CRANFIELD UNIVERSITY

Thomas Mourouzidis

Research on Environmentally Friendly Fire Suppression Systems for Aircraft Cargo

School of Aerospace, Transport and Manufacture
PhD in Aerospace

Doctor of Philosophy (PhD)
Academic Year: 2018 - 2019

Supervisor: Dr Suresh Sampath
Associate Supervisor: Dr Theoklis Nikolaidis
August 2019

CRANFIELD UNIVERSITY

School of Aerospace, Transport and Manufacture
PhD in Aerospace

Research on Environmentally Friendly Fire Suppression Systems for Aircraft Cargo

Academic Year 2018 - 2019

Thomas Mourouzidis

Doctor of Philosophy (PhD)

Supervisor: Dr Suresh Sampath
Associate Supervisor: Dr Theoklis Nikolaidis
August 2019

This thesis is submitted in partial fulfilment of the requirements for the degree of PhD

“Everything flows and nothing abides,
everything gives way and nothing stays fixed”

HERACLITUS

ABSTRACT

It is widely known in the aviation community that the use of Halon1301 as fire suppression agent has been banned as it presents high ozone depleting potential. This fact dictates that there is a necessity for fire suppression systems replacement on all existing aircraft within a limited timeframe. So far, Nitrogen (IG-100) was proven to be the most promising replacement agent for future aviation. The present research project attempts to assess the handling, performance and installation of a Nitrogen (IG-100) fire suppression system on aircraft cargo in order to accelerate the transition to Halon-free systems. The research has been conducted under the umbrella of the EU Clean Sky 2 (CS2) “Environmentally Friendly Fire Suppression System for Cargo using Innovative Green Technology” (EFFICIENT) project.

The methods used to achieve the project targets are based on analytical and numerical 3D-CFD modelling as well as both in-house and public domain experimental information of respective cargo fire suppression systems. Additionally, they are aligned with FAA requirements and follow the Minimum Performance Standard (MPS) required for testing and certification. The Nitrogen (IG-100) system design space exploration focused on the examination of exchange rates between parameters such as the number and location of discharge nozzles and ventilation ports with the system effectiveness, operability and safety. The resulted fire suppression system design was also used for the development of the detailed design and operation strategy of the Cranfield in-house test rig as well as the experimental testing and procedures, the risk assessment and installation cost estimation.

The outcomes of CFD simulations presented satisfactory agreement with the theoretically expected analytical calculations. Additionally, they were validated against the experimental data coming from the above mentioned Cranfield based test rig. The data regarded No-Fire and Open Surface Liquid Fire tests using Jet-A fuel. Both CFD and experiments showed that system achieved the desired average Oxygen concentration within 60 seconds discharge, while maintaining it below 16% for more than 45 minutes, satisfying the FAA MPS. Additionally, the

average overpressure level inside the compartment remains within limits both during and after agent discharge. Finally, based on their comparison, numerical model adaptations and calibration are suggested in order to improve modelling fidelity and simulation accuracy.

The proposed Nitrogen based design suggests minimum modifications to the already existing Halon1301 based systems in order to accelerate the replacement process. Furthermore, the system provides ease in handling and operation with capabilities of minimising Nitrogen wastage by varying the agent mass used based on the level of the cargo load and the nature of its content. Finally, recommendations for future improvements regarding the system response time, the fire protection time, the weight and complexity are included.

Keywords: MPS tests for aircraft cargo, Nitrogen (IG-100) inert concentration, cargo ventilation modelling, fire extinguishment

ACKNOWLEDGEMENTS

Initially, I would like to express my deep gratitude to Professor Pericles Pilidis for being a great mentor and a role model, providing continuous support and guidance throughout this hard task.

I would like to thank Dr Suresh Sampath and Dr Theoklis Nikolaidis, my research supervisors, for their patient guidance, enthusiastic encouragement and useful critiques of this research work.

Special thanks to my beloved brother Dr Christos Mourouzidis for his motivation, constant support and belief in my capabilities, without which I wouldn't be able to achieve my goals. 6 years ago, he was the one who suggested and supported me to follow a career in aerospace engineering in the UK and pursue the demanding challenge of a PhD project.

Thanks to the CS2 EU EFFICIENT project partners', Dr R. Beuermann from AIRBUS and the Cranfield University Test Area staff for their invaluable scientific and technical support on this research project.

Many thanks to my colleagues Dr Alvise Pellegrini, Dr Alozie Ogechukwu, Dr Bjorn Cleton, Dr David Bentley, Dr Eduardo Anselmi Palma, Dr Michalis Diakostefanis, Dr Evangelos Chrysochoidis and Dr Areti Malkogianni for sharing our thoughts and worries, and for making me feel less lonely in this personal research journey.

I would like to extend my gratitude to my good friend and mentor Nikos Triantafillidis, who is always like a father to me, and to my devoted friends Giorgos Petridhs, Panagiotis Papadopoulos and Spiros Tsakiropoulos for honouring me all these years with their love, support, reliance and care. Additionally, thanks to my friends/colleagues from the Sports Centre Roy, Craig, Ed, Joan and Evangelia, my good friend and best UK taxi driver Abs and my housemates Shaila and Yash for being a real family to me in the UK, making me feel welcome from the beginning to the end of this journey.

Finally, I would like to dedicate this work to my close family. My farther Petros, who initially inspire and constantly support me to define and follow my life dreams and become the person I am today. His wife Sofia, with her unconditional love and support for the last at least 20 years. My beloved mother Sofia, who is always loving, caring and supportive with all my choices. My aunt and uncle, Lena and Dimitris and my cousins Christos, Pavlos and Vasiliki, who are always following me in my life's journey with their love and support. My beloved grandma and grandpa, Maria and Christos, who recently passed away, for implanting into me traditions and moral standards that allow me to withstand life challenges with dignity and keep focus on my life targets even in hard times.

Last but not least, I would like to specially dedicate this work to the memory of my beloved friend, coach and a real fighter of life Mr Raymond Cummins, who left us too soon, by quoting one of his signature phrases "God Bless".

TABLE OF CONTENTS

LIST OF FIGURES

LIST OF TABLES

LIST OF EQUATIONS

LIST OF ABBREVIATIONS

DBCS	Density based couple solver
EFFICIENT	Environmentally Friendly Fire Suppression System for Cargo using Innovative Green Technology
FAA	Federal aviation administration
Full Cargo	Full cargo volume
Full Cargo-Load	Full cargo loaded with 30% boxes
GWP	Global Warming Potential
Halon 1301	Fire extinguish agent using halogens
HFC-125	Fire extinguish agent using halogens
ICAO	International Civil Aviation Organization
IG-100	Inert gas ≈100% Nitrogen
IHRWG	International Halon Replacement Working Group
MPS	Minimum performance standard for cargo
MQF	Model quality factor
OBIGG	On-board inert gas generators
OBOGG	On-board oxygen gas generators
ODP	Ozone depletion potential
Partial Cargo	Partial volume of the full cargo
PBCS	Pressure based couple solver
SPGG	Solid particle gas generator
SS	Steady-state
TR	Transient

LIST OF NOMENCLATURE

A_1	Initial cross-sectional area (m^2)
A_f	Floor area of the compartment (m^2)
A_n	Nozzle area (m^2)
$A_{orifice}$	Nozzle orifice area (m^2)
C	Agent concentration (% v/v)
Cv	Initial volumetric concentration (%)
C_{agent}	Agent concentration (%)
C_d	Design concentration (v/v)
D	Cylinder Diameter (m)
ΔP	Pressure drops from reducer (Pa or bar)
$F_{vertical,jet}$	Nozzle vertical jet force (N)
F_{jet}	Nozzle jet force (N)
F_{nozzle}	Nozzle total force (N)
g	Acceleration due to gravity ($9.81 m/s^2$)
$G1$	Safety Factor (%)
H_d	Height of the agent/air layer (m)
h	Cylinder Height (m)
H_d	Height of the agent mixture (m)
H_o	Height of protected enclosure (m)
$\dot{m}$	Total mass flow rate (kg/s)

$\dot{m}_A$	Discharge mass flow rate (kg/s)
$\dot{m}_{jet}$	Nozzle jet mass flow rate (kg/s)
$\dot{m}_N$	Nozzle mass flow rate (kg/s)
$\dot{m}_{N1}$	Nozzle 1 mass flow rate (kg/s)
$\dot{m}_{N2}$	Nozzle 2 mass flow rate (kg/s)
$\dot{m}_{N3}$	Nozzle 3 mass flow rate (kg/s)
$\dot{m}_1$	Mass flow rate split 1 (kg/s)
$\dot{m}_2$	Mass flow rate split 2 (kg/s)
m_{excess}	Excess mass (kg)
m_{final}	Final quantity (kg)
Mn	Design Mach No.
M_1	Mach No. station 1
M_2	Mach No. station 2
Mn_{exit}	Exit Mach No.
N	Number of cylinders
Nn	Number of nozzles
P_1	Pressure station 1 (Pa or bar)
P_2	Pressure station 2 (Pa or bar)
P_c	Column hydrostatic pressure (Pa or bar)
P_{atm}, T_{atm}	Enclosure conditions (atm or Pa)
Po	Initial pressure (Pa or bar)
$Ps, Ts, \rho_{\mathrm{s}}$	Static conditions (Pressure, temperature and density)

Q_e	Total volumetric flow rate (kg/s)
R	Gas constant
r_a	Air density (kg/m^3)
r_m	Agent/air mixture density (kg/m^3)
r_v	Vapour density
s	2.2062 + 0.005046*T (ft^3/lb) (experimental factor)
T	Minimum anticipated volume temperature (°F or ^{o}C or K)
t	Activation/discharge time (s)
$t_{constant\ discharge}$	Main discharge time (s)
$t_{drain-out}$	Time till drain-out (s)
$t_{extra\ mass}$	Extra mass time (s)
t_d	Design activation time (s)
t_{excess}	Excess time (s)
t_{op}	Operation time (s)
T_s	Temperature drop taken from the diagram (^{o}C or K)
T_o	Initial temperature (^{o}C or K)
T_1	Temperature station 1 (^{o}C or K)
T_2	Temperature station 2 (^{o}C or K)
V	Agent quantity (m^3)
V_{agent}	Agent volume (m^3)
V_{AIR}	Air volume (m^3)
Vc	Cylinder Volume (m^3)

Vh	Net volume of hazard (m^3 or ft^3)
V_{jet}	Nozzle jet velocity (m/s)
V_L	Out-flow velocity across leakages (m/s)
$V_{leakage}$	Leakages volume (m^3)
Vo	Enclosure volume (m^3)
W	Agent weight for design concentration (lb or kg)
X	Volumetric concentration due to leakage (%)
Y	Height of the pure air layer (m)
Y_d	Design height of the pure air layer (m)
γ	Ratio of specific heats
ρ	Density (kg/m^3)
ρ_1	Density station 1 (kg/m^3)
ρ_2	Density station 2 (kg/m^3)

1 INTRODUCTION

1.1 Background

For the last 60 years, worldwide fire suppression systems use Halons as fire extinguishing agents. This is due to the fact that Halons (1211, 1301, etc.) present impressive fire suppression characteristics, which also provided great leverage for low complexity and lightweight installation of the storage and delivery systems. Such systems were proved to be successful in industrial, marine, aviation and spacecraft applications.

Nevertheless, during the Montreal Protocol in 1989, it has been decided that Halon production must be completely stopped (fully active by 1994) and the existing systems to be replaced as soon as possible [1, 2]. This was mainly due to the fact that Halons present strong ozone depletion potential. London agreement (1990) and Copenhagen treaty (1992) also offered more restrictions on chlorofluorocarbon (CFC) emissions [3].

Despite the facts mentioned above, a temporary exception has been allowed for aircraft systems to use Halon through a recycling process, until a replacement system is completely operational [2].

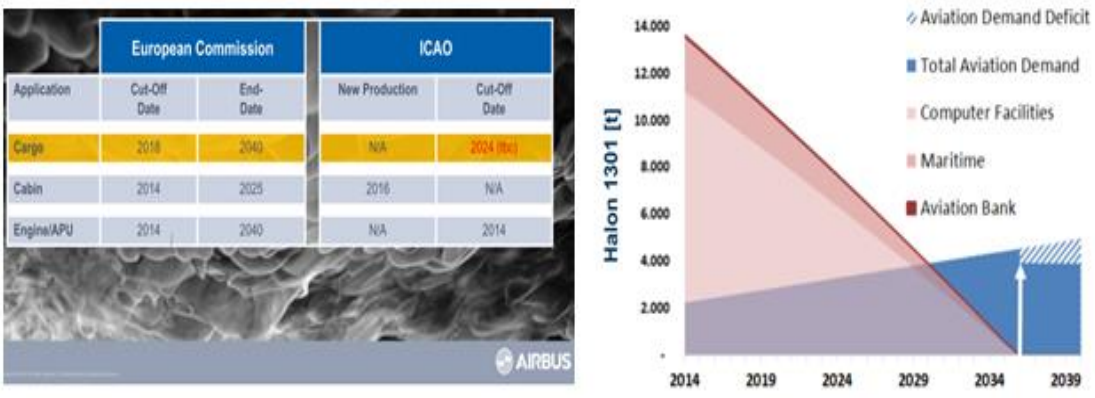

(a) (b)

Figure 1 - a) European commission and International civil aviation deadlines for Halon replacement b) Halon global reserve bank compared to aviation demand [4]

The International Civil Aviation Organisation (ICAO) is in the progress of implementing a deadline for replacing Halon in aircraft cargo fire suppression

systems (Figure 1 a). In addition, European legislation prohibits the Halon use in the future aircraft. Thus, only already existing aircraft will still use the rest of Halon reserves.

In any case, Halon stocks are depleting and the future long term availability is under risk. Figure 1 (b) illustrates the Halon global bank reserves compared to the aviation demand and thus its inadequacy to support civil aviation for next 20 to 40 years [4]. These facts lead to the conclusion that there is limited time available for certified system replacement on all existing aircraft and thus, any contribution towards accelerating this process becomes a vital target for aviation.

On the same basis, Federal Aviation Administrator (FAA) and generally the civil aviation community have initiated research studies focusing on Halon1301 replacements [5]. For this purpose several activities have been developed such as fire suppression simulations (analytical, numerical) and experimental tests (Minimum Performance Standard (MPS) tests, Gup burner test, etc.). The International Aircraft Fire Protection Working Group IAFPWG (FAA sponsored) has fully defined the MPS requirements for Halon replacements in order to identify and classify the candidate agents. The main target of all the above was to examine the fire suppression characteristics of each candidate agent, establish certification requirements and assesses their suitability for each application. The aircraft applications under considerations are commercial aircraft cargo and cabin fire protection along with the powerplants.

Although the research on replacing the Halon based fire suppression systems has progressed significantly, the integration with the aircraft and operation challenges are not yet fully addressed. EU Clean Sky 2 project EFFICIENT (Environmentally Friendly Fire Suppression System for Cargo using Innovative Green Technology) [6] has been specifically set to address such challenges for aircraft cargo applications. This four year research activity, which started in 2017, is the base of the present research project.

Specifically, for aircraft cargo fire suppression systems, the candidate agent must demonstrate the ability to achieve the MPS requirements successfully through experimental testing. The MPS tests [7] are specific large scale fire scenarios

inside a ground based cargo compartment using Halon1301 as baseline agent. Additionally, each replacement agent that will satisfy the MPS will be suggested by FAA for testing on a flying test bed. According to the outcome, FAA will either approve the agent or suggest extra testing. Finally, the considerations for the applicability and economics of the actual replacement of the complete fire suppression system, along with the supply lines and procedures, introduce extra time and complexity in order to overcome these challenges.

Furthermore, FAA categorised the candidate fire extinguishing agents in “replacements” and “alternatives” (see Table 1) [5].

Table 1 - Halon1301 candidate replacement fire extinguish agents [5]

"Alternatives"		"Replacements"	
Classical	**New**	**Halon compounds**	**Chemical synthesis**
Foams	Water misting	HCFCs	Hydrochlorofluorocarbons
Water sprinklers	Particulate aerosols	FCs (PFCs)	Perfluorocarbons
Dry chemical	Inert gases	HFCs	Hydrofluorocarbons
Carbon dioxide	Gas generators	FICs	Fluoroiodocarbons
Loaded stream	Combination	-	-

The candidate agents were tested following mainly the MPS procedures, environmental and aviation requirements. This research provided the list of most promising agents as well as the main system approval criteria for aircraft cargo applications (see Table 2 and Table 3).

Table 2 - State-of-the-art agents

a/a	Agents	Comments
Cargo system	Halon1301	used as baseline (FFA, MPS)
Replacements	HFC-125	currently tested for engine nacelles (FAA)
Alternatives	Nitrogen	recently under development (Airbus, Boeing)
	Water mist	
	Combination	

Table 3 - Overall system approval criteria

1	Environment (ODP, GWP, Lifespan)
2	Toxicity
3	Applicability, cost and complexity
4	MPS for aircraft cargo

On the other hand, a recent promising development under this context regards the *On-board Inert Gas Generators* (OBIGGS), *On-board Oxygen Gas Generators* (OBOGGS) and the *Solid Particle Gas Generators or Cold Gas Generators* (SPGG or CGG). These devices are intended to work as main or in collaboration with the main aircraft fire suppression system [41].

Summarising, two significant challenges have been identified regarding the near future aircraft fire suppression systems:

1. Develop an efficient, reliable and environmentally friendly fire suppression system, suitable for future aircraft applications.

2. Minimise the time required for the development of a certified replacement system, as well as its installation on-board all existing aircraft.

The time required for the development and deployment of the replacement system depends on several factors such as:

1. Selection of appropriate replacement agent
2. Cargo systems current technology level
3. System design process
4. Testing and certification processes
5. System installation on-board the aircraft

All factors must achieve their time goals in order to meet the requirements. Recently, numerical simulation methods have been improved significantly providing further advantages in terms of simulation time and cost for case studies such as that in the present research project. 3D-CFD numerical simulations enable detailed representation of the flow characteristics, providing valuable information regarding nozzle discharge performance and overall cargo conditions. Such capabilities provide a further insight on the physical problem which enhances and accelerates the system design process while reduces the

experimental tests. The elements that can be improved regarding the system design process using numerical simulations are the agent storage and delivery systems sizing, the discharge nozzles selection, the cargo ventilation requirements and the system controls. These would also support in achieving accurately the desirable fire suppression and protection times, while minimising the agent consumption. Regarding the experimental tests, the same elements can support the design, installation and operation of the test rig targeting the minimisation of installation cost, number of experiments, number of spare parts, agent quantity and emissions.

1.2 Scope of Work

The scope of this work is to support the research towards quick transition to Halon1301-free fire suppression systems for aircraft cargo. The main focus of the research locates on the thematic areas below:

- Replacement agent performance and operability characteristics, along with design criteria for the testing procedures
- Fire suppression system general arrangement and modifications required on the existing system based on the replacement agent
- Fire suppression system numerical (3D-CFD) modelling supporting both the design and setup of experiments, as well as the system on-board the aircraft

1.3 Aim & Objectives

The project aim is to develop a fire suppression system concept based on the most promising Halon1301 replacement agent and predict its operational performance. System general arrangement, firefighting strategy, analytical and numerical modelling, simulation strategy, test rig design and experimental procedures setup are the main elements that comprise the fire suppression system concept. The prediction of the system performance aims to provide a top level assessment of its applicability on-board aircraft cargo. Finally, the proposed design will include considerations regarding system installation on aircraft, which

complies with the requirement for quick transition to environmentally friendly systems before Halon1301 reserves are depleted.

The individual objectives specified to meet the project aim are listed below:

1. Based on the most promising replacement agent, examine current aircraft cargo fire suppression systems and derive the conceptual system general arrangement and firefighting strategy.
2. Develop an analytical model for the sizing and performance prediction of the hydraulic and ventilation systems as well as the agent discharge process. The model will be used to provide geometric dimensions and boundary conditions for the numerical 3D-CFD models.
    a. Develop the agent distribution piping network design along with the necessary equipment
    b. Develop the cargo ventilation system design
    c. Adapt all designs based on the existing aircraft cargo fire suppression systems, minimising installation time and weight
3. Develop numerical (3D-CFD) models to perform simulations of the fire suppression system operation (MPS tests) and support the test rig design and operation. The simulations are separated in two categories:
    a. Steady state, for the study of cargo conditions during discharge. This study will support the sizing of the agent delivery system, the discharge nozzles and the ventilation requirements. Additionally, it will provide relatively quick solutions suitable for system architectural design assessments and parametric studies. Main targets:
        i. Assure acceptable compartment overpressure levels during operation based on experimental information from public domain (FAA, AIRBUS) [5, 9].
        ii. Assure safe discharge conditions preventing human hazards, baggage damage and direct agent losses
    b. Transient, to study the agent concentration and overpressure inside the compartment against time. The complete simulation is separated in two time periods: a) beginning to end of discharge and b)

immediately after discharge and until the targeted protection time (landing). Main targets:

   i. Achieve the agent extinguish concentration level proposed by the small scale tests (cup burner tests, LSBU data [8])

   ii. Assure acceptable compartment overpressure levels during operation based on experimental information from public domain (FAA, AIRBUS) [5, 9].

   iii. Achieve compartment conditions acceptable to human health

4. Verify overall system operation and propose adjustments on the existing on-board arrangement.
5. Develop the designs and support the installation of the test rig required for the fire suppression system experimental testing (based on MPS). Individual sub-system designs, test rig automations and controls, experimental tests setup and risk assessment are to be included.
6. Run large scale tests, assess the final system performance based on MPS requirements and verify/calibrate the analytical/numerical models

1.4 Research Contribution

The current research project contributes towards the development of an environmentally friendly and effective replacement of the existing aircraft cargo fire suppression systems. This contributes to the global effort towards a “Greener” future for aviation. Such novel systems will include more demanding environmental and human health requirements during operation.

The outcomes of this research provide an insight on the potential challenges regarding the integration and performance of the system on-board the aircraft as well as on test rigs. The resulted system sizing dimensions, weight estimations and automation requirements support the development a low cost and complexity retrofit system. Such information contributes to the global effort for transition to Halon1301 free aircraft cargo fire suppression systems before the reserves banks are depleted.

The project case study was focused on the proposed Nitrogen (IG-100) fire suppression system for aircraft cargo. The methodologies developed, along with

the outcomes of the analytical/numerical modelling of the replacement system, provide a first assessment of the technology and a proof of concept. This fact combined with the established testing procedures and firefighting strategy, support the transition of the technology to a higher Technology Readiness Level (TRL).

The numerical (3D-CFD) simulation strategy developed assures acceptable representation of the phenomena that occur during fire suppression system operation, for the purposes of the current project. It provides information on the settings and running computationally expensive numerical simulations regarding high gas discharge velocities in large control volumes. Finally, the solution convergence strategy presents properties of removing complexity, reducing computational cost and increasing accuracy. Thus, it is expected to deliver relatively fast and accurate solutions for the sizing and conceptual design of such systems for all aircraft sizes and types.

The numerical (3D-CFD) models produce detailed information regarding the agent concentration and distribution inside the cargo, as well as the complex interaction between the agent discharge and ventilation systems. Using such data, the design of the agent delivery and discharge system, as well as the design criteria for the ventilation system can be established.

The experimental data provided herein enrich the database regarding Nitrogen based fire suppression systems for aircraft applications. They support the proposed Nitrogen based system design by proving its potential to pass the required MPS fire tests for certification. Additionally, they provide valuable information that can support all research activities using numerical models to simulate aircraft cargo fire suppression systems in operation.

Finally, based on the outcomes of the present research, a journal paper has been produced with title:

Conceptual Design, CFD Modelling and Experimental Testing of Eco-Friendly Nitrogen Based Fire Suppression Systems for Aircraft Cargo

The paper has been submitted to the Journal of Aeronautics & Aerospace Engineering (open access) and it is under review.

1.5 Thesis Outline

The thesis was structured in five chapters. A general description of the chapters after Chapter 1 is presented below:

Chapter 2 – Literature review

This chapter contains the theoretical background regarding the fire suppression system operation and the flow phenomena that occur within an aircraft cargo compartment. Also, it highlights the most promising replacement agents and systems for such applications and the performance acceptance criteria (MPS). Finally, it presents the current state-of-the-art, the challenges they face and their relation to the present research project.

Chapter 3 – Methodology

This chapter presents the methodology developed in order to meet the project objectives. The methodology is separated in three work streams: analytical, numerical CFD and experimental studies. It explains the approach and methods used for analytical and numerical CFD models development, and presents the general system arrangement, test rig design and the setup for the experimental procedures.

Chapter 4 – Results & Discussion

This chapter includes the main outcomes of the current research project and follows the structure of the methodology chapter. It highlights the main design challenges for system assessment as well as the adaptations required to meet the acceptance criteria and derive the finally proposed system.

Chapter 5 – Conclusions & Recommendations for Future Work

This is the final chapter of the thesis which summarises the major outcomes and conclusions. Additionally, it includes suggestions for future system improvements as well as recommendations for the continuation of the research on this topic.

Finally, at the end of the thesis there is a number of Appendices attached. Those present general information regarding the background of the research of Halon replacement agents. Furthermore, they include details on the experimental work performed at Cranfield University in order to support the EU CS2 EFFICIENT project fire tests. Safety analysis, hazards classification and details regarding the MPS tests acceptance criteria, setup and equipment are also provided.

2 LITERATURE REVIEW

This chapter includes the theoretical background that describes the phenomena that occur within an aircraft cargo compartment during fire suppression system operation. In addition, it highlights the most promising replacement agents for these applications and summarises the public domain information about their behaviour, storage and handling. Furthermore, it provides a brief description of the candidate agent performance requirements to succeed the MPS tests. Finally, it presents the current state-of-the-art for these systems, along with their future design challenges and research gaps.

2.1 Fire Suppression for Aircraft Cargo Fundamentals

The design of the fire suppression system for aircraft cargo is highly depended on the fire extinguishing agent. Fire extinguishing agents are selected based on the mechanism they use to attack and extinguish fires. Therefore, both the type of fire and the extinguishing agent are of high importance for the development of the fire suppression system.

The type of fire depends mainly on the burning material. Therefore, different agents are used depending on the burning material or type of fire. The types of fire are categorized also into Classes (see Table 4 [10])

Table 4 - Fire classes [10]

ISO Standard 3941	*NFPA 10*
Class A: Fires involving solid materials, usually of an organic nature, in which combustion normally takes place with the formation of glowing embers	***Class A***: Fires in ordinary combustible materials, such as wood, cloth, paper, rubber and many plastics.
Class B: Fires involving liquids or liquefiable solids.	***Class B***: Fires in flammable liquids, oils, greases, tars, oil-based paints, lacquers and flammable gases.
Class C: Fires involving gases.	***Class C***: Fires which involve energized electrical equipment where the electrical non-conductivity of the extinguishing medium is of importance.
Class D: Fires involving metals.	***Class D***: Fires in combustible metals, such as magnesium, titanium, zirconium, sodium, lithium and potassium.

Halons are bromines containing gaseous or volatile liquid chemicals and mostly used on aircraft applications. Halon1301 is used primarily as a total flood agent in cargo fire suppression systems. These chemicals are applicable for fire Classes A, B and C and they cannot be used for Class D.

2.1.1 Fire Extinguishment Considering the Fire Tetrahedron

Four basic components constitute the fire tetrahedron: (a) Fuel, (b) Oxygen, (c) Heat and (d) Chain Reaction (Figure 2).

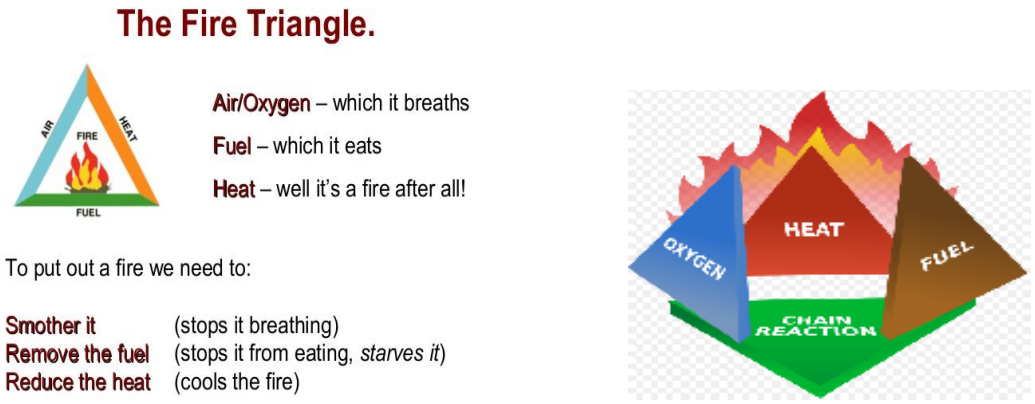

Figure 2 - Fire triangle and tetrahedron [11]

Considering the fire tetrahedron, each one of the components is essential for either the ignition or maintenance of fire. Generally, each of the extinguishing agents attacks and removes one or more sides of the tetrahedron.

Fuel is the "food" of fire and can be found in all three phases: solid, liquid or gaseous. The behaviour of the fuel when it burns is highly depended on its properties, used to initiate, maintain or extinguish fire. For example if the fuel is solid with the use of foam as an extinguishing agent the fuel is protected with a shield preventing the contact with the other components and the fire shuts down. Typically, the way to extinguish fire through fuel, for all substances, is to physically separate it from the fire (e.g. cut-off supply).

Oxygen is the oxidiser contained in the surrounding air at about 21% volumetric concentration. The concentration of the rest of the elements contained in air are 78% Nitrogen and 1% others, mainly Argon. The sufficient amount of oxygen in order for the fire to exist is around 16% [10]. Typical examples of agents, used to extinguish fire by reducing the amount of oxygen, are Nitrogen and CO_2. These agents are taking the place of oxygen close to the combustion process and extinguish the fire. The seal of an enclosed space is very important in order to maintain the concertation of Nitrogen or CO_2 to extinguish or prevent a fire.

Nevertheless, it has been proven challenging for these agents to be used in open spaces.

Heat is released during the oxidation process and increases the fuel molecule temperature resulting in a self-supporting fire. This is the third component of the tetrahedron of fire. Water, due to its high heat capacity, is able to reduce the temperature and extinguish the fire by removing heat. Water is a very effective heat absorber and reduces the vapour production by cooling down the fuel surface. Actually, water absorbs heat from the fuel as well as the radiation heat feedback affecting also the chain reaction both on the fuel surface and flames.

Chain reaction is the forth component of the tetrahedron of fire. It shows how the other three components react with each other in order to maintain the fire. Once this chain reaction interrupted, the heat generation reduces resulting in a reduction of both fuel vapour production and oxidiser temperature rise. Common examples of agents which interrupt the chain reaction are Halons, Halon replacements and dry chemicals. These agents attack the molecular structure of products formed during the chain reaction by search and collect the oxygen and OH^- radicals. These agents do not cool down the fuel and must be maintained on the fire until the fuel cools down naturally.

2.2 Fire Suppression Systems for Aircraft Cargo

Generally, the fire suppression systems, land-based or airborne, can be separated in five types [4]:

I. Total flood fire extinguishment (aircraft hand extinguishers etc.)

II. Total flood fire suppression

III. Streaming fire extinguishment

IV. Explosion suppression

V. Inertion against explosions and fires

The fire suppression systems for aircraft cargo are classified as total flood applications, where the extinguishing agent is discharged in order to rapidly and

sufficiently suppress an existing fire and prevent any potential explosion or re-ignition inside the cargo compartment until landing. A representative example of current fire suppression systems for cargo can be seen in Figure 3.

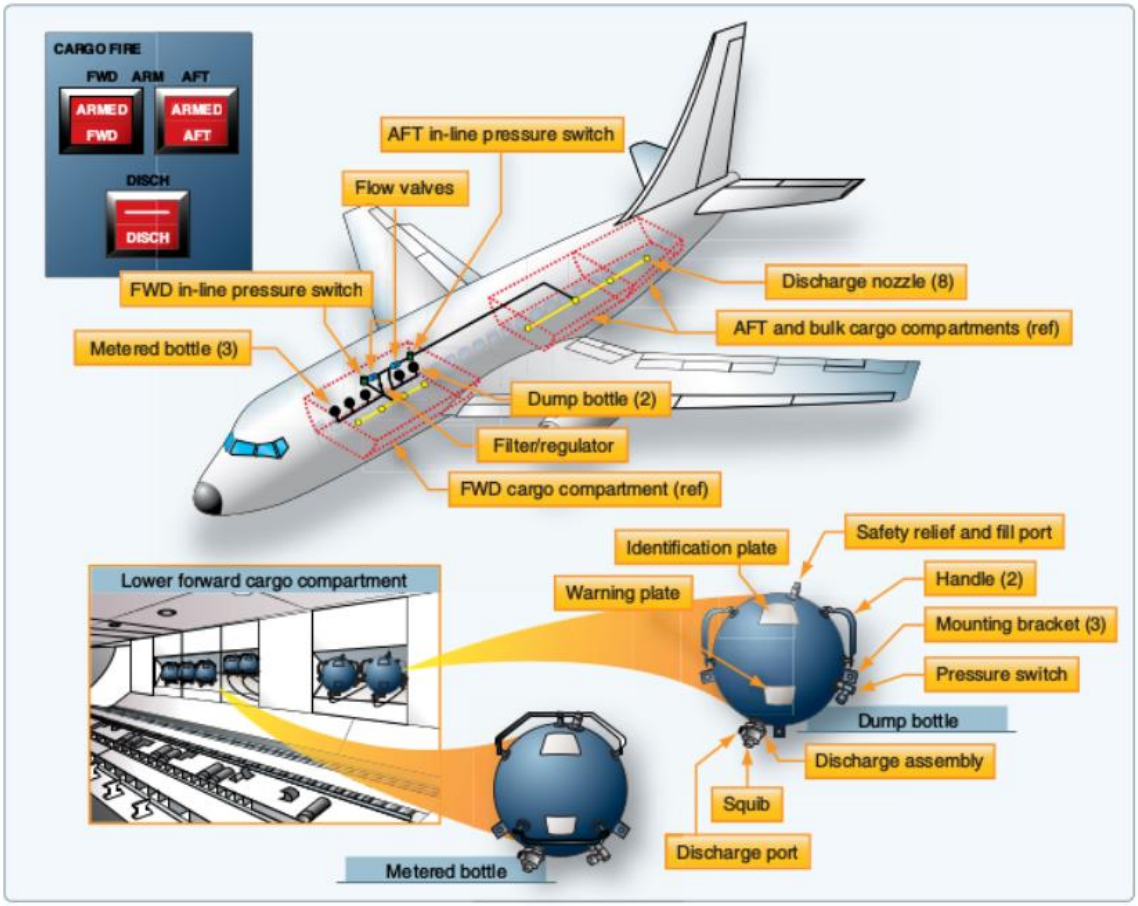

Figure 3 - FAA document Fire Protection Systems [12]

The system operation is comprised by two stages: a) using the dump bottles in order to quickly suppress the fire and b) using the metered bottles in order to maintain the agent required concentration inside the enclosure until the aircraft lands.

Such systems use both manual and automatic activation after the detection of fire. Their control and indication panel includes the following components [13]:

1. Detector select switch
2. Cargo fire test switch
3. Detector fault indicator

4. Master fire warning light and bell
5. Cargo fire warning lights and armed switches
6. Extinguisher test lights

In Class A, the fire can be easily discovered by the crew members and is located in fully accessible areas, where there is no need for heat resistant compartment liner. In Class B, approved smoke or fire detection systems are used to alert the pilot or flight engineer and the compartment is accessible for the crew members to reach with a manual fire extinguisher. The liner design is based on flame penetration resistance standard requirements in order to prevent the fire to spread. Class C systems are similar to B, with the main difference being that only the automatic build-in extinguishing system is utilised to control the fire. Moreover, the fire detection systems as well as the compartment liner require more demanding capabilities in order to be certified. In Class D, the firefighting strategy is based on restricting the supply of the available oxygen. The liner capability to resist the flame penetration must be exceptional for this class. Additionally, due to uncontrolled fires happening into cargo compartments causing accidents and loss of life, this class is still under revision and modifications. The growing danger of fire/explosion caused by aerosol cans in passenger luggage led FAA to conduct tests with aerosol can explosions in burning luggage and investigate the transition from Class D to Class C [15]. Finally, the case of aircraft used only for goods transportation is represented by Class E. The compartment here is the entire cabin of an all-cargo airplane and uses smoke or fire detection systems. After the fire detection, the flow of ventilation air stops, reducing the oxygen and extinguishing the fire. In this class the compartments can handle procedures such as depressurizing airplanes in order to extinguish fire due to the lack of passengers. The tables below present typical aircraft cargo dimensions and a summary of the characteristics for each of the main Classes of interest.

Table 5 - Typical Boeing Aircraft Cargo Dimensions [13]

	737-800	747-400	757-300	767-300	777-300
Cargo compartment free air space volume					
Forward	719 ft^3	5,000 ft^3	1,071 ft^3	3,096 ft^3	6,252 ft^3
Length	298 in	510 in	495 in	486 in	590 in
Width	125 in	184 in	80 in	140 in	164 in
Height	42 in	80 in	44 in	68 in	80 in
Percent of compartment volume occupied by cargo	Up to 50%	**Up to 67%**	Up to 75%		Up to 67%
Aft	961 ft^3	5,000 ft^3	1,295 ft^3	3,152 ft^3	5,667 ft^3
Length	221 in	680 in	558 in	572 in	817 in
Width	123 in	184 in	80 in	140 in	164 in
Height	45 in	80 in	54 in	68 in	80 in
Percent of compartment volume occupied by cargo	Up to 50%	Up to 67%	Up to 75%	Up to 67%	**Up to 67%**

Table 6 - Summary of Different Cargo Compartment Characteristics [14]

	Class C	Class E	Class B	Class D
Fire Detection	Smoke detection	Smoke detection	Smoke detection	No Detection
Crew Action	Push button	Set FL 200/250	Hand held fire Ex.	No Action
Aircraft fire fighting means	Built-in fire suppression system	Flight level procedure, reducing oxygen partial pressure	Active firefighting via held extinguisher	Isolation
Fire Fighting Principle	Fire suppression via Inhibition (Halon 1301)	Oxygen starvation	Extinguishing	Fire Containment and Oxygen consumption
Conditions	Until end of flight	Increase of oxygen partial pressure during descent phase	Monitoring	Gradual Increase of oxygen partial pressure during descent phase
Expected steady-state conditions	Cargo Compartment temperature>200^0 C	Similar condition as class C cargo	Extinguished	Smoldering fire, depend on oxygen concentration left

Focusing on the Halon1301 replacement systems, three main requirements for a potential replacement agent have been established:

1. Particularly for Classes A and B, it must be capable to provide fire suppression over a period up to 180 minutes depending on the case (aircraft type and route) and approved by the authorities [15].

2. The agent must be compatible with the materials or equipment it will come in contact during a fire event. This is to prevent corrosion or any type of decomposition of the surrounding materials.

3. Finally, the agent must comply with the Montreal Protocol restrictions (near zero ozone depleting potential, low global warming potential and atmospheric lifespan).

Furthermore, the toxicity of the agent must be low or the agent must be able to extinguish fire at low concentrations to avoid any health problems for animals inside the cargo. Regarding failure modes, the agent cannot be allowed to leak into occupied areas in toxic concentrations. Basically, it should prevent any potential issues regarding its integration with the aircraft, causing delays or false discharge. These are some of the reasons for the cargo to contain fiberglass liners which are tested with flame penetration burners and smoke generators for leakage. The most likely fire to occur in this case is an open surface fire, supplied with an ignition source and usually flammable material in solid and liquid form. A wide variety of fires can be initiated both by human and cargo ignition sources. Typically, the minimum normal pressures and temperatures inside a cargo flying at 8000ft are maintained above water freezing point, ventilation included.

2.2.1 Current Aircraft Fire Suppression System Arrangement

The general arrangement of a typical fire suppression system along with the main description of its operation at ground level is presented in Figure 4 and Figure 5 [16]. The quick discharge activation system uses a number of high-rated bottles depending on the aircraft mission and size. The high rated bottles are discharged rapidly to suppress the fire quickly (1 or 2 minutes after the fire detection) and achieve concentration above the required level for extinguishment. The diverter valve delivers the agent directly to the affected area (forward or aft cargo). This process was also designed to maintain concentration above the required level for 90 minutes without any more discharge. Figure 5 (left) illustrates the operation of the quick discharge activation system in order to maintain agent concentration above the required level for 90 minutes. In a two stage case, the metered activation system (see Figure 5 right), follows a different approach in order to minimise the leakages and thus the amount of Halon1301 discarded to the environment. The bottle discharges the agent in a controlled fashion in order to

maintain the agent concentration at the required level without exceeding it until the aircraft lands.

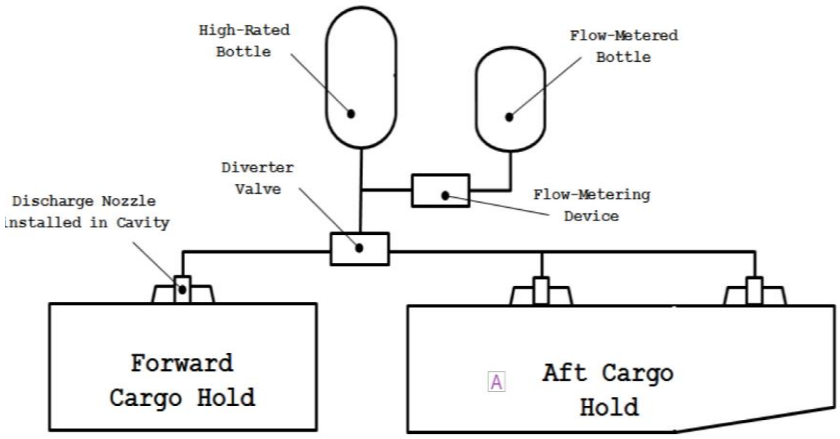

Figure 4 - Lower deck cargo hold fire suppression system- general arrangement [16]

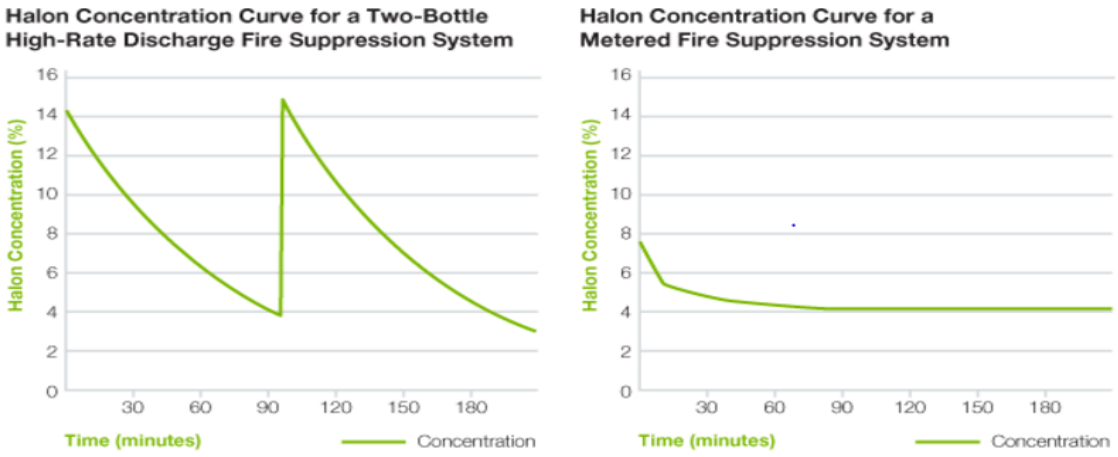

Figure 5 - Fire suppression activation systems [17]

The system activation uses smoke detectors (automatic) or thermocouples (manual – through indications) and a flow-metered device for agent discharge control. The agent discharge nozzles are placed in cavities preventing interference with the cargo baggage while the purpose of the system design is only to suppress the fire and contain the damage until the aircraft lands and specified personnel fully takes over.

Besides the agent distribution and discharge system, a typical aircraft cargo fire suppression system operates in collaboration with the cargo ventilation system. Figure 6 illustrates typical cargo ventilation system in two different types [18]. The target of these systems is to maintain acceptable levels of pressure and

temperature inside the cargo in order to assure life sustaining conditions. A typical range of pressures inside aircraft cargo during flight is 0.8 – 1.0atm, while for temperatures 10 – 37°C.

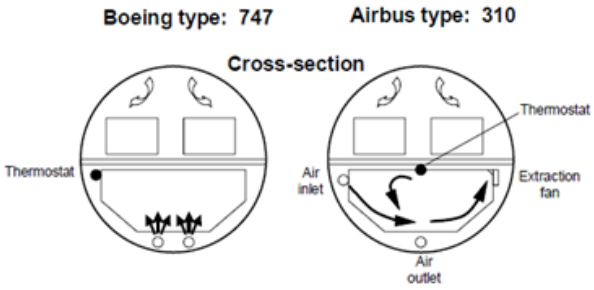

Figure 6 - Ventilation system in two different types of aircraft [18]

2.2.2 Halon1301 Fire Suppression System Characteristics

Halon is a chemical compound that contains group of organic halogen compounds such as bromine and fluorine with one or two carbons. The Halon fire extinguish agents have low boiling point and are commonly used to suppress fires and protect against explosions [5]. The term Halons refers to fire extinguishing agents such as Halon1301, 1211 and 2402 (Table 7).

Table 7 - Halon extinguish agents [5]

Halon Number	Halocarbon Number	Chemical Name	Formula	Boiling Point, °C
Halon 1301	BFC-13B1	bromotrifluoromethane	$CBrF_3$	-58
Halon 1211	BCFC-12B1	bromochlorodifluoromethane	$CBrClF_2$	-3
Halon 2402	BFC-114B2	1,1-dibromotetrafluoroethane	$CBrF_2CBrF_2$	47

Halon1301 (CBrF3) was first used in gaseous form, within fixed fire suppression systems around 1960s in aircraft applications [20]. It is used successfully in total flood applications such as aircraft, marines, mainframe computers and telecommunications and it is injected as vapour spray. It is an electrically non-conductive, non-corrosive, volatile or gaseous fire extinguish agent which does not leave residue upon evaporation. It is very effective even at low concertation and chemically reacts by breaking/interrupting the chain reaction of fire and stopping the fuel, the ignition or oxygen mixing together [21]. The main reason of the interruption is the bromine and chlorine atoms in Halon molecule which are

aggressive scavengers of hydrogen atoms. Hydrogen atoms are very important to maintain the combustion chain reaction. Therefore, it is very attractive for fire extinguishing in closed spaces because it is very effective in relative low levels of concentration, it is not harmful for humans in reasonable exposure and it does not damage electrical equipment. Halon1301 is suitable for protection against fires involving flammable solids, liquid chemicals, gases and electrical systems. Also, it is the most widely used in total flooding agent applications which cause minimum damage inside the aircraft cargo preserving the integrity of the equipment [21]. Table 8 presents the properties of the total flooding agent Halon1301.

Table 8 - Halon1301 properties [22]

Important Halon 1301 properties	
Chemical formula	CBrF3
Relative molecular mass	148.91
Gas constant (J/kg*K)	55.8346
Boiling point at 1.013*105 (Pa)	215.4
Freezing point (K)	105.2
Critical pressure (Pa)	3.9628*10^6
Critical temperature (K)	340.08
Critical specific volume (m3/kg)	1.3089*10^9
Critical density (kg/m3)	745
Vapour pressure at 293 K (Pa)	14.63*10^5
Vapour pressure at 333 K (Pa)	34.58*10^5
Saturated liquid specific entropy at 293 K (kJ/kg*K)	1
Saturated liquid specific enthalpy at 293 (kJ/kg)	200
Saturated vapour density at 293K (kg/m3)	115.6
Liquid density at 293K (kg/m3)	1575
Specific volume of superheated vapour at 1.013*10^5 Pa and 293 K	0.159
Application	Total flooding agent-Fixed installations, engine and cargo bays

In Figure 7 a typical schematic representation of two nozzles discharge using Halon1301 [23] is presented. The appropriate design for the storage, delivery and discharge of Halon1301 could be able to withstand pressures from the bottle at 600 or 360psia (41.36 or 24.82bar) when pressurized with Nitrogen and at

200psia (13.78bar) without, at a temperature of 130°F (55°C). More details on the fire suppression system operation and design can be found in [24, 25, 26].

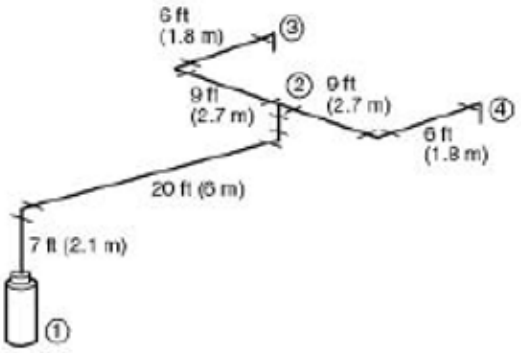

Section	Pipe	L (ft)	EQL (ft)	Elevation (ft)	Rate	Start (psig)	End (psig)
1-2	1 in. Sch. 40	27	58	7	8	243	197
2-3	¾ in. Sch. 40	15	19	0	4	197	181
2-4	¾ in. Sch. 40	15	19	0	4	197	181

Figure 7 - Typical schematic representation of two nozzles discharge using Halon1301 [23]

In order for Halon1301 to be effectively used, the storage and distribution system along with the discharge process itself need to be specifically designed for multiphase flow. Figure 8 illustrates typical design parameters used for the sizing of Halon based storage cylinders and piping networks. The top right plot can be used for the sizing of the piping network depending on the cylinder conditions. The three remaining plots can be used for the storage cylinders sizing depending on the design requirements. Initially, the fire extinguishing agent (in super-pressurized cases it mixes up with Nitrogen) flows through the piping network, absorbs heat, increases its temperature, decreases its pressure and begins to boil inside the pipes. The piping network must be designed targeting minimum pressure losses (pipe friction loss, elevation loss, etc.) balanced flow split between the different nozzles and fairly high flow rates. Also, the design of the evaporation process through the piping network aims to ensure uniform agent or mixture properties and reduced pressure losses before discharge. Finally, the

nozzle design determines the pressure, temperature, density and shape of the final sprayed jet of the agent or mixture, which enters the compartment. A successful design allows the mixture of Halon1301 and Nitrogen to form a very stable mixture with air.

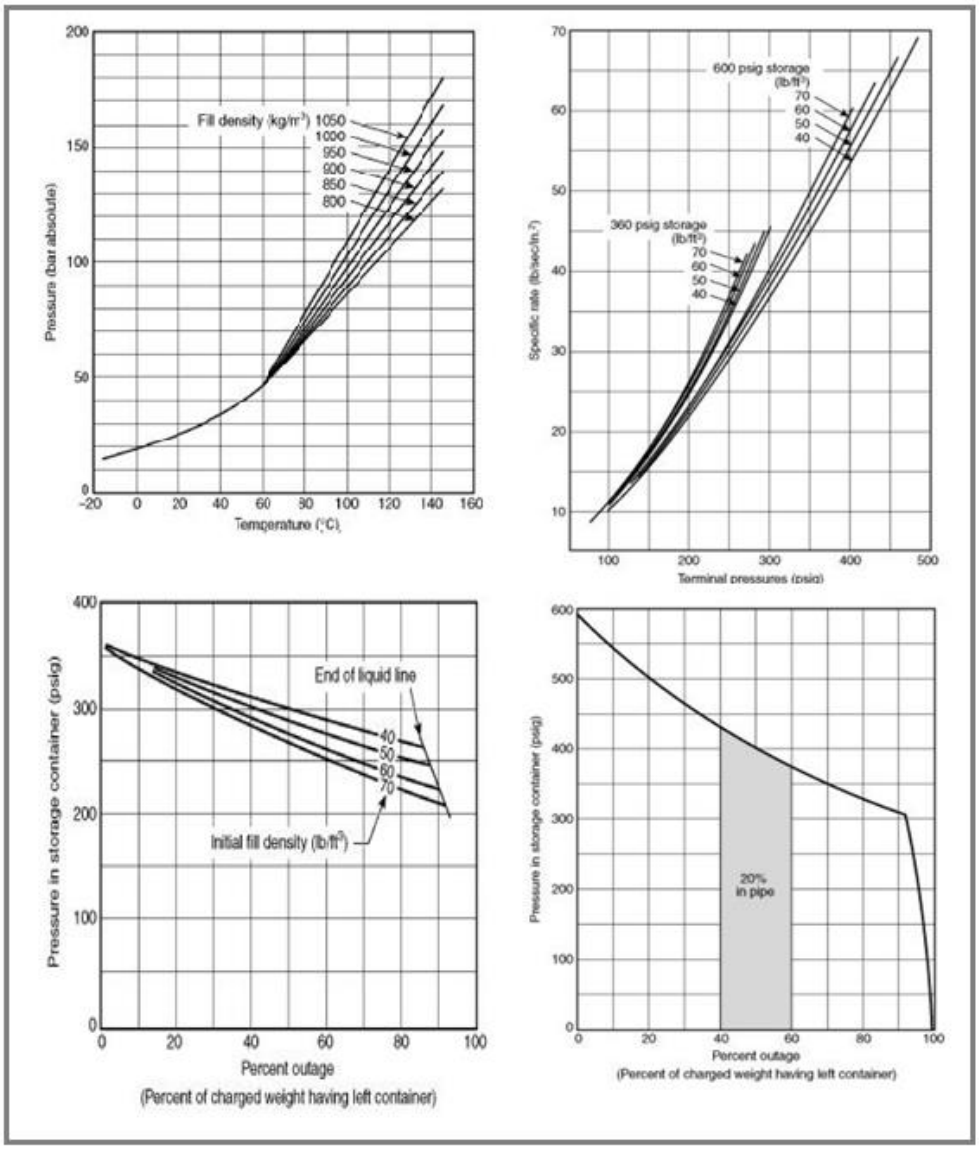

Figure 8 - Design parameters estimated using Halon1301 system [23]

Nevertheless, the details of the Halon1301 mechanism that extinguishes fire are not yet fully understood. It appears, however, to be a physicochemical inhibition of the combustion reaction. Halon1301 has also been referred to as a “chain breaking” agent, meaning that it acts to break the chain reaction of the combustion process. Halon1301 dissociates in the flame as below [23]:

$$CBrF_3 \rightarrow CF_3 \cdot + Br \cdot$$

Two inhibiting mechanisms have been proposed, one that is based on a “free radical (·)” process, and the other based on ionic activation of oxygen during combustion. The “free radical” theory supposes that the bromide radical reacts with the fuel to give hydrogen bromide:

$$R - H + \mathrm{Br} \cdot \rightarrow R \cdot + \mathrm{HBr}$$

which then reacts with active hydroxyl radicals in the reaction zone:

$$HBr + \mathrm{OH} \cdot \rightarrow Br \cdot + H_2 O$$

The bromide radical again reacts with more fuel, and so on, with the result that active H·, and OH· radicals are removed, and less reactive alkyl radicals are proceed.

The “ionic” theory supposes that the uninhibited combustion process includes a step in which Oxygen ions are formed by the capture of electrons that come from ionization of hydrocarbon molecules. Since bromine atoms have a much higher cross section for the capture of slow electrons than Oxygen, the bromine inhibits the reaction by removing the electrons that are needed for activation of the oxygen. The released Br, after the reaction between fire and Halon1301, reacts with the ozone molecules in stratosphere as follows [27].

$$Br \cdot + O_3 \rightarrow BrO \cdot + O_2$$

$$BrO \cdot + O_3 \rightarrow BrO_2 + O_2$$

Halon1301 is a stable compound and not open to break up by UV wavelengths, which is the basic mechanism for subtracting compounds from the upper atmosphere. It has a very long atmospheric lifetime (around 65 years [28]) and high potential to react and consume the ozone layer [29]. A number of advantages and disadvantages are summarized in Table 9.

Table 9 - Halon1301 advantages and disadvantages [29]

Advantages	Disadvantages
Fast chemical suppression	Minimal extinguish effectiveness on reactive metals and rapid oxidisers
Penetrating vapour	Side-effects on Class A fires
No residue	Environmentally harmful (ODP)
Non-corrosive	High cost
Non-conductive	Ineffective against Ti fire
Colourless (No obscuration)	Ineffective against fuels carrying their own oxidizer
Compact storage due to high density	Ineffective against auto-thermal decomposition
Low toxicity in concentrations required for fire to extinguish	

Therefore, due to the high restrictions of the environmental policies, the FAA, aircraft industry, researchers and other authorities are investigating new “clean” agents for Halon1301 replacement.

2.2.3 Approval Criteria & Main Requirements

Generally, the primary fire extinguishment criteria for the agents include: Ozone Depletion Potential (ODP), Global Warming Potential (GWP) and atmospheric lifespan. These characteristics need to be in agreement with the international laws but also with the national, state and local laws [5]. An agent with zero or near zero ODP and the lowest practical GWP and atmospheric lifetime may have problems of international availability and commercial longevity. In addition, the toxicity levels of the agent need to be in acceptable limits preventing health risks. The fire suppression systems in areas with workers or animals must be protected avoiding agent leakages and also the discharge agent concertation must be within the safety limits. Most of Halon compound agents break down after contact with fire and the by-products could be harmful to health. The environmental impact and the toxicity levels of the agents are calculated based on mathematical relationships comparing their impact with a known gas. However, in order to certify and approve a fire extinguishing agent as Halon1301 replacement for

aircraft cargo, the complexity/cost and the fire extinguishing performance of the agent needs to be acceptable by both airframe manufacturers and aviation authorities (FAA, MPS, flight tests, etc.) [29].

FAA conducted a program to establish performance criteria and certification methods with objective to develop Minimum Performance Standards for non-Halon fire suppression systems for aircraft. This program was a collaboration of Joint Aviation Authorities in Europe, Civil Aviation Authority in UK and Transport Canada Aviation [5]. The International Halon Replacement Working Group (IHRWG) was established by FAA and several other agencies (such as aviation regulatory authorities, government agencies involved in research and development, airplane manufacturers, industry associations, suppliers of fire protection equipment and researchers) to provide input for this program. This group has developed MPS tests which describe full-scale fire tests. These tests examine and compare the effectiveness of the fire suppression system comparing the candidate agent with Halon1301 in the case of cargo compartment. Similar MPS were developed for lavatories, hand-held extinguishers and engine/auxiliary power units [30]. The optimum replacement agent would be the agent with the capability to extinguish sufficient the fire in both cargo compartment and engine nacelle. The published MPS [7] for cargo compartments describe the criteria and instrumentation used to demonstrate equivalent performance to Halon1301 for four separate fire scenarios: bulk-loaded cargo, containerized cargo, surface burning fire, and exploding aerosol scenario and the performance requirements for each (see Table 10).

Table 10 - MPS test performance criteria requirements [7]

Fire Scenario	Maximum Temp. °F (°C)	Maximum Pressure psi (kPa)	Maximum Temp-Time Area °F-min. (°C-min.)	Comments
Bulk Load	720 (382)	Not Applicable	9940 (5504)	Use the data that is between 2 and 28 minutes after suppression system activation. See figure 11.
Containerized Load	650 (343)	Not Applicable	14,040 (7,782)	Use the data that is between 2 and 28 minutes after suppression system activation. See figure 11.
Surface Fire	570 (299)	Not Applicable	1230 (665)	Use the data that is between 2 and 5 minutes after suppression system activation.
Aerosol Can Explosion Simulation	Not Applicable	0.0	Not Applicable	There shall be no evidence of an explosion. No enhancement of explosion at below inert concentrations.


Surface Burning Fire


Bulk-Load Fire


Containerized Fire


Exploding Aerosol Can Test

The FAA in collaboration with airframe manufacturers, fire extinguisher companies and agent suppliers are evaluating a number of Halon1301 replacement agents, including commercially available agents approved by the EPA as well as developmental systems and concepts (more info in FAA official website). The current update on limitations and requirements can be found in Advisory Circulation (AC), 25.857-1, Class B and F Cargo Compartments [31]. FAA website also provides all the updated advisory circulations, meeting minutes on Halon replacement research progress of Working Group (IHRWG) until now and other regulations for fire suppression system for aircraft cargo. The link to the latest version of the FAA website is in reference [32]

2.2.4 Potential Halon1301 Replacements

There are several options of placement agents that could be used in aircraft cargo. FAA, in their latest update report 2012 [5] has collected all possible Halon1301 replacement agents for aircraft cargo. These options can be

separated in two categories: Halon compounds and all the other agents. The Halon compounds are usually referred as “replacements” and all the others as “alternatives”.

“Replacements”-(Halon-compounds)

As mentioned previously, all approved agents must have acceptable levels of environmental impact, toxicity, and complexity/cost. Halon compounds are preferable compared to the “alternatives” such as foams or dry chemical due to the fact they have similar characteristics to Halon1301 (clean, volatile and electrical non-conductive). Also, the uses of some of these compounds as fire extinguishers have zero ODP and high extinguish capabilities comparable to Halon1301. Their disadvantage is that they need higher concentration to extinguish fire, which leads to slower extinguishment process, while the produced by-products results to be more toxic and corrosive [33].

Three primary elements exist in Halon compound agents: fluorine, chlorine and bromine. Their behaviour during fire suppression depends on the relative quantities they exist in the compound. Some of the main parameters affected are their chemical and thermal stability, toxicity, boiling point, volatility and fire suppression effectiveness (see Table 11). For example, Fluorine contributes to increased chemical and thermal stability, reduced toxicity and boiling point, while it presents no significant influence on the fire suppression effectiveness. Table 12 presents the families of the Halon compounds [29].

Table 11 – Halon compounds composition and performance characteristics [29]

Property	Fluorine	Chlorine	Bromine
Stability	↑	-	-
Toxicity	↓	↑	↑
Boiling point	↓	↑	↑
Thermal stability	↑	↑	↑
Suppression effectiveness	-	↑	↑

Table 12 - Halon compound families [5]

Halon compound family	Chemical synthesis
HCFCs	Hydrochlorofluorocarbons
FCs (PFCs)	Perfluorocarbons
HFCs	Hydrofluorocarbons
FICs	Fluoroiodocarbons

Most of the available “replacements” are acting physically, mainly by heat absorption such as HCFCs, HFC and FCs and only CF_3I is acting chemically. The CF_3I in general is more effective than the physically acting agents. Halon1301 acts 20% physically and 80% chemically in the extinguishment of n-heptane in air [21]. HCFCs family has non-zero ODP and probably they will eventually be banned. They are denser than Halon1301 and present very good extinguish capabilities. PFCs are fully fluorinated compounds and they have several attractive characteristics such as are non-flammability, low toxicity and practically zero ODP. This family can be used only in specific applications due to the GWP and their long atmospheric lifetime. The HFCs look more promising for three reasons. First, they are usually volatile and have low toxicity. Second, they present similar ODP to HCFCs and third, because they have lower atmospheric lifetime, similar to PFCs. The HFC-125 belongs to this family and FAA examines the use of it in aircraft nacelles. Nevertheless, several studies showed that there might be implications with the HFCs as they present an increase in greenhouse gas emissions and a concern about GWP. The last family is FICs, containing only the CF_3I, which is a commercialised compound. Due to the fact that FICs produce large amount of iodine, their fire extinguishment speed needs to be reduced (lower concentrations) in order to control the by-products generation. Therefore, there are serious concerns about toxicity. Some cargo fire-extinguishing tests were conducted with triodide, CF_3I but were discontinued because of toxicity concerns [5]. All the Halon compounds present high fire extinguishing capabilities and are more suitable for aircraft applications. However, it is fact that Halon-carbons have been banned in several countries and possibly are going to be

banned globally in the future. In Table 13, typical values for the density of commercialized total-flood replacement agents are presented.

Table 13 - Typical density of commercialized total-flood replacement agents [5]

Generic Name	Vapor Pressure at 20°C, Bar	k1 (m^3/kg)	k2 ($m^3/kg/°C$)	Vapor Density, at 20°C and 1 atm (kg/m^3)	Liquid Density at 20°C (kg/m^3)
Halon 1301[1]	14.3	0.14781	0.000567	6.255	1574
HCFC Blend A	8.25	0.2413	0.00088	3.861	1200
HCFC-124[2]	3.30	0.1585	0.0006	5.858	1373
HFC Blend B[2]	12.57	0.2172	0.0009	4.252	1190
HFC-23	41.80	0.3164	0.0012	2.933	807
HFC-125	12.05	0.1825	0.0007	5.074	1218
HFC-227ea[3]	3.89	0.1269	0.0005	7.282	1408
HFC-236fa	2.30	0.1413	0.0006	6.544	1377

Table 14 Total-flood replacement agents design concentrations [5]

Agent	Minimum Design Concentration for *n*-Heptane, vol%	NOAEL, vol%	LOAEL, vol%
Halon 1301	5	5	7.5
HCFC-124	8.5	1.0	2.5
HCFC Blend A	11.9	10.0	>10.0
HFC-23	16	30	>50
HFC-125	10.9	7.5	10.0
HFC-227ea	7	9.0	10.5
HFC-236fa	6.4	10.0	15.0
FC-218	8.8	30	40

Information about the minimum required fire extinguishment concentration for each commercialised Halon-based agent can be seen in Table 14. The environmental impact and the implications of using each one of these agents can be found in the latest report of the Group 2012 [5, 34]. More information from FAA regarding the thermodynamic properties of candidate Halon compounds can be seen in Appendices 7.1.

"Alternatives"-(All Non-Halon compounds)

The use of non-Halocarbon substitutes as alternative fire extinguishment agents to replace Halon1301 has increased lately. The "alternatives" are separated to "Classical" and "New" (see Table 15).

Table 15 - Alternative agents [5]

Classical	New
Foams	Water misting
Water sprinklers	Particulate aerosols
Dry chemical	Inert gases
Carbon dioxide	Gas generators
Loaded stream	Combination

Water sprinklers have already replaced Halon1301 in many applications such as marine [35]. Dry chemical extinguishers and CO_2 are also attractive and their use has also been increased the last years [36]. Water misting and particulate aerosol could be more effective due to better distribution, reducing the amount of agent [37, 38]. This could decrease the probability of secondary damage allowing protection and minimizing the problems concerning the water and solids.

An interesting approach that passed the cargo compartment MPS fire test criteria was a water mist / Nitrogen gas hybrid system concept [39]. Despite the fact that this is most likely to satisfy the proposed FAA regulation, including fuel tank protection technics (OBIGG or OBOGG, etc.), such systems are not yet developed for commercial transport aircraft [40, 41, 42].

Finally, the recent technology improvements allow the use of inert gases in new applications in occupied areas (Table 16). Inert gases such as Nitrogen are suitable for Class A, B and C flames (see Appendix B) and the tests showed that increased (150 to 200bar typical effective range of discharge pressure for cargo systems) discharge pressure reduced extinguishment time [43]. This happens due to the fact that Nitrogen is under higher pressure and this reduces quickly the oxygen concentration for the fire during the combustion process. This fire suppression strategy applies two mechanisms: a) decreasing the oxygen concentration and b) inerting the combustible environment. Generally, inert gasses (N, CO_2, hypoxic air, etc.) are very promising candidates due their high fire extinguishment capability (Table 15). The CO_2 storage system uses even higher storage pressure (around 720 psia or 49.64bar) compared to Halon1301

(NFPA [20]). More details about properties of Nitrogen and CO_2 can be found in Appendix 7.1-C. Finally, foams could also be effective fire extinguishment agents [44] but they are increasing the complexity of the fire suppression system and it is relatively hard to apply on aircraft applications.

Table 16 - Inert gasses and hypoxic systems [45]

Agent Trade Name	CO_2	Argotec	Argonite	ProInert	N-100	Inergen	Hypoxic Systems(6)
Manufacturer	N/A	Minimax	Ginge-Kerr	Ginge-Kerr	Koatsu	Ansul	Various
NFPA #	CO_2	IG-01	IG-55	IG-55	IG-100	IG-541	N/A
Type of Agent	Inert (8)	Inert	Inert	Inert	Inert	Inert	N/A
Chemical Make Up	CO_2	100% Argon	50% Nitrogen 50% Argon	50% Nitrogen 50% Argon	100% Nitrogen	52% Nitrogen 40% Argon 8% CO2	N/A
Conc. %	34% to 75%		37.9% Minimum	Class A & C = 34.2% Class B = 45.5%	40.30%	34.9% Minimum	N/A
Global Warning Potential (GWP)	1	0	0	0	0	0	0
Ozone Depletion Potential (ODP)	0	0	0	0	0	0	0
Atmospheric Lifetime (ATL)	-10	0	0	0	0	0	0
No Observable Adverse Effect Level (NOAEL)	-9	43% (7)	43% (7)	43% (7)	43% (7)	52%	N/A
Lowest Observable Adverse Effect Level (LOAEL)	-9	52% (7)	52% (7)	52% (7)	52% (7)	62%	N/A
Discharge Time per NFPA	30 Seconds to 20 Minutes or more	60 Seconds	60 Seconds	60 Seconds	60 Seconds	60 Seconds	N/A

2.3 State-of-the-Art Fire Suppression Systems Research

Numerous studies using Halon1301 and promising replacement agents have been attempted in order to explain the fire suppression system operation in cargo during flight. One of the main challenges of these studies is to simulate the fire extinguishment process in a large volume for different types of fires and in “adverse” conditions (see Appendices 7.1). Based on the author’s best knowledge, the most relevant studies can be separated in two categories:

1. Simulations on fire suppression systems for aircraft cargo.

    a. Development of mathematical models simulating the fire suppression system operation. A number of assumptions are required in each

application. Such models provide design guidelines for the fire suppression system development.

b. Development of numerical models using CFD tools (ANSYS, etc.). These studies provide information about the flow phenomena and fire extinguishment process during system operation inside the cargo compartment in more detail. Additionally, they can also enhance the overall system design as well as allow for educated experimental setup which leads to significant savings in time and cost. The running time of the simulations is of key importance and must be kept at minimum.

2. Experimental testing of fire suppression systems for aircraft cargo.

   a. The studies involving experimental tests include both small scale and large scale tests. Generally, in experimental tests the setup can be very expensive and restricted to follow regulations in order to be approved for aircraft applications. Thus, initially, small scale experimental tests, laboratory tests (cup burner tests) are performed to provide information about the chemical behaviour of the agent during the fire extinguishing process and suggest modifications (additives). Large scale experiments are performed for the complete agent testing and approval and they include MPS tests, flight tests and some additional fire extinguishment or explosion avoidance tests. Finally, it can be mentioned that the link between small and large scale experiments presents several challenges.

2.3.1 Simulations

Peteado 2004 [46] presents a numerical simulation using the lumped parameter method and simulates the Halon1301 extinguishing system inside cargo. The numerical results were taken for both rapid and slow (lower volume) discharge bottle cases and presented satisfactory agreement with experimental data. Kurokawa [47] also applied the same lumped parameter approach and the differential equation system solved using a fourth-order Runge-Kutta scheme. These mathematical models simulate the Halon1301 concentration during time inside the cargo using mass continuity equations and assuming perfect gasses.

A schematic representation of Kurokawa's model and results are shown in the figures below.

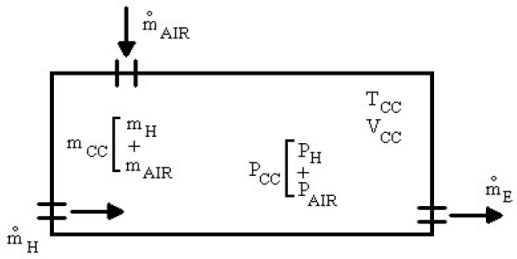

Figure 9 - Schematic of the model [47]

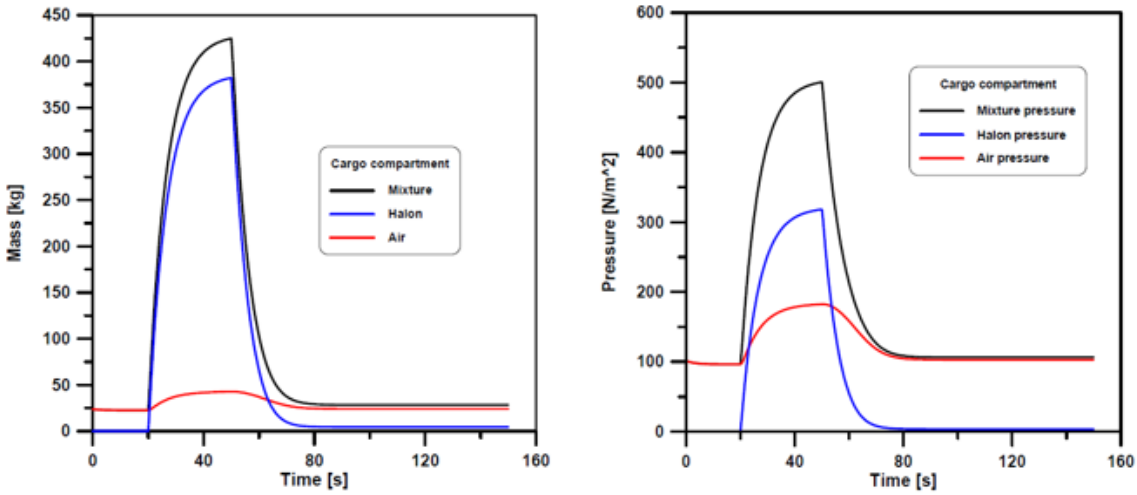

Figure 10 - Results for mass and pressure during time [47]

The adopted methodology allowed the estimation of the transient behaviour inside the cargo, providing information for parameters such as: agent volumetric concentration, agent and air masses and the compartment differential pressure. Despite the fact that this formulation did not include spatial distribution or non-uniformities of agent concentration, it provides rapidly useful information regarding the design and performance of the aircraft cargo compartment fire extinguishing system.

Golberg [48] also applied a mathematical model in order to predict the aircraft cargo compartment pressurization and extinguish hold time. This is a one-zone numerical model which solves the conservation of mass and energy during the discharge of FK-5-1-12 (with Nitrogen). The model is applied either for the case of an A330-200 forward cargo compartment in flight or the DLR test chamber in

the ground level. The results showed that during flight, the cargo compartment equipped with a twin fluid suppression system will not activate the emergency pressure relief venting at any point during discharge, irrespective of the cargo load volume (see Figure 11). FAA also tested this promising EPA-approved agent, FK-5-1-12, and experienced two major failure modes: i) increased overpressure during the aerosol can explosion test and ii) sudden flare-up during the suppression of bulk-loaded cargo fire.

The international fire protection research foundation (NFPRF), in 1988, presented an extended report in Halon1301 discharge testing. The technical analysis focuses on three predominant areas of uncertainly: i) methods of flow calculations, ii) mixing of nozzle flows and initial distribution of agent and iii) post discharge leakage from enclosures. An extremely detailed description of the fire suppression system operation and flow/discharge calculations using Halon1301 is presented in reference [49]. Additional information about modelling flow properties and discharge of Halon1301 replacement agents can be found in previous older reference [22, 50].

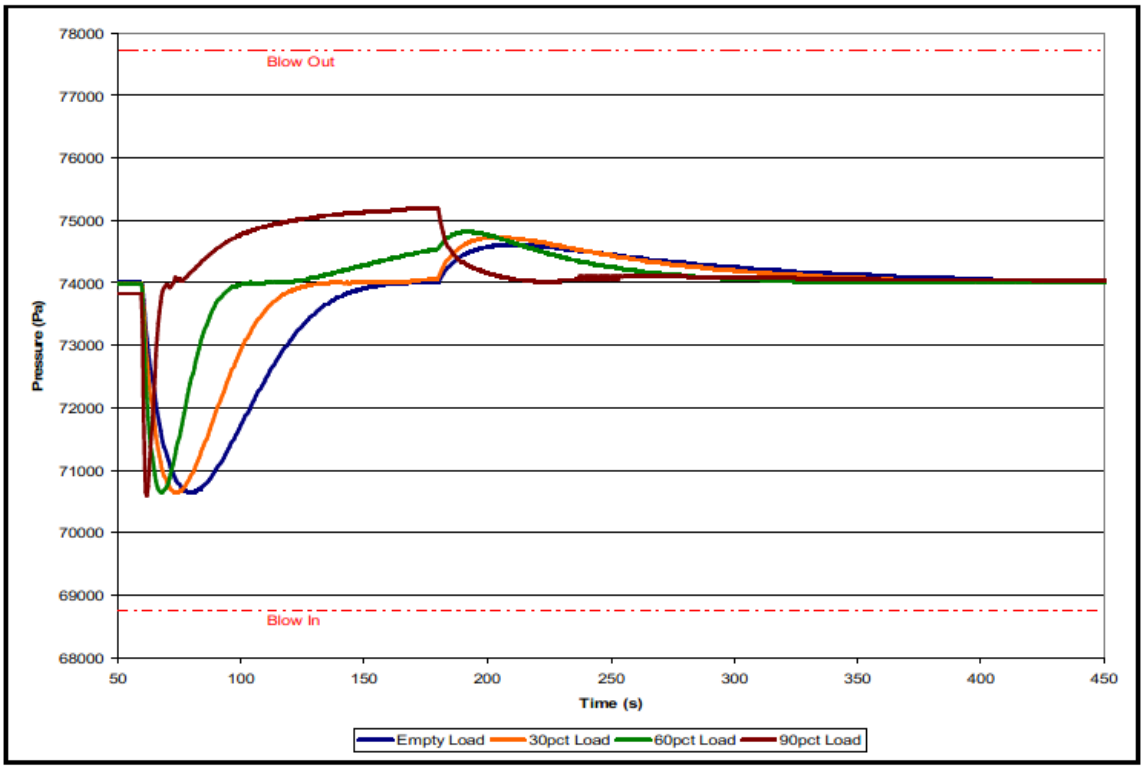

Figure 11 - Pressure during time inside cargo compartment [48]

Papa [51], presented a CFD model regarding fire and smoke generation inside an aircraft cargo compartment. This flexible model can provide information on smoke transport under various conditions and is able to simulate various fire scenarios in a short period of time. The sensors positioning effects were also evaluated.

Another CFD study [52], attempts to analyse the time–space evolution of Halon1301 volumetric concentration for certification purposes. It also allows the examination of the influence for different parameters such as infiltration rate and mixture leakages. The results of the selected cases showed good agreement with the certification requirements, indicating that as lower mass flow rate as lower the agent leakages after discharge, resulting higher oxygen concentrations inside cargo (see Figure 12). This model can be used in the preliminary analysis during the aircraft conceptual design or to modify a pre-existing fire suppression system.

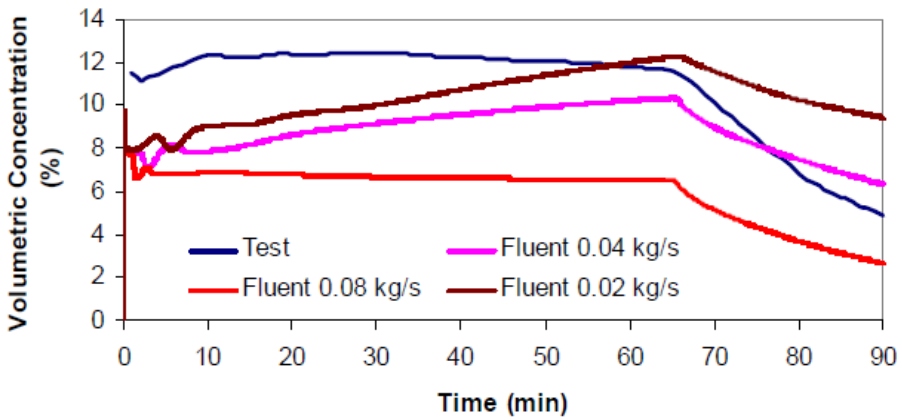

Figure 12 - Comparison between test and CFD results for the plane 67% of height inside cargo compartment [52]

The study in reference [53] can be very useful to develop a simple and accurate CFD model for further insight on fire safety design (flame propagation and temperature profile). It presents a comparison of CFD simulation results of fire field models with experiments. The volumetric heat source method as well as the sub-models of combustion and radiation was compared with the available experimental data under different fire scenarios. Additionally, it provides methods on the determination of fuel area and volume for a given heat release rate. According to the study, two different methods can be used to characterize fire

source in the fire field model: a) volumetric heat source and b) combustion model. Both methods can provide good results that agree quite well with the experimental data. Figure 13 below illustrates the comparison between the experimental and the predicted temperature profiles when burning propane fuel, using both the combustion model (eddy dissipation break-up) and the volumetric heat source method for small, medium and large size heat sources. It can be noticed that the combustion model and the small size heat source shows good agreement with the experiments, proving that the combustion models are more sufficient to describe the temperatures profiles.

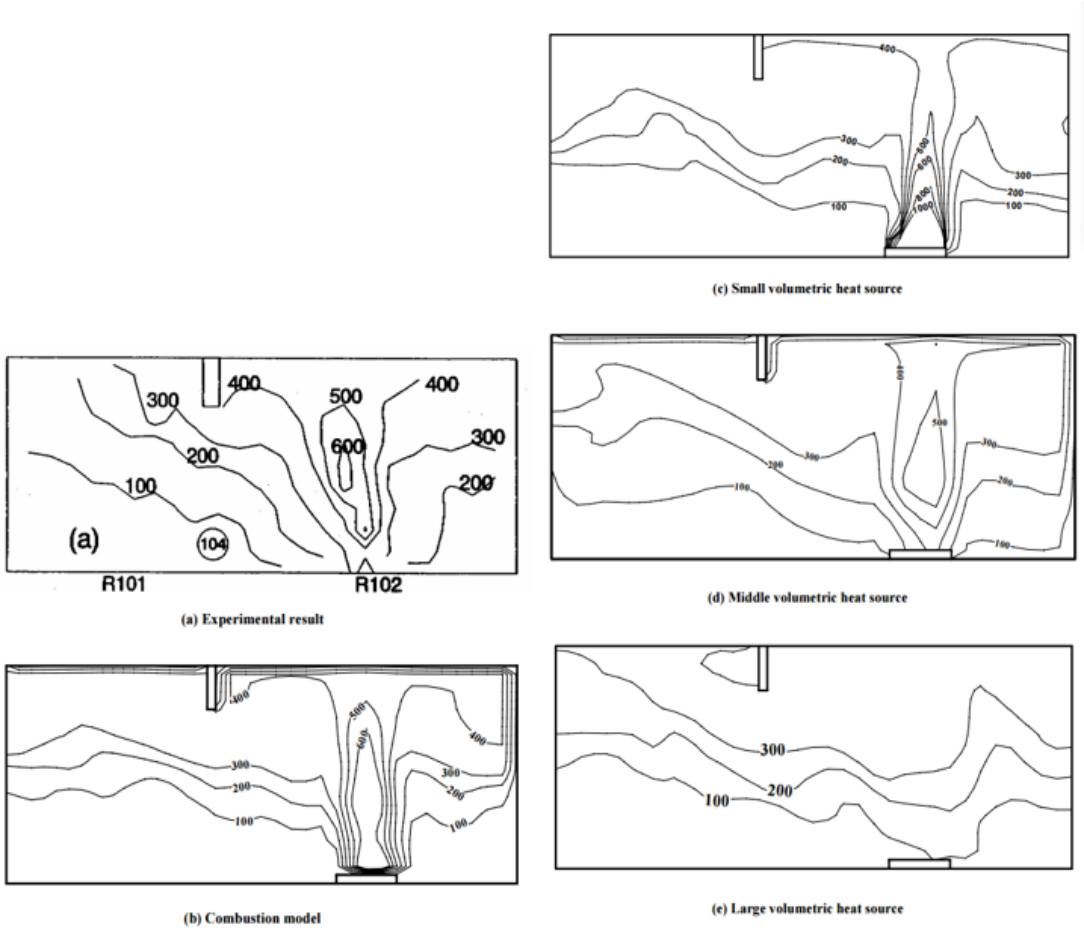

Figure 13 - Comparison between experimental, combustion model and heat source [53]

Summarizing, a CFD model with combustion sub-model could provide:

1. Good prediction of temperature distribution in the flame
2. Useful information for the forensic fire accident investigations

However, due to the fact that combustion models are quite challenging and computationally expensive, they have not yet been fully adopted in industry.

On the other hand, a CFD model with volumetric heat source could also provide satisfactory results in room fire scenarios. It could be applied for studies regarding:

1. Smoke and toxic-gas movement in buildings
2. Smoke filling processing of rooms
3. Effectiveness of smoke detection system
4. Effectiveness of smoke extraction system
5. Effectiveness of smoke protection barriers or curtains
6. All other studies that are mainly concerned on smoke in large spaces.

The CFD methods vary depending on the agent properties/phases (gas, liquid or mixture) during the fire suppression system operation. In Lee's [54] work regarding the simulation methods for fire suppression process inside the engine core and APU compartments, the vapour and liquid phases of the mixture (agent-air) are simulated using CFD tools. This is achieved by coupling the Eulerian transport equations of the gas mixture with the Lagrangian equations of the discrete-droplet phase in order to account the interaction between evaporating and moving suppressant droplets and the gaseous suppressant/air mixture (see Figure 14).

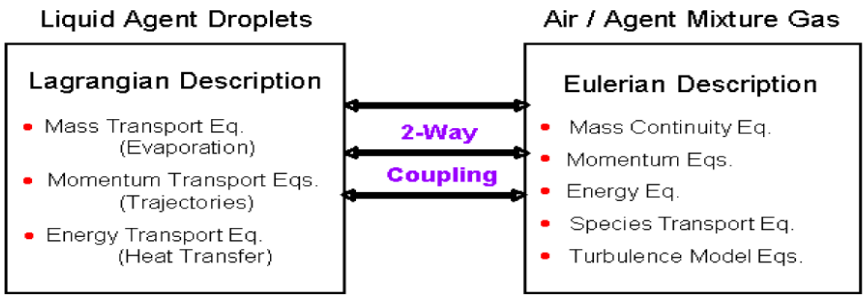

Figure 14 - Coupling Lagrangian and Eulerian description [54]

One of the significant challenges in CFD simulations is to simulate the fire, considering the flame interaction with the agent in a real fire scenario. In order to simulate fire or the fire extinguishment process accurately, the burning material, the agent properties and the interaction between the flames and agent mixture are some of the additional problem variables. This increases the complexity of the problem and even more for liquid agents due to the fact that they attack fire in more ways than gases. One of the most promising liquid agents for the future is water mist. Zhigang Liu [55], showed in his work five different fire extinguishing mechanisms for water mist. Depending on the behaviour of the droplets, these are:

1. Droplets are blown away before reaching the fire
2. Droplets that penetrate the fire plume, or otherwise reach the burning surface under the fire plume, to inhibit pyrolysis by cooling, and the resultant steam dilutes the available oxigen
3. Droplets that impact on the walls, floor and celling of the compartment and cool them, if they are hot, or otherwise run-off to waste
4. Droplets that vaporise to steam while travelling the compartment and contribute to the cooling of the fire plume, hot gases, compartment and other surfaces
5. Droplets that pre-wet adjacent combustibles to prevent fire spread

A method to develop a fire suppression system CFD simulation model that uses water mist as fire extinguishing agent is described in reference [56]. This work illustrates possible methods and equations that can be used in order to simulate the fire extinguish process. These are typically the Lagrangian and Eulerian methods for gas and liquid phase flows of the agent (mixture). They also include non-premixed flames and Large Eddy Simulations (briefly) for combustion models.

Similar studies focusing on the CFD modelling of fire suppression and it rule in optimizing suppressant distribution and analytical methods for modelling

characteristics of Halon1301 could be found in reference ([54] and [58], respectively).

Finally, reference [59] includes CFD simulation of pool fires which describes the fuel behaviour during explosions in various rates. These results can potentially support the test rig design for the aerosol can explosion tests (MPS). In this work the three well-known flame zones of pool fires are captured by recording the axial flame temperature profiles. Additionally, the safety distances were captured satisfactory by recording the time averaged maximum flame temperatures resulted from the CFD simulations.

2.3.2 Experimental Testing

A comprehensive overview of the challenges for installing and certifying a safe, reliable and economic cargo fire suppression system onto a large commercial airplane is presented in reference [4]. Suggested operating limits for the environmental conditions can be found in Appendices 7.1-B. A typical analysis of the agent concentration inside the cargo using Halon1301 fire suppression system is illustrated in Figure 15.

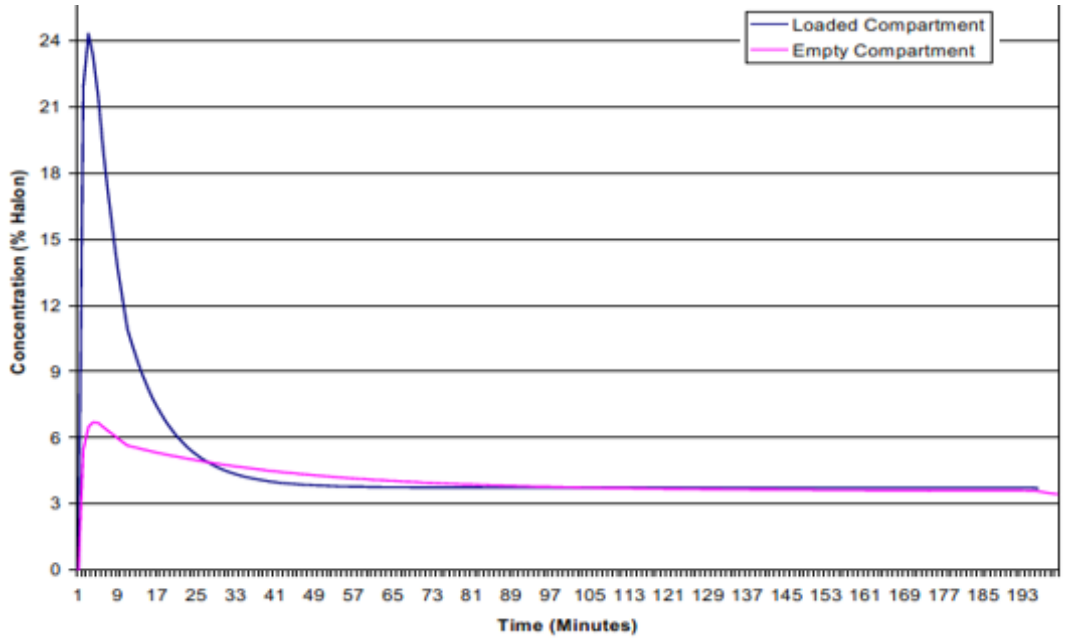

Figure 15 - Typical analysis of cargo suppression system using Halon1301 [4]

Additionally, a useful table containing the agents tested in MPS tests so far and the several technical challenges recorded is presented in Table 17.

Interesting results were shown in experimental studies performed using Halon-compound agents. One of the most promising agents is the HFC-125 (Pentafluoro-ethane, CHF_2CF_3). Figure 16 and Figure 17 present the temperature profiles during bulk-load fire suppression for Halon1301 and HFC-125 respectively [60]. They also present the results of cup burner test measurements for agent desired concentration during the fire suppression event. Such data provide in detail the designed fire suppression strategy.

Table 17 - Agents technical issues [4]

Agent	Type	MPS Status	Technical Issues
Halon 1301	Gas	Baseline	High Ozone Depletion Potential (ODP). Production Ceased.
Agent A	Solid Aerosol	Not tested	Failed corrosion testing. High temperature discharge onto cargo. Light residue requiring clean-up. Less weight than Halon.
Agent B	Solid Aerosol	Not tested	Failed corrosion testing. Less weight than Halon. Light residue requiring clean-up.
Agent/System C	Water mist/ nitrogen	Passed MPS	Complex temperature feedback system.
Agent/System D	Water mist/ nitrogen	Not tested	MPS used long version of aerosol can test – Boeing designs to the short version of test. Development of new delivery system. Approximately 3 times weight of Halon system with temp feedback system, approximately 4+ times weight of Halon system with programmed discharge. Low temperature discharge issues.
Agent E	Gas	Not tested	Tests demonstrate significant weight penalty (2x wt had no effect on fire). 4 times weight of Halon system.
Agent F	Gas (liquid at room temp – but vaporizes quickly)	Failed Preliminary MPS Tests	Failed Aerosol Can Explosion Test. Approx. 1.75 times the weight of a Halon 1301 system.
Agent G	Foam	Not Tested	Clean-up required. Low Temp Discharge not demonstrated. More than 10 times the weight of Halon.
HFC-125	Gas	MPS Tests Suspended	Lots of HF gas generated during fire suppression. At lower concentrations, acted as fuel for fire. High GWP. Approximately 4 times weight of Halon 1301.
CF3I	Gas	Not Tested	Minor corrosion concerns as gas. ODP at altitude. Cold temperature not as effective. Toxic after combustion at 2 ppm.

Comparing the methods for the establishment of the desired agent concentration, the cup burner tests approach provides better control of the discharge conditions resulting in satisfactory concentration measurements, while the agent consumption is minimum. Regarding the MPS test aerosol can explosion, screening fuel explosion small vessel tests could be used in order to measure more accurate (such cup burner tests) agent concentration to prevent the fuel explosion. The HFC-125 has been tested for aircraft nacelle by FAA using a

benchmark method and the results showed that the HFC-125 could be as effective as Halon1301 [57]. HFC-125 has similar boiling point with Halon1301 (224.7K or -48.48^{O}C when 215,4K or -58.15^{o}C for Halon1301) and approximately 10.5% higher extinguish concentration. Recent studies on HFC-125 development show that the volumetric distribution profile matches with Halon1301 for various fire extinguish scenarios (see Figure 18) [28, 61]. Many aircraft engines have been tested with HFC-125 and the results showed that it has been tested successfully as simulant flooding agent and could become a comparative baseline for MPSe (Minimum Performance Standards for engine nacelle evaluations) [62].

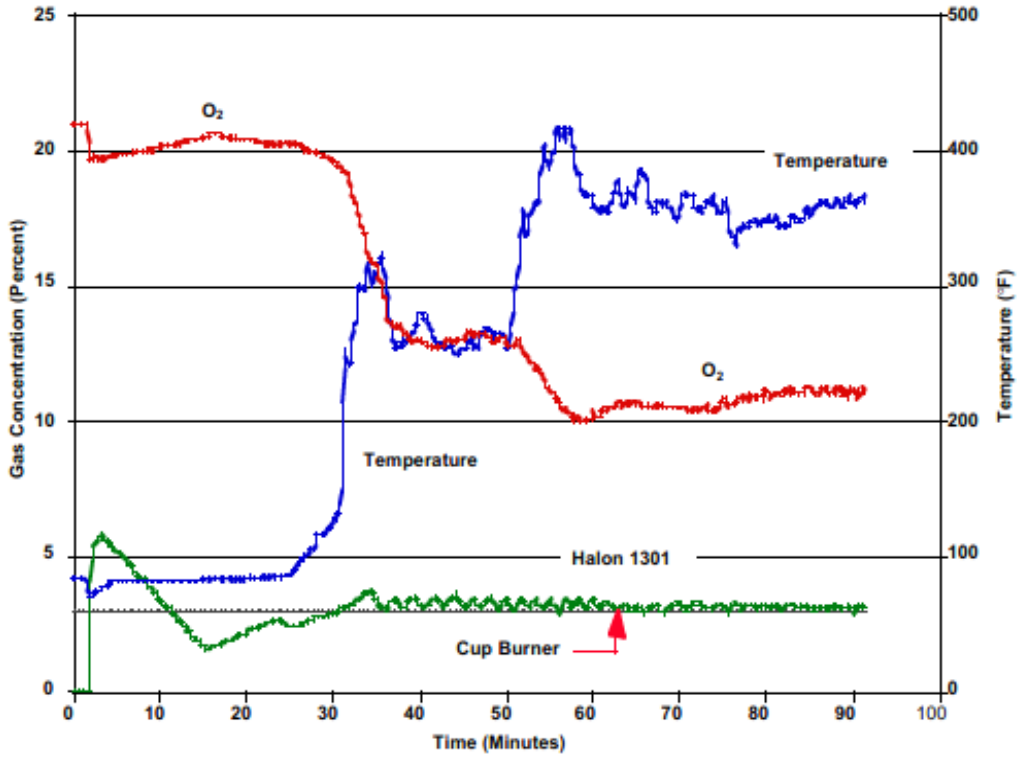

Figure 16 - Gas and temperature profiles during bulk-load fire suppression test with Halon1301

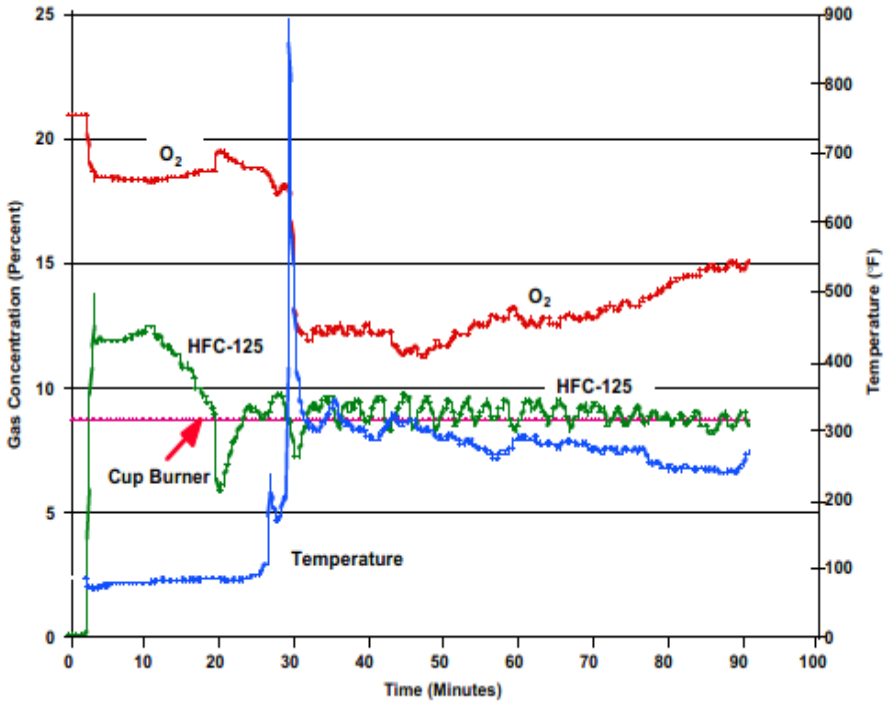

Figure 17 - Gas and temperature profiles during bulk-load fire suppression test with Halon1301 and HFC-125 [60]

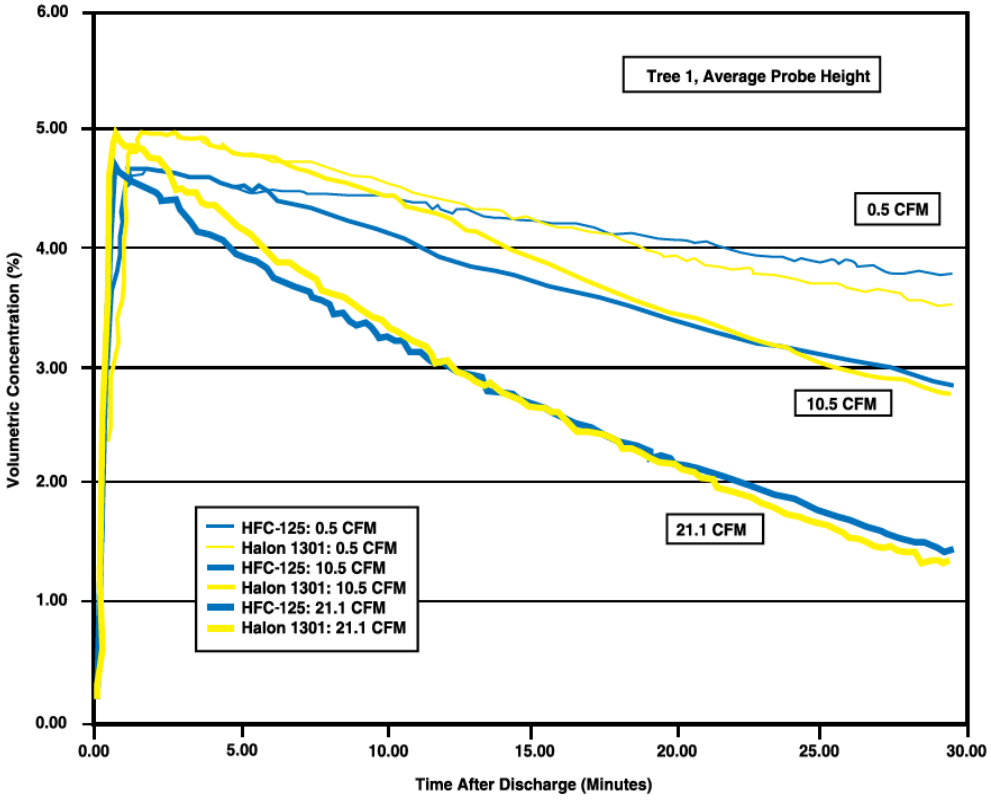

Figure 18 - Halon1301 comparing with HFC-125 [28]

Robins [45] presents some recent technical progress of Halon alternatives in large scale fire tests. The tests focused on the extinguishment of n-heptane pool fires by using: a) FM-100 (bromodifluoromethane), b) FM-200 (1,1,1,2,3,3,3-heptafluoro-propane) and c) HFC-23 (trifluoromethane). Tables of saturation and superheated vapour properties have been generated for both FM-100 and FM-200 as well as pressure-enthalpy diagrams. A complete set of thermodynamic properties is made available for use in the design of fire suppression systems employing these new agents (Table 18)

The main challenges faced by FAA were during the aerosol can explosion tests. There is a potential that the replacement agents may enhance the explosion severity instead of mitigating the event at values below inerting concentration. At UTC Aerospace Systems test program two agents were selected, HFC-125 and Novec1230, in order to assess the behaviour below inert concentrations in a fire event (burning propane). The results showed that both agents enhanced the explosion and the addition of N_2 with the agent mitigated the event [63].

Table 18 - Thermodynamics and other properties of the agents [45]

	FM-100	FM-200	**HALON** 1301	HALON 1211
Chemical Formula	CF_2HBr	CF_3CHFCF_3	CF_3Br	CF_2BrCl
Molecular weight	130.92	170.03	148.91	165.37
Boiling point	4.14 °F	2.55 °F	-71.95 °F	24.80 °F
	-15.48 °C	-16.36 °C	-57.75 °C	-4.00 °C
Melting point	-229 °F	-204 °F	-270 °F	-256.00 °F
	-145 °C	-131 °C	-168 °C	-160.00 °C
critical Temperature	281.89 °F	215.02 °F	152.60 °F	308.84 °F
	138.83 °C	101.68 °C	67.00 °C	153.80 °C
critical Pressure	744 psia	422 psia	575 psia	595 psia
	5.132 MPa	2.912 MPa	3.964 MPa	4.102 MPa
critical Density	49.0 lb/ft^3	38.7 lb/ft^3	***46.5*** lb/ft^3	44.4 lb/ft^3
	0.784 kg/L	0.62 1 kg/L	0.745 kg/L	0.7 13 kg/L
Extinguishing Concentration, cupburner, % v/v (n-heptane)	3.9	6.0	3.5	3.7
Inerting Conc %v/v (Stoichiomemc)				
Methane	6	8	4	-
Propane (Reference 3)	8	12	8	
LC_{50} (4 hour)	108,000	>800,000	800,000	131,000

In order to explore the experimentally observed combustion enhancement during fire extinguish process, the combustion properties of pure mixtures of fire suppressants and air/oxygen need to be analysed. In reference [64] “Combustion properties of halogenated fire suppressants”, adiabatic combustion temperatures, ignition delays and burning velocities were calculated for several typical fluorinated fire suppressant mixtures with air, and oxygen. The results showed that the fluorinated agents possess sufficient energy to participate in the combustion processes and support combustion with measurable burning velocities at slightly elevated initial temperatures. The adiabatic combustion temperatures of stoichiometric mixtures of fluorinated suppressants with air (1 bar, 300K or 26.85^{o}C) are illustrated in Table 19.

Table 19 - Adiabatic combustion temperatures of fluorinated suppressants [64]

Fire suppressant	Stoichiometric concentration in air, % by volume	T (K)
C_2F_6	29.58	1381
C_3F_8	17.36	1552
C_4F_{10}	12.28	1743
CF_3H	29.57	1669
C_2F_5H	17.36	1809
C_3F_7H	12.28	1800
$C_3F_7COC_2F_5$	7.749	1823
CF_3Br	45.65	1248
CF_3Br, 1 bar, 400 K	45.65	1323
CF_3Br/O_2, 3 bar,400 K	80 (oxygen atmosphere)	1497
CF_3I	45.65	1340
CF_3I, 1 bar, 400 K	45.65	1432
CF_3I/O_2, 3 bar, 400 K	80 (oxygen atmosphere)	1593

Generally, it has been observed that Halon compounds can be as effective as Halon1301. However, both their density and required concentration are higher. Halon compounds tested with the cup burner method presented higher concentration levels to extinguish fire compared to Halon1301. This produces a negative impact on the system size, weight and complexity as well as the agent quantity disposed.

Effects of mixed agents with Halon1301 and inert gases (argon, Nitrogen and carbon dioxide) on flame extinction have been investigated in [65]. The fire extinguishment efficiency was determined by using n-heptane in a cup burner

test and measuring the agent concentration in different conditions. Generally, during cup burner tests, the agent concentration is set to increase step by step until the fire is extinguished. In this case, the n-heptane is ignited and burned inside the cup for 120sec and the agent is injected with the initial concentration which continues to increase using a 2% step until suppression is achieved. The chemical effect of Halon1301 was enhanced by the decreased flame temperature with the addition of inert gasses. Table 20 illustrates the measured flame extinguishing concentrations (%).

Table 20 - Measured flame extinguish concentration (%) [65]

Agent	Flame-extinguishing concentration (%)
Halon 1301	3.4
Argon	43.3
Nitrogen	33.6
Carbon dioxide	22.0

An extensive study focused on the investigation of scale effects on Halon1301 and Halon alternatives is presented in reference [66]. It examines the flame extinguishing process regarding the agent inerting properties, the concentration required and the thermal decomposition of the products. This is done using gas tubular burner test, in order to tackle the challenge of scaling up the tests to the real fire scenario. Similarly, a detailed recent study, normally used before the aerosol can explosion test, on how to determine the burning rate of various flammable liquids at large scales from small-scale experiments is presented in [66]

FAA working group, in the prevention of aerosol can explosion report [68], describes experimental tests performed (MPS tests) in order to determine the concentrations of Halon1301 and Nitrogen (oxygen depletion) required to prevent a propane and alcohol explosion. This applies varying the concentration of each gas from zero to its inerting value. These tests aim to support the Halon1301 replacement efforts by clearly defining the baseline requirements for the fire suppression systems.

In 2011, the International Halon Replacement Working Group (IHRWG) presented details about the understanding on the combustion promotion by halogen suppressants [69]. They tested several halogen agents in aerosol can explosion tests in the effort to understand deeper the behaviour of the combustion process using propane/ethanol/water. The main result was that most of the agents enhanced the combustion. The figure below illustrates the complicated physics during the combustion process.

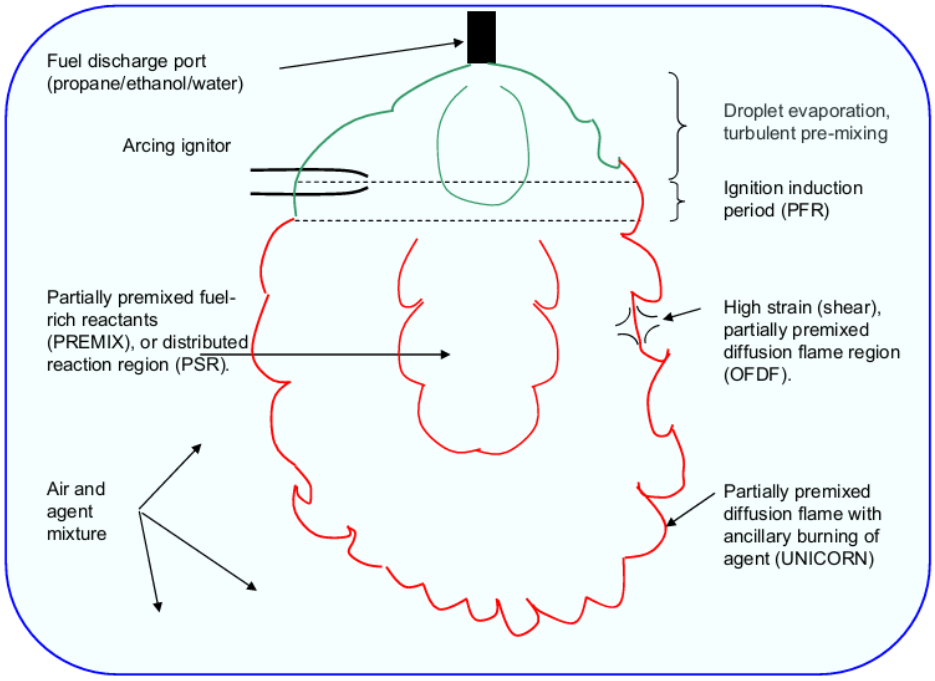

Figure 19 - Combustion physics [69]

In addition, a table which presents several similar studies indicates that most of the agents enhanced the combustion (Table 21). More details about hydrogen fluoride formation in suppressed fires can be found in the work of Linteris, member of the IHRWG in references [70, 71].

Table 21 - Studies showed combustion enhancement [69]

Researchers	Fuel	Agents	Experiment	Phenomena	Explanation		
Grosshandler and Gmurczyk	Propane, ethylene	CF3I, CF3Br, HFCs	Detonation - Deflagratoin Tube	Higher Ma, flame speed, pressure ratio	None		
Shebeko et al.	methane, hydrogen	C2HF5, C4F10	Deflagration	Higer pressure rise and dP/dt	Added heat release from agent		
Moriwaki et al.	methane, ethane	CH3Cl, CH3I, CH3, Br	Shock tube	Shorter ignition delay	None		
Ikeda and Mackie	ethane	C3HF7	Shock tube	Shorter ignition delay	None		
Mawhinney et al.	heptane	water mist	Heptane pool fi	Higher heat release	Enhanced fluid-dynamic mixing		
Hamins et al	hydrocarbons	HFCs, water mist, N2, powders	Full-scale tests	Higher pressure, visual flames	Enhanced fluid-dynamic mixing		
Holmstedt et al.	propane	C3HF7, C2H2F4, CF3Br,	Diffusion flame	Higher heat release	None		
Katta et al.	methane	CF3H	Cup burner	Higher heat release	Agent reaction		
Ural	none	C3HF7, C2H2F4, CHClF2	Flammability tube/chamber	Visual observation	Heat loss/ gain		

As mentioned in MPS for cargo, the 4th test is the aerosol can explosion test. This is the most demanding test because the agent must be capable to extinguish the fire in low concentration and prevent the explosion inside the cargo when the fire suppression system is already activated. The overpressure inside the compartment must be minimised. Figure 20 below illustrates the overpressure caused using Halon1301 and several promising Halon compounds, tested by IHRWG, using the FAA aerosol can explosion simulator [72]. The results showed that none of the replacement agents acts on the fire as Halon1301, in terms of sustaining the overpressure to low values. The replacement agents, in some degree, initially enhance the combustion process as well as produce higher levels of overpressure inside the cargo compartment.

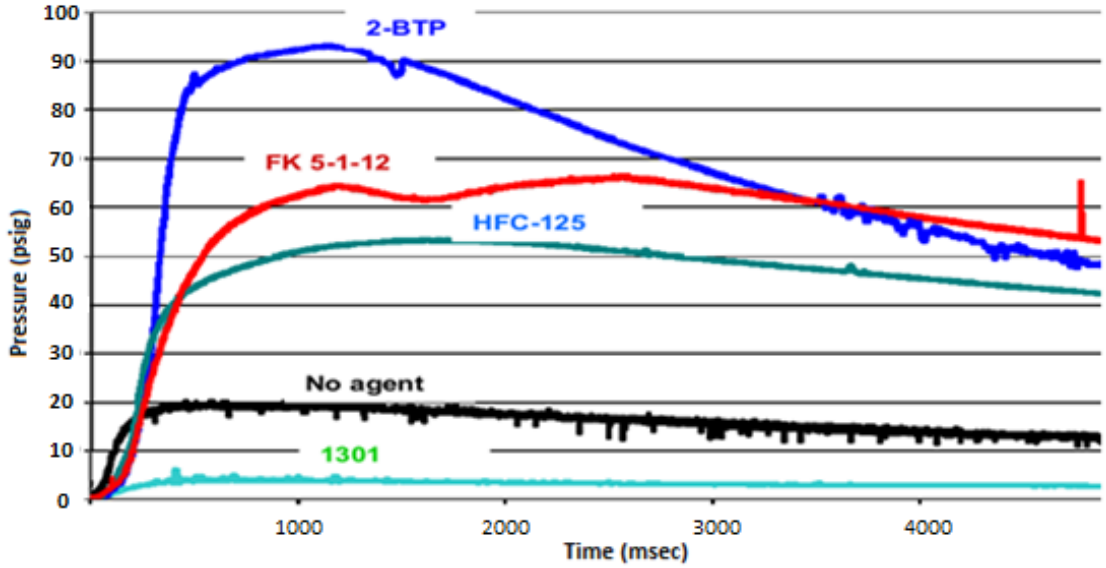

Figure 20 - Halon1301 and halon compounds additional pressure during operation [72]

The fire safety branch at FAA selected and tested two candidate agents capable of withstanding the aerosol can explosion test (MPS) [73]. The agents were selected by the members of the International Aircraft Systems Fire Protection Working Group, based on their work on potential Halon1301 replacement agents. Bromotrifluoropropene (BTP) and HFC-125 were subjected to a series of tests in order to determine if they are capable to succeed the aerosol can explosion test (propane can). The results showed specific values of overpressure and used to establish a comparison benchmark. The benchmark test was conducted with 2.5% Halon1301 concentration and showed significantly lower overpressure, proving that Halon1301 is extremely capable to handle explosion scenarios. In Figure 21, the results of BTP and HFC-125 are presented. Both agents enhance the explosion and create higher overpressure. HFC-125 was able to prevent the explosion with 13.5% concentration. In cargo compartment systems the agent requires to cause overpressure below the limiting value.

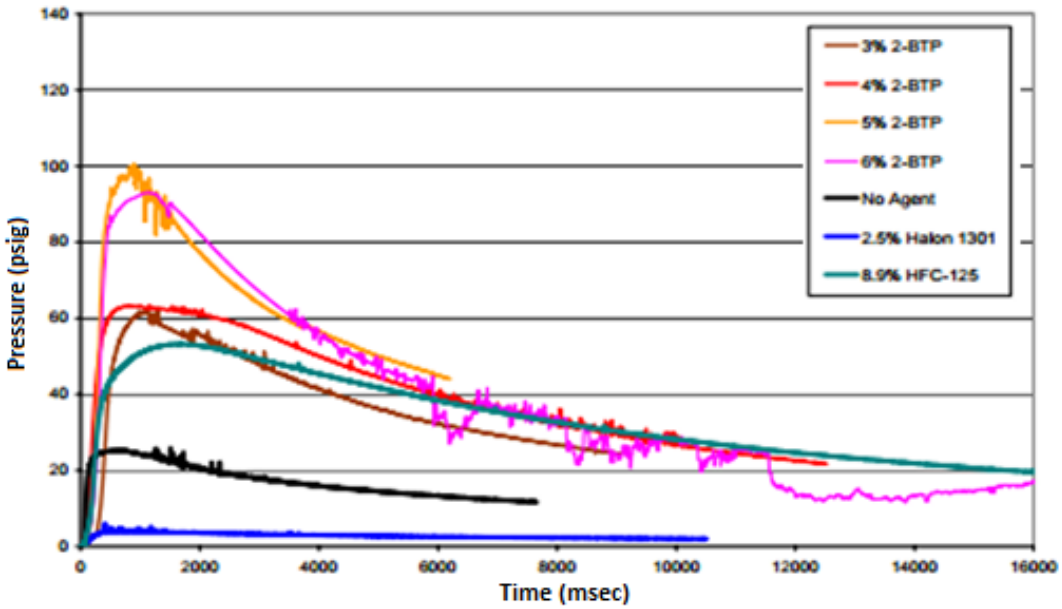

Figure 21 - Tests results for BTP and HFC 125 [73]

Due to the fact that Halon compounds in general could cause environmental or toxicity issues, many countries have stopped the use and production of Halon compounds for reasons similar to Halon1301 [74]. Therefore, the interest is turning more towards Halon alternatives. Several studies performed with the use of water mist for fire protection showed that it is a very effective agent with good distribution. As mentioned previously, FAA Group conducted tests with the use of water mist and the water was not able to pass the aerosol can explosion test [30]. Therefore, due to the high effectiveness of the mist they suggested that the use of water mist with Nitrogen could solve the problem but the system also needs a Nitrogen generator [31].

Airbus “Nero” project was intended to provide extensive development and testing to prove the concept of water mist / Nitrogen fire suppression in aircraft cargo holds and to determine actual installation parameters to replace Halon1301 systems aboard Airbus manufactured planes [75]. The results of the project showed that Nitrogen systems presented several complexities regarding storage, size and high operation pressures.

A very interesting collaboration program called FIREDASS was created inside the EU by the partners shown below [76].

Table 22 - FIREDASS partners [76]

Marconi Avionics (MA) (Project Coordinator)	UK
CAA, Safety Regulation Group	UK
Siemens Cerberus (SC)	France
DLR	Germany
National Technical University of Athens (NTUA)	Greece
SINTEF-NBL	Norway
University of Greenwich (UoG)	U.K.

This program was developed after the generation and validation of methods based on fire detection and suppression systems. These methods were integrated with the CFD tool in order to model a fire suppression system that uses water mist and interacts with fire [77]. In addition, these CFD models are validated based on experimental tests simulating MPS for airplane cargo using water mist (Figure 22). The target was to create a computational platform in order to reduce the number of experimental tests for possible Halon1301 replacements. Additionally, it can provide information about agents to the FAA Group in order to enrich the MPS data bank and influence the rules applied on fire detection systems.

Figure 22 - Experimental test rig of FIREDASS for MPS tests using water mist [77]

Due to the fact that water mist can be more effective and is a liquid non-Halon compound suppression system, it is preferred in the latest research studies. In several occasions it has been shown that water mist has good potential to replace Halon1301. Similar study on experimental and CFD modelling can be found in reference [82]

Recently, water replaced Halon1301 in marine applications and many studies were performed using water mist as fire extinguishing agent (CFD and experiments) [78].

Water mist systems are facing major difficulties associated with design and engineering [79]. It is very difficult to maintain an adequate concentration of a proper droplet size inside the compartment when the gravity and the agent deposition loss on surfaces deplete the concentration. In addition water mists are more suitable to extinguish fire from close distance. Many problems arise with fires away from the discharge nozzle and extinguishing deep seated Class A fires (Appendix B). Other concerns regard: collateral damage from the water deposition, electrical conductivity of the mist, the cooling of the combustion products, deposition of smoke particles to the water droplets, loss of visibility and clogging for small nozzle orifices. Finally, no MPS requirements or regulations regarding their design and application have yet been finalised and thus they not yet approved for aircraft applications.

Focusing more on water mist suppression systems, there are two basic types: single and dual fluid. Single fluid systems can be high (51.71bar), medium (12.06 to 51.71bar) and low (less than 12.06bar) pressure systems [79]. These systems utilize stored water under pressure with spray nozzles which deliver droplets in size between 10 and 100 μm. Dual fluid in general uses air or Nitrogen to atomize water at the nozzle and produce higher spray energy for a given pressure for example the pressure of a dual system at maximum reaches 100 psi (6.89bar) and for single fluid for many applications could reach 1000psi (68.94bar) or more depending on the size of the nozzle.

Another interesting study was conducted using hypoxic air and showed that it did satisfy the MPS but presented potential health issues [80]. FirePASS [81] developed hypoxic air for fire extinguishing purposes as it aggressively occupies the space and reduces the Oxygen content. This study showed that people were able to stay in environment with oxygen concentration below 16% for sufficient amount of time. FirePASS proposes that future airplanes could be pressurized with hypoxic air before the flight takes-off and therefore fire will never ignite in such environment. MPS tests (Figure 23) were also performed with dual fluid nozzle and the results showed that the agent satisfies the requirements. In these tests, the experiments began with small scale and cup burner tests.

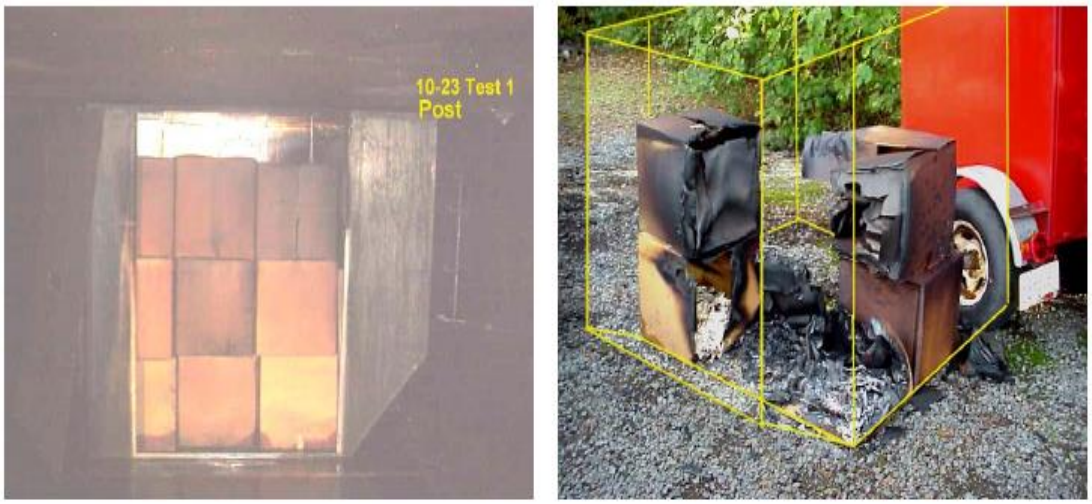

Figure 23 - Container tests MPS from FirePASS using water mist and hypoxic air [81]

Finally, Nitrogen, Argon and a combination of both have been tested for Class A and B fires with large and small scale experiments (

Table 23 - Inert gases properties [45]) [45]. The resulted data along with the scaled up laboratory cup burner and inertion data present that with agent concentration between 33.6 and 43.5vol% the fire extinguishment is achieved in around 16-18sec, with minimum oxygen concentration between 11.7 and 14.2vol%.

Table 23 - Inert gases properties [45]

Designation	Composition	Manufacturer
IG-541	Nitrogen 52 ± 4% Argon 40 ± 4% Carbon Dioxide 8 ± 1%	Tyco International, Ltd., USA, and Fire Eater A/S, Denmark ("INERGEN")
IG-55	Nitrogen 50 ± 5% Argon 50 ± 5%	Unitor Denmark A/S ("ARGONITE")
IG-01	100% Argon	Minimax GmbH ("Argotec")
IG-1	100% Nitrogen	Cyberus; Koatsu ("NN100")

The systems using Nitrogen gas as fire suppression agent, utilise pressurised cylinders for storage, satisfy the MPS requirements and are not causing any material degradation or by-products [83]. Table 24 presents some of the main advantages and disadvantages of the Nitrogen systems compared to Halon1301. Typical fire suppression system arrangement and Nitrogen extinguishment specifications are presented in Appendix E.

Table 24 - Advantages and disadvantages of Nitrogen [83]

Advantages	Disadvantages
Will extinguish fire at life supporting O_2 concentrations.	Not as effective as halons.
Extremely environmentally friendly (benign).	Heavy steel cylinders and pipes required when compared to halon, equipment is similar to other inert gases.
Wide range of applications.	
Nontoxic.	Low cooling potential.
Nitrogen gas is by far the cheapest inert gas.	Anoxia potential, especially at high altitudes.
No halogen acid decomposition products.	
Acceptable for occupied areas.	
Readily available worldwide (existing infrastructure).	
Simple flow calculations.	
Available in solid form (additional research required).	

2.4 Summary

Summarising, Halon1301 fire suppression systems for aircraft cargo must be fully replaced by the year 2040. The increasing environmental restrictions for Halon compounds globally lead researchers towards “alternatives”. One of the suggestions by FAA was the use of dual fluid water mist with Nitrogen as most promising agent (successfully past all MPS tests). Current water nozzle technology has reached to a point where the nozzles are capable to produce droplets in the order of micrometres increasing dramatically the effectiveness and extinguishing capabilities of the agent. Thus, recent Boeing efforts focused on testing dual systems with water mist as main agent and the support of Nitrogen.

Halon compounds also presented some promising properties and more importantly most suitable with the current Halon1301 fire suppression system. Nevertheless, there will always be concerns about the continuously increasing environmental restrictions. Thus, for example, HFC-125 could be used as Halon1301 substitute baseline agent in specific cases (MPSe, etc).

The most challenging requirement for the replacement system is to prevent the aerosol can explosion or if the explosion occurs, to minimise the overpressure in the cargo. Considerations for fire ignition or re-ignition after discharge are also required for the agent approval. Additionally, there is a need to maintain the agent concentration higher than a minimum level for a pre-specified amount of time. This is in order to avoid any potential fire enhancement by the agent.

Another important aspect of the fire suppression system successful operation regards the collaboration with the ventilation system. The ventilation system regulates the air conditions inside the cargo as well as the leakage rates (Door fan, outlet valve, etc.). Since the fire extinguishing agent changes dramatically, the required operating conditions change and thus the ventilation system needs to be adjusted accordingly.

Finally, very promising capabilities have been demonstrated by inert gasses due their high effectiveness and low toxicity without facing Halon1301 or water issues. Recently, the focus is growing on Nitrogen systems using different approaches,

such as storing Nitrogen as gas, liquid or solid, identifying the advantages and disadvantages for each. The main design challenge of these systems is to create a hypoxic environment below 12% Oxyegn concentration inside the cargo and maintain this concentration level for the time required and as close to the floor as possible. Additionally, the weight penalties associated to inert gas (Nitrogen) system operation on the aircraft could result to be comparable to water systems if not carefully designed.

2.4.1 Identification of Research Gaps

The literature survey showed that the research focus moves towards the installation and operation of fire suppression systems, using replacements agents, on-board the aircraft. Currently, several promising agents successfully passed the MPS tests. Nevertheless, there are still several challenges in order to progress the research towards system certification and in-flight testing. The list below presents some of the areas that require further development:

1. There is insufficient information on the behaviour of the proposed agents during operation. Most of the existing data on these agents are based either on numerous assumptions (CFD simulations) or on a small number of experiments performed in a relative small scale.

2. Very limited information exist on system architecture requirements and especially on system integration/installation on-board the aircraft (accounting for the Halon1301 reserves exhaustion). Additionally, existing cargo architectures are insufficient to fully integrate the proposed agents without significant modifications. However, very limited information was found on the suitability of each of the proposed systems as potential solutions which account for minimum modifications on the currently existing aircraft cargos.

3. No information was found on cargo ventilation systems design requirements, including fire suppression considerations based on replacement agents.

4. In terms of simulation strategies, there are very limited data on the public domain regarding running such computationally expensive numerical simulations with high fluid discharge velocities in large control volumes.

5. Finally, due to the fact that they were designed considering halogens, the MPS fire test scenarios do not seem to satisfy the requirements for the most demanding fire scenarios identified when replacement agents are used. Additional considerations in terms of fire ignition/re-ignition as well as agent mass losses during discharge are required. Thus, adjustments on the MPS designed tests and test rigs are required, aiming to cover all existing aircraft cargo arrangements.

The intended outcome of the present research aims to contribute to the above research gaps by:

1. Adding information on Nitrogen (IG-100) based systems during operation

2. Enriching the database on the proposed system arrangement and installation (design criteria, sizing methods, sub-systems drawings, system integration layout, etc.), as well as testing procedures

3. Adding information on the design methodology and sizing of cargo ventilation systems from a fire extinguishment point of view for the proposed agent

4. Enriching the experimental database on the proposed system operation against MPS fire test scenarios (evolution of cargo average Oxygen concentration, overpressure and Nitrogen discharge conditions with time)

5. Adding information about the meshing, boundary conditions settings and solution convergence strategies of computationally expensive numerical simulations with high fluid discharge velocities in large control volumes

3 METHODOLOGY

This chapter contains the complete methodology setup as well as the individual methods developed to meet the project objectives. The overall approach follows the sequence of the list of objectives presented in section 1.3. The problem setup was mainly based on the selected replacement agent for the near future.

3.1 General Methodology

Generally, the study was divided into two levels in terms of project development and modelling fidelity:

1. Preliminary Approach: includes the problem definition, agent selection, system requirements, general arrangement, the analytical modelling and the preliminary numerical modelling and simulations.
2. Main case study: includes the complete test rig design, the experimental procedures setup and based on the results, the modifications required in order to achieve a higher level of modelling fidelity, more realistic solutions and verify the outcomes.

In terms of activities, the study involved three main streams:

1. The analytical work on the overall system and sub-systems preliminary design and operation.
2. The numerical (3D-CFD) modelling and simulations.
3. Test rig design and experimental procedures setup.

All activities progressed through both levels of the study. The workflow for each work stream of the project is illustrated in Figure 24.

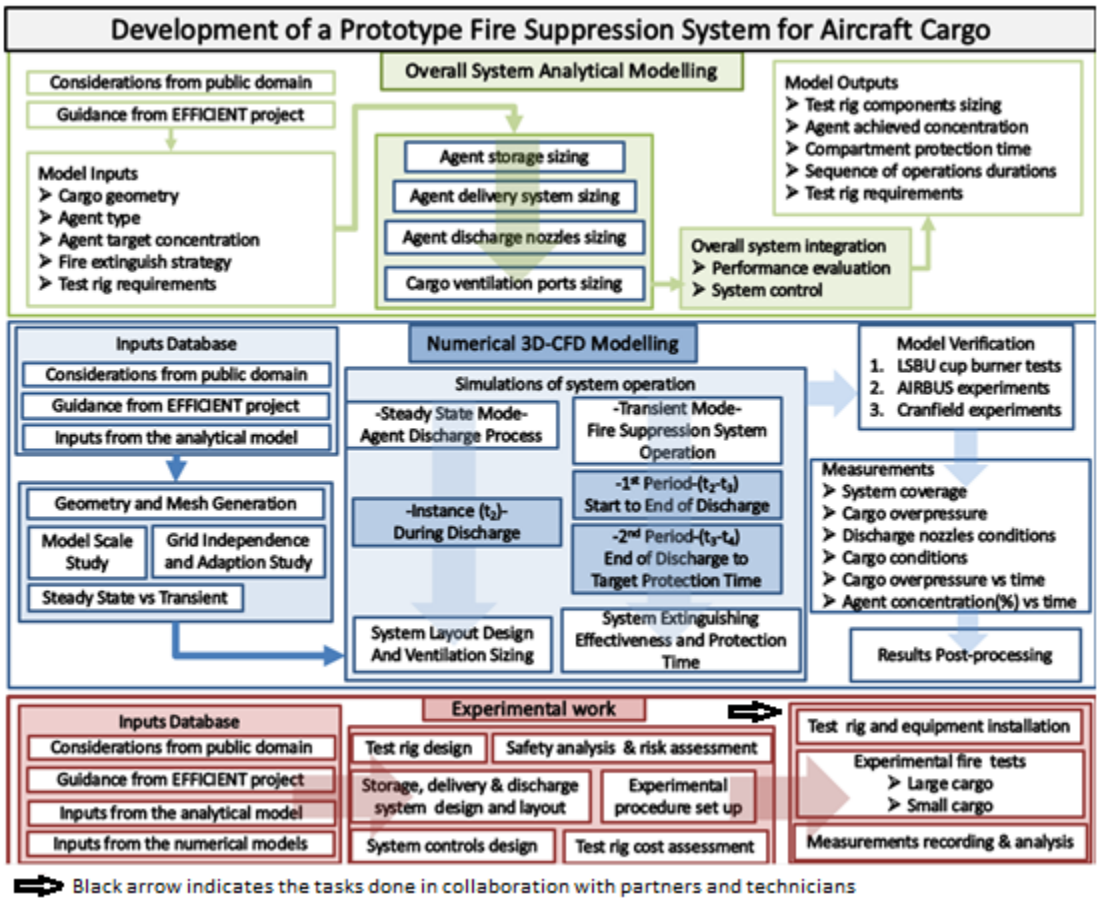

Figure 24 - Project General Methodology

As mentioned, the project begins with the selection of the most promising fire suppression agents in terms of environmental impact, toxicity and performance. Considering the latest achievements in the research of Halon1301 replacement agents, the candidate categories are:

a) Halon compounds
b) Inert gasses
c) Combinations of gasses
d) Dual fluid water mist and Nitrogen

Due to the potentially increased computational complexity and cost and the risk associated, water based agents were excluded and the research focused only on inert gases. This decision was supported also by the fact that the current aircraft fire suppression systems discharge Halon1301 very effectively (high coverage capabilities) in gaseous state. Finally, the most important factor was that inert gasses practically do not present any environmental threat.

Halon1301 was defined as the baseline agent for the MPS tests and thus it has been selected as baseline for comparison the CFD simulations. Additionally, due to the limited availability of Halon1301, it was decided that a model using the halon-compound HFC-125 should also be produced as a sub-baseline agent. Finally, the replacement agent which presented the most promising overall properties and deemed suitable for future aircraft cargo applications is Nitrogen (IG-100). More details about the problem definition and agent selection are presented later in this chapter.

The final selected case was the pressurized gas single flow Nitrogen (IG-100) system, with the potential future collaboration with OBIGGs or respective technologies.

The results of the analytical model were then passed towards the second work stream of the project, the numerical (3D-CFD) modelling and simulations. Initially, full scale simulations of the MPS tests, using complex nozzle geometry, were tested in order to assess the computational demand and design requirements. Progressive simplification/improvement of the geometry and mesh along with a model scale study resulted the final simulation models. The selection of the final models was based also on the grid adaptation and independence study. Three final cases were selected:

1. Cargo compartment empty
2. Cargo compartment with 30% of the volume load with boxes
3. Partial cargo compartment (1/3 of the full cargo volume)

The numerical (3D-CFD) simulations required to meet the objectives were separated in two categories:

1. Steady state, to study the cargo conditions during discharge adapt the ventilation and discharge nozzle arrangements through an iterative process in order to ensure adequate performance and overpressure control.
2. Transient, to study the agent concentration, coverage and overpressure inside the compartment against time. The complete simulation is

separated in two time periods: a) start to end of discharge and b) immediately after discharge till the targeted protection time.

Single phase flow 3D-CFD models were developed using the FLUENT species transport (no reaction) model and the k-ε turbulence model with a pressure-velocity coupled solver.

For model verification purposes, both cases were compared with AIRBUS respective experimental results. The transient cases were also compared against the data from LSBU cup burner tests.

The third and final work stream regards the experimental work. Based on the outputs of both analytical and numerical modelling, the detailed designs for the test rig along with the agent storage, delivery and discharge systems have been performed. Additionally, the established fire suppression strategy was built into the design of the indications and control system and the necessary risk assessment and safety analysis were performed for the proposed test rig installation. Finally, after the completion of the experiments, the data received are post-processed and compared to the analytical/numerical model outputs.

3.2 Preliminary Approach

The research begins with the problem setup and the analytical work. The problem definition was based on the considerations below:

1. FAA MPS, Options and advisory circulars [5,7,31]
2. NFPA 2004 Halon and NFPA 2015 Clean agents 2015 [23,90]
3. Recent development regarding fire suppression systems [9,15,16,93]

3.2.1 Agent Selection

It was mentioned in the previous section that the fire extinguishing agents selected for this study were three: a) Halon1301, b) HFC-125 and c) Nitrogen. Since Halon1301 reserves are very limited, only HFC-125 and Nitrogen have the potential to be used in experimental procedures. This is one of the reasons that HFC-125 was selected as second baseline. HFC-125 is a halon compound agent with very similar properties and behaviour to Halon1301. This fact allows for

reduced modifications to the Halon1301 based system and similar performance. Additionally, it was approved by FAA in previous studies to be used as sub-baseline especially for bulk and containerised load fire MPS tests and is currently tested for engine nacelles [94]. The Halon compound agents are compatible with the already existing cargo fire suppression systems. Thus, they can provide an edge on the time required to transit from research and technology development to full system integration, test and operation. This increases the confidence regarding meeting the deadlines set for complete Halon1301 replacement. Nevertheless, HFC-125 presented complications related to fire re-ignition below inert concentration during the MPS tests, thus it will be used only at the preliminary approach.

Another very promising replacement agent who passed MPS tests (FAA) was the dual fluid water mist with Nitrogen [39]. Water based systems have been also tested and examined in more detail within NERO [75], FIREDASS [76] and other projects. Generally, they present higher effectiveness than Halon1301 but increased complexity on the system design, integration and modelling. Although this could be an interesting selection for the future, due to the increased risk regarding modelling and simulation time it has been excluded from this study.

Inert gasses, considering also using additives (or other gasses such as CO_2), and Hypoxic air were the originally selected category of the most promising agents for this study. Generally, they do not present similar environmental impact to halon compounds. They present some challenges regarding their storage and integration on-board aircraft applications. Nevertheless, these challenges are significantly less compared to those existing for water based solutions and can be tackled with the current technology level.

Nitrogen (IG-100) is the most popular from the inert gases as it exists in large quantities in the atmosphere. Thus, it comes at a lower cost in the market and the possibility of reserves exhaustion is zero. Additionally, it mixes very well with atmospheric air, providing effective and rapid distribution in space. Most importantly though, it is also one of the agents that have passed the MPS tests

(FAA) [5] and it is compatible with the existing aircraft cargo systems operation and architecture.

Concluding, in the Preliminary Approach both HFC-125 and Nitrogen based models were developed while the Main Case Study focused solely on the Nitrogen system.

3.2.2 Agent Design Concentration

The value of the agent design concentration is one of main inputs of any fire suppression model. Small scale experiments have been performed for the purpose of establishing such values for different agents. The main categories of data required are two:

I. Flame extinguishment data, which determine the agent concentration necessary to extinguish a flame of a particular fuel [8]
II. Inertial behaviour data, which determine the minimum premixed agent concentration to suppress propagation of a flame front at the “flammability peak,” or stoichiometric fuel/air composition [8]

3.2.3 Analytical Modelling

Following a design approach similar to that described in reference (NFPA), the main targets of the analytical model are:

1. Model the cargo fire suppression system discharge process, utilising public domain data and basic principles, for:
    - Halon1301
    - HFC-125
    - Nitrogen
2. Establish boundary conditions for the numerical 3D-CFD models

The analytical model was applied to simulate the filling process of the agent mixture inside the enclosure. The first model concerns the case of a single nozzle discharging Halon1301 inside a control volume. This model was designed based on reference [23] for comparison. A respective model setup was also used for the replacement agents.

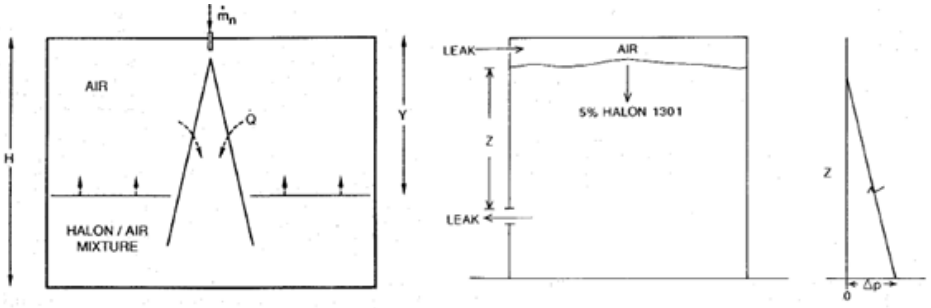

Figure 25 - Analytical simplified model [23]

In the case of Halon1301, the agent is discharged downwards, filling up the compartment from bottom to top (see Figure 25). This happens due to the fact that Halon1301 has higher density than air in such conditions. The Halon1301/air mixture layer formed close to the floor progressively rises towards the ceiling. In order to assure uniform distribution of Halon1301 inside the enclosure, pure air is also entrained in order to enhance the Halon1301/air mixing process. Finally, some of the mixture escapes the enclosure in an effort to simulate the leakage process.

The exact same approach is followed for the case of HFC-125, as it presents very similar properties to Halon1301. Nitrogen on the other hand behaves in a different way. Since air consists of approximately 79% Nitrogen and 21% Oxygen, its density is relatively higher. In this case, the jets are still discharged downwards. However, the formed layer of agent/air mixture fills-up the compartment from top to bottom. Additionally, since the Nitrogen system requires significantly higher quantity of agent to achieve fire extinction, successful distribution is assured. However, there is still need for representation of the leakage flows as well as an additional opening, which instead of being used for air infiltration it is designed for overpressure control.

The calculation procedure for this analytical model followed a physics based approach combined with empirical correlations. The calculations aim to deliver the boundary conditions for the agent, in order to achieve the required concentration levels and successful fire extinction. These boundary conditions mainly refer to the mass flow of the agent discharge, the pure air infiltration and the leakages. The “Leaks” illustrated in Figure 25 represent the air infiltration rate

(top) and the compartment leakages (bottom) (door, sealing/lining, connections, etc.). The compartment leakages are calculated based on the hydraulic height of the mixture zone. The assumptions applied are:

1. Homogenous flow regime (mixture)
2. Perfect/ideal gasses
3. Incompressible flows
4. Constant mass flow rates
5. Constant compartment leakage rate after discharge
6. Agent design concentrations (e.g. 6% for Halon1301)
7. Uniform agent concentration within the mixture zone
8. Discharge times:
    a. Quick discharge: Extinguish fire in 10 seconds and maintain agent concentration capable to prevent re-ignition for 30 minutes (MPS)

The imposed input parameters based on each agent are:

1. Agent design concentrations [v/v] [27, 28].
    a. Halon1301 = 6%, targeting >3.5% for 30min after discharge
    b. HFC-125 = 8.5%, targeting >6% for 30min after discharge
    c. Nitrogen = 32%, targeting >30% for 30min after discharge
2. Volume of enclosure: 56 m^3 for Full Cargo and 9.41m^3 Partial Cargo (1/8 of the full)
3. Height of enclosure: 1.67m (minimum acceptable 2m)
4. Temperature inside: 18°C, outside: 21°C
5. Allowable enclosure overpressure without discharge:
    a. Halon1301 = 10Pa (1*10^-4bar)
    b. HFC-125 = 10Pa (1*10^-4bar)
    c. Nitrogen = 250Pa (2.5*10^-3bar)

The required agent quantity to achieve the design concentration is calculated as:

$$W = \frac{Vh}{s}\left(\frac{C}{100 - C}\right) \quad \text{3-1}$$

where,

W = weight of agent required to achieve design concentration (lb)

Vh = net volume of hazard in (ft^3) (enclosed volume minus fixed structures)

s = 2.2062 + 0.005046* T (ft^3/lb)

T = minimum anticipated temperature of the protected volume (°F)

C= agent concentration (% v/v)

The density of agent/air mixture was calculated using the following equation:

$$r_m = r_v * \frac{C}{100} + \left(r_a * \frac{100 - C}{C}\right) \quad \text{3-2}$$

where:

r_m = agent/air mixture density (kg/m^3)

r_a = air density (kg/m^3)

r_v= vapour density (kg/m^3)

Typically, the main enclosure leakages depend on:

1. Hydrostatic pressure developed from the agent/air mixture in the enclosure
2. Leakages across the enclosure boundaries and the forced ventilation system
3. Environmental conditions

The overpressure developed inside the compartment forces the flow to pass through the available leakage paths. The direction of the flow depends on the operating conditions.

The fluid hydrostatic pressure differential depends on the height the mixture reached and its density compared to that of pure air. In addition, the mixture is cooler than the air and in case of Halon1301 it is approximately 5 times heavier. The resulting density difference causes the hydrostatic pressure differential

across the enclosure boundaries. The hydrostatic pressure difference is calculated as:

$$P_c = g * H_o * (r_m - r_a) \quad \text{3-3}$$

where:

P_c = Hydrostatic pressure due to agent density difference (Pa)

g = acceleration due to gravity (9.81m/sec^2)

H_o = height of protected enclosure (m)

The out-flow velocity across the leakages where calculated:

$$V_L = (2 * g * H_o * \frac{(r_m - r_a)}{r_a}) \quad \text{3-4}$$

And the total volumetric flow rate:

$$Q_e = (2/3 * g * C_d * A_L * V_L) \quad \text{3-5}$$

Where:

V_L: Outlet velocity (m/s)

Q_e: Total volumetric flow rate (kg/s)

The same applies for the case of HFC-125. However, in the case of Nitrogen, the primary mechanism for the generation of compartment overpressure is the rapid discharge of compressed Nitrogen. After the discharge stops, the large amount of the added agent causes an increase on the compartment pressure. The level of overpressure reached depends on the area of the openings that represent the leakages and ventilation.

As mentioned above, Figure 25 right illustrates the pure air inflow at the upper part and the mixture leakages at the lower part of the enclosure. In this case an interface is formed between the pure air and the mixture. In real fire extinguish scenarios the agent discharge flow rate is reducing with time. Additionally, the mixture leakage flow rate will increase with time, due to the hydrostatic pressure

head of the mixture. A critical assumption applied here dictates that hydrostatic pressure difference will be calculated after the mixture layer reaches the mid-height of the enclosure (excluding cases where the primary combustible load is close to the ceiling and all the leakages are concentrated at or close to the celling). The combination of the above assumptions results in a decreasing agent concentration in the mixture after discharge.

The analytical model treats the problem as the smoke filling process. Initially, the whole space of the enclosure is filled with pure air and conservation of mass applied. The concentration of Halon1301/air mixture for each layer is calculated by the volume of Halon1301 discharged at a specific time divided by the volume of the total gas inside until that layer, following the equations [23]:

$$C = \frac{\frac{\dot{m}_A * t}{\rho_v}}{(H - Y) * A_f} \quad \text{3-6}$$

$$C_d = \frac{\frac{\dot{m}_A * t_d}{\rho_v}}{H_d * A_f} \quad \text{3-7}$$

$$\frac{C}{C_d} = \frac{\frac{t}{t_d}}{1 - \frac{Y}{H}} \quad \text{3-8}$$

where:

Y: Height of the pure air layer (m)

H: Height of the agent/air layer (m)

H_d: Height of the agent mixture for total height of the enclosure (H_o) (m)

A_f: Floor area of the compartment (m)

$\dot{m}_A$: Total discharge rate (kg/sec)

t: Activation time (sec)

t_d: Design activation time (sec)

C_d: Design concentration (v/v)

The final parameter required for the analytical model is the discharge nozzle area. The nozzle area required to achieve the concentration for each layer within a specified amount of time is estimated by [23]:

$$A_n = \frac{-0.4 * C_d * H}{\ln(Y_d) * A_f} \qquad 3\text{-}9$$

where;

Y_d: Design height of the pure air layer (m) (0.1 m for design purposes)

A_n: Nozzle area (m^2)

Neglecting the agent distribution and mixing requirements, the number and size of the nozzles for each agent can be calculated based on the above area. The above correlation shows that the nozzle design highly depends on the specific case. Nevertheless, it includes extra degrees of freedom for the designer. Some of the main considerations required for a proper nozzle design are:

1. Agent discharge flow rate
2. Air infiltration position and flow rate
3. Geometry of the enclosure
4. Obstacles, loads and the quality of ceilings
5. Number of nozzles
6. Nozzle positions relative to the air infiltration and leakages for maximum agent effectiveness, proper mixing and distribution and minimum agent loss

This analytical model is sufficient to predict the agent discharge flow, mixture leakages and air infiltration in order to set representative boundary conditions for the preliminary 3D-CFD simulations. There are already numerous studies for Halon1301 systems, illustrating the size of the system and sub-systems (bottles,

pipes, nozzles, etc.) for 600 psia and 360 psia bottle pressure, which can verify the analytical model. However, the final nozzle design will also need to account for agent optimum mixing and distribution. The agent mixing and distribution can only be evaluated using CFD tools and thus the final nozzle design will result as a consequence. Figure 26 below illustrates typical example of the nozzle discharge pressure using Halon1301 from a bottle pressurized at 24.82bar. More examples for Halon1301 cargo fire suppression systems could be seen at table in Appendix 7.1-B.

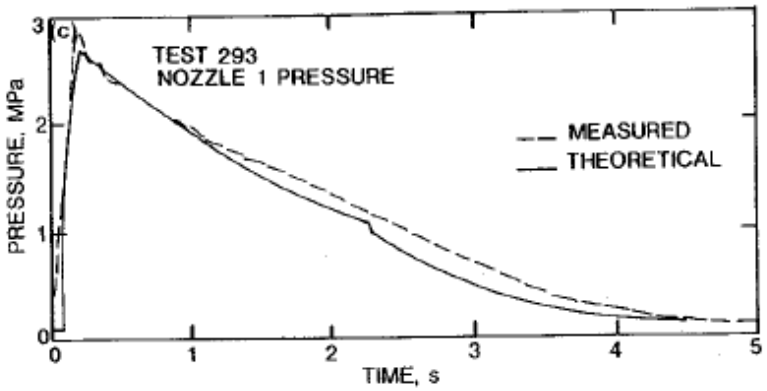

Figure 26 - Experimental Halon1301 nozzle discharge [24]

3.3 Main Case Study

3.3.1 Analytical Modelling & System Design

The analytical modelling of the selected Nitrogen (IG-100) system was based on current state-of-the-art cargo ventilation system architecture (see Figure 27). The system design targets are:

1. Fire suppression performance
2. Minimisation of system size and weight
3. Identification of the optimum system arrangement (bottles, pipes, nozzles, ventilation, etc.) for current aircraft cargo
4. Delivery of experimental procedures setup and test rig design
5. Collaboration with 3D-CFD models

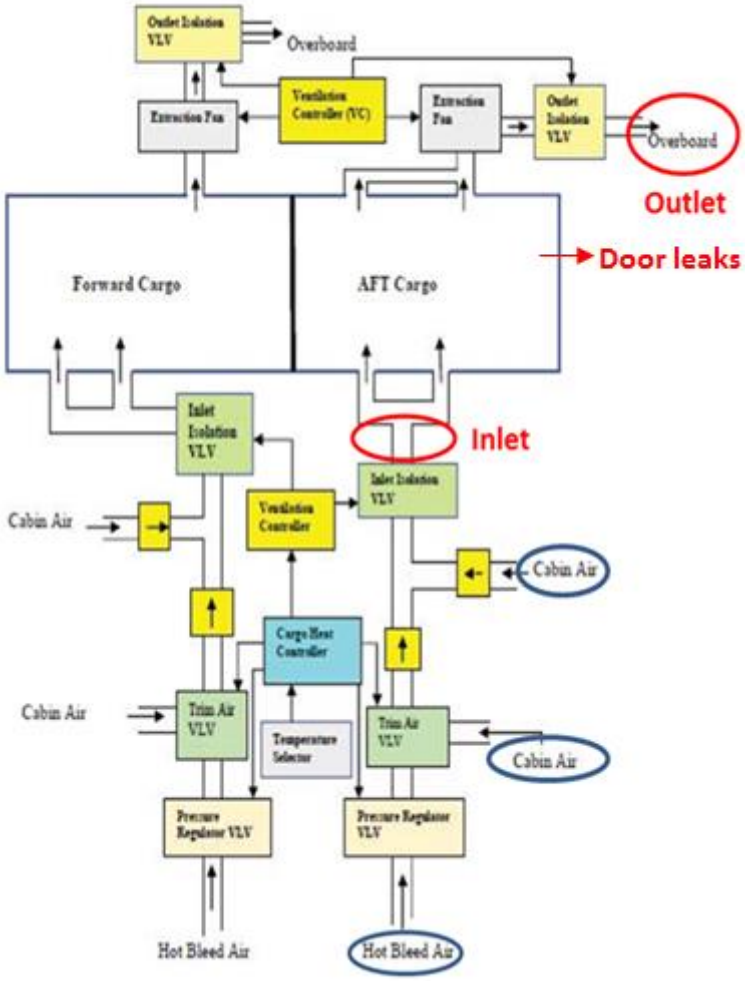

Figure 27 - Typical cargo ventilation and heating system [92]

The main elements considered for the Nitrogen (IG-100) model are listed below:

i. Aircraft cargo fire suppression system requirements [2,16]
ii. MPS requirements [7]
iii. Advisory circulars [15,31]
iv. NFPA 2015 Clean agents 2015 [90]
v. NFPA 2004 Halon discharge [23]
vi. Recent technology development regarding fire suppression systems [19,41]
vii. Preliminary Approach results

General design considerations for Nitrogen (IG-100) system

i. Nitrogen (IG-100) extinguishes fire by diluting the air and decreasing the Oxygen content. Bellow 16% of Oxygen concentration at normal atmospheric pressures the fire cannot survive.
ii. Current Oxygen design concentration requirements for aircraft cargo are below 12% (effective for Class A and B fires) [8]. Furthermore, based on the present research and the EFFICIENT project consortium suggestions, values ≤10% were considered for increased system reliability and effectiveness. However, due to human and animal health considerations, the Oxygen concentration minimum limit was set to 10%.
iii. Maintain the Oxygen concentration below 16% at least for 30min (MPS requirement), ensuring no re-ignition until the aircraft lands.
iv. Maintain the cargo overpressure limits before and after agent discharge
v. Achieve agent design concentration at a horizontal plane (parallel to the floor) as close to the cargo floor. This challenging design requirement leads to increased discharge time in order to achieve the desirable hypoxic environment using an agent lighter than air.
vi. Collaboration with OBIGGs or SGPGG for extended time of fire protection and increased overall system performance. Such collaboration is very likely to happen as OBIGG or SGPGG devices are already examined in order to be installed on aircraft for other applications.

3.3.1.1 Nitrogen (IG-100) System Discharge and Firefighting Approach

In the case of Nitrogen, both the compartment filling-up mechanism and the firefighting strategy differs to Halon1301. Figure 28 presents a simplified view of the fire suppression system. Each arrow represents mass flow direction. One of the main requirements for this system is to assure that the ventilation system operates with a constant leakage rate ($m_{mix\ leak}$), even when there is no agent discharge. This is the reason behind the two arrows that represent the flow exiting the control volume. Also, it is obvious that within an air sealed cargo, discharging agent will require the respective mass flow to exit the control volume in order to avoid developing overpressure. Thus, the ventilation system was designed to

deliver the required constant leakage rate before agent discharge, then regulate the leakage rate ensuring minimum overpressure during agent discharge and finally continue with the same constant leakage rate after agent discharge.

The main assumptions applied within this process are:

- Constant discharge mass flow rate for 60sec
- Maximum acceptable overpressure during discharge (1500Pa or 0.015bar)
- Maximum acceptable overpressure after discharge (250Pa or 0.0025bar)
- Constant leakage flow rate (0.023m^3/s, MPS) at no agent discharge
- No pure air inserts the enclosure during agent discharge
- Mixture uniformity at any given time / Nitrogen diffusion in air infinitely fast

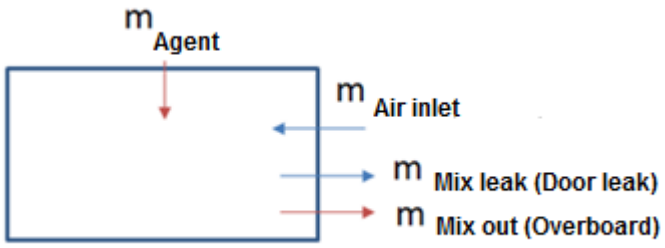

Figure 28 - Simplified analytical model for the agent discharge process

As mentioned, the storage and delivery system for Nitrogen (IG-100) can be designed for:

1. Single gas flow
2. Two-phase flow (Liquid/gas)
3. Solid gas flow (SPGG)

The single flow gas was selected as the most suitable case for this study. The technical challenges introduced by the two-phase (liquid/gas) or solid gas flow made these systems unsuitable for the current research. Solid gas generators could be considered as support systems for the experiments while for aircraft applications they could provide further reduction on the overall system size and weight as well as longer fire protection duration.

The design of the fire suppression system aims uniform distribution and adequate agent effectiveness inside the enclosure. The piping system will be installed on the roof of the cargo/test rig, while considerations relative to equipment installation capabilities were taken into account. Some of the desirable system features are presented in the list below:

i. Ease in handling the operating conditions
ii. Flexibility on modifications/adjustments (e.g. piping, nozzles, hydraulics)
iii. Suitability for alternative agents
iv. Easy to maintain
v. Minimum pipe elevation pressure losses
vi. Safe operation of the system (e.g. hydraulic system maximum pressure 300 bar, minimum safety distance)
vii. Acceptable behaviour during operation (noise, high pressure load, etc.)
viii. Low weight
ix. Low cost

Figure 29 illustrates the developed firefighting strategy, operation approach and limitations. The suggested system operation was separated in four time periods, including two future system upgrades for the extension of the fire protection time. The first time period refers only to experimental scenarios while the rest apply also for the on-board operations.

Period 1: t_0-t_1 (Fire ignition and detection time)

The experiment begins the moment the fire ignition switch in on (t_0). This period is completed after successful fire ignition has been achieved and one of the fire detection sensors (temperature or smoke) gets activated at instance t_1. The recording of this time period aims to categorise the severity of each fire scenario.

Period 2: t_1-t_2 (System response time)

This period begins when the signal from one of the sensors (temperature or smoke) reaches the fire suppression system control unit. At that instance, the control unit activates the valves and the Nitrogen expands in the piping network, traveling towards the discharge nozzles. This phase is completed after successful

discharge has been achieved at instance t_2. The recording of this time period aims to categorise the hydraulic system and overall automations response time and performance.

Period 3: t_2-t_3 (System activation and firefighting time)

This period begins right at the start of discharge process and lasts until the Oxygen concentration measurement probe signals the control to shut down the Nitrogen valves and stop the discharge at instance t_3. The allowed overpressure during discharge is limited to 1500Pa (0.015bar) in order to avoid damage and reduce agent leakages. The design target concentration should be below 12% Oxygen as suggested by cup burner tests (LSBU). The recording of this time period aims to categorise the fire suppression system overall effectiveness inside the cargo.

Period 4: t_3-t_4 (Cargo fire protection time)

Finally, period 4 begins right after discharge stops and lasts until the Oxygen concentration measurement probe reaches the value of 16% at instance t_4. The allowed overpressure after discharge limited to 250Pa (0.0025bar) in order to keep low the agent leakages targeting values close to zero. The recording of this time period aims to categorise the protection time achievable

System Upgrades: The potential existence of OBIGGS or SGPGG on future aircraft provides the opportunity of potential integration with the fire suppression system. Such devices can provide relatively small quantities (e.g. for OBIGGs approximately 0.009kg/s for 4 continuous minutes) of Nitrogen on-board the aircraft. Connecting this small feed of Nitrogen coming from one of the OBIGGS or SGPGG devices can provide the capability of extending the fire protection time.

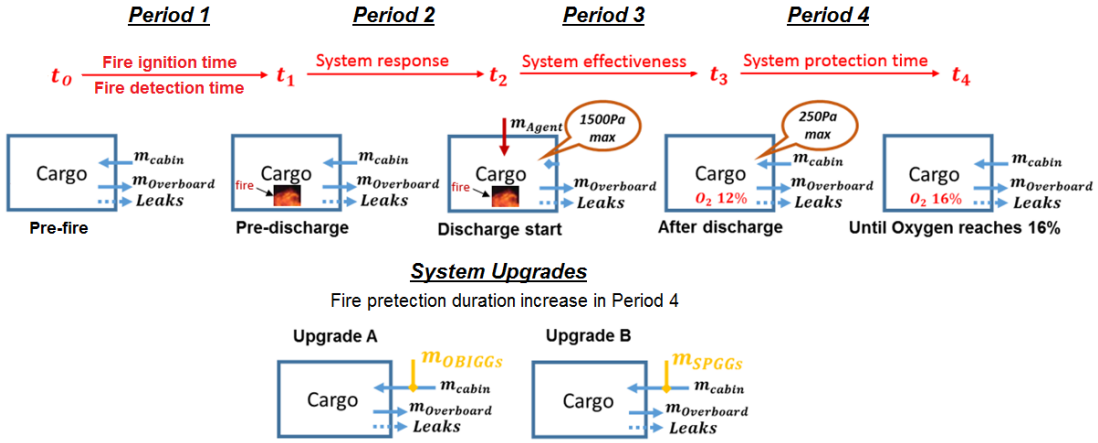

Figure 29 - Firefighting strategy

3.3.1.2 Storage, Delivery and Discharge Systems Design

The design of the delivery system is based on:

i. D1.1 deliverable for WP1.0 of the EFFICIENT project [6]
ii. NFPA 2001/2004/2015 guidelines [23, 90]
iii. MPS tests requirements for aircraft cargo [23]
iv. Considerations for aircraft applications [95, 96, 97]

Based on market research, two container cylinders were sized targeting minimum system weight while meeting the required discharge time period described in the previous section. The sizing of the pipes was based on the compartment dimensions and the agent distribution requirements. The methodology selected for the calculation of the characteristics of adiabatic compressible gas flow inside constant cross-sectional area tubes follows the *Fanno* approach [96, 97]. The selection of the *Fanno* instead of the *Rayleigh* method for calculating flows inside pipes was based on the criteria below:

i. The system is considered adiabatic, fact which agrees with the *Fanno* but disagrees with the *Rayleigh* method, which includes heat transfer phenomena
ii. The system dissipates energy through friction with the pipe wall, fact which agrees with the *Fanno* but disagrees with the *Rayleigh* method, which considers frictionless flow characteristics inside the pipe
iii. Although a combined approach might provide some extra accuracy on the results, the actual system resembles sufficiently the adiabatic behaviour and

thus increasing modelling complexity and computational power demand is deemed unnecessary

The main assumptions taken are:

1. No heat transfer – adiabatic system (pipes insulation)
2. Darcy friction factor for pipe roughness = 0.002 (smooth pipes)
3. The boundary conditions selected are:
    a. Design initial Mach number: $Mn_{initial}$ = 0.3, in an effort to keep it low without penalising the size significantly. This ensures relatively low turbulence levels minimising total pressure losses and heat transfer, as well as avoiding adverse compressibility effects.
    b. Total temperature = 18^0C, assuming that the cylinders will be stored in ambient temperature.
    c. Total pressure = 41bar, in an effort to keep it relatively high and minimise the system size and weight, while respecting safety requirements (value commonly used in fire knockdown systems).

Additionally, the ‘Joule-Thomson’ effect due to flow throttling [91] was considered in order to estimate the temperature drop expected at throttling points such as pressure reducers and discharge nozzles. Figure 30 presents the isenthalpic throttling of Nitrogen in a temperature-entropy diagram. At high storage pressure, the Nitrogen gas state inside the storage cylinders presents a level of entropy which allows higher temperature for the same enthalpy. The storage pressure of the gas sets the initial level of entropy. High initial storage pressure leads to low initial entropy level, below which isenthalpic pressure changes affect the total temperature (observe the region of isobars between 10 and 1000bar). Below 10bar storage pressure, isenthalpic throttling doesn’t present any practical temperature change

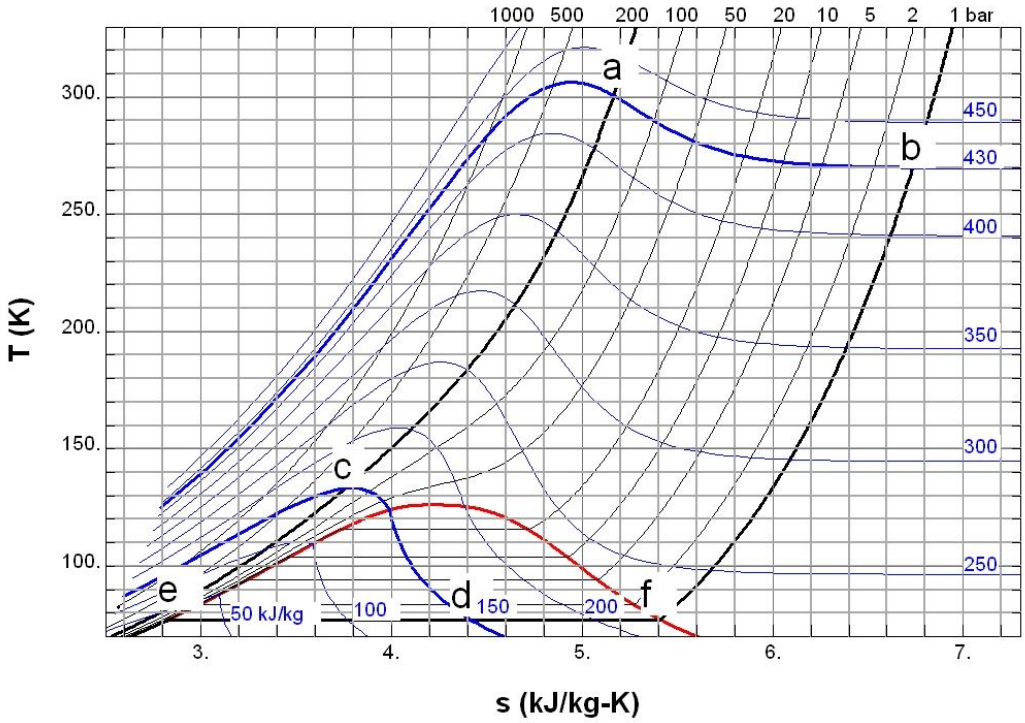

Figure 30 - Nitrogen isenthalpic throttling in T-s diagram [91]

The detailed analytical method developed for the system design is presented below. The method is presented in a sequential manner starting from the inputs.

Nitrogen quantity calculation

1. Enclosure volume,

$$Vo = x * y * z\ (m^3) \qquad 3\text{-}10$$

2. Main discharge time, $\mathrm{t}_{constant\ discharge} = 60\ s$

3. Initial volumetric concentration,

$$Cv = \frac{V}{Vo}\ (\%) \qquad 3\text{-}11$$

4. Volumetric concentration increased due to leakage,

$$X = \ln(\frac{100-C}{100})\ (\%) \qquad 3\text{-}12$$

5. Agent required quantity in m^3,

$$\mathrm{V} = Vo * \mathrm{X} \tag{3-13}$$

6. Physical properties

    a. Density

$$\rho = \frac{m}{V}\ \left(\frac{kg}{m^3}\right) \tag{3-14}$$

    b. Ratio of specific heats

$$\gamma = \frac{C_p}{C_v} \tag{3-15}$$

    c. Gas constant

$$R = \frac{R^*}{MW} \tag{3-16}$$

7. Safety Factor $G1 = 1.15\%$

8. Cylinder storage dimensions

    a. Diameter, D

    b. Height, h

    c. Volume

$$Vc = \ \pi * \mathrm{D}^2 * \mathrm{h}\ (\mathrm{m}^3) \tag{3-17}$$

9. Number of cylinders

$$N = [\frac{V^{\cdot}}{Vc}]_{top\ integer} \tag{3-18}$$

10. Final quantity

$$\mathrm{m}_{final} = N * Vc * \rho \quad (3\text{-}19)$$

11. Excess mass

$$\mathrm{m}_{excess} = \mathrm{m}_{final} - \rho * \mathrm{V} \quad (3\text{-}20)$$

12. Excess discharge time

$$\mathrm{t}_{excess} = \frac{\mathrm{m}_{excess}}{0.5 * \rho * \mathrm{V}/\mathrm{t}_{constant\ discharge}} \quad (3\text{-}21)$$

13. Time till drain-out

$$\mathrm{t}_{drain-out} = \mathrm{t}_{constant\ discharge} + \mathrm{t}_{extra\ mass} \quad (3\text{-}22)$$

The discharge mass flow rate was assumed to decrease linearly from its constant design value all the way to zero.

Piping network definition

1. Basic considerations
    a. Constant flow rate in pipelines
    b. Network geometry and number of nozzles ($Nn = 3$)
2. Total mass flow rate

$$\dot{m} = \frac{\mathrm{m}_{final}}{\mathrm{t}_{op}} \ (\frac{kg}{s}) \quad (3\text{-}23)$$

3. Nozzle mass flow rate

$$\dot{m}_N = \frac{\dot{m}}{N_n} \ (\frac{kg}{s}) \quad (3\text{-}24)$$

4. Boundary conditions

a. Initial pressure P_o (Pa)

b. Initial temperature T_o (K)

c. Enclosure conditions P_{atm}, T_{atm}

d. Pressure drop from reducer

$$\Delta P = P_1 - P_0 \tag{3-25}$$

e. Temperature drop from reducer taken from the diagram in Figure 30

f. Select design Mach No.

$$Mn = \frac{V}{\sqrt{\gamma * R * T_s}} \tag{3-26}$$

5. Static conditions (Pressure, temperature and density)

$$Ps = \frac{P_T}{(1 + \frac{\gamma - 1}{2} * Mn^2)^{\gamma/\gamma - 1}} \tag{3-27}$$

$$Ts = \frac{T_T}{1 + \frac{\gamma - 1}{2} * Mn^2} \tag{3-28}$$

$$\rho = \frac{P_S}{R * Ts} \tag{3-29}$$

6. Initial cross-sectional area and velocity

$$A_1 = \frac{\dot{m}}{\rho_1 * V_1} \tag{3-30}$$

$$V_1 = Mn_1 * \sqrt{\gamma * R * T_{S_1}} \tag{3-31}$$

7. Basic network dimensions (isometric diagram)

8. Pipes sizing

   a. Adiabatic system

   b. Darcy friction factor = 0.002

   c. *Fanno* flow calculation inside constant cross-sectional area pipes

      i. Mass conservation

$$\frac{d\rho}{\rho} + \frac{dA}{A} + \frac{dV}{V} = 0 \qquad \text{3-32}$$

      ii. Momentum conservation

$$\frac{d\rho}{\rho} + \frac{\gamma * Mn^2}{2} + \frac{f * dx}{D} + \gamma * Mn^2 * \frac{dU}{U} = 0 \qquad \text{3-33}$$

      iii. Transformation for $\frac{dMn}{dx}$:

$$\frac{dMn}{dx} = \frac{Mn * (1 + \frac{\gamma - 1}{2} * Mn^2)}{(1 - Mn^2)} * (\gamma * Mn^2 * \frac{f}{D} + \frac{(1 + \gamma * Mn^2) * dT_T}{2 * T_o * dx} - \frac{\gamma * Mn^2 * dA}{A * dx}) \qquad \text{3-34}$$

      iv. Final correlation: Ordinary 1st order differential equation

$$\frac{dMn}{dx} = \frac{\gamma * f}{D} * Mn^2 * \frac{Mn * (1 + \frac{\gamma - 1}{2} * Mn^2)}{(1 - Mn^2)} \qquad \text{3-35}$$

      v. Initial boundary condition: $Mn_1 = \text{Guess Station 1}$

      vi. Mn calculation for each subsequent station

      <u>Station 2</u>

$$Mn_2 = Mn_1 + \int_1^2 (\frac{dMn}{dx}) * l_1 \,, \qquad T_{2S} = \frac{T_{2T}}{1 + \frac{\gamma - 1}{2} * Mn_2^2} \qquad \text{3-36}$$

$$P_{2T} = P_{1T} * \frac{Mn_1}{Mn_2} * \left(\frac{T_{S_2}}{T_{S_1}}\right)^{\gamma+1/2*(1-\gamma)} \quad 3\text{-}37$$

$$P_{2S} = \frac{P_{2T}}{\left((1 + \frac{\gamma - 1}{2} * Mn_2^2\right)^{\gamma/\gamma-1}} \quad 3\text{-}38$$

$$\rho = \frac{P_S}{R * Ts} \quad 3\text{-}39$$

$$A_2 = \frac{\dot{m}_2}{\rho_2 * Mn_2 * \sqrt{\gamma * R * T_{S_2}}} \quad 3\text{-}40$$

$$D_2 = \sqrt{\frac{4 * A_2}{\pi}} \quad 3\text{-}41$$

vii. Network junctions and mass flow splits

$$\dot{m}_2 = {}^2/_3 * \dot{m}_1 \quad 3\text{-}42$$

$$\dot{m}_{N1} = \frac{\dot{m}_1}{3} = \dot{m}_{N2} = \frac{\dot{m}_2}{2} = \dot{m}_{N3} \quad 3\text{-}43$$

viii. Repeat the previous two steps for the next stations

ix. Expansion in the nozzles

a. Choked flow at the exit $Mn_{exit} = 1$

b. Isentropic expansion

c. No total pressure losses

d. Total temperature drop taken from diagram in Figure 30

At this point, a suggestion for future work would be to simulate the delivery pipes in 3D-CFD and improve the estimation of the friction factor.

Agent concentration reduction rate calculation

The agent concentration was calculated against time for the final time Period 4. Since the agent discharge has stopped, the agent concentration begins to drop from its initial value $C_{agent}(1)$ due to the leakages. Mass continuity and the current set of assumptions suggest that pure air enters the enclosure at the same rate as the leakages. Thus, the agent concentration reduction rate can be calculated as:

$$V_{agent}(t) = V_O * C_{agent}(t) \quad \text{3-44}$$

$$V_{AIR}(t) = V_O * \left(1 - C_{agent}(1)\right) + V_{leakage} * t - V_{leakage} * \left(1 - C_{agent}(t)\right) * t \quad \text{3-45}$$

$$V_O = V_{AIR} + V_{agent} \quad \text{3-46}$$

The combination of the above provides:

$$C_{agent}(t) = \frac{V_O * C_{agent}(1)}{V_O + V_{leakage} * t} \quad \text{3-47}$$

The correlation above combined with the value of the agent minimum level of concentration which assures no fire re-ignition, provides the fire protection time.

Nozzles design specifications

Three nozzles in a row or one way pipeline system was selected in order to model the real cargo agent discharge system and assure agent quick coverage. The nozzle design aims to provide a conical discharge pattern based on the coverage demands and aircraft cargo requirements.

i. 360° angle of coverage
ii. 150° angle of discharge cone

Summarising, the key considerations taken for the nozzle design are:

i. The selection and positioning of the nozzles is based on the design concentration of the agent, while targeting uniform and rapid agent distribution inside the enclosure.

ii. Geometry and dimensions of the enclosure, obstacles, loads and the quality of lining/sealing.
iii. The positions of the air infiltration and leakages for maximum agent effectiveness and proper mixing and distribution.
iv. The nozzle installation is designed to withstand the expected loads from the jets while ensuring safe interaction with the luggage space.
v. Special cones are designed as part of the nozzles installation in order to prevent any component from entering the compartment control volume and interacting with the luggage or personnel.
vi. Position of one of the nozzles close to outlet (worst case).

Nozzle pipe structure load calculation

The jet formed by the agent during discharge produces a force on the structure of the nozzle pipe. Each nozzle injects 6 jets of agent from 6 symmetrically placed circular orifices (see Figure 31). The orifice planes are placed at an angle of 15° compared to the vertical axis. The force generated by each jet and the total discharge force are calculated by the correlations below.

$$F_{jet} = \dot{m}_{jet} * V_{jet} + A_{orifice} * (P_{exit,S} - P_{atm}) \quad \text{3-48}$$

$$\dot{m}_{jet} = \frac{\dot{m}_N}{6} \quad \text{3-49}$$

$$V_{jet} = Mn_{exit} * \sqrt{\gamma * R * T_{exit,S}} \quad \text{3-50}$$

$$T_{exit,S} = \frac{T_{exit,T}}{1 + \frac{\gamma - 1}{2} * Mn_{exit}^2} \quad \text{3-51}$$

$$P_{exit,S} = \frac{P_{exit,T}}{((1 + \frac{\gamma - 1}{2} * Mn_{exit}^2)^{\gamma/\gamma - 1}} \quad \text{3-52}$$

$$\rho = \frac{P_S}{R * Ts} \quad \text{3-53}$$

$$A_{orifice} = \frac{\dot{m}_{jet}}{\rho * V_{jet}} \quad \text{3-54}$$

$$F_{vertical,jet} = F_{jet} * \sin 15° \text{ (jet vector at 105° angle from vertical axis)} \quad \text{3-55}$$

$$F_{nozzle} = 6 * F_{v,jet} \quad \text{3-56}$$

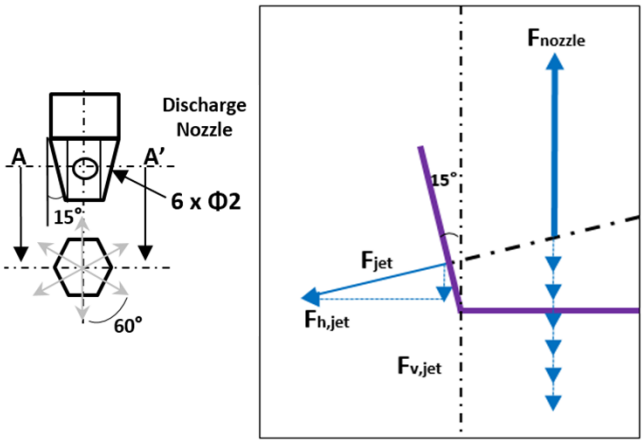

Figure 31 - Nozzle discharge force

In such geometry, the failure modes are determined considering some of the orifices being blocked.

System weight estimation

The system weight estimation is also an objective of the analytical approach. Weight is an important factor when aircraft applications are considered. Since most of the major components of the system have been sized, the weight can be estimated based on the storage cylinders and piping network dimensions, material properties, agent quantity and the masses of the rest of the components.

3.3.1.3 Ventilation System Design and Operation

The ventilation system was designed based on the enclosure dimensions, the MPS requirements and the agent properties. Since Nitrogen is the most demanding case in terms of agent quantity, the ventilation system sizing will result with a solution adequate for the complete range of potential replacement agents such as inert gases.

The leakages of the enclosure can be identified based on:

1. Door fan method (measuring pressure inside and outside of the door fan)
2. Gas tracer method (measuring agent concentration on time)

The Equivalence Leakage Area (ELA), which combines all the leakage paths through the enclosure, represents the theoretical area of a sharp-edged orifice that would be used if all incoming and outgoing flows of the enclosure at a given pressure were to pass solely through it. ELA was calculated targeting a limit value of overpressure using the door fan method approach [23].

Regarding experimental testing, U-shape tube is installed on the test rig in order to simulate the aircraft cargo door leakages (Figure 32). On the test rig, the U-shape tube is connected to a fan before exiting the enclosure. The fan is driven by a variable speed electric motor. The fan speed will be set to ensure that the targeted leakage rate is achieved before the agent discharge. FAA suggests that the targeted leakage is set according to confirmation testing conducted with the carbon di-oxide decay rate calculation. Since FAA was using Halon1301 as baseline, there was no need for another inlet to control the cargo overpressure. Based on that, the MPS suggested the use of only outlets (leakages), which resulted in under-pressurised enclosure when simulating aircraft cargo fire suppression system operation. This original design was applied to simulate the air entering the ‘cheek’ area as well as any leakages from doors or openings (see example in Figure 33). However, it was found that after a number of tests, the level of metal deformation to the U-shape tube can significantly alter its geometry (by FAA [7]). Thus, either the tube has to be replaced with a simple pressure relief outlet or its material has to be carefully selected.

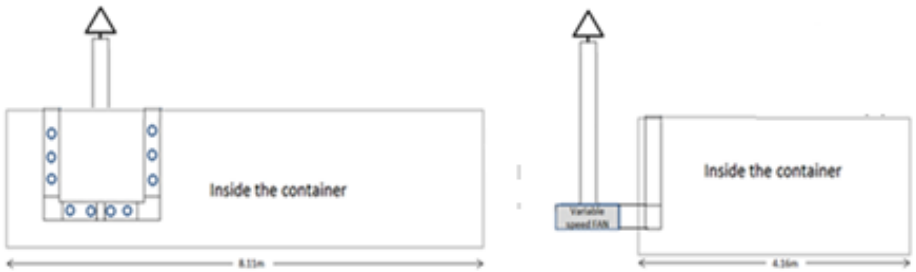

Figure 32 - Test rig ventilation system arrangement for Halon1301 (FAA)

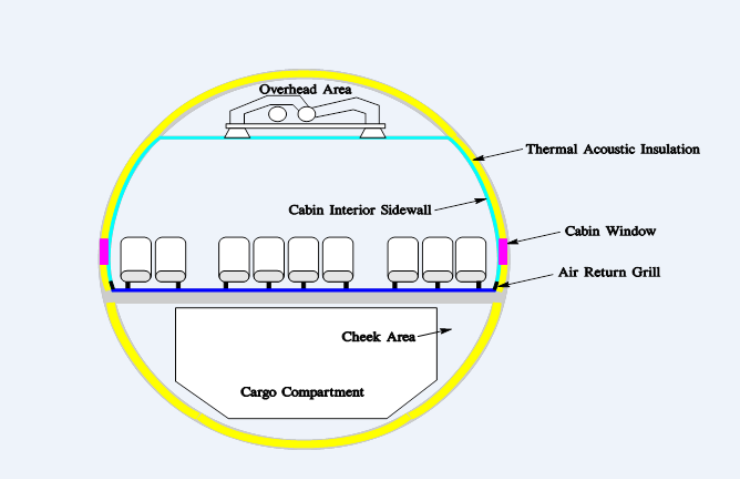

Figure 33 - MPS cargo arrangement case (Boeing arrangement)

However, based on the present research, it was found that in the case of Nitrogen there is need for an additional outlet port or an increase of the original (original diameter 0.084m based on MPS outlet area while maintaining the MPS leakage flow rates to control over-pressure inside the compartment during and after discharge. Considering increasing the existing outlet area would allow only for one function each time, either only as outlet or inlet. Thus, although it can potentially control the overpressure levels, it cannot fully represent the fire scenarios for aircraft cargo. Considering the additional outlet port can lead to a more accurate representation of the cargo pressurisation flow coming from the engine. As illustrated in Figure 34, the ventilation system arrangement should contain two ports, one outlet and one switching between inlet and outlet. The first port will be connected to the fan and act as the permanent outlet flows (leakages). The second will be open to the atmosphere and act as both inlet and outlet depending on the period of operation. During agent discharge, the system will modulate fan speed based on the pressure difference between inside and outside of the cargo. The location of the opening outlet/inlet was selected based on worst case scenario in terms of fire ignition or re-ignition and agent loss during discharge. This suggestion can be respectively applied to all possible cargo ventilation system architectures and agent acceptance capabilities when executing MPS tests, with minimum adaptations and modifications.

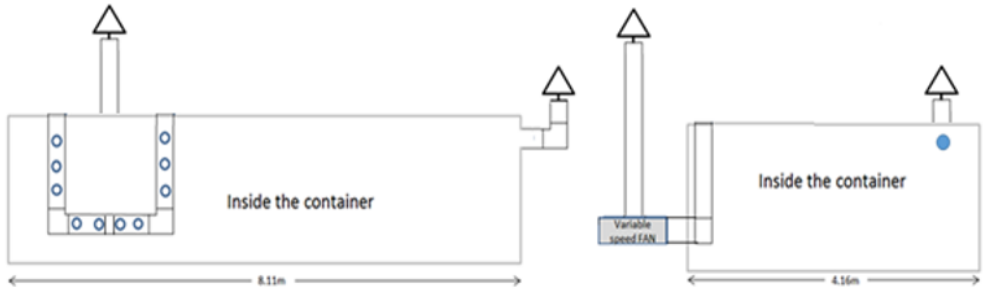

Figure 34 – Test rig ventilation system arrangement for Nitrogen

Finally, the addition of another pressure equalisation valve, sized for fire suppression purposes, has to be considered as it is a component already existing on-board current aircraft cargo systems.

3.3.2 Test Rig Design & Experimental Procedures Setup

3.3.2.1 Description of the Test Rig General Arrangement

The test rig arrangement is illustrated in Figure 35. The design was based on representative cargo dimensions. It can also be used as a preliminary design for the flying test bed or even the final system on-board the aircraft. The design method provides weight and effectiveness optimisation capabilities, while respecting all technical or certification constraints.

The system sizing was based on the case of an empty cargo compartment, which represents the most demanding scenario. Combining the criteria for uniform agent distribution and minimum system weight, the system design included three discharge nozzles, placed symmetrically on the rig roof centreline. Extra degrees of freedom are embedded on the piping network installation for potential future nozzle re-positioning.

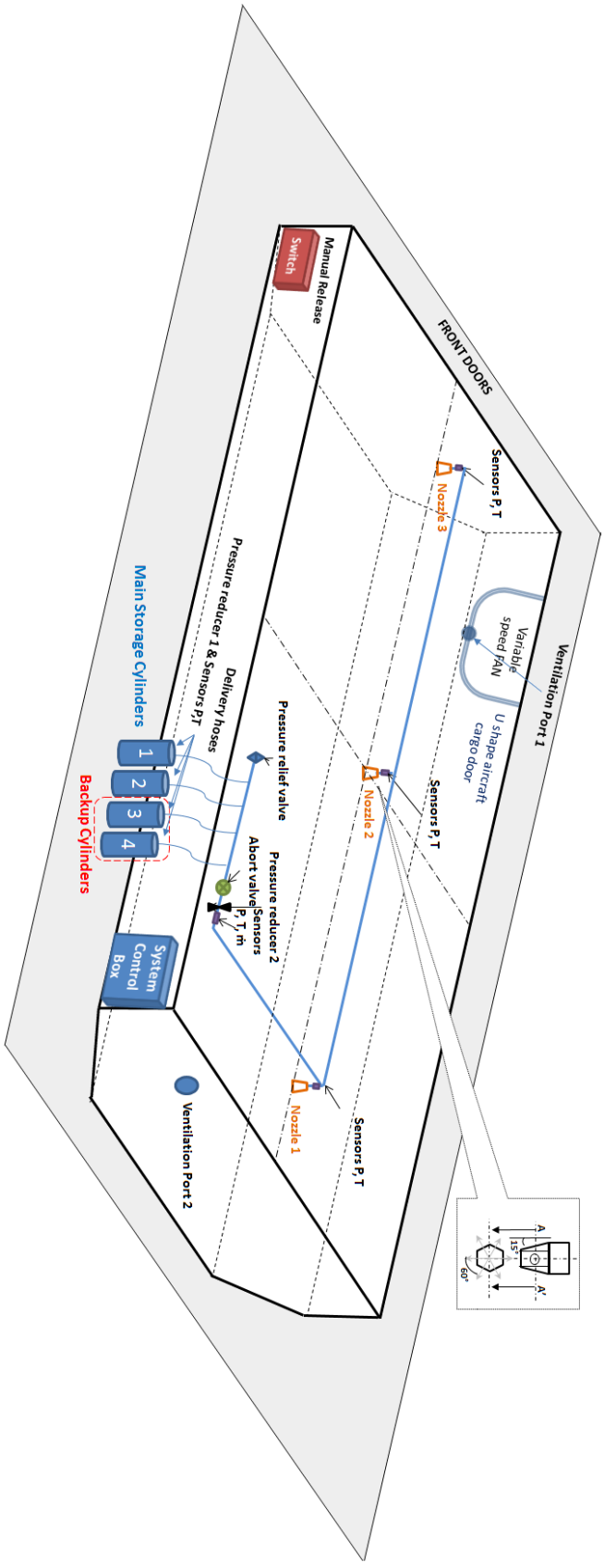

Figure 35 - Schematic of the system arrangement

The agent flow path begins with the 2 container cylinders. For safety reasons during experiments, 2 additional agent cylinders are installed in parallel on the test rig as a secondary system. Additionally, a pilot cylinder will be used for the system activation. This represents the pneumatic activation systems which are normally on-board the aircraft.

The main system is activated by smoke detectors or when one of the internal thermocouples reaches 93.33^0C (MPS). After system activation, the agent travels from the container cylinders, through the actuation valves to the delivery hoses. The cylinder actuation valves are also acting as high pressure reducers, dropping the pressure from 300bar to 100bar. Thus, the agent pressure within the delivery hoses will be 100bar.

The delivery hoses are connected to the piping manifold, which collects the agent flow from all cylinders. On one side, the manifold contains a pressure relief valve, in order to assure that high pressure agent will not enter the rest of the piping system. On the other side it is connected to a system abort valve, in case there is a need for urgent stoppage of the agent flow through the piping.

In a typical operating scenario, the abort valve will be normally open and the agent will flow directly towards the second and low pressure reducer, in order to drop the pressure to around 41bar. The pressure, temperature and flow capacity of the agent will be measured right after the second pressure reducer and their values will represent the boundary conditions for the agent flow through the main piping system.

The agent will then flow through the main piping, which reduces diameter each time the agent has to pass through a flow splitter (T-junction). This is due to the fact that at one of the junction's outlets, the agent will flow towards the discharge nozzle, while the other outlet will lead towards the next junction. In total, two T-junctions will be installed. After the agent reaches the second, it splits into two equal parts, each travelling towards its respective discharge nozzle. Finally, the agent is discharged through the orifices of each nozzle, forming a wide cone of 150° angle and covering the full circumferential. The system will continue the agent discharge until the cylinders drain-out.

After the agent is discharged, it mixes up with the air to achieve the design concentration and fills-up the enclosure. Although this creates the desirable turbulence levels which enhance mixing and distribution, the mixture eventually flows towards the outlet ports. The ventilation system is designed to regulate the flow exiting the enclosure relatively to the agent discharge rate. This is mainly to avoid overpressure during discharge while ensuring realistic leakage rates.

For the cases with cargo load, the discharge time will be adjusted in order to deliver the new requirement and maintain the same discharge effectiveness. Finally, for the simulation of flight conditions the variable speed fan will adjust the speed accordingly.

Additional considerations

A more detailed view on the discharge of Nitrogen separates the agent flow path from the storage cylinder into the piping and nozzles network in three stages [90]:

a. The initial transient phase as the gas flows into the piping and fills the pipes up to the nozzles.
b. The phase of agent discharge through the nozzles. This is a dynamic phenomenon, during which the agent flow rate initially increases from 0 to its design value and then it is maintained constant until just before the cylinders begin to drain-out. Additionally, the pressure also behaves similarly.
c. The final transient phase during which the system drains-out. The agent flow rate drops from its design value to 0. Additionally, the pressure, which is kept constant until the pressure limit value on the pressure reducer, progressively drops to atmospheric.

Discharge time and delays

Based on NFPA 2015, the discharge time is defined as time required achieving 95% of minimum design concentration for flame extinguishment using 15% safety factor and it shall not exceed 60sec. This time period is also defined as the required time period for the nozzles to discharge 95% of the agent mass (at 15°C) to achieve design concentration [90]. Exposure limits shall be applied depending on the agent (worst case scenario).

For example, for Nitrogen (IG-100) 5 minutes exposure [90] allowed for 40% design concentration inside the test rig according to NFPA 2004.

The time delays of the system operation could be separated into:

i. System activation delays

ii. Time delays for personnel evacuation before agent discharge (pre-discharge alarm)

iii. Time delays for area preparation

Finally, extra time delays should be applied in the cases of hazardous areas, subject to fast growth fires, where the lack of time delays would seriously increases the threat to human life and property.

3.3.2.2 System Controls, Indications and Measurements

Regarding the experimental procedures, the full scale experiments will be set based on the MPS. The system control, measurements and automation concept is illustrated in Figure 36.

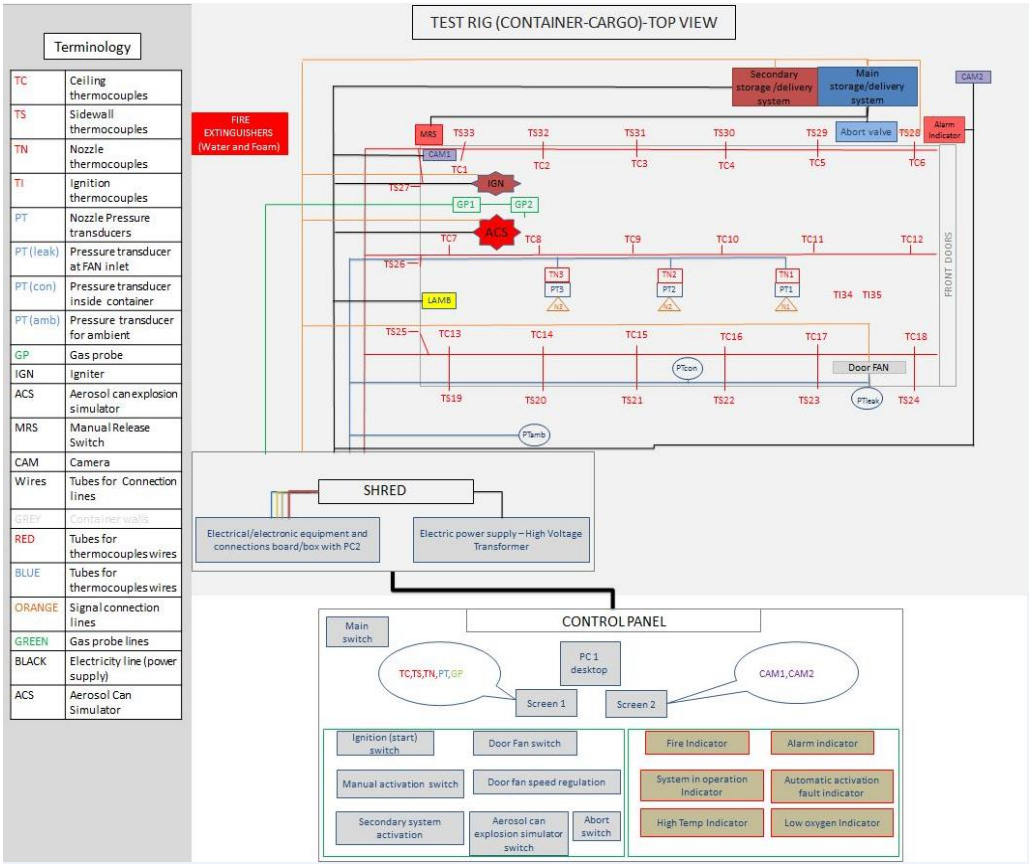

Figure 36 - Test rig control system arrangement

Main system operation and control

In any fire scenario, the fire will be ignited using the ignition switch on the main control panel (experiment start). For the aerosol can explosion case, after the ignition, the aerosol can simulator (ACS) will be released using the respective switch. The same switch will activate also the test rig rotating light (alarm indicator), in order to notify personnel that the experiment is on-going. As soon as the fire starts, the fire indicator will light up, signalling the operator to shut down the ignitor switch manually. The fire suppression system will be automatically activated when either one of the thermocouples (TC, TS) reaches at 93.3°C or when smoke reaches the smoke detector. During operation, the fire suppression system indicator light is on and the fire extinguishment agent is continuously discharged inside the compartment until the container bottles drains out.

For each experiment, the ventilation system is set to adjust the rotational speed of the door fan based on indications coming from the pressure transducers. Using the door fan switch, the rotational speed regulator is activated in order to achieve the desirable leakage rate. At the end of every successful experiment, the fire suppression system will shut down while the ventilation system will continue to operate until the room temperature and the oxygen concentration return to normal conditions. After the end of each experiment, a full hour has been selected as the appropriate amount of waiting time before the doors of the test rig can be opened.

The piping system will be compressed with air for leakage checks, while operation checks will be performed on system equipment and automations before the experiments begin.

Secondary system procedures

In case of system activation malfunction, the respective fault indicator will light up, informing the operator and activating the secondary system. The secondary system activation can be performed both automatically and manually. For the cases where the agent fails to extinguish the fire, the secondary system will be activated automatically using the high temperature indication sensor or manually based on the operator’s judgment.

Abort procedures

In case of failed ignition, the system programmed operation will be disrupted and the experiment will stop immediately. The supply line for electrical power will need to be replaced while the ignitor will need repositioning and the command switch thorough checking for malfunctions.

Additionally, an abort switch, accessible manually from the control panel, is installed for cases of undesirable outcomes of any nature which require immediate system shut down.

Emergency procedures

For cases where the temperature inside the test rig exceeds a predefined level, the high temperature indicator will light up. In this case the door fan will shut down in order to avoid feeding air to the fire.

For dangerously low oxygen concentrations, the respective indicator will light up. In this case, the abort switch will need to be used, along with the door fan speed regulator, in order to stop the agent discharge, increase the air inlet flow rate and restore oxygen concentration.

For uncontrolled fires, the secondary system will be also activated and depending on the fire scenario, additional manual water or foam fire extinguishers will be placed close to test rig.

Safety requirements

The alarm indicator will be on throughout the complete duration of the experiment, which is finished at least one hour after the fire extinguishment is achieved.

The personnel will be equipped with specific clothing, gloves, shoes and helmets during the test rig set up. No personnel will be allowed close to the test rig during the experiment.

After fire extinguishment is achieved, the temperature and oxygen concentration inside the enclosure must reach a level which is safe for humans before the test rig doors are allowed to open.

More details regarding safety analysis (risk and mitigation) and hazards classification and signs developed for MPS tests are presented in Appendices 7.2, 7.3.

Experimental measurements instrumentation and connections

Figure 36 illustrates both the required instrumentation for the experimental measurements and the main control panel. The test rig will be equipped with 33 thermocouples, 18 ceiling and 15 sidewall (TC and TS). Also, 3 thermocouples will be placed to the pipes close to the nozzles (TN). All thermocouples will pass through three main tubes (red lines) and will be connected to the hardware board/box. 6 pressure transducers will be installed, 3 for measuring the pressure in the pipes close to the nozzles, 1 for ambient pressure (barometric transducer), 1 for the volume inside the test ring and one for leakages close to the FAN. Like the thermocouples, through tubes (blue lines) the transducers wiring will be connected to the hardware board/box. The gas probes (GB) will be placed closed to the ignition (IGN) (figure shows only two gas probe locations) and connected with the hardware box (green lines). All the rest of the equipment will be fed with electric power, represented by the black lines, while the signal lines are shown in orange.

All the measurements (TC, TN, PT, GP, etc.) will be transferred to PC1 (Ethernet connection). In screen 1, using LabVIEW software, all recorder data will be displayed. Respective graphs will created such for the parameters of interest:

i. Compartment temperature vs time
ii. Agent concentration (or oxygen concentration) vs time
iii. Nozzle discharge pressure and temperature vs time
iv. Pressure inside the compartment vs time
v. Leakage flow rate vs time
vi. Agent mass flow discharge vs time
vii. Total agent quantity for every experiment

Finally, two cameras will be installed, one for fire/ignition verification inside the test rig (CAM1) and one for test rig safety precaution outside the test rig (CAM2). The second camera will be used for checks regarding the test rig surrounding

area, any approaching personnel during the experiments or other similar complications. Both cameras are to be displayed in Screen 2.

More details regarding the test rig, equipment and experimental procedures setup for the necessary MPS tests are presented in Appendices 7.4, 7.5 and 7.6

3.3.3 Numerical 3D-CFD Modelling

The numerical 3D-CFD modelling of aircraft cargo fire suppression systems in operation is the final task which completes the theoretical study of the system. Depending on the specific targets and the required level of fidelity, this task can become very challenging and time consuming. The specific targets set for the numerical models in order to meet the project objectives are:

1. Perform system design space exploration, investigating agent distribution and concentration inside the enclosure, while respecting the constraints on overpressure and leakages.
2. Prove that the model can achieve desired agent concentration within the targeted amount of time and maintained it for the required protection time
3. Prove that the model can be used for validation purposes against MPS experimental tests
4. Prove that the system doesn’t present any residual risk for human safety

From a system performance point of view, the numerical models are designed to provide information about the agent concentration and distribution in space and time, the cargo internal conditions and the ventilation properties. The methodology followed for the development of these models illustrates how numerical methods (steady-state and transient) can be used to support the overall fire suppression system design and operation. Additionally, it includes an effective method for 3D-CFD model validation with experimental measurements for aircraft cargo fire suppression system operation. Finally, the numerical model outcomes are compared to the analytical in order to verify the conceptual design and improve overall system architecture, performance and weight.

3.3.3.1 Case Study Setup

The computational simulations demand for the present research project is defined based on the nature of the problem and the current technology level. Besides cases involving fire/combustion simulations, current software capabilities dictate that for the specific project requirements, a relatively lower order of simulation fidelity is adequate. Simulations targeting volume-averaged values of the cargo conditions are enough to evaluate system effectiveness on possible fire threats during flight. The main conditions of interest are:

a. Cargo average overpressure
b. Cargo average agent concentration
c. Cargo leakages

The nature of the problem dictates that only a general knowledge of the flow-field inside the compartment is satisfactory for the assessment of the system design. There is no need for detailed flow-field analysis on surfaces or any potential pressure field for force generation calculations like in aerodynamic design cases. Thus, CFD simulations can offer relatively low cost and quick solutions for aircraft cargo fire suppression systems sizing and performance assessments.

The development of representative and accurate simulations for aircraft cargo fire suppression system operation can be separated into three subsequent steps:

1. System design and analysis: A top level approach using isolated models for testing the discharge performance of gaseous agents as well as the agent/air mixture flow behaviour inside cargo. In this step, a preliminary assessment of the computational cost of fire inside the enclosure is also performed.
2. Design space exploration and final selection: Parametric study, adaptations and selection of the final 3D-CFD models for verification against analytical and public domain data.
3. Model validation and calibration against experimental data

The numerical 3D-CFD modelling work was performed using ANSYS software. ANSYS 16.2 workbench contains geometry and mesh generator, solver (Fluent)

and results post-processing tools for complete 3D CFD simulation and analysis (see an example in Figure 37).

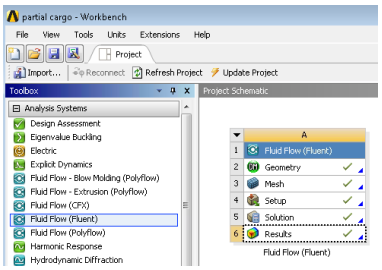

Figure 37 - ANSYS workbench software

Taking into account the software capabilities and the specifics of the present numerical problem, the model development processes were defined, along with the simulations setup [98-106] (see Figure below).

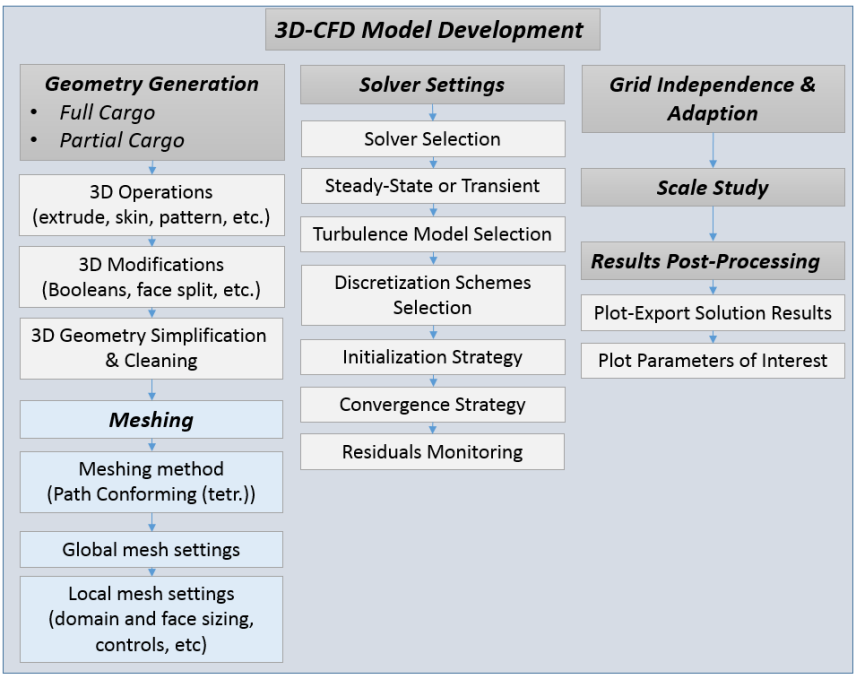

Figure 38 - CFD Models development

The complete operation of a fire suppression system on aircraft cargo includes the processes of:

i. agent delivery through the piping network
ii. agent discharge inside the enclosure
iii. fire ignition/extinguishment
iv. cargo ventilation

Although the agent delivery is one of the processes, it was excluded from the numerical simulations. The same applies also for the fire ignition/extinguishment processes. The reasons behind these decisions are:

1. Models complexity and computational cost inappropriate for the purposes and duration of the project
2. Cup burner and explosion screening vessel tests proved that at specific levels of agent concentration fire cannot occur
3. The nature of the problem doesn't require that level of fidelity, while their influence is not expected to provide significant improvement to the outcome

The agent discharge process has been separated in three main phases: a) from the start of discharge until the design mass flow is achieved, b) constant mass flow discharge period and b) cylinders drain out process. From these phases, the first is neglected as it is extremely fast and third is also excluded from the simulations due to reasons similar to those above. However, for the final models, the agent discharge duration at constant mass flow was increased in order to discharge the total amount of agent and achieve the same level of concentration as that of the analytical model. This way, the simulation including only the cargo ventilation and leakage process can start with boundary conditions similar to the analytical model, allowing for a direct comparison of the outputs. Nevertheless, although the agent discharge time at constant mass flow is increased, it still represents a pessimistic design in terms of fire protection time since the actual cylinder drain out process would last significantly longer compared to the extra discharge time at constant mass flow.

Based on the above, proving that the model can achieve the desired level of agent concentration provides a satisfactory level of certainty for the system fire suppression performance. Thus, only the agent discharge at constant mass flow rate and cargo ventilation processes are required for the numerical 3D-CFD simulations. Nevertheless, as part of the first step of development, small scale models including combustion of two different fuels (liquid and gas) were developed in order to access the model complexity and computational demand as well as the heat release and temperature profiles.

The control volume of the models was set to include the complete interior of the cargo compartment, the discharge nozzles and the ventilation ports. The simulation is set to begin when agent jets start to be ejected from the discharge nozzle outlets with constant mass flow, mix up with the surrounding air and diffuse in all directions inside the compartment. In addition, the simulation includes the operation after discharge and until the required protection time is reached, using the two ventilation ports representing the actual aircraft ventilation system.

Regarding model scaling, both full-scale and scaled models have been developed. This was done in an effort to reduce computational time and cost and avoid post-processing challenges, especially for the full-scale models transient simulations. For the same reason and based on geometrical symmetries, an additional ‘partial cargo’ model was developed with control volume a given fraction of the total cargo volume, covered by only one of the discharge nozzles. Finally, for the cases of loaded cargo, 30% of the complete volume of the cargo is covered with boxes as it would have in an average real mission. Thus, the numerical models developed are:

A. Full Cargo
    a. Full-scale
        i. Empty
        ii. Loaded 30% boxes
    b. Scaled
        i. Empty
        ii. Loaded 30% boxes
B. Partial Cargo
    a. Full-scale
    b. Scaled

The full cargo models aim to record the overpressure and agent concentration and distribution inside the enclosure. The partial cargo models aim to verify the boundary conditions coming from the analytical models and support the scale independence study as well as the full-scale simulations.

Finally, the numerical simulations are performed both in steady-state and transient modes. The steady-state mode simulations aim to record information regarding cargo conditions and verify the delivery, discharge and ventilation systems designs. The transient simulations aim to provide information about overpressure, agent concentration and distribution inside the enclosure as well as their evolution with time, both during and after discharge. The system goal is to achieve spatially uniform fire suppression concentration level within a given discharge duration and maintain it for a given protection time. Additionally, they aim to produce information regarding the nozzles and ventilation ports positioning in order to improve the overall system design and performance.

System Design & Analysis

At first, the numerical models development focused on two different agents: Nitrogen and Halon1301 (HFC-125 was excluded due to similarity). The initial models were designed to narrow down the design space of interest by providing information about boundary conditions and design selections. The simulation scenarios set for the initial phase of the numerical 3D-CFD modelling are listed below:

1. **Delivery & discharge system analytical design verification**. Based on the Halon1301 system design requirements, agent discharge pressure of 5bar was set for the initial steady-state simulations. Accounting for the boundary conditions and overpressure coming from the analytical model, the numerical 3D-CFD models were used to verify the design capability to satisfy the fire suppression scenario.
2. **System effectiveness and protection time estimation**. For all different agents tested here, the assessment of the system fire suppression and re-ignition avoidance capabilities is achieved through transient simulations on full cargo and partial cargo scaled, as well as full-scale partial cargo models. The discharge time for all these simulations was set for 10sec.
3. **Positioning of ventilation ports (leakages)**. For both full and partial cargo models, the agent/air mixture flow path was examined during discharge as well as the air inlet after discharge while maintaining the cargo overpressure

below 250Pa (10Pa for Halon1301). Through such steady-state simulations, the position of the nozzles as well as the ventilation ports inside the compartment can be assessed with respect to their effect on the system fire suppression and protection capabilities.

4. **Computational demand for fire simulations**. Two different fuels (Jet A and propane) were tested on a partial cargo scaled geometry to assess the computational cost of the combustion models.

The table below contains a summary of the simulation cases set up.

Table 25 - System Design & Analysis main set up

Design space setup for System Design & Analysis			
Parameter	**Comments**	**Case 1**	**Case 2**
Geometry	Full Cargo [FC] Partial Cargo [PC]	FC	PC
Scale		1:1	
Nozzles No.	#	8	1
Nozzle layout			
Simulation Mode	Steady-State [SS] Transient [TR]	SS	SS - TR
Discharge pressure	bar	5	
Discharge time	sec	10	
Leakage rate	lit/s	0.023	
Overpressure	Pa	10	
Ventilation ports No.	inlet [IN] outlet [OUT]	2 IN & 2 OUT	
Ventilation port diameter	inch	2	1

Design Space Exploration & Final Selection

In this phase of development, the system design space exploration is performed, the results of which led to the selection of the final models. The final models selected are:

1. Full Cargo – Full-scale – Empty – Steady-state
2. Full Cargo – Scaled – Empty – Transient
3. Full Cargo – Full-scale – Loaded 30% boxes – Steady-state
4. Full Cargo – Full-scale – Loaded 30% boxes – Transient

5. Partial Cargo – Full-scale – Empty – Steady-state

The final models selection was based on all criteria mentioned previously in this chapter, the overall system requirements (see Table 26) and the identified flow phenomena that occur in a typical cargo fire suppression scenario. Additional factors that influenced the decision were the capability to simulate accurately the MPS tests scenarios as well as the resulted model complexity and computational cost.

Table 26 - Overall System Performance Requirements

Parameter	Units	Value
Allowable discharge timeframe for successful extinguishment	seconds	60 - 120
Agent concentration requirement at 60 seconds	%	≥ 40.3
O_2 concentration requirement after agent bottles drain-out	%	≤ 12
Time required for O_2 concentration to reach 16% concentration, when the compartment suffers from a constant leakage rate of 23L/s	minutes	28

The system design space exploration was performed during the steady state simulations due to the significantly reduced complexity and computational cost. This was done by systematic modification of the design variables, in a parametric fashion, until the design satisfies all requirements. The main design variables are divided into 3 groups:

1. Number, location and size of discharge nozzles
2. Location, size and operation of cargo ventilation ports
3. Piping network arrangement and dimensions

The piping network and dimensions was not simulated in the numerical models and its design and weight were calculated analytically based on the setting of the first group of variables. The system technological constraints were based on existing state-of-the-art aircraft cargo systems. These are related to:

1. System number and type of components
2. System geometric characteristics (piping network, nozzles, ventilation ports)
3. Cargo overpressure limitation
4. Cargo Oxygen concentration limitation
5. Rapid discharge and fire suppression ($t_2 \rightarrow t_3$, 60 - 120sec)
6. Ensure extended fire protection time ($t_3 \rightarrow t_4$, 30min).

The steady state simulations were found to be adequate for the system sizing and satisfy most of the project's requirements. After narrowing down the available design space for such systems, the steady state simulations were used to refine the design of the nozzles and ventilation ports, in an effort to respect the overpressure limitation and achieve the desirable agent discharge conditions and distribution inside the enclosure before exiting through leakages. Thus, the main requirements of the system design can be met by using only steady state simulations.

Nevertheless, in order to assure that the agent concentration requirements inside the aircraft cargo, transient simulations of the system during operation are used. The transient simulations are used to further improve the system design to ensure that the targeted fire extinguishment and protection time requirements are met.

Figure 29 illustrates the time periods for the fire suppression system operation during a fire event. The steady state models simulate the system design point which was considered to be the instance of full agent discharge at the design mass flow rate. The targets set for the steady state simulations are summarised below:

1. Confirm system spatial arrangement/layout as well as nozzle and ventilation ports dimensions and positions ensuring safe operation and minimum agent leakages
2. Achieve desirable nozzle discharge pattern and cargo interior conditions for successful agent recirculation and distribution (such data will be used for analytical calculations of the piping network dimensions and weight)
3. Respect technological limitations:
    a. cargo interior overpressure lower than 1500Pa and 250Pa, during and after discharge respectively.
    b. cargo interior Oxygen concentration higher than 12%

The targets set for the transient simulations are:

1. Ensure the system capability to achieve the agent fire extinguishment design concentration levels inside the enclosure within 60sec.

2. Ensure the system capability to prevent fire ignition or re-ignition inside cargo for 30 minutes after fire detection.
3. Ensure acceptable cargo overpressure throughout the complete discharge duration and minimise leakage losses and thus total agent quantity required.

The rest time periods regarding the system response to a fire threat are excluded and will be evaluated during experimental tests.

As mentioned previously, the numerical models aim to support the test rig design and experimental procedures setup. Therefore, the computational cost must be controlled in order to minimise the simulations duration.

The table below contains a summary of the simulation cases set up

Table 27 - Design Space Exploration & Final Selection main set up

Design space setup for Design Space Exploration & Final Selection							
Parameter	**Comments**	**Case 3**	**Case 4**	**Case 5**	**Case 6**	**Case 7**	**Case 8**
Geometry	Full Cargo [FC & FC Load] Partial Cargo [PC]	FCL	PC	FC			
Scale		1:4	1:1		1:1 to 1:8	1:1	1:4
Nozzles No.	#	3	1	6-4-3	3		
Nozzle layout							
Simulation Mode	Steady-State [SS] Transient [TR]	TR	TR-SS	SS			TR
Discharge pressure	bar	5, 41		41			
Discharge time	sec	10, 60		60			
Leakage rate	lit/s	0.023					
Overpressure	Pa	10, 250		250			
Ventilation ports No.	inlet [IN] outlet [OUT]	1 IN & 1 OUT					
Ventilation port diameter	inch	6	2	6			

Model Validation & Calibration against Experimental Data

For the CFD model validation, the final cases are generated by updating the geometry and boundary conditions using the actual test rig specifications. The finalised and fully integrated test rig will provide information regarding technical limitations and the adaptations required for the CFD models. Additionally, considerations regarding the 'Joule-Thomson' effect on agent discharge temperature are taken into account in more detail. Finally, the solver is switched from ideal to real gas.

Both steady-state and transient simulations are used for the CFD model validation. Steady-state simulations require reduced computational power and time compared to the transient. However, they can only provide partial validation of the system due to their limited capabilities. The transient simulations on the other hand are costly and complex. Nevertheless, they provide a more detailed view of the system operation, adequate for complete system validation. Finally, if fire is included in the simulations, the models could provide the capability to simulate the phenomenon in more detail. However, since the increase in complexity and computational demand is significant, it was suggested for future studies.

The simulation cases selected to represent the experimental tests for aircraft cargo MPS fire suppression scenarios are:

1. Full cargo - empty
2. Full cargo - loaded 30% boxes
3. Partial cargo (1/3) - empty
4. Full cargo scaled (1/8) - empty
5. Full cargo scaled (1/8) – loaded 30% boxes

The above cases support also the design of the test rig the experimental tests. The outcomes of these CFD cases are used to finalise test rig design features such as ventilation ports and discharge nozzles positions and dimensions as well as operating parameters such as discharge pressures and mass flows.

The categories of the respective experimental tests required for the CFD models validation are:

1. Complete system operation on empty and loaded cargo without fire (MPS load 30% with boxes scenario)
2. System fire detection, suppression and protection times against solid fuels (MPS 30% boxes load fire scenario)
3. System fire detection, suppression and protection times against liquid fire (MPS Open fire or Surface burning fire scenario)
4. System fire detection, suppression and protection times against explosion (MPS Aerosol can explosion fire scenario)
5. System effectiveness against large container obstacles (MPS Containerized-Load fire test)

The first category refers to the tests designed for the test rig systems operational checks. In this category, the agent is discharged using the design values of pressure and discharge duration. Such tests can provide most of the validation data required for the CFD models as they represent fully the simulations. This category is designed to provide data regarding the effect of fire and the differences to the first category tests, the fire suppression system effectiveness and the protection time.

The next four categories refers to the system response and effectiveness against the main cargo fire challenges for solid, liquid, explosion and cargo covering with large containers fires. With this four categories the fire suppression system concept is completed proving its overall effectiveness on any cargo fires. The increase in number of this tests could result the desirable replacement fire suppression system

Finally, the outcomes of the experimental tests are compared to those of the CFD simulations and based on their differences, model calibration factors are generated in order to increase the accuracy of the simulations and the validity of the CFD models.

3.3.3.2 Geometry Development

The 3D cargo compartment geometry suggested in the MPS was the one used to model the aircraft cargo compartment. A sketch of the geometry containing the main dimensions, the forced ventilation system geometry and the positions for the temperature and pressure sensors as well as the proposed gas probes is presented in Figure 39. In the same figure, the shaded volume represents a portion of the cargo volume which can be assumed covered only by one of the discharge nozzles. Since in that case 8 nozzles were installed symmetrically inside the compartment in two rows of 4, the shaded area equals to the 1:8 of the total volume. In the final models developed for the present project, 3 nozzles were selected to be installed in a row at the centre of the compartment. Thus, the respective shaded area contains the 1:3 of the total cargo volume. Finally, the geometry selected for the loaded cargo cases was the same with the empty, with the only difference the existence of boxes, covering 30% of the total volume from bottom to top.

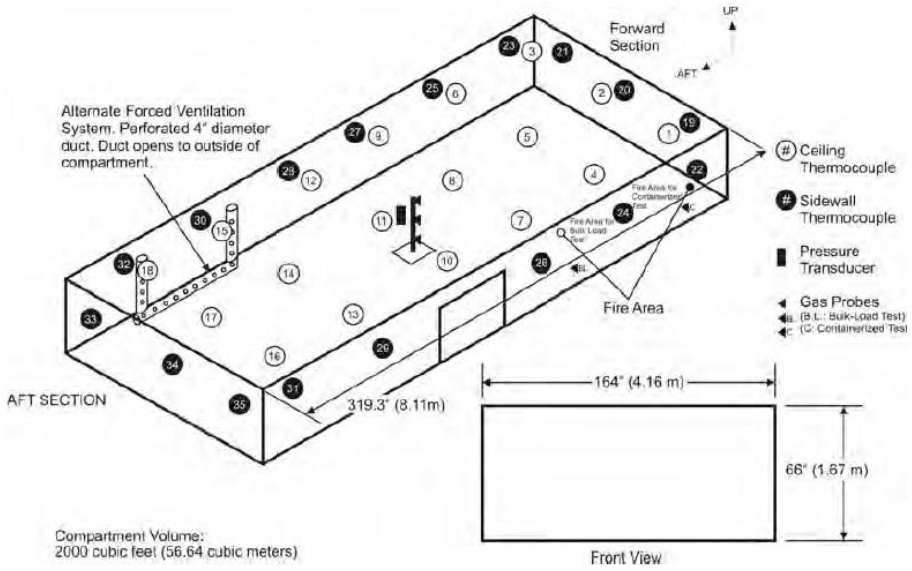

Figure 39 - Full and partial cargo volumes based on MPS [7]

Geometry Design & Setup using ANSYS

The software used for the development of the model geometries was the ANSYS design modeller. The geometry drawings were produced using a top-down

approach. The pre-processor software was the same to that used to create the mesh in order to avoid compatibility issues during meshing and simulation running. The computational domain was generated and further developed by applying logical operations on the geometrical shapes such as those used for the cargo interior, nozzle walls and ventilation ports. The basic operations required for geometry generation:

- ✓ **Extrude** , in order to generate 3D cargo rectangular shape, cylindrical nozzles and ventilation pipe from 2D drawings
- ✓ **Skin,** in order to create pyramid shape nozzles
- ✓ **Projection,** in order to project the circular orifices of the nozzle on the top of the ceiling wall surface representing the nozzle discharge jets. With this operation the installation cones were excluded and the nozzles geometry replaced with elliptical orifices as inlets.
- ✓ **Pattern**, in order to generate copies of the nozzle geometry and place them in different patterns on the enclosure geometry.
- ✓ **Face or volume split tool**, in order to develop separated geometry domains for walls, which are used for the mesh and solver modifications and settings.
- ✓ **Boolean**, in order to generate the full geometry as one part body and exclude mesh complexity preventing solver stability issues (no interfaces).The process followed in steps:
  a. Boolean /imprint feature 3 part bodies (nozzles) to the 4 part (cargo).
  b. Boolean/subtract feature 3 part bodies (nozzles) from the 4 part (cargo).
  c. Boolean/unite feature in order to unite all final parts and recognise the entire model as one part body.
- ✓ **Repair**, in order to check and repair geometry holes

Based on the outcomes of the initial phase of the numerical 3D-CFD models development and the results of the analytical modelling, the geometries suggested in the MPS were adapted. The modifications performed regarding model geometries include the identification of the appropriate number and location of discharge nozzles, the ventilation ports positions and the simulation of the door leakages. Each geometrical improvement performed aimed to increase the accuracy, stability, convergence and flexibility of the models.

The suggested MPS fire test scenarios are four. However, due to the geometric complexities, the containerised fire test case was deemed unsuitable for 3D-CFD simulations. The 3D-CFD models suitable to simulate the three scenarios are:

1. Full cargo – Empty
2. Full cargo –Loaded 30% boxes
3. Partial cargo

The modifications were applied to the model geometries in a subsequent progressive manner. For the first cases, the cargo interior was represented by a rectangular box, containing four symmetrically positioned air inlet and mixture outlet (leakages) ports (2 inlets, 2 outlets) as shown in Figure 40. This was done in an effort to force air recirculation inside the enclosure and enhance agent mixing and distribution. This fact combined with the relatively large number (8) of discharge nozzles selected for the first cases assures that the agent concentration inside the enclosure will result as uniform as possible.

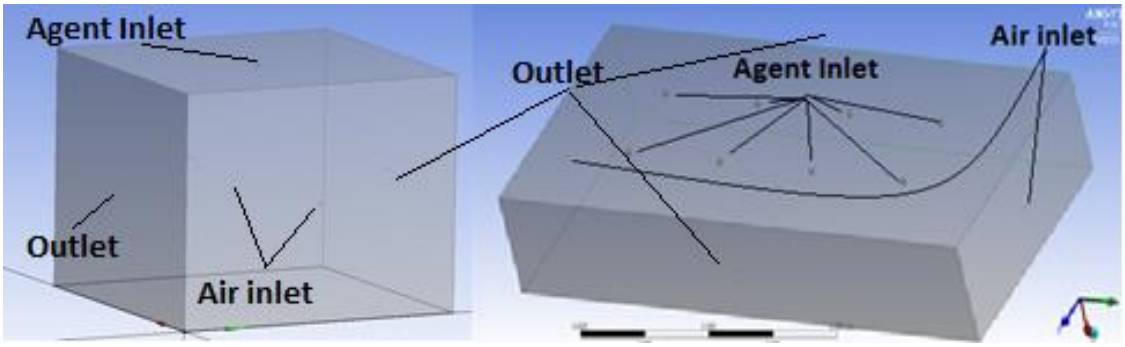

Figure 40 - Initial geometries for partial (left) and full (right) cargo models

The original Halon1301 nozzle designs (see Figure 41) were resized based on the tested agent properties, phase and concentration level target for a 10sec discharge. In the initial cases, 8 nozzles were placed symmetrically in two rows of 4 on the top of the ceiling, protruding inside the enclosure. This nozzle design contains seven orifices in total, six circumferentially and one vertically at the front face of the nozzle.

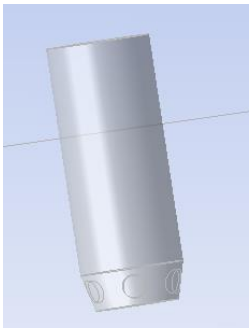

Figure 41 - Halon1301 original nozzle geometry

After the first set of simulations finished, a better understanding regarding the distribution capabilities of Nitrogen was gained. Thus, for the next step of development, the number of nozzles was then progressively reduced from 8 to 3, which was the number of nozzles current typical aircraft cargo systems have. The nozzle positions were adopted accordingly to assure uniform agent coverage. Furthermore, the air inlet and mixture outlet ports were reduced to 2 (1 for air inlet and 1 for the mixture outlet) for the cases of partial cargo models (Figure 42). For the full cargo models, the modifications for the door leakages and air inlet ports were based on the MPS (see Figure 43).

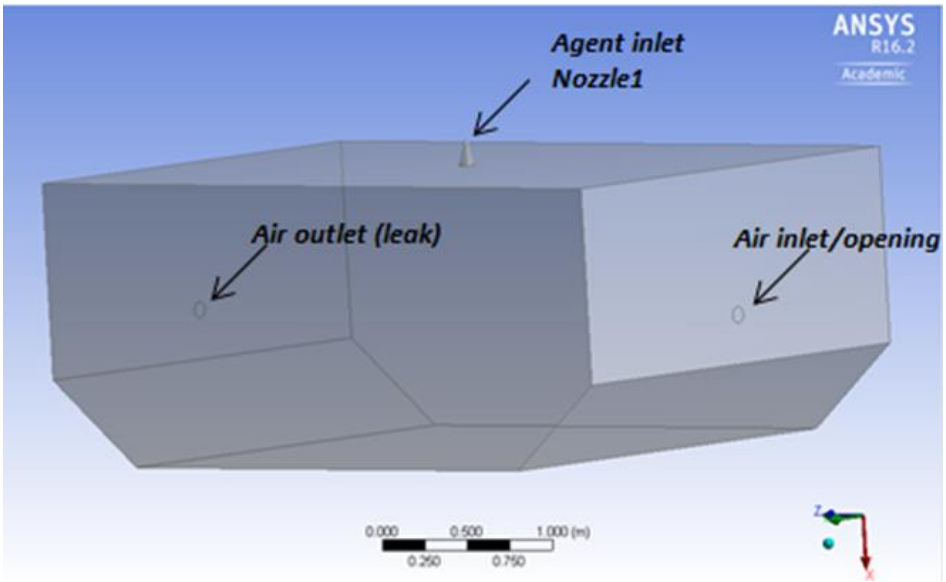

Figure 42 - Partial cargo air inlet and mixture outlet ports symmetric positions

Figure 43 - Full cargo model for the door leakages based on MPS

Based on the outcomes of the above cases, the geometry modifications were continued for all models. In the full cargo models, the tube resembling the door leakages and inlet ports was replaced with a slot of rectangular shape in an effort to simulate the actual door leakages more accurately (see Figure 44). Moreover, in all models, the nozzles were redesigned for the updated requirements resulted out of this study for a Nitrogen based system (60sec instead of 10sec discharge). Additionally, in order to avoid any tangling between the nozzles and the luggage or personnel, specifically designed nozzle installation cones have been attached on the top of the ceiling (see Figure 45). The final nozzle design contains six orifices around the circumference, achieving the same discharge angle and coverage area while removing the front face orifice existing in the original design. This decision was made in an effort to avoid any potential luggage damage or personnel injury during the discharge of high velocity jets, ejected vertically inside the enclosure.

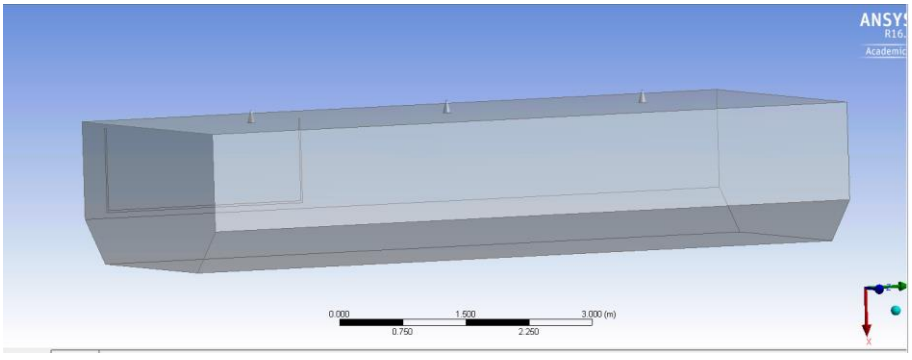

Figure 44 - Full cargo improved representation of the door leakage opening

Figure 45 - Discharge nozzle installation cone

The nozzle geometry modifications continued due to the fact that the outcomes of the simulated cases so far indicated that the meshing process, solver settings and simulations execution requires further improvement. By removing completely the installation cones and nozzles and replacing each one with six ellipses representing the cross-sectional area of the agent jets entering the control volume (see Figure 46). Assuming that the agent jets are cylindrical close to the orifices, the ellipses are a product of the cylindrical section with a 15° inclined plane. This was done in an effort to represent only the part of the jets that enters at a 15° angle in the control volume. Another important assumption taken into account is that the boundary conditions on the elliptical cross-sections are equal to those at the throat area of the nozzle orifices. This is an acceptable approximation as the cylindrical section plane was designed tangential to the nozzle orifices lowest points. This modification reduced the number of elements but most importantly removed model complexity, improving both solution convergence and calculation execution time. In addition, several geometries generated vary the location and number of nozzles to examine ventilation system and agent coverage.

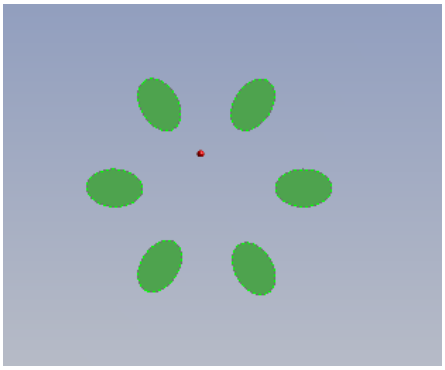

Figure 46 - Final nozzle representation as 6 elliptical orifices

Concluding, the geometries selected for the final simulations are presented in Figure 47 and all geometries general dimensions in Table 28

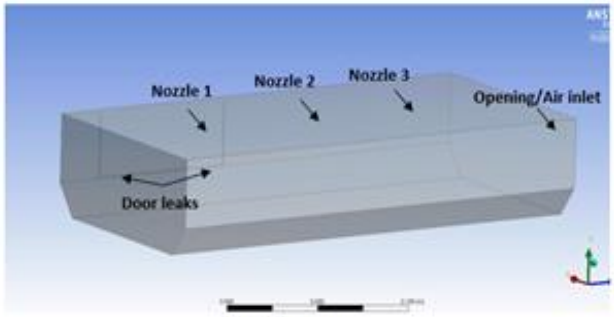

Full cargo

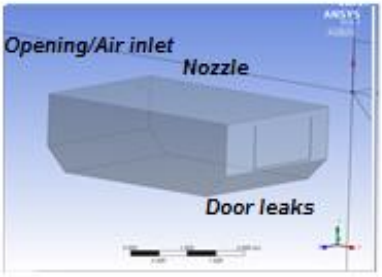

Partial cargo

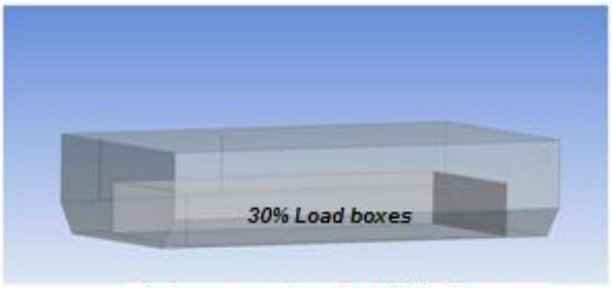

Full cargo- Loaded 30% boxes

- The scaled model provides better stability, less accuracy and ease in convergence

Figure 47 - Final numerical 3D-CFD model geometries

Table 28 - Geometries dimensions

Compartment	Length (m)	Width (m)	Height (m)	Volume (m^3)
Full Cargo	8.1	4.16	1.67	56.3 (54)[4]
Partial Cargo[1]	2.025	2.08	1.67	7.03
Partial Cargo[2]	2.7	4.16	1.67	18.8 (16)[4]
Full Cargo Loaded[3]	8.1	4.16	1.67	39.9
Cargo load boxes	6.8	2.7	0.9	16.4

[1]: 1/8 of the Full Cargo volume

[2]: 1/3 of the Full Cargo volume

[3]: 30% of the Full Cargo loaded with boxes

[4]: Cargo geometry- Rectangular shape excluding volume created from two sides inclined planes (more details regarding the incline sides could be seen in Figure 125)

Component	Diameter (m)	Num. of holes	Cone angle (º)	Num. of nozzles
Initial Nozzle[5,6]	0.01	7	15	8
Final Nozzle[7,8]	0.002	6	15	3
Symmetric inlets/outlets[5]	0.0508	4	Location mid-section	
Symmetric inlets/outlets[6]	0.0254	4		
Air inlet/ Opening[7]	0.0838	1	Location close to celling	
Air inlet/ Opening[8]	0.0308	1		
Component	Length (m)	Height (m)	Cone angle (º)	Gap size
Door leakages[7,8]	2.6	1.05	location MPS	0.002

[5]:Full Cargo initial case set up

[6]:Partial Cargo initial case set up

[7]:Full Cargo final case set up

[8]:Partial Cargo final case set up

Comment: For scale study all dimensions scaled down to 1/2, 1/4 and 1/8

3.3.3.3 Mesh Development

A bottom-up approach was followed during the mesh development using clean geometries and sizing subsequently the mesh cells edges, faces, volumes etc. Regarding mesh type, both structured and unstructured meshes were developed in order to assess their capabilities, solution accuracy and convergence rate. The unstructured meshes were generally found more suitable for the requirements of the present project.

The first setting regards the critical cell sizes near walls or areas of interest. This was based on the wall treatment method and the y^+ calculated values for: nozzles, floor, side walls, load walls and ceiling. Since the interest of the simulation is focused on the mixing rather than the forces on the walls, the main guides for the Y+ values suggest that [102]:

- First grid cell, $30< y^+<300$
- High-Re turbulence model for solver

The cell sizes for the majority of the control volume were set based on the size of the compartment and the target for minimum acceptable number of cells. The criteria of acceptance were adequate representation of the flow field and acceptable solution accuracy and computational time. The cell size needed to be large enough to reduce the number of cells, while respecting an acceptable maximum distance between cells. The maximum cell size reached 35mm. Finally, a consideration regarding the models flexibility to modifications was taken into account.

Path conforming algorithm method was used in order to develop tetrahedra cells with the acceptance quality ≥0.4 and skewness ≤0.65 according to the basic solver stability demands [99]. The automatic refinement was based on both curvature and proximity. The figures below illustrate the representative meshes during the development.

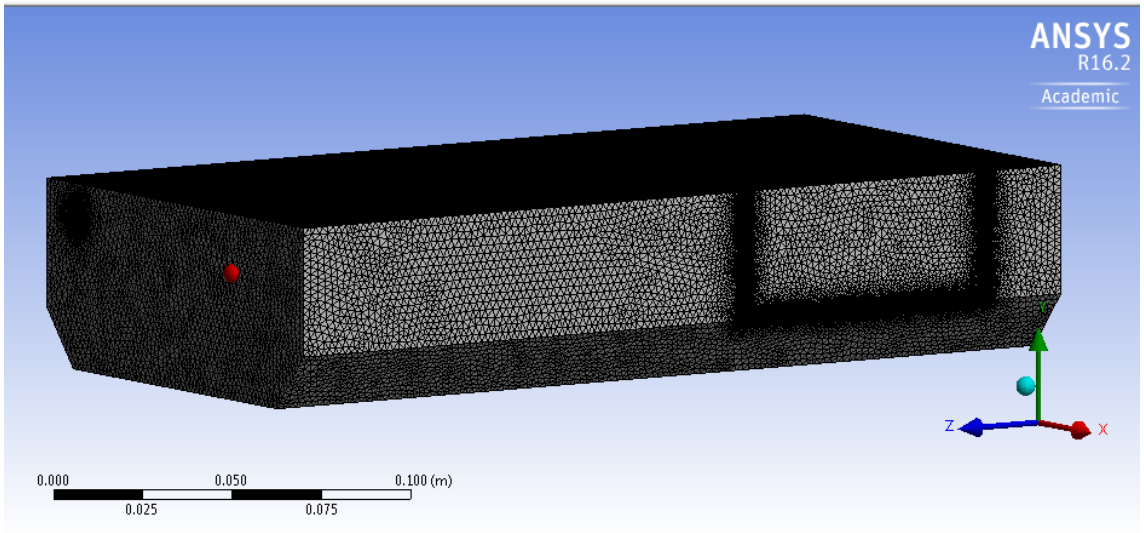

Figure 48 - Mesh of the empty full cargo model

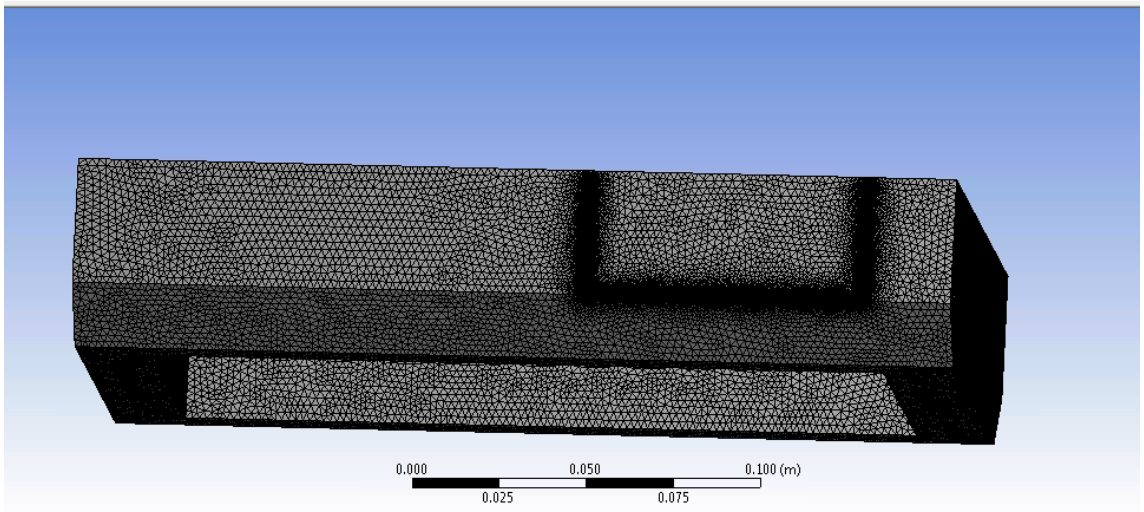

Figure 49 - Mesh of the loaded 30% full cargo model

The meshes were developed to be denser around and close to the nozzles ventilation ports, door leakages and walls. The figures below illustrate the meshes around the areas of interest.

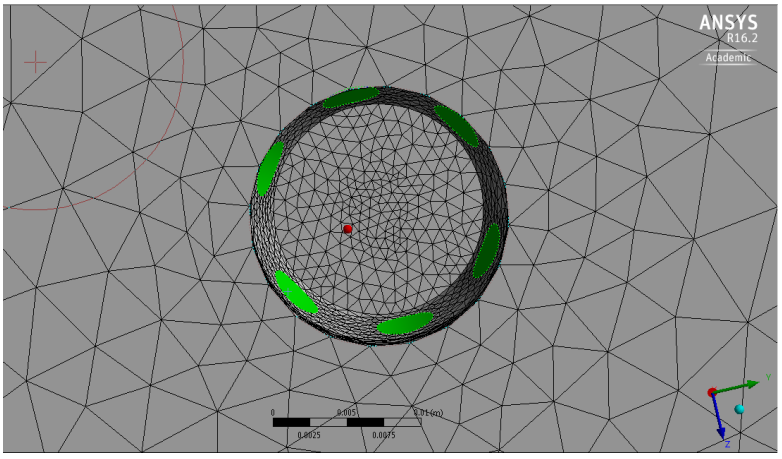

Figure 50 - Mesh around and close to the nozzle

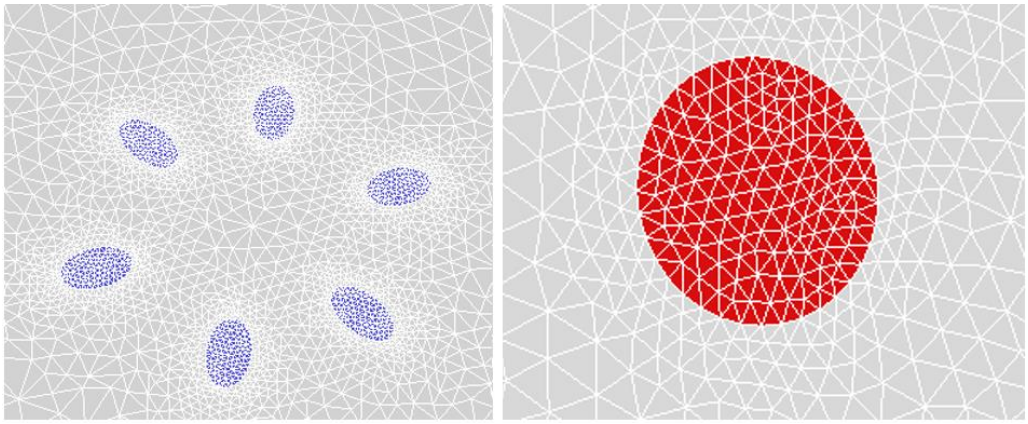

Figure 51 - Mesh close to discharge orifices and ventilation port

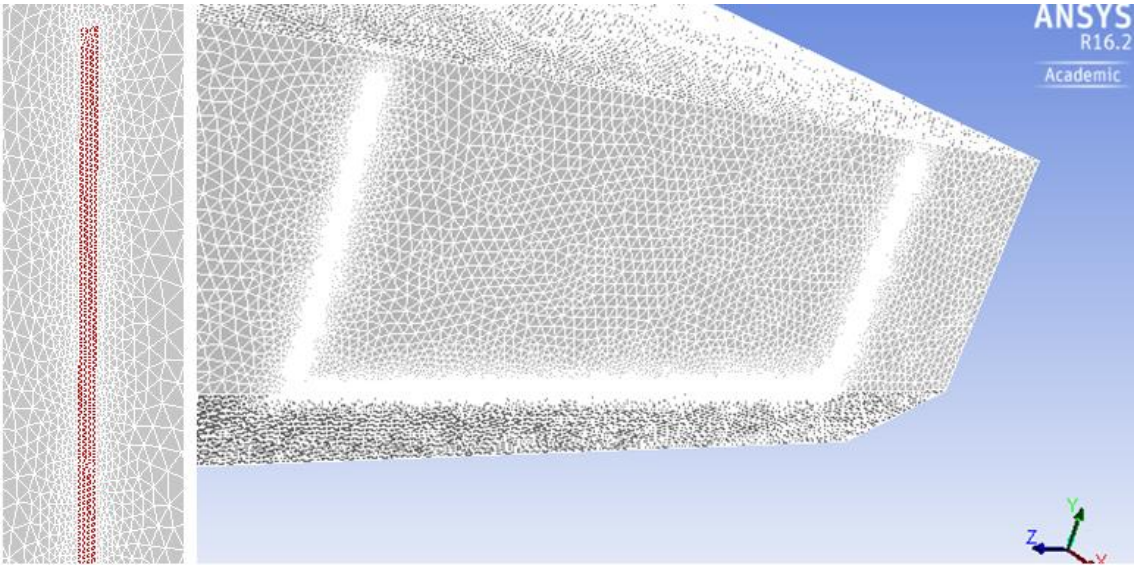

Figure 52 - Mesh close to the door leakages

3.3.3.4 Grid Independence & Adaptation

The grid independence study was performed following the steps below:

1. Generate new meshes subsequently, changing the cell size approximately 1.5 times at the time.
2. For each new mesh, use the solution-based adaptation approach in ANSYS for adaptation based on the original mesh.
3. After convergence is achieved, the results are compared between the meshes.

The convergence criteria were to achieve balanced residuals below 10^{-3} deviation with no fluctuations [101]. The process stopped when the improvement observed in the mesh results was lower than 0.1%. The minimum number of repetitions to achieve balanced residuals was approximately 200. Besides the main parameters of interest, the checks included the boundary conditions and mass and energy conservation.

The grid adaptation was performed in order to refine or coarsen the meshes and perform cell repair and local modifications, especially in the regions of interest. An illustration of the grid adaptation can be seen in Figure 53.

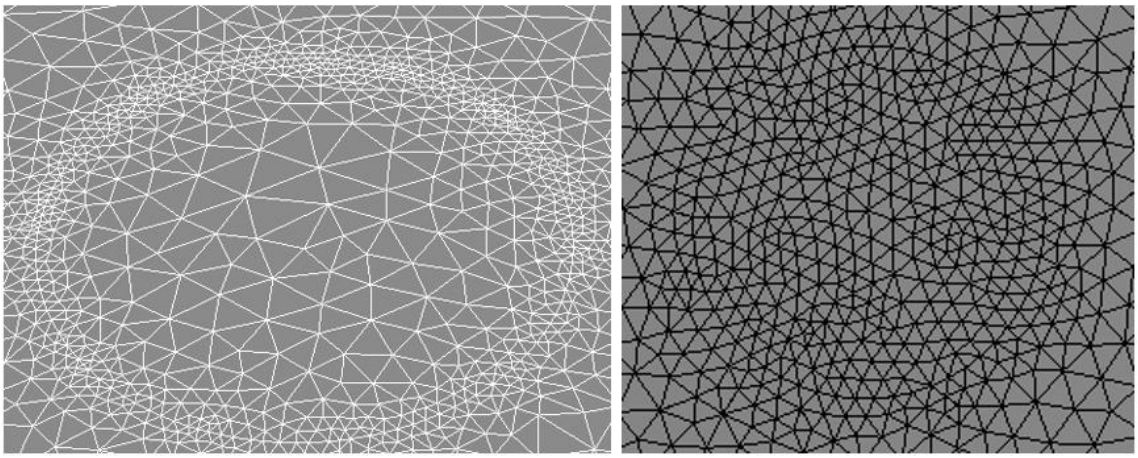

Figure 53 - Grid adaptation on the ventilation port (left: Before, right: After)

3.3.3.5 Model Scale Independence

The real size of the model is that of a typical aircraft cargo. From a simulation point of view, large volumes associate with many complexities such as stability

issues, high computational power demands, long running time and the respective challenges in results post-processing. These challenges become even more demanding in the case of transient simulations, especially for simulation cases with extended time duration. These challenges are the main reason behind the investigation performed on model scaling.

Two methods for model scaling were applied during the scale independence study:

1. Scaling of all dimensions of the original control volume
2. Identifying symmetries and use part of the original control volume

The acceptance criteria in this case are the same as those mentioned in the previous section for the grid independence. Additionally, appropriate sanity checks regarding the expected flow phenomena assured successful representation. For the dimensions scaling method, the effort focused on identifying the maximum acceptable cell size that can allow appropriate representation of the process of agent discharge in air. The original control volume was scaled by a factor of 2 to generate 3 subsequent scaled models (1:2, 1:4 and 1:8). This range of dimensions was selected based on the physical dimensions of the discharge nozzle orifices, which were in the order of 2mm. Dimensions smaller than the 1:8 were deemed comparable to the dimensions of the turbulent flow structures and thus inappropriate to fully represent the physical phenomena.

Regarding the division of the original control volume in a number of identical parts, the system symmetries were taken into account. The components defining the levels of symmetry and the number of identical parts are the discharge nozzles. Each discharge nozzle is simulated in isolation, with the domain it covers, including ventilation ports. Since the partial cargo models are in full-scale, they are of particular interest for the transient simulation cases where the computational demand increases substantially.

Finally, the value of the scaled models increases if both scaling methods are applied separately for the same original control volume and their outcomes are combined for a complete investigation of the system operation.

3.3.3.6 Solver Selection & Settings

The models are developed targeting solution stability, accuracy and speed while minimising the resources required. The available computational resources were 32GB RAM memory on a 4core desktop PC and Cranfield University super computer (for running large transient simulation).

The solvers available in ANSYS are two:

1. Pressure-Based Segregated or Coupled Solver (PBCS)
2. Density-Based Coupled Solver (DBCS)

The pressure-based segregated solver solves the fluid dynamics equations (mass continuity, momentum and energy) in a segregated manner. The PBCS represents the latest version of the pressure-based solver in ANSYS, solving the momentum and pressure-based continuity equations in a coupled manner (pressure-velocity coupling scheme). The Coupled algorithm was selected for steady-state simulations, which enables full pressure-velocity coupling scheme [102]. As for the transient simulations, the Pressure-Implicit with Splitting of Operators (PISO) pressure-velocity coupling scheme is preferable with relative large time step [101]. The DBCS was found more computationally expensive and since the PBCS and PISO were found suitable, it was not used. Table 29 presents some of the main computational properties of the available solvers [103].

Table 29 – Capabilities of ANSYS solvers [103]

Solver	Memory (MB)	Time per Iteration (seconds)	Iterations to Convergence	Time to Convergence (hours)
Segregated	172	2.10	2570	1.50
PBCS	259	3.26	298	0.27
DBCS	317	3.82	976	1.04

Additionally, the solution approach for the solvers can be either Implicit or Explicit. The Implicit approach is generally preferred to the Explicit, due to the very strict limit on time step size. The Explicit approach is usually used for cases where the

characteristic time scale of the flow is on the same order as the acoustic time scale.

The transport equations selected to simulate the agent flow through the orifices are based on the species transport model (non-reaction Eulerian approach for gases) using inlet diffusion. The turbulence specification method that was found to be suitable to describe the flow phenomena inside the enclosure was by setting the viscosity ratio and turbulence intensity.

Finally, the turbulence model families available are two: a) Reynolds Averaged Navier-Stokes (RANS) and b) Large Eddy Simulation (LES). The LES family represents a much higher simulation fidelity level, associated with high computational demand, which is not necessary for the purposes of the present project. The turbulence models available for the RANS simulations are: a) k-ε and b) k-ω. The flexible RANS Realizable k-ε turbulence model, used on coupled solvers, was proved to be sufficient for the simulation of single phase compressible flows discharged through orifices and diffused inside the control volume.

Taking into account the software capabilities, the physics of the problem and after testing all possible options, the final solver selections are:

1. Steady-state: PBCS – Explicit,
2. Transient: PBCS/PBS PISO-Implicit

The PBCS presented improved convergence time and reduced computational demands while achieving acceptable solution accuracy. However, it presented significant challenges regarding solution stability for the transient simulations. Thus, despite the penalty on solution accuracy, the PISO solver was chosen as it presented acceptable levels accuracy and stability.

Regarding the wall treatment, the scalable wall function was adequate for the simulation goals, providing improved stability. The Green-Gauss Node Based, second order upwind interpolation method provided improved solution accuracy and suitability for meshes using tetrahedra cells.

The solver general settings and main boundary conditions in Table 30 targeted to provide the verification capabilities against the analytical model that describes the physics of the problem. At this point, it is worth to mention that for model validation against experiments, the settings for gas properties need to change to Real Gas and mass-weighted mixing law, for improved model representation.

Table 30 - Main final case boundary conditions and solver settings for 3D-CFD models

A/a	Dimensions	Total Pressure (Bar)	Total Temperature (°C)
Full Cargo	8.11 x 4.16 x 1.67m = 56.34 m^3	1	15
Full Cargo baded 30% boxes	39.4 m^3	1	15
Partial Cargo	2.7 x 4.16 x 1.67 m = 18.78 m^3	1	15
Door fan	0.017 m^2	1	15
Air inlet	0.008 m^2	1	15
Nozzles discharge jets	6 Orifices, D = 0.002m	41	15
Fluent General Settings			
Steady state	Pressure based couple/explicit	Hybrid initialization	
Transient state	Pressure based PISO /implicit	Hybrid initialization	
Turbulence models	Species transport and k-ε	Scalable wall functions	
Discretization theme (interpolation method)	Green-Gauss Node based	Second-Order Upwind	
Mixture	Ideal gas (compressible flow)	Ideal gas mixing law	
Materials	Cp piecewise-polynomial	Kinetic theory	
Species	Nitrogen	Oxygen	

The time steps for transient simulations were set following the FLUENT [102] guides. For the agent discharge process, the time steps were $1.2*10^{-4}$sec for the full scale and $1.1*10^{-5}$sec for the scaled models. For the simulation after discharge, the scaled model time step was set to $2.5*10^{-4}$sec.

During the simulation processes, the solver settings are being systematically modified in order to reach the final cases. Table 30 presents also the main boundary conditions and general solver settings (More details on boundary conditions can be found in the next chapter). Finally, before launching the simulations, the mesh quality was improved using the respective FLUENT commands for this purpose.

3.3.3.7 Solution Monitoring & Convergence Strategy

In numerical iterative problems, a common way to measure their convergence is through observation of the so called *Residuals*. They represent the errors in the iterative solution of the system equations. As expected, if the residual errors result to be zero, then the solution is fully converged. However, for solutions coming from numerical iterative methods, the residuals would never reach zero. The solution convergence criteria are:

1. The residuals to reach a level of error acceptable for the nature of the problem
    a. Steady-state: x,y,z-momentum, continuity, k, ε $<10^{-4}$, energy $<10^{-6}$ and species $<10^{-5}$
    b. Transient: x,y,z-momentum, continuity, k, ε $<10^{-3}$, energy $<10^{-6}$ and species $<10^{-5}$
    c. Scaled Model Transient: x,y,z-momentum, continuity, k, ε $<10^{-4}$, energy $<10^{-6}$ and species $<10^{-5}$
2. The residuals to stabilize without presenting any peaks or periodic fluctuations for a specified number of iterations
3. Steady-state: Boundary conditions and mass/species conservation <0.1%
4. Transient: Boundary conditions and mass/species conservation <0.5%

The residuals monitoring represents the current method used in 3D-CFD simulations for solution progress tracking and convergence assessment. Typical acceptable level of error for a converged solution in any CFD case is 10^{-4} or less. Nevertheless, such levels of convergence are not always achievable and the selection of another limit falls to the judgment of the designer and the nature of the problem.

Fluent uses the Residuals Monitor Solution (RMS) to record the history of the flow characteristics (x, y, z velocity (momentum), energy, k, ε and species) and produce live images of the solution residuals.

Additionally to the RMS, several parameter monitors were placed to the models in order to record also all the parameters of interest for the project (see Figure 54). Such monitors where also used to verify boundary conditions, evaluate

solution and assess their compliance to physics and the theoretically expected outcomes.

1. Nozzles discharge total and static pressure,
2. Nozzles discharge total and static temperature
3. Nozzles discharge velocity
4. Nozzles discharge density
5. Nozzles discharge Mach number
6. Nozzles discharge turbulence ratio
7. Nozzles discharge ε
8. Nozzles discharge k
9. Nozzles discharge mass flow
10. Compartment total and static temperature
11. Compartment density
12. Outlet total and static pressure
13. Outlet total and static temperature
14. Outlet total and static pressure
15. Vent out/air inlet total and static pressure
16. Vent out/air inlet total and static temperature
17. Total inlet and total outlet mass flow
18. Cargo species mass fraction and molar concentration

Figure 54 - Additional monitor parameters

The initialisation strategy using the FLUENT hybrid method was proved to be suitable for the specific problem, providing improved accuracy and confidence that the outcome is correct. This was due to the fact that this strategy complies with the compressible nature of the flow.

The approach followed in order to initialise the simulations was the one suggested in FLUENT for hybrid initialisation of high velocity compressible flows. The under-relaxation factors were estimated respectively to the flow limitations and cell sizes, with the density factor set to 0.9 [102]. This was done in order to initialize the solution preventing instabilities and improving convergence.

For the steady-state cases, during the simulations, the Flow Courant Number was progressively reduced in order to accelerate solution convergence [106]. For the simulation of the process after the discharge stops, the initialization was performed using the outlet conditions. The Flow Courant Number for the transient cases was set based on the appropriate selection of the time step for each specific case [101, 102]. The boundary conditions, cell size and geometry of each case are the main parameters considered. For the simulation of both phases of the system operation, after the completion of the agent discharge the simulation stops, solution boundaries and time step are adjusted and the new simulation without discharge begins (incompressible flow). A constant leakage rate of $0.023m^3$/sec was set to door outlet until the end of the simulation. Table 31

presents the selected settings for the explicit, implicit and under-relaxation factors.

Table 31 - Solver general settings

Steady State Pressure Based Pressure-Velocity couple						
	Explicit Relaxation Factors		Under-Relaxation Factors			
Flow Currant Number	Momentum	Pressure	Density	Body Forces	Turbulent Viscosity	Energy
200	0.3	0.4	0.9	1	0.9	1
Courant number reduced to 50 to accelerate convergence			Turbulent Kinetic Energy	Turbulent Dissipation Rate	Nitrogen Species	Oxygen Species
			0.7	0.7	1	1
Transient Density Based Pressure-Velocity couple						
	Implicit Relaxation factors		Under-Relaxation factors			
	Momentum	Pressure	Density	Body Forces	Turbulent Viscosity	Energy
	0.6	0.7	0.9	1	0.9	1
Courant number seleted respecting boundary conditions, time step size and flow characteristics			Turbulent Kinetic Energy	Turbulent Dissipation Rate	Nitrogen Species	Oxygen Species
			0.7	0.7	1	1

Generally, the resulted mesh size was relative large and thus the models are more susceptible to simulation inaccuracies/instabilities. Using common practices, the actions performed to achieve successful problem initialisation are based on the progressive running of subsequent simulations, refining the initialisation guesses each time, and checking solution accuracy and converge [101]. Furthermore, regarding the solver settings for the flow inlets in the control volume, mass flow was the control parameter selected in order to achieve smooth initialisation, after which it is switched to pressure in order to prevent simulation instabilities (follows more appropriate solution strategy, commonly used for flow velocities close to Mn=1).

3.3.3.8 Results Post-Process Analysis

The CFD models setup for the outputs recording was aligned to the outcomes of the analytical model as well as the instrumentation setup on the test rig for comparison purposes. The selection of the locations of interest was based on considerations for adequate mapping of the test rig interior conditions. The measurement locations for gas flows (gas probe), pressures (pressure transducers) and temperatures (thermocouples) inside the test rig as well as the fire ignition locations define the necessary locations for the interior flow characterisation. Thus, they were also selected for the CFD simulations outputs recording. The parameters of interest were selected based on the MPS requirements and the analytical model setup.

The recording of the CFD outputs regarding the system critical operating parameters at the locations of interest provides the capability to assess the

system fire suppression effectiveness, verify it against public domain data and validate it against experimental data. A list presenting the CFD recorded critical parameters in more detail, along with their locations, is presented below:

1. Cargo internal mass-weighted average pressure, temperature (total and static) and density
    a. Location: Complete control volume
2. Cargo internal agent mass-weighted average concentration
    a. Location: 4 horizontal planes, the first at 0.35 m from the floor and then the rest every 0.4m
3. Nozzles discharge pressure and temperature (total and static)
    a. Location: Nozzle discharge orifices
4. Nozzles discharge velocity, Mach number and density
    a. Location: Nozzle discharge orifices
5. Agent concentration at the fire ignition point
    a. Location: 0.35m from the floor for loaded cargo
    b. Location: 0.305m from the floor for open surface fire
    c. Location: 0.61m from the floor for aerosol can explosion
6. Pressure, temperature (total and static) and mass flow
    a. Location: Ventilation port
    b. Location: Door leakages

Recording the cargo internal mass-weighted average gas properties is essential in order to verify that the model produces results close to the theoretically expected coming from the analytical models. For similar reasons, the conditions of discharge at the nozzle orifices are also of great importance. Besides the obvious parameters and locations, the author has included the recording of the agent concentration close to the fire ignition point, which is considered one of the critical locations inside the enclosure. Additionally, the selection of 4 representative planes to record the agent concentration was based on the location of the thermocouples, pressure transducers and gas probe inside the test rig. Finally, the gas conditions at the inlet and outlet ports and door leakages are recorded for reasons similar to the previous parameters, as well as for verification of the ventilation system design for overpressure avoidance.

Regarding software availability, both methods offered in FLUENT for results post-processing are used:

1. FLUENT Legacy version post-processing tools
2. ANSYS CFD-Post application (workbench)

3.3.4 Model Verification/Validation & Calibration with Experiments

The achievable levels of solution fidelity and model credibility for 3D-CFD numerical simulations are case sensitive. In order to quantify and assess them, the 3D-CFD models must be designed targeting adequate representation of the real scenarios. An adequate representation is characterised through the verification, validation and calibration processes.

Verification is the process of determining if a model implementation accurately represents the developer's conceptual description, complies with first principles and produces theoretically expected solutions. It is performed through comparisons between the CFD model outputs and theoretical/analytical model outputs or respective experimental outputs. On the other hand, validation refers to the process of determining the degree of which a model can capture real world effects. In order to perform a validation process for CFD models, experimental measurements or in-flight recorded data are required. Comparisons between the CFD model outputs and data coming from sensors and generally instrumentation are used for this purpose. If the verification and validation processes are completed successfully, the CFD model could be used to represent reality at a satisfactory order of fidelity and credibility.

The validation process outcomes are designed to provide an insight on the CFD model ability to reproduce the real measurements. In case of success, the experimental data are then used to perform CFD models calibration. Model calibration focuses on the evaluation of a variety of appropriate metrics, used for measuring the consistency of a given CFD model solution with experimental data. Both errors and uncertainties of these metrics will be quantified in order to align the CFD model output to experiments or real scenarios.

The model verification criteria were based on respective experimental studies found on the public domain, the analytical model design and the theoretically expected flow phenomena. The list below presents the necessary monitoring parameters along with the components they refer to:

1. Agent discharge properties and required quantity
    a. Storage cylinders, piping network and nozzle dimensions verification
2. Agent mixing and distribution capabilities through velocity contours
    a. Nozzle dimensions, discharge angle and location and ventilation ports locations verification
3. Flow-field streamline observations of the agent flow path and enclosure coverage capability before exiting through the ventilation ports
    a. Number and location of nozzles and ventilation ports verification
4. Cargo mass-weighted average pressure and temperature
    a. Ventilation inlet/outlet ports dimensions verification
5. Cargo mass-weighted agent concentration at the vicinity of the ignition point, as well as at 3 additional points as described in Section 3.3.2.2
    a. Agent storage and delivery system dimensions, fire extinguishment effectiveness and protection time verification
6. Turbulence level (Re number) of all inlets and outlets of the enclosure
    a. Observations for turbulence level verification

Since the model validation depends on the data coming from experiments or real scenarios, a top level assessment on the achievable level of fidelity and credibility of the measurements is required. Aircraft cargo compartment typical sizes range between 30 – 120m^3. Such large volumes present significant technical challenges when trying to record in detail spatial ambient properties for the entire enclosure. A large number of sensors is required, while their available locations inside the enclosure are not enough to fully cover the control volume and capture in detail conditions and flow phenomena. Additionally, the technology level of the available instrumentation along with the measurement technics applied further increase the level of difficulty to represent reality. This would result in an increased number of experiments necessary to capture the desired phenomena at an acceptable level of fidelity. Nevertheless, the system controls, indications

and measurements setup presented in Section 3.3.2.2 is designed to minimise the required number of experiments needed for validation.

Focusing on the test rig design and experimental setup presented in Section 3.3.2, the expected mapping of the recorded properties is limited and focuses on specific areas of the compartment. This limits the CFD model validation capabilities to only capturing a reduced number of properties and on specific locations. Thus, careful selection of the properties to be monitored as well as strategic placement of both instrumentation sensors and CFD model solution recording points are needed in order to increase the levels of fidelity and credibility. The above selections also depend on considerations regarding computational time and model flexibility to adaptations, in an effort to generate a practical and user-friendly model. Figure 55 illustrates the envisaged model validation and calibration approach.

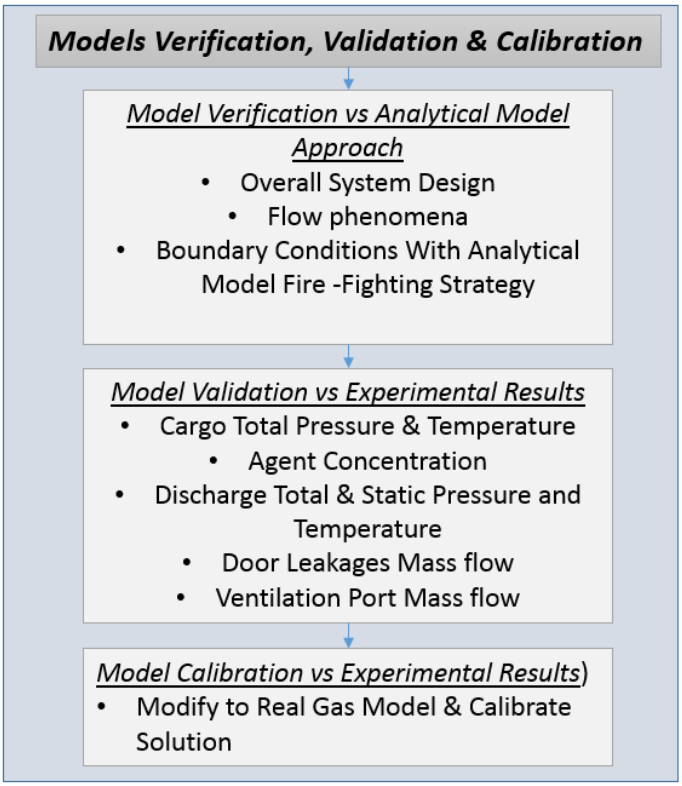

Figure 55 - General approach for CFD fidelity and credibility assessments

4 RESULTS & DISCUSSION

This section contains the main outcomes of the present research project and follows the same structure as that in the methodology section.

4.1 Preliminary Approach Outcomes

The initial part of the study includes the preliminary approach. The results coming from the analytical models for Halon1301, HFC-125, Nitrogen and water vapour are presented herein. The calculated values for the agent mass required to reach the targeted level of concentration inside each enclosure volume are presented in Figure 56. The relationship between the agent total quantity and the achieved agent concentration for each specific compartment volume illustrates the impact of the selected agent design concentration on the system size and weight.

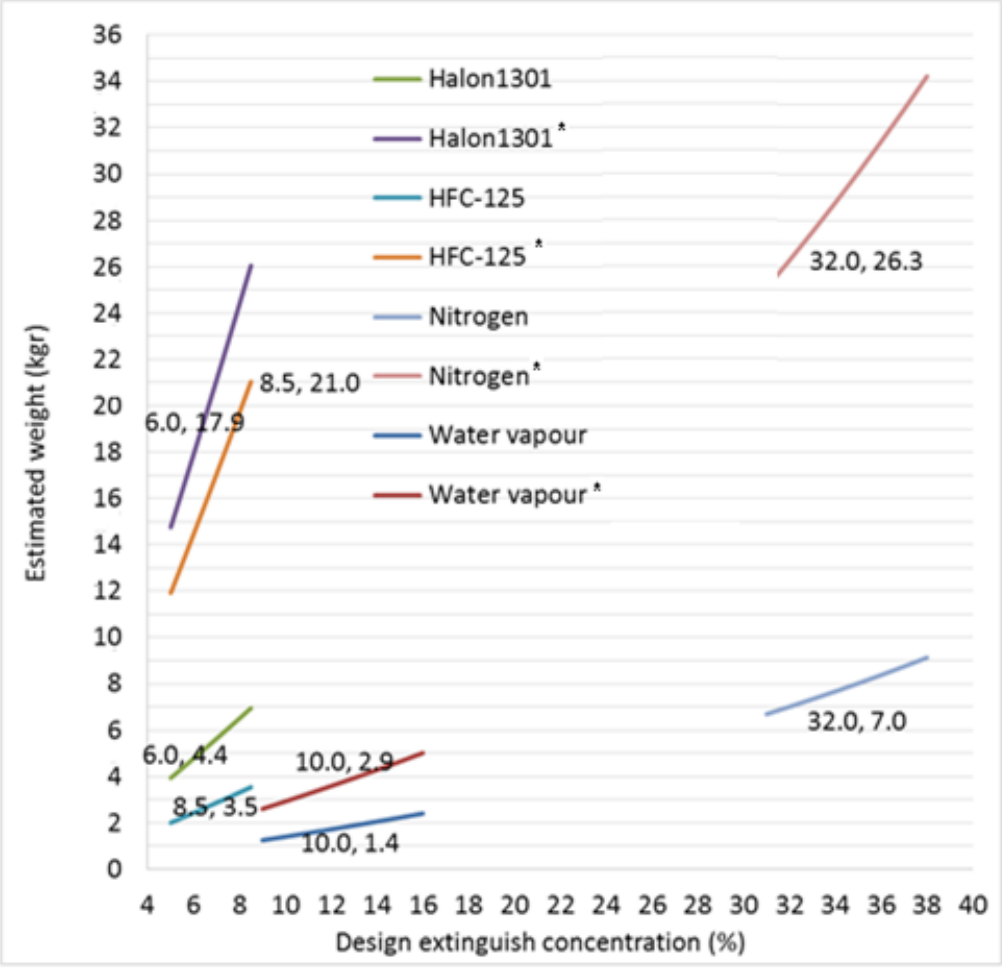

Figure 56 - Estimated agent weight against concentration inside the enclosure (full cargo (*) and partial cargo)

The results show that there is an order of magnitude difference between the quantities required for Full cargo and Partial cargo volumes. For each individual volume, the quantities calculated to achieve the required level of concentration for Halon1301, HFC-125 and Nitrogen are at a similar order of magnitude and thus the weight penalties associated are expected to be similar. However, the case of Nitrogen requires special attention due to the challenging storage and handling, which introduce extra weight penalties. For the water vapour case, the above method underestimates the quantity needed. The quality of the water vapour selected, was based on current water nozzle technology. The indicative value of concentration came out of test measurements near the fire region [5]. Although the concentration value is correct, the calculation of the quantity of water required to achieve it should capture the water quantity that gets condensed on the surrounding surfaces. Improvements on the water based method are planned for the future systems. However, they fall out of the scope of the present study. Nevertheless, the figure above can be used to derive boundary conditions regarding agent mass flow rates.

Targeting a specific value of concentration and activation time, the agent mass flow rate can be estimated. Figure 57 illustrates the agent concentration during the 10 seconds activation time. The system design considers the Halon1301 activation time of 10 seconds as baseline, while depending on the agent effectiveness this duration can vary. The target is to achieve the desirable concentration inside the enclosure as soon as possible. The selected mass flow rates will be used in the CFD simulations in order to evaluate the agent distribution, the air infiltration and the leakage flows. The evaluation through CFD simulations will include also the phase after the system deactivation and until the Oxygen concentration returns to 16%.

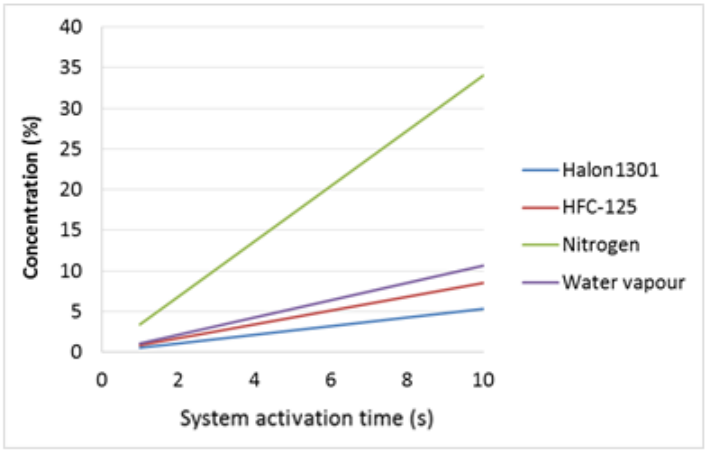

Figure 57 - Agent concentration for 10 seconds system activation

For different system activation times, the mass flows for the Halon compounds vary following the correlations presented in Figure 58 and Figure 59.

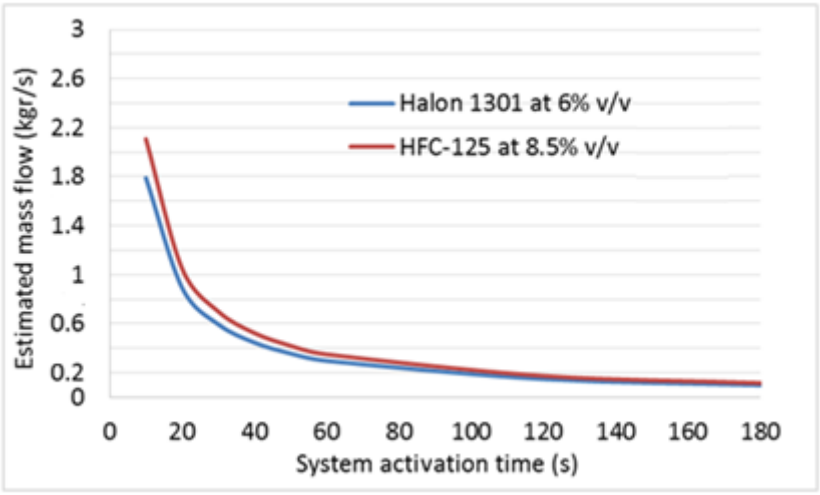

Figure 58 - Estimated mass flow rate versus system activation time for Full cargo

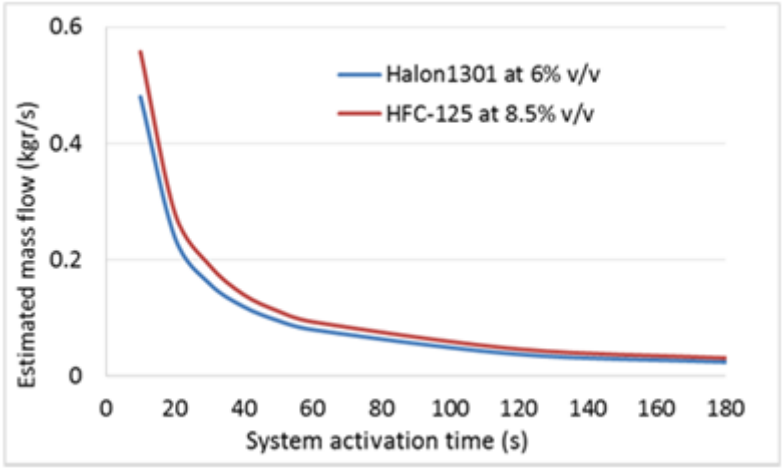

Figure 59 - Estimated mass flow rate versus system activation time for Partial cargo

The results from the analytical model of the compartment filling process are presented in Figure 60. An interface layer is assumed that separates the agent mixture from the pure air. The agent concentration is presented against the compartment height reached, assuming a “bottom to top” filling process. For the Halon1301 case, the interface layer formed reaches a height of 20cm for 100% agent concentration and as the filling up continues the agent spreads upwards reducing its concentration. This system has been designed to reach the required agent concentration at 90% of the available height.

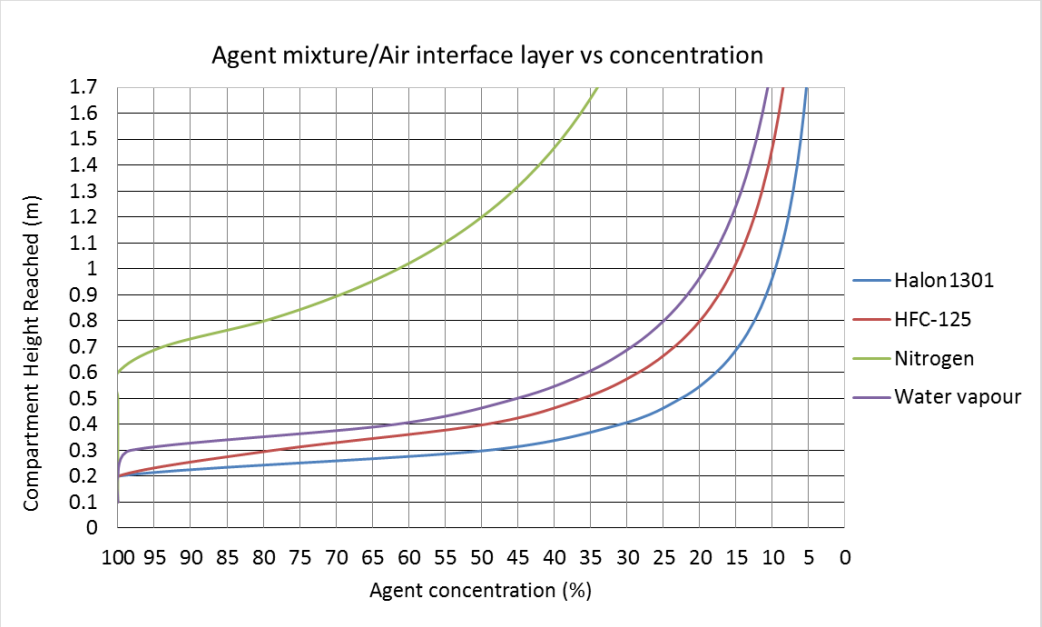

Figure 60 - Agent concentration versus height reached

The agent concentration inside the compartment after the system deactivation reduces with time. This is due to the leakages imposed to the model. The evolution of the agent concentration with time, after the system deactivation, is presented in Figure 61. The agent discharge must be designed to maintain the minimum required concentration level for 28 minutes (time indicated for MPS tests duration, without the 2 minutes activation time). Thus, the minimum required concentration during system activation for each agent was set to satisfy this time target. However, in the case of Nitrogen, the fixed value used for the constant leakage rate caused a quicker reduction in agent concentration than targeted. Thus, leakage rate control might be essential for the case of Nitrogen.

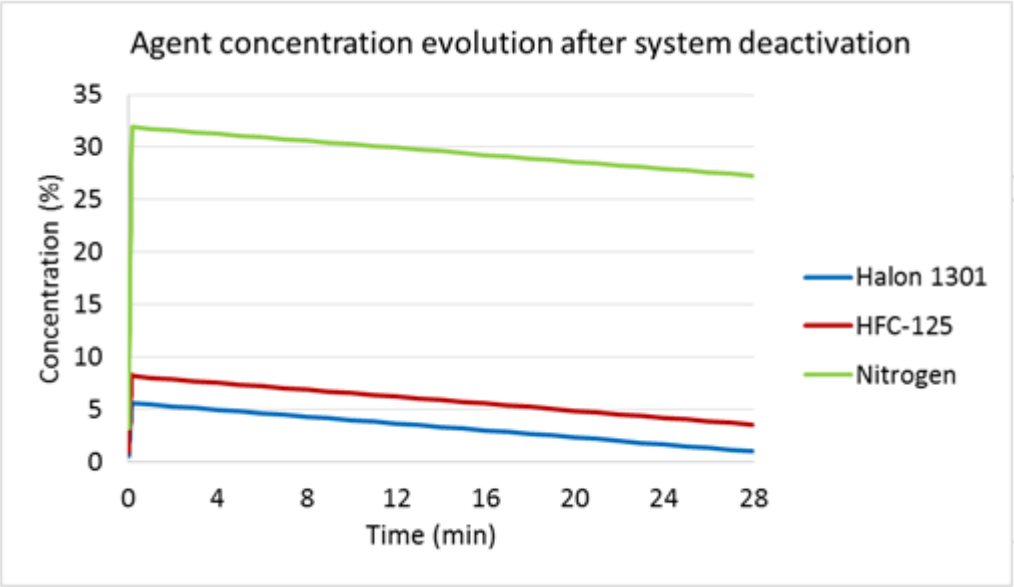

Figure 61 - Agent concentration after the system deactivation

Figure 62 presents the results for the same model, excluding the Nitrogen case, following the NFPA approach. The system is these cases was designed to extract a constant flow of 0.023m^3/s without agent discharge. In this approach, the model calculates the agent concentration against time, both during and after discharge, for a fixed effective height of protection inside the cargo compartment.

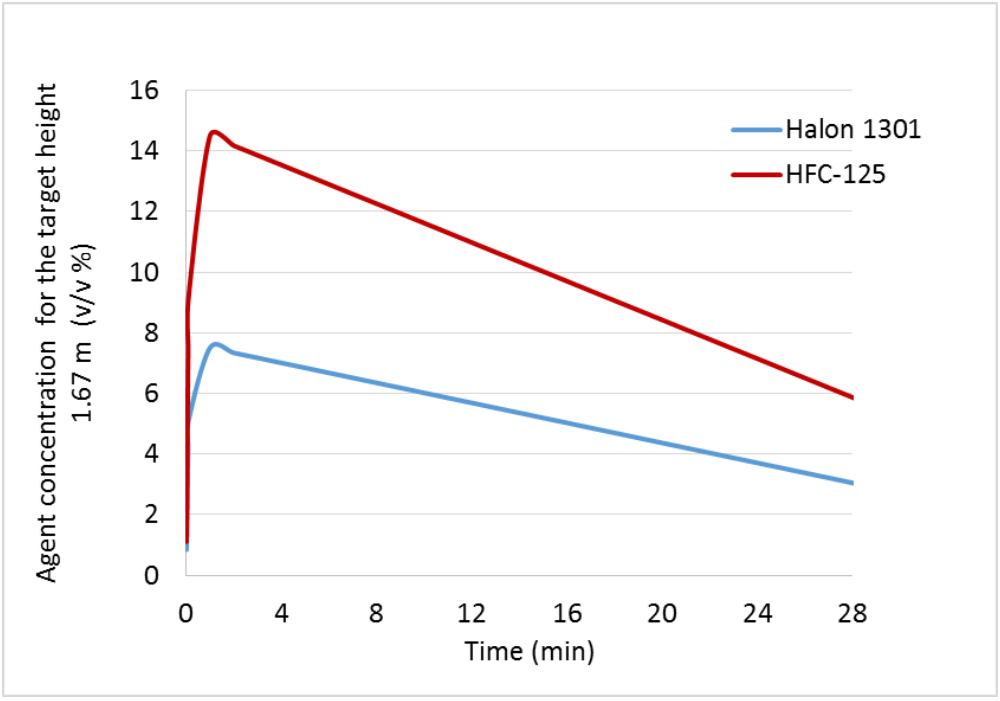

Figure 62 - Agent concentration after the system deactivation using NFPA model

The resulted protection time for each agent can be seen in Table 32. The model results show that for all examined agents, the system is able to maintain agent concentration above the required value for the required protection time. The effective height used for both Full and Partial cargo cases is 1.67m, equal to the full height of the compartment.

The nozzle design for each agent was based on the commercial Halon1301 nozzle design, resized appropriately. Additionally, the approach followed for the definition of the number of nozzles and their positions was based on considerations regarding agent distribution and effectiveness as well as numerical simulation demands.

Table 32 contains the main parameters of interest for the analytical model. The overpressure was found to be less than 10Pa for all cases. Hence, the value of 10Pa was selected as representative for realistic scenarios.

Table 32 - Main inputs and outputs for the analytical models

A/A	Halon1301	HFC-125	Nitrogen	Water
Density gas vapour (kg/m³)	6.283	5.074	1.251	0.5896
Design agent concentration (%)	6	8.5	32	10
Density mixture (kg/m³)	1.507	1.531	1.218	1.141
Effective area Partial cargo (m²)	16.17			
Effective area Full cargo (m²)	33.738			
Design mixture/air interface height	0.1% of the total protection height			
Target height of protection (m)	1.67			
Leakage inlet area (m²)	0.0041			
Leakage outlet area (m²)	0.0041			
Lower leak fraction	0.5			
Agent hydrostatic pressure (Pa)	5.0	5.4	0.3	
Gauge pressure Limit (Pa)	10	10	250	
Velocity exit (m/sec)	8.31	8.97	0.44	
Volume flow rate exit (l/sec)	9.12	9.84	0.48	

Another interesting observation concerns the estimation of the quantity of agent required for successful fire extinguishment, against the compartment load. Increasing the load inside the cargo area reduces the empty volume that the pure air can occupy. This output results in reduction of the required agent quantity (see Figure 63). Nevertheless, the sizing design of the system must comply with the

100% empty volume of the compartment. The cargo load effect could provide information about the number of activations before the replacement/refilling of the bottles.

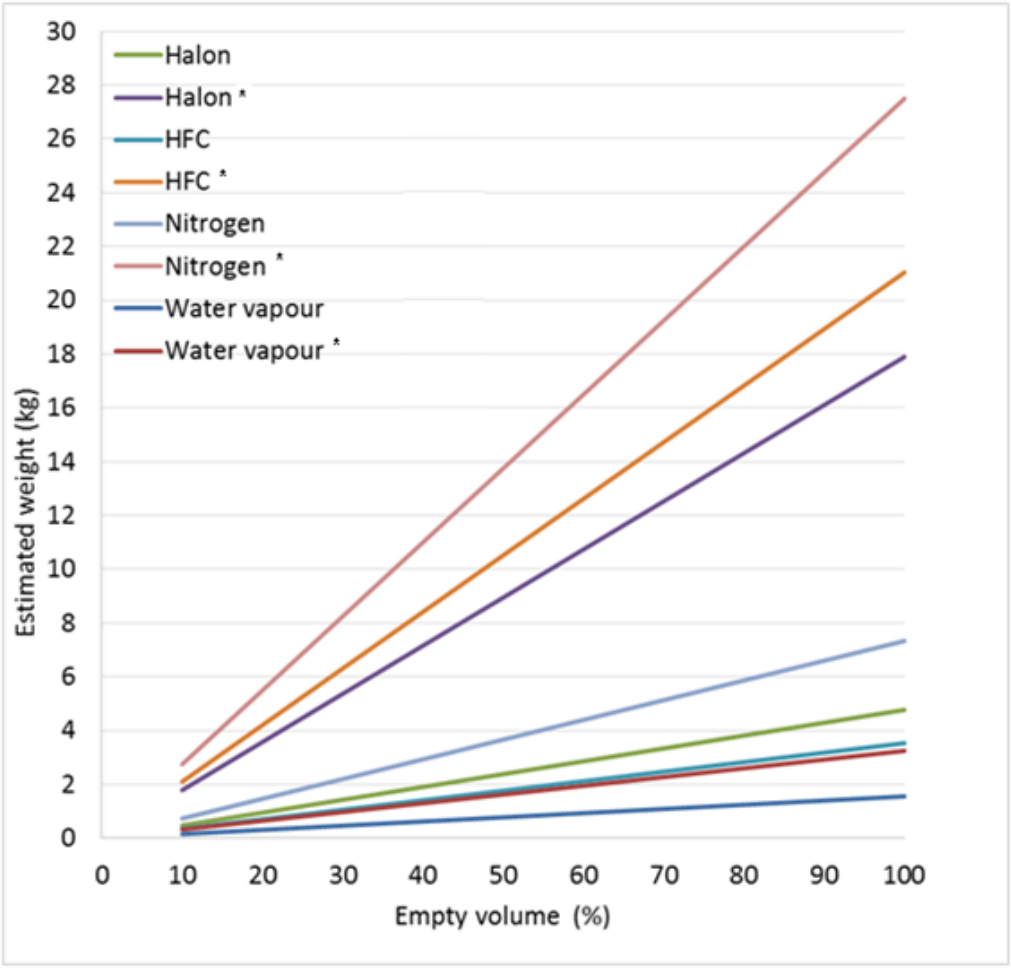

Figure 63 - Estimated weight versus empty volume of the compartment (full cargo (*) and partial cargo)

Finally, the main sizing parameters and criteria for the ventilation system design were based on the requirement for a constant leakage rate and for a limited value of overpressure. Based on the MPS requirements, the final system was designed to extract a constant flow of 0.023m^3/s without agent discharge. During discharge, the door fan is designed to modulate the flow capacity in order to avoid cargo overpressure that exceeds 10Pa(0.001bar).

The main outcome of this activity is that it provides the necessary boundary conditions for the CFD simulations, as well as an insight about the quantities and concentrations of the agent inside the enclosure.

4.2 Main Case Study

4.2.1 Analytical Model Outcomes

The results coming out of the analytical model for the final system design were inserted in INVENTOR software and produced the isometric diagram of the piping network (see Figure 64).

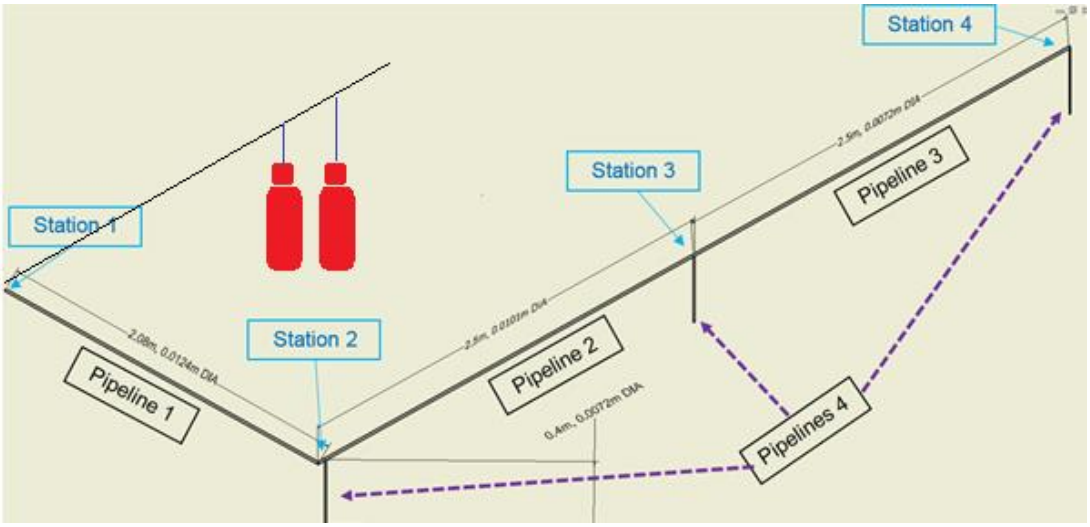

Figure 64 - Isometric design of the piping network

The table below shows the main dimensions of the piping network components.

Table 33 - Delivery system specifications

Piping Network			
Parameter	**Quantity**	**Length [m]**	**Diameter [mm]**
Pipeline 1	1	2.08	12.4
Pipeline 2	1	2.5	10.1
Pipeline 3	1	2.5	7.2
Pipeline 4	3	0.4	7.2
T-junction1	1	-	12.4x7.2x10.1
T-junction 2	1	-	10.1x7.2x7.2
90° Angle 1	2	-	12.4
90° Angle 2	1	-	7.2

Table 34 and Table 35 contain the main dimensions for the nozzles with their installation cones.

Table 34 - Discharge nozzles specifications

Discharge Nozzles				
Parameter	**Quantity**	**Orifices**	**Inlet diameter (mm)**	**Orifice diameter (mm)**
Nozzles	3	6	7.2	2

Table 35 - Discharge nozzles installation cones specifications

Discharge Nozzle Installation Cones				
Parameter	**Quantity**	**Height (mm)**	**Inlet diameter (mm)**	**Outlet diameter (mm)**
Cones	3	150	100	400

The operating conditions that were selected for a representative experimental process are presented below:

1. Storage pressure and temperature: 300bar/18°C
2. Overpressure relief: 370bar
3. Operating pressure after first reducer: 120 bar
4. Operating temperature after first reducer: 3.85^{o}C
5. Max working pressure: 310bar
6. Operating pressure after second reducer: 41bar
7. Operating temperature after second reducer: -14.55^{o}C
8. Nozzles Discharge Temperature: -20.15^{o}C

The resulted agent storage cylinders characteristics are based on the agent quantity requirements and the market availability. The main parameters are presented in the table below.

Table 36 - Agent cylinders specifications

Agent Storage		
Parameter	**Units**	**Quantity**
Number of Cylinders	-	2
Cylinder Diameter	m	0.345
Cylinder Height	m	1.76
Cylinder Pressure	bar	300
Cylinder Nitrogen Content	kg	24.13

In case of real aircraft cargo applications, these cylinders must be designed refillable with filling level indications. They should be checked and/or refilled if necessary, depending on the containerised load % or luggage load. Finally, if technology allows it, they can be connected to OBIGGs.

The performance properties of the final piping system can be observed in the figures below. All results presented here are plotted normalised against their reference inlet values. Figure 65 illustrates the evolution of the main gas properties within the piping network between stations 1 and 4 (see Figure 64).

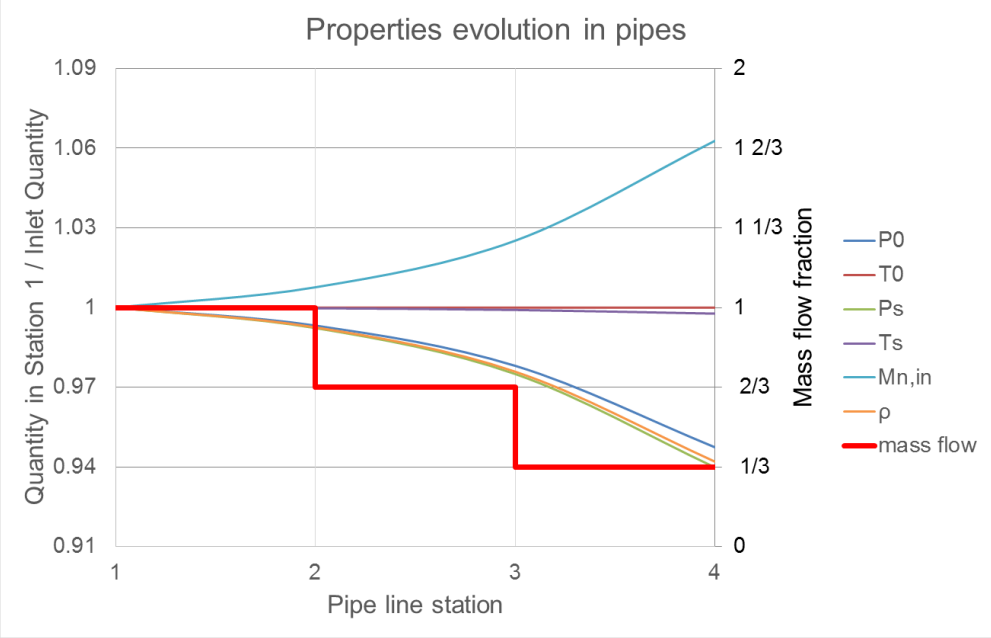

Figure 65 - Agent properties evolution in the piping system

The evolution of gas properties inside the piping network is a direct outcome of the *Fanno* calculation method for pipes of constant diameter. The total pressure reduction exceeds the value of 5% at the furthest station. This is due to the imposed friction within the pipes, which increases the flow Mach number. The effect of flow friction and thus energy dissipation within the pipes is expressed by the increased Mach number. The rest of the fluid properties are only following the changes in the flow velocity.

Generally, it can be observed that the changes in the fluid properties resulted to be within the range of ± 6% compared to their respective inlet value. Figure 66 includes the respective outcomes for the evolution of the main gas properties

within the small pipes that lead to the nozzles. It can be seen that the agent presents a similar behaviour, with the total pressure dropping a bit further. Also, it can be seen that the nozzle inlet conditions are different for each one of the nozzles. These results imply that in order to achieve the same mass flow exiting each nozzle at chocked conditions, the nozzle exit areas should be different. However, due to the fact that the differences between the fluid properties in absolute values are small, the differences in nozzle exit areas are negligible from an engineering point of view. Thus, in order to develop one single nozzle design for all three positions, the greatest area was selected for all three nozzles (see Table 34).

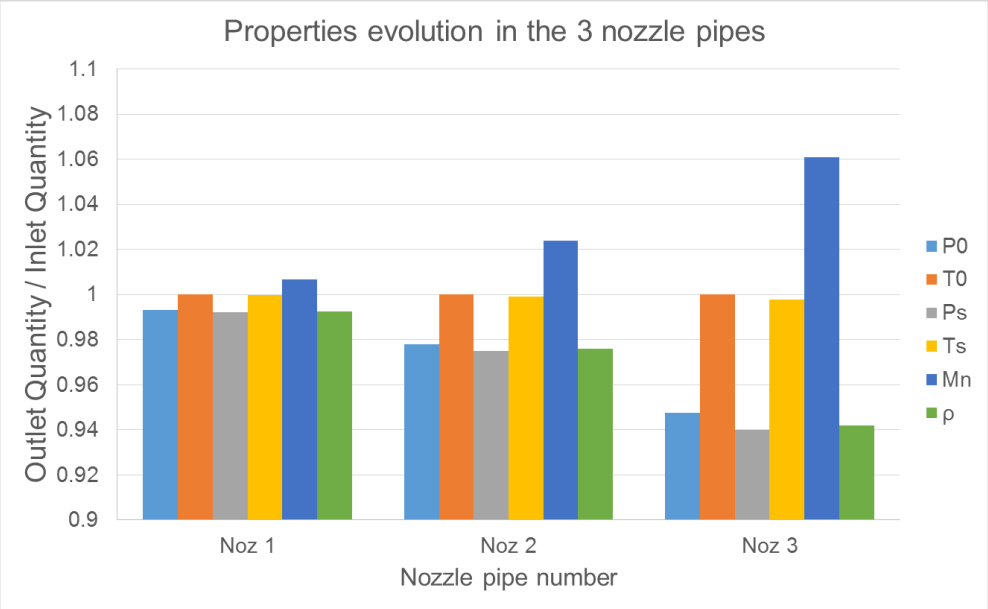

Figure 66 - Agent properties evolution in the 3 nozzle pipes

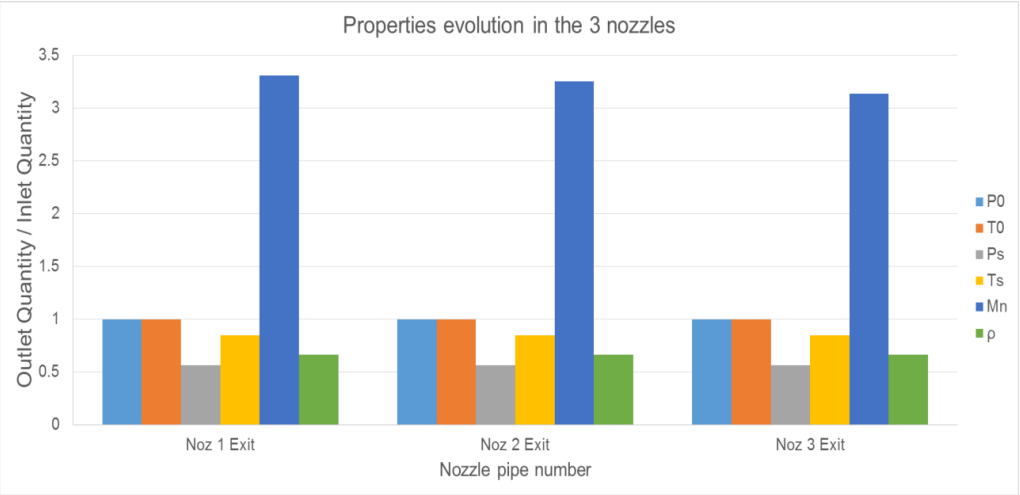

Figure 67 - Agent properties evolution in the 3 nozzles

Figure 67 presents the gas expansion in the nozzles. The total pressures and temperatures remain constant due to the assumed adiabatic and isentropic expansion. However, there is a significant drop in the static properties, due to the fact that the flow was forced to expand in ambient conditions and accelerate rapidly to Mach number equal to unity at the nozzle exit.

The ventilation system sizing was based on the assumption that there is a top limit for the compartment overpressure. This limit was set to 1500Pa or 0.015bar during discharge and 250Pa or 0.0025bar after discharge. The ventilation port size affects both the resulted interior static pressure as well as the agent mass loss. During discharge, the level of overpressure is allowed to be higher in order to maintain a reasonable ventilation port size compared to the current state-of-the-art. However, it needs to be small enough to assure minimum possible agent mass loss during discharge. After discharge, the overpressure level selected assures minimum possible agent mass loss due to leakages and thus maximum fire protection time.

The outputs for the final system overall performance in both Full Cargo and 30% Loaded with Boxes are presented in the tables below:

Table 37 – Main system design parameters: Full Cargo Empty

Overall System Performance		
Parameter	**Units**	**Quantity**
Agent Main Discharge Time	s	60.0
Agent Main Discharge Pressure	bar	41
Agent Concentration at 60sec	%	32
Oxygen Concentration at 60sec	%	14.2
Agent Discharge Time till Drain-out	s	158.6
Agent Concentration after Drain-Out	%	50.3
Oxygen Concentration after Drain-Out	%	10.4
Time till Oxygen Concentration Reaches 16% - Constant Leakage Rate 0.023m^3/s	min	45

Table 38 – Main system design A parameters: 30% Loaded with Boxes

Overall System Performance		
Parameter	**Units**	**Quantity**
Agent Main Discharge Time	s	60.0
Agent Main Discharge Pressure	bar	28.7
Agent Concentration at 60sec	%	32
Oxygen Concentration at 60sec	%	14.2
Agent Discharge Time till Drain-out	s	252.3
Agent Concentration after Drain-Out	%	63.4
Oxygen Concentration after Drain-Out	%	7.7
Time till Oxygen Concentration Reaches 16% - Constant Leakage Rate 0.023m^3/s	min	47.7

The main discharge pressure for the Full Cargo Empty case was 41bar, mainly in order to achieve quick fire extinguishment (32% v/v Nitrogen Concentration with 60sec discharge) as explained earlier. Given that the piping network and discharge nozzles were designed for the Full Cargo Empty case, the main discharge pressure for the 30% Loaded with Boxes case was 28.7bar in order to achieve the same target. The Nitrogen storage cylinders shown in Table 36 are assumed to be used fully in both cases. This is the driver behind the resulted values of the parameters relative to cylinders drain-out, such as time till drain-out, etc. However, the resulted 7.7% level of Oxygen concentration is considered toxic. Thus, another iteration of the analytical design using 70% of the total agent quantity and discharging at 41bar, while assuming constant discharge mass flow for 42sec. Maintaining the discharge pressure the same as in the Full Cargo, assures that 42sec are enough to discharge 70% of the total agent mass, while maintain below 16% oxygen for only 32 minutes. This shows that besides the discharge pressure, the discharge time control provides another lever for variability on the system effectiveness. Considering the proposed Nitrogen system operation on a real aircraft scenario, the discharge time can be adjusted depending on the level of the cargo load (Table 39).

Table 39 – Main system design B parameters: 30% Loaded with Boxes

Overall System Performance		
Parameter	**Units**	**Quantity**
Agent Main Discharge Time	s	42.0
Agent Main Discharge Pressure	bar	41
Agent Concentration at 60sec	%	32
Oxygen Concentration at 60sec	%	14.2
Agent Discharge Time till Drain-out	s	72
Agent Concentration after Drain-Out	%	50.9
Oxygen Concentration after Drain-Out	%	10.3
Time till Oxygen Concentration Reaches 16% - Constant Leakage Rate 0.023m^3/s	min	32.4

The results of the analytical models show that such system can provide variable effectiveness capabilities. Considering current state-of-the-art land-based systems, discharge pressures up to 60bar are usually selected. Allowing discharge pressure to increase up to 60bar can provide significant reduction of discharge time and thus the fire extinguishment time. Additionally, in cases with relaxed time requirements, it allows the discharge pressure to reduce and provide leverage for compartment overpressure control. The main discharge pressure selection affects greatly the design values of the enclosure overpressure level and leakage area dimensions (see Figure 68).

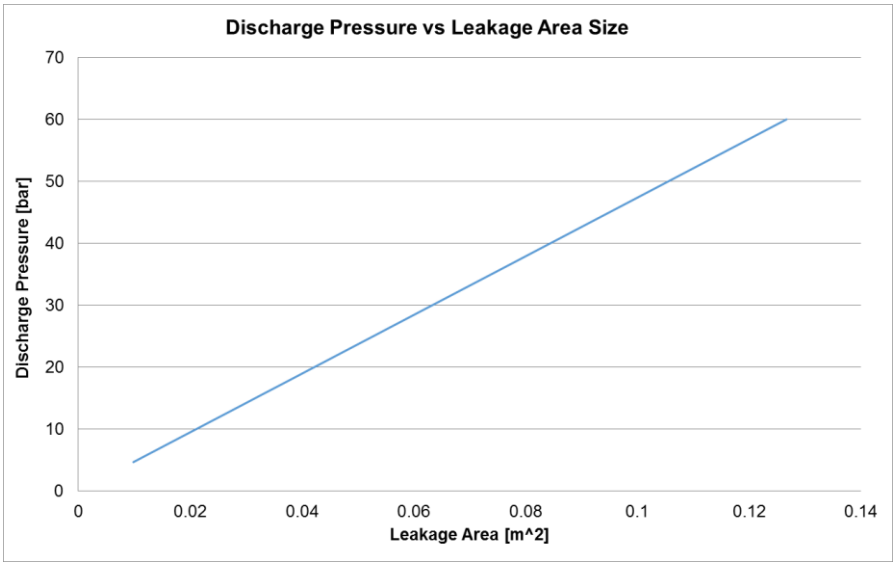

Figure 68 – Leakage area size vs discharge pressure (Overpressure Limit: 1500 Pa)

The final criterion for the selection of the discharge pressure is based on considerations regarding the 'Joule-Thomson' effect and the potential agent temperature drop before discharge. Assuring that the temperature will not reduce below acceptable values inside the enclosure during discharge, such mechanism provides advantageous cooling capabilities for the agent, enhancing its fire suppression performance.

The agent discharge temperature and its effect on the enclosure conditions is estimated based on Figure 69, the agent quantity and the original ambient conditions. This conservative approach considers fully adiabatic and isenthalpic expansion processes. Nevertheless, the enclosure internal conditions must satisfy the requirement for life support, avoiding water freezing point during system activation. For aircraft applications, the piping network design as well as the enclosure conditions during discharge need to be thoroughly assessed.

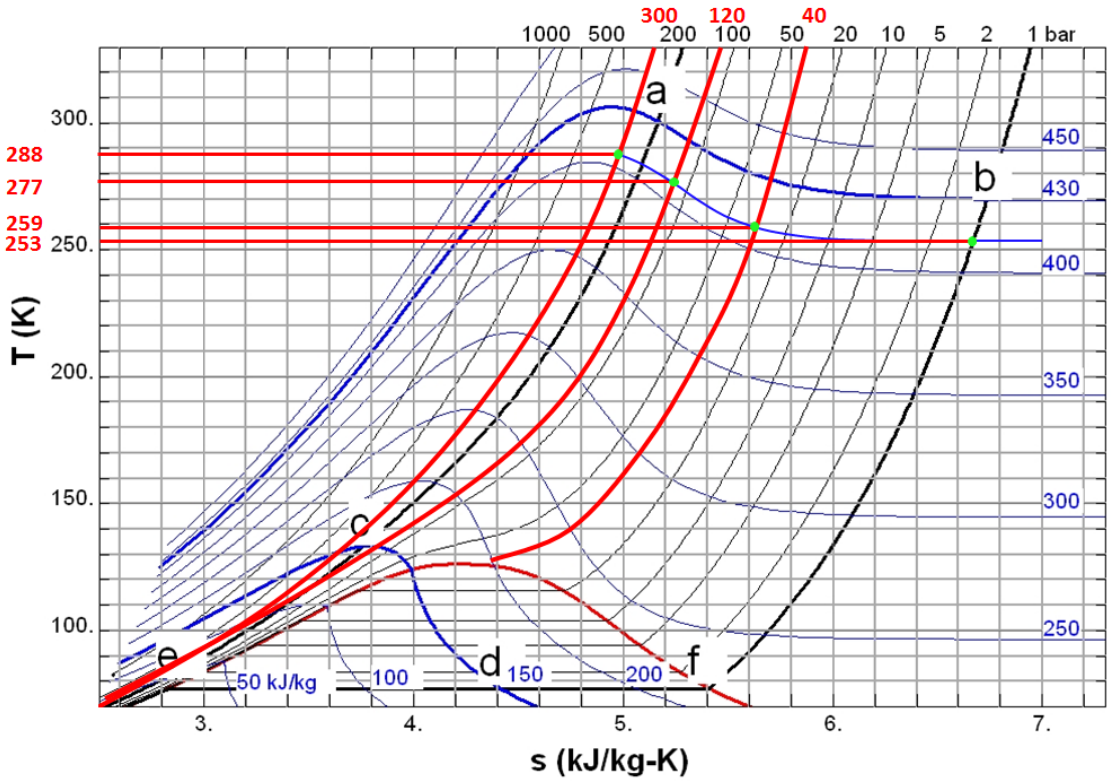

Figure 69 - Agent theoretical temperature drop during isenthalpic expansion

The final system design assures that the enclosure temperature will never reach extremely low values. In the worst case for the Full Cargo, assuming that the complete quantity of the agent inside the compartment was at its minimum temperature (-20°C), the volume weighted average enclosure temperature results to be -1°C. Of course this approach neglects important factors related to the system heat transfer and thus the anticipated enclosure temperatures are expected to be above the water freezing point.

4.2.2 Numerical 3D-CFD Outcomes

This section contains the 3D-CFD results, including verification against public domain and alignment against experimental tests for model validation and calibration scheduled for the near future.

4.2.2.1 Grid Independence & Adaptation

Beginning from coarse meshes, progressive mesh refinement was performed in order to assess solution appropriate representation and stability. Five mesh refinements were performed subsequently. The comparison between the

solutions showed that after the 4th mesh refinement, the solution wasn't practically improved. Thus, all mesh solutions were compared based on the 4th refined mesh, which was considered as baseline for a satisfactory solution. Considerations for computational cost reduction are an important factor since the deviation observed in all cases was relatively low (see Figure 70). Nevertheless, the cell size was kept small enough to ensure solution stability and desired resolution of flow representation. Based on the given problem requirements a 3.5 mm maximum cell size was set as max limit.

For the steady state simulations of the partial cargo models, it was observed that smaller number of cells can achieve accuracy of 0.1% providing solution in less than 40 minutes. These models are suitable for rapid assessments of the design space with reduced computational cost. Additionally, they can provide data relative to system operation that can be used for verification purposes.

For the scaled models, the maximum cell size was reduced from 0.035m to 0.012m, assuring appropriate case representation while all residuals reached values below 10^{-4} (convergence criteria). During this process, it was proved that the transient cases could achieve residuals in the order of 10^{-4}, allowing the simulation of a complete operation for the full cargo scenarios. The mesh comparisons along with the selected meshes are presented in Figure 71.

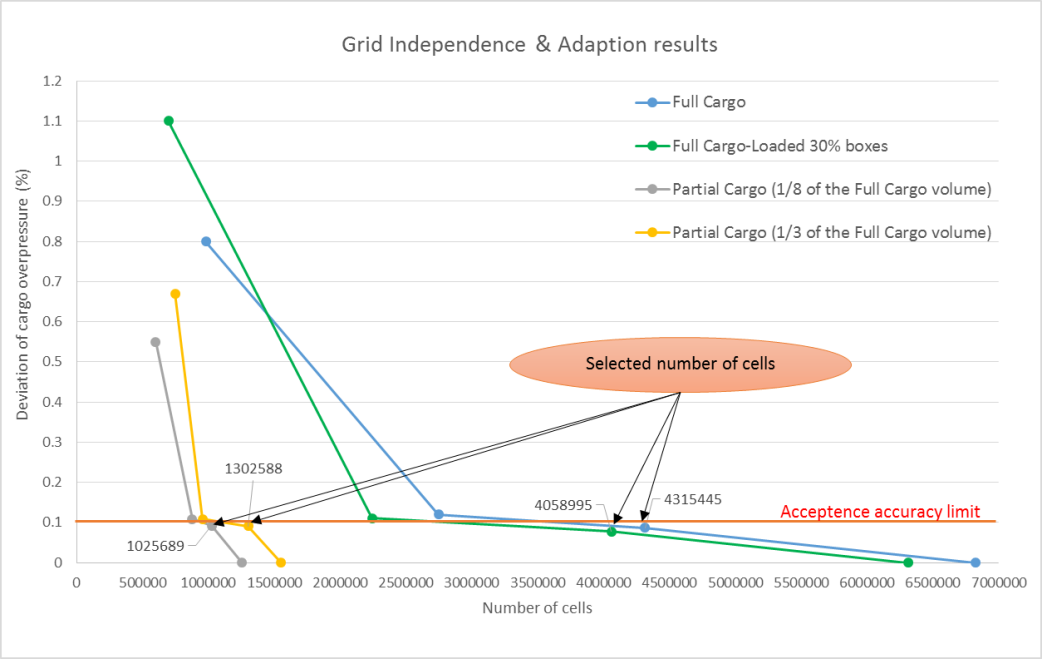

Figure 70 - Grid independence & adaptation study for all models (steady state)

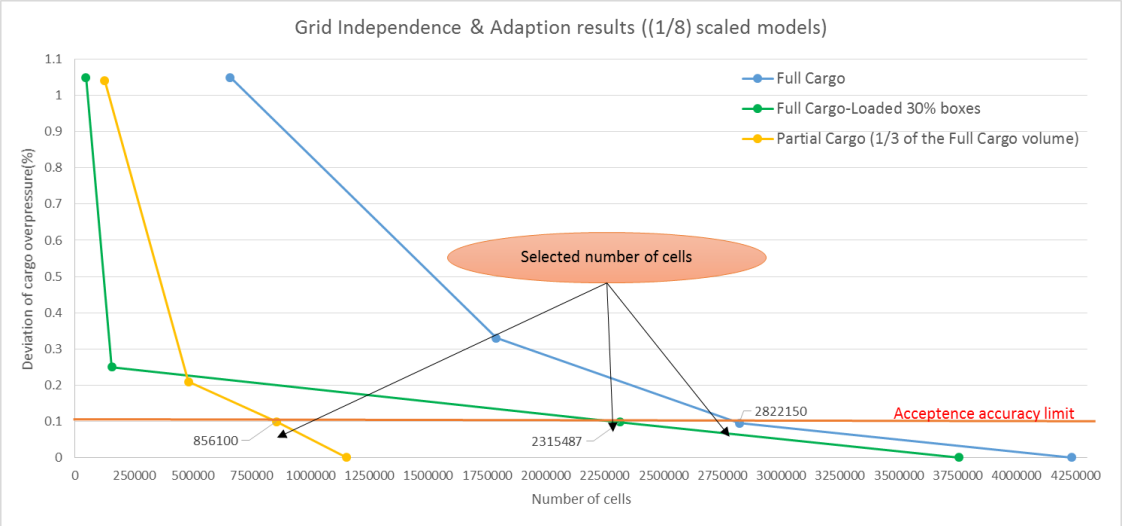

Figure 71 - Grid independence & adaptation study for (1/8) scaled models (steady state)

4.2.2.2 Model Scale Independence

The 3D-CFD models applied for these simulations resulted out of a scale independence study. The model scaling was deemed necessary in order to achieve transient simulations for the time requirements of the problem, as the full-scale models were proved unfeasible with the given computational power. Figure

72 presents an example of the comparisons between scaled models, using the full-scale as baseline. It can be seen that the level of deviation is generally low (below 0.5%, acceptable for transient cases). Both scaling methods were proven satisfactory when applied independently and combined. However, the flow representation and resolution (mapping parameters required) of the scaled Full cargo model was higher than the full scale Partial cargo model (see Figure 73).

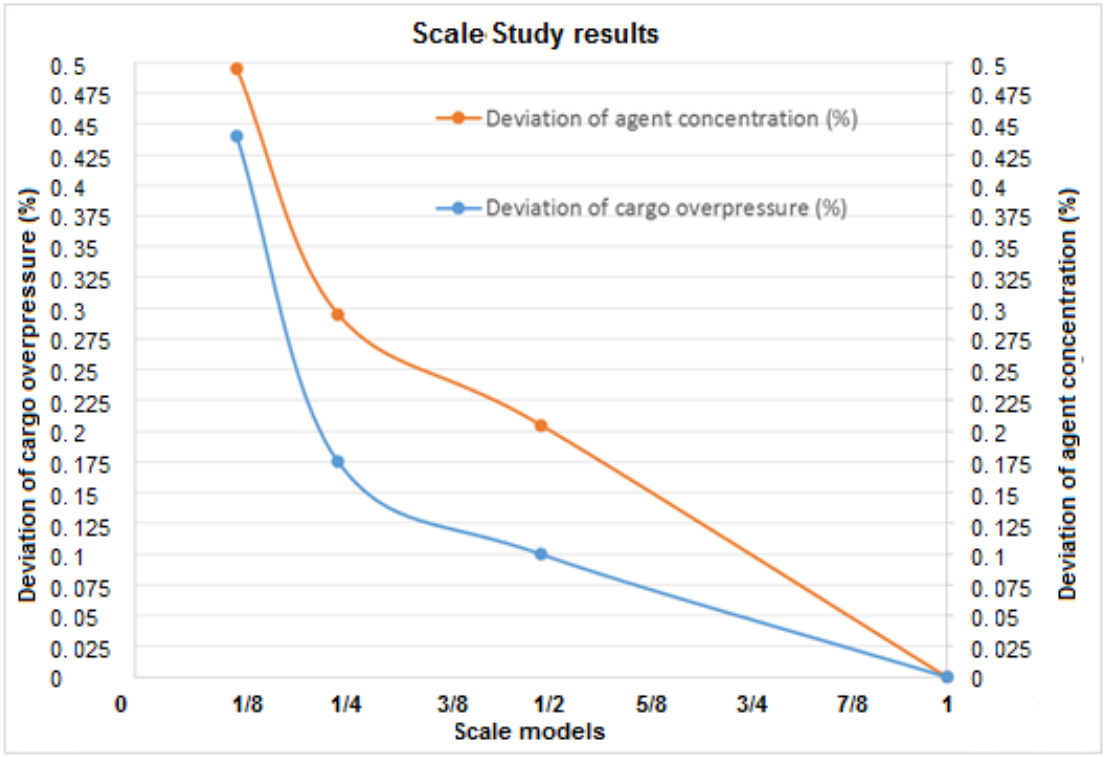

Figure 72 - Model scale study – Cargo overpressure & agent concentration comparisons

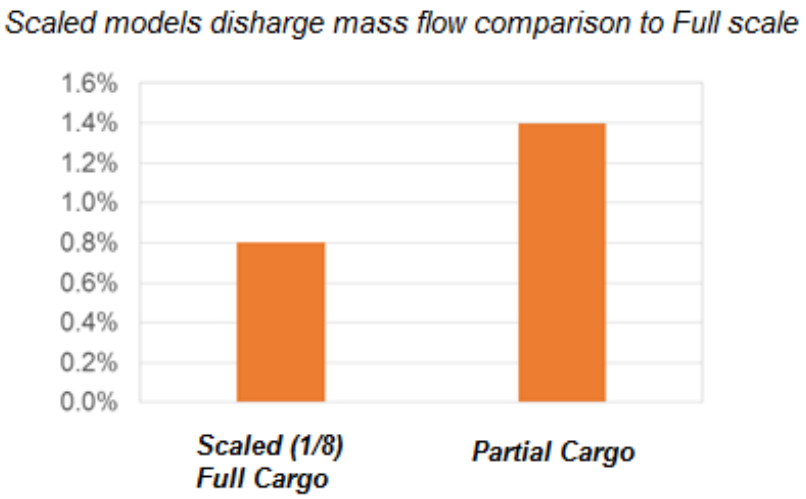

Figure 73 - Model scale study – Scaling methods comparison (transient)

4.2.2.3 Turbulence Model Selection & Convergence Strategy

The selection of the appropriate turbulence model was based on considerations regarding the nature of the problem and the expected flow phenomena of interest. Additionally, mesh size and structure as well as software computational capabilities were proved to be important factors for the final selection.

Based on the problem specification, both *k-ε* and *k-ω* were appropriate. However, several challenges were identified during the application of both. The list below presents some of the main challenges observed during the steady-state simulations:

a. *k-ω*: solution unable to achieve residual values below 10^{-2} using maximum cell size 0.035mm due to the restricted wall treatment requirements
b. *k-ε*:
   - when using large maximum cell sizes, e.g. 0.055m, the solution becomes unstable
   - unable to achieve residuals value below 10^{-3} using maximum cell size 0.045mm
   - acceptable residuals achieved 10^{-4} at 0.035m maximum cell size

An additional strategy followed to improve initial guesses, solution convergence and stability regards the data exchange between initialisations using mass flow and pressure inlet boundary inputs. Based on the requirements of the present

research, the pressure inlet boundary input is preferable as this is the main handle of the actual system. However, using first the pressure inlet with the initial guesses coming from the analytical model presented solution stability challenges. In order to improve the initial guesses, the mass flow inlet was used as it was found to be satisfactory using guesses coming from the analytical model. The mass flow is used as handle in order to achieve discharge flow Mach numbers close to unity. The generated outputs are then used for the initialisation using pressure inlet boundary input. This strategy was found to provide satisfactory solutions and an optimum compromise between accurate problem representation and system design flexibility and handling.

4.2.2.4 System Design Analysis

In order to achieve the desirable system characteristics, the CFD models are aligned with the system main features. This allows the finalised system design to include considerations based the outcomes of the CFD simulations.

4.2.2.4.1 Partial Cargo Steady-State & Transient Simulations

During the initial stage of the CFD models development, the Partial Cargo models were used in steady-state mode. These models represent the least demanding simulation case regarding computational cost. This provided the capability to perform parametric adjustment of boundary conditions and design features like the number and location of nozzles, in order to achieve the desirable conditions and provide the necessary inputs for the Full Cargo models. Additionally, the outcomes of the Partial Cargo steady-state simulations are used to investigate the agent distribution capabilities and overpressure level as well as assess of the effect of the ventilation ports location on local agent concentration levels.

The effect of the number of nozzles was assessed by targeting improved system effectiveness. The system effectiveness is examined by evaluating the agent uniformity and distribution inside the domain as well as the elimination of low concentration regions and the possibility for fire re-ignition. The Partial Cargo models were tested initially with their size based on an excessively large number of nozzles (8) for the Full Cargo, in order to assure adequate agent distribution. The system arrangement included a single discharge nozzle placed at the centre

of the ceiling and two pairs of ventilation ports, one for inlets and one for outlets, each placed at the centres of the two opposing side walls.

The main outcomes of these simulations are compared with the analytical design values, the results of which are summarised in Table 40. The values presented here for the CFD parameters refer to the mass weighted average quantities.

Table 40 - Main CFD outcomes verification for Partial Cargo steady-state simulations

Partial Cargo - Steady-State	Analytical design				CFD predictions				Absolute Delta (%)			
	Nozzles	Door Leaks	Vent Port	Cargo	Nozzles	Door Leaks	Vent Port	Cargo	Nozzles	Door Leaks	Vent Port	Cargo
Total Pressure (bar)	5	NA	NA	<0,015	5,0025	NA	NA	0,0085	0,0500	NA	NA	NA
Static Pressure (bar)	2,36	NA	NA	NA	2,3607	NA	NA	0,0009	0,0297	NA	NA	NA
Total Temperature (K)	253,2	288,2	288,2	288,2	253,09	288,09	288,1	288,12	0,0434	0,0382	0,0486	0,0278
Density (kg/m3)	4,36	1,205	1,205	1,205	4,361	1,206	1,206	1,206	0,0229	0,0946	0,0929	0,0830
Velocity (m/sec)	314,8	NA	NA	NA	314,61	NA	NA	NA	0,0617	NA	NA	NA
Mach Number	1	NA	NA	NA	0,9997	NA	NA	0,101	0,0290	NA	NA	NA
Inlet Mass Flow (kg/s)	0,3288	0	0	NA	0,3288	0	0	NA	0,0000	NA	NA	NA
Outlet Mass Flow (kg/s)	NA	0,1644	0,1644	0,3288	NA	0,16448	0,16454	NA	NA	0,0634	0,100	NA
Agent volumetric fraction	1	1	1	1	0,9998	0,9998	0,9998	0,9997	0,0200	0,0200	0,0200	0,0300
											MQF	0,0461

In Table 40 it can be seen that the CFD results present acceptable deviations from the analytical design values. Additionally, it can be seen that the mass flow balance between inlet and outlet flows is achieved. Based on the table above, a Model Quality Factor (MQF) was generated in order to provide an overall characterisation for comparison purposes. The MQF summarises the deviations found in all parameters in one average value.

$$ABSOLUTE\ DEVIATION\ \% = \left|\frac{CFD - Analytical}{Analytical}\right| \times 100$$

$$MQF_{Partial\ Cargo,SS} = AVERAGE(ALL\ ABSOLUTE\ DEVIATIONS\ \%) = 0.0461\ \%$$

The resulted MQF presents a value below the acceptance limit of 0.1%. However, the closer it gets to zero the better the model quality is.

Figure 74 illustrates the Nitrogen mass fraction within the Partial Cargo model. The operation of the nozzle presents expected patterns, with the jets distributing the agent within the entire volume in a symmetric fashion. This model is also suitable to capture the ventilation system effects on the agent mixing and distribution processes. Thus, the appropriate positions and operating conditions for the ventilation system, combined with the effects of the expected leakages can be identified.

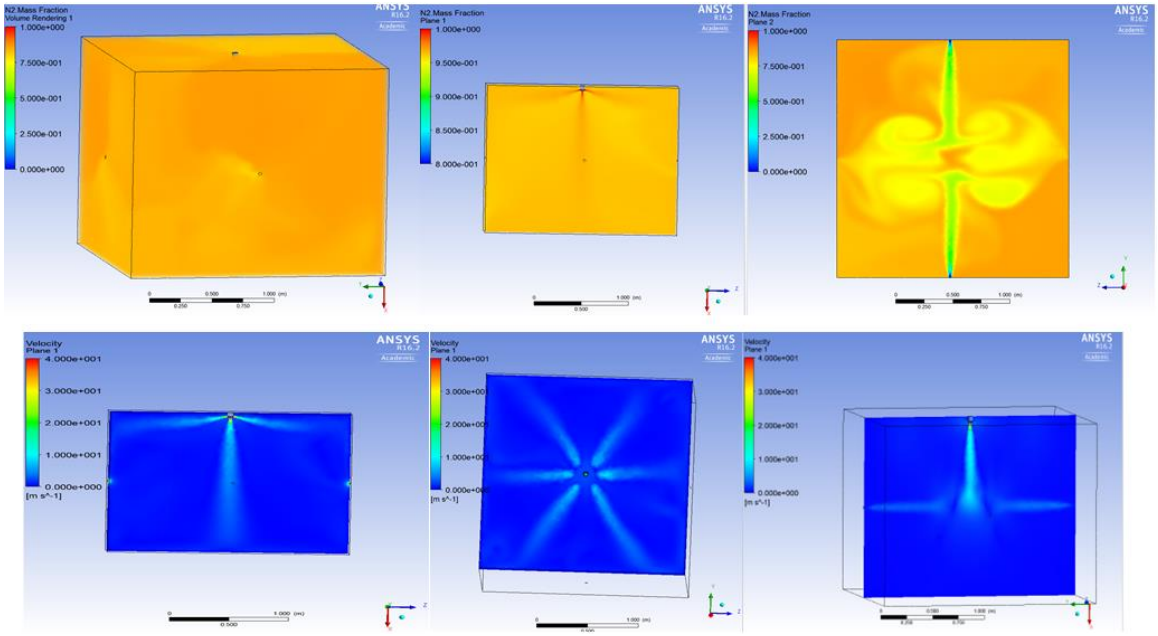

Figure 74 - Partial Cargo agent mass fraction, mixture leakages and air infiltration

Observing Figure 75, it becomes obvious that the air entering the control volume moves towards the ceiling and the agent towards the floor. Thus, it has been found that the suitable locations are close to the floor for the leakages and close to the ceiling for the air infiltration depending on the agent density. In these simulation cases, both leakages and air infiltration are introduced in the centre of the side walls for symmetry reasons. Nevertheless, the Full Cargo models will include a more realistic representation of the ventilation system and a favourable location for the openings.

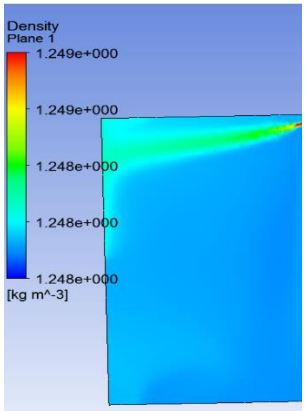

Figure 75 – Partial Cargo leakages for Nitrogen discharge at 5bar

Since the targeted protected height of the enclosure is usually 90% of the total, it is advised that the air should enter close to the ceiling, in an effort to maintain

uniform concentration within the protected zone and avoid feeding the fire with oxygen. As for the leakages, it can be seen that the agent directly moves towards the extraction ports. Thus, they should locate as far from the discharge nozzles as possible, in an effort to minimise the agent mass loss to the environment.

Aircraft cargo fire suppression systems discharge the agent with variable mass flow rate and pressure. When the system is activated, both parameters begin at their maximum values and then drop progressively until the storage cylinders drain-out. This process introduces the challenge of overpressure inside the compartment and thus needs to be controlled. To control the overpressure, both discharge mass flow rate and pressure must be designed talking into account the expansion and mixing processes inside the pipes and properly size the agent delivery circuit.

Based on public domain information about the agent discharge, appropriate range for the discharge pressure has been set in order to examine the resulted levels of overpressure inside the compartment, especially close to the leakage locations [5]. The targets in this case were to assure acceptable overpressure and investigate the potential to satisfy the requirements for all agents of interest using the same model. This capability can be valuable, increasing the flexibility and applicability of the models. Figure 76 illustrates that the level of overpressure during the discharge of Nitrogen is within the acceptable limit of 1500Pa.

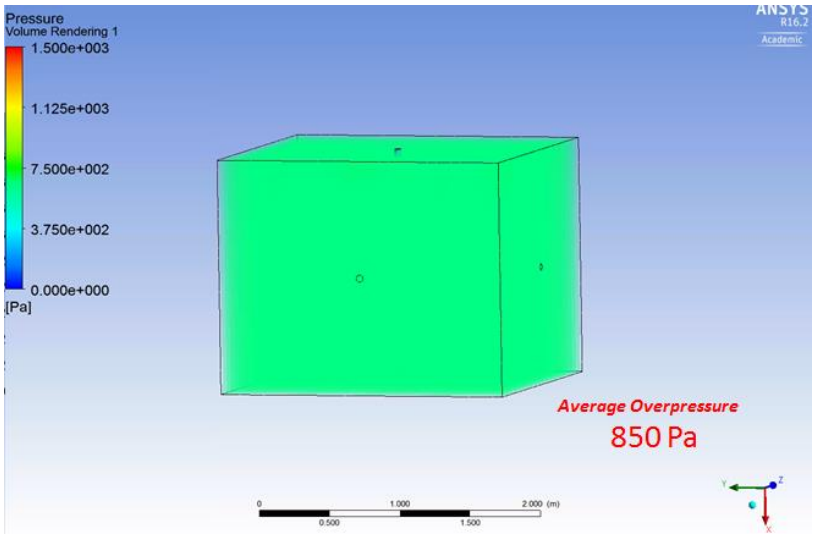

Figure 76 - Partial Cargo overpressure for Nitrogen discharge at 5bar

Figure 77 shows the difference in the Nitrogen jets generated for two different discharge pressures at the acceptance boundary. It was found that for a discharge pressure of 5bar, the model proved that it can achieve mass flow necessary to meet the time requirements at their top limit, while providing effective agent mixing and distribution. Reducing the discharge pressure to 4bar presented challenges in achieving sufficient mass flow to meet the time requirements. Additionally, the agent distribution capabilities are reduced. The value of 5bar discharge pressure was found to be satisfactory for the rest of the agents of interest (Halon1301, HFC-125) and thus it was set as the bottom limit.

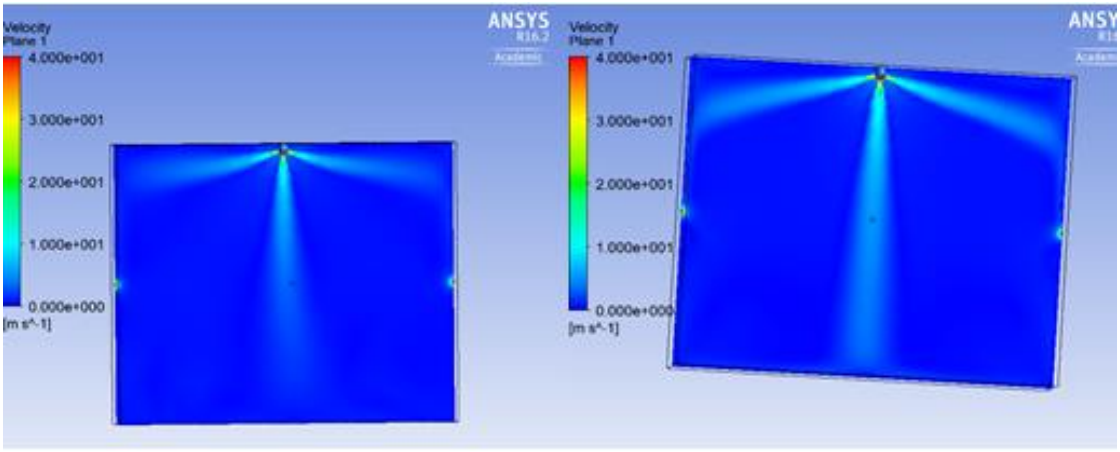

Figure 77 - Partial Cargo Nitrogen discharge velocity patterns at 4 (left) and 5bar (right)

The Partial Cargo simulations also represent the least demanding transient simulation cases regarding computational cost. The main outcome for the transient case for 10 seconds discharge is presented in Table 41. The MQF value achieved was:

$$MQF_{Partial\ Cargo,TR} = 0.2792\ \%$$

Table 41 - Main CFD outcome for 10sec Partial Cargo transient simulation

Partial Cargo - Transient	Analytical design				CFD predictions				Absolute Delta (%)			
	Nozzles	Door Leaks	Vent Port	Cargo	Nozzles	Door Leaks	Vent Port	Cargo	Nozzles	Door Leaks	Vent Port	Cargo
Total Pressure (bar)	5	NA	NA	<0,015	5	NA	NA	0,00825	0,0000	NA	NA	NA
Static Pressure (bar)	2,36	NA	NA	NA	2,364	NA	NA	NA	0,1695	NA	NA	NA
Total Temperature (K)	253,2	288,2	288,2	288,2	253,4	289,2	289,3	288,4	0,0790	0,3470	0,3817	0,0694
Density (kg/m3)	4,36	1,205	1,205	1,205	4,3615	1,210	1,208	1,209	0,0344	0,4149	0,2490	0,3320
Velocity (m/sec)	314,8	NA	NA	NA	315,74	NA	NA	NA	0,2988	NA	NA	NA
Mach Number	1	NA	NA	NA	0,9965	NA	NA	0,101	0,3479	NA	NA	NA
Inlet Mass Flow (kg/s)	0,329	0	0	NA	0,3302	0	0	NA	0,4263	NA	NA	NA
Outlet Mass Flow (kg/s) at t3	NA	0,164375	0,164375	0,329	NA	0,1651	0,1652	NA	NA	0,4	0,5	NA
Agent volumetric fraction at t3	1	NA	NA	<0.86	0,996	NA	NA	0,862	0,4000	NA	NA	NA
											MQF	0,2792

These simulation results shown above presented good agreement with the analytical model, providing confidence on the capturing of the agent discharge

and distribution processes. Compared to the steady-state simulation residuals, levels of error 10^{-5}, the transient cases reached the acceptable values of $>10^{-4}$ (when for both the acceptable values of residuals for species $>10^{-5}$ and energy $>10^{-6}$ respectively). The time step was set to 1.2×10^{-4} sec, for 10 concequtive seconds of agent discharge. The number of iterations required for such simulation was approximatelly 8333333. Generally, running such transient cases was found to be relatively expensive computationally.

In order to assess the convergence of the transient simulation, a snapshot of the residuals evolution for the first 5 time steps of the Partial Cargo case is presented in Figure 78. In this case, the residuals reached the required level of convergence in each time step, while the average number of iterations per time step was found to be around 110. Illustrating a small number of time steps allows enough image resolution for analysis, since the number of iterations for the complete simulation is very large. Nevertheless, after the 5th time step (between 550 and 8333333 iterations), the simulation followed a very similar trend.

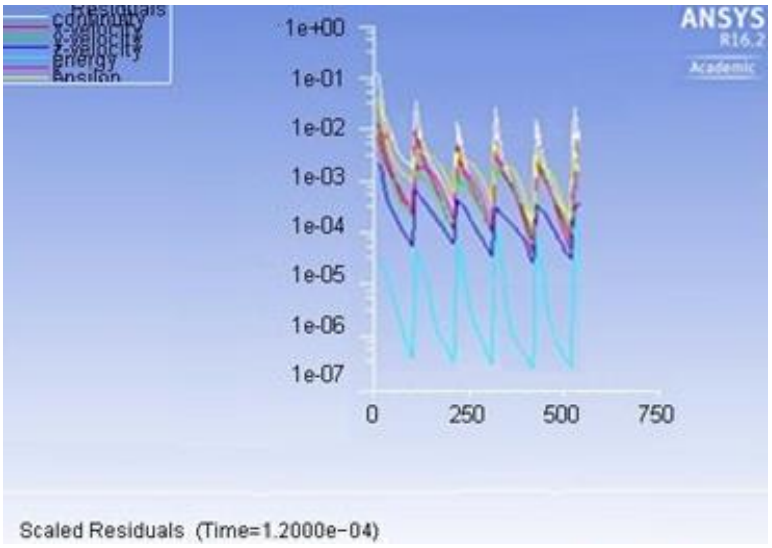

Figure 78 - Output of the residuals convergence for the transient Partial Cargo case

Regarding the solution evolution with time, the transient simulation was set to output and record the oxygen concentration during discharge at every 1sec (around 83333 time steps) of real time. Figure 79 illustrates the trend of the average Oxygen concentration during the complete discharge period. It can be seen that for constant agent discharge mass flow rate, the Oxygen concentration

reduces linearly. Such trends represent the system performance and thus are used for overall system evaluation as well as comparisons with the experimental results.

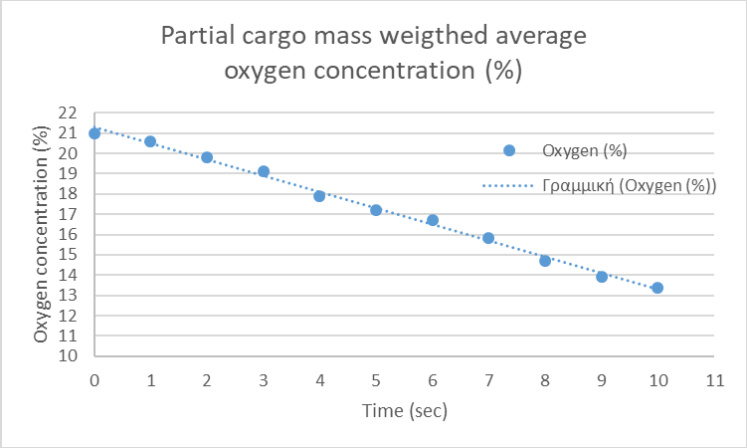

Figure 79 - Oxygen Concentration for Partial Cargo Transient simulation

Finally, for Nitrogen agent discharge, a 5bar discharge pressure was used in the transient simulations in order to be comparable to the steady-state. The transient simulations were set to converge below 100 iterations for each step. Comparing the predictions from the transient model after 1 second of agent discharge with the steady-state showed satisfactory matching. Figure 80 presents the velocity contours comparison between staedy-state and transient.

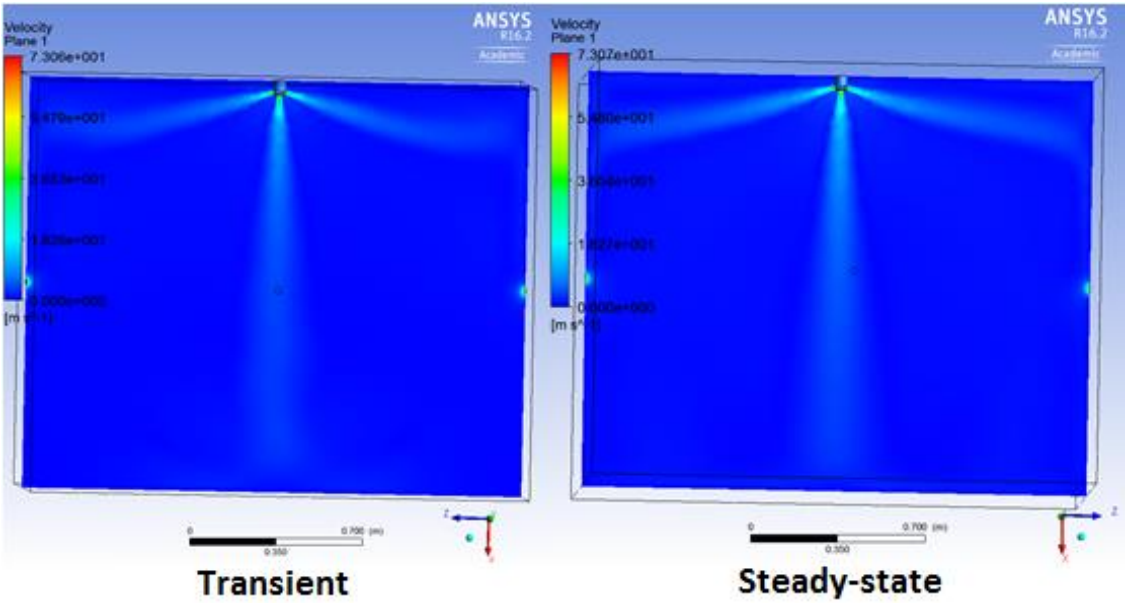

Figure 80 - Steady-state (right) against Transient right (left) at 1sec

4.2.2.4.2 Full Cargo Steady-State Simulations

Although, the Full Cargo models present the highest computational demand, it is also the most representative for the purposes of the present research. Table 42 includes the main outcomes of the Full Cargo steady-state simulations. For the discharge nozzles, average values between all individual nozzles are shown, while ensuring that each nozzle presented very low deviation ($<10^{-3}$) from its desirable value. As mentioned previously, the Full Cargo models were tested initially with an excessively large number of nozzles (8), in order to assure adequate agent distribution. The system arrangement included 8 discharge nozzle placed symmetrically on the ceiling in two rows of four while two pairs of ventilation ports, one for inlets and one for outlets, were placed at the centres of the two opposing side walls.

Table 42 Main CFD outcomes verification for Full Cargo steady-state simulations

Full Cargo - Steady-State	Analytical design				CFD predictions				Absolute Delta (%)			
	Nozzles	Door Leaks	Vent Port	Cargo	Nozzles	Door Leaks	Vent Port	Cargo	Nozzles	Door Leaks	Vent Port	Cargo
Total Pressure (bar)	5	NA	NA	<0,015	5,0042	NA	NA	0,0088	0,0836	NA	NA	NA
Static Pressure (bar)	2,36	NA	NA	NA	2,3624	NA	NA	0,0009	0,1030	NA	NA	NA
Total Temperature (K)	253,2	288,2	288,2	288,2	253,08	288,05	288,04	288,05	0,0474	0,0520	0,0559	0,0536
Density (kg/m3)	4,36	1,205	1,205	1,205	4,362	1,206	1,206	1,206	0,0459	0,0996	0,0931	0,0913
Velocity (m/sec)	314,8	NA	NA	NA	314,62	NA	NA	NA	0,0572	NA	NA	NA
Mach Number	1	NA	NA	NA	0,9996	NA	NA	0,101	0,0390	NA	NA	NA
Inlet Mass Flow (kg/s)	2,63	0	0	NA	2,63	0	0	NA	0,0000	NA	NA	NA
Outlet Mass Flow (kg/s)	NA	1,315	1,315	2,63	NA	1,3157	1,3161	NA	NA	0,0556	0,0837	NA
Agent volumetric fraction	1	1	1	1	0,9997	0,9998	0,9998	0,9996	0,0300	0,0200	0,0200	0,0400
											MQF	0,0564

The outcomes of the Full Cargo steady-state simulations presented low deviation levels while the MQF reached the value of:

$$MQF_{Full\ Cargo,SS} = 0.0564\ \%$$

Figure 81 (right) illustrates the Nitrogen agent discharge velocity contours within the Full Cargo model. The operation of the nozzles presents expected patterns, achieving satisfactory agent distribution within the entire volume. Additionally, the overpressure inside the compartment was found to be below 1500Pa (see Figure 81 (left).

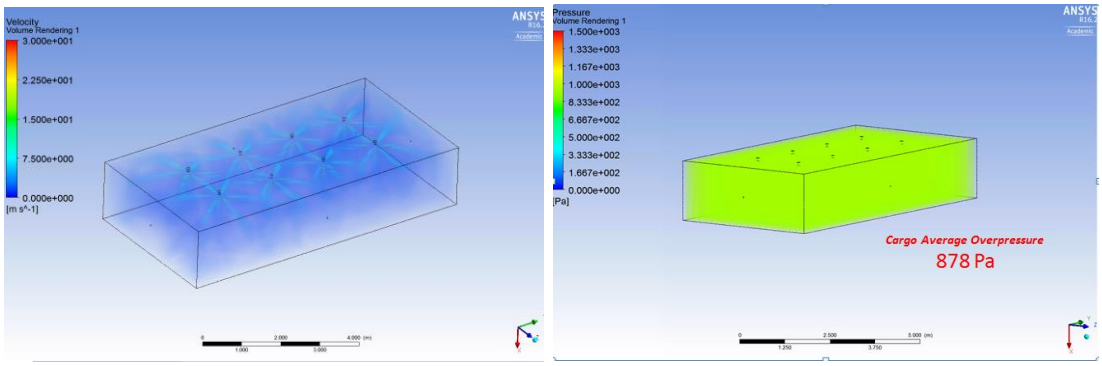

Figure 81 - Full Cargo Nitrogen discharge velocity at 5bar (right) and cargo overpressure (left)

For the above simplified version of the Full Cargo model, where both air infiltration and leakages are positioned in the mid-section of the compartment, the results showed similar behaviour to the Partial Cargo results. The location of the leakage ports affects the agent discharge patterns. In this case, the pressure differential at the leakage ports remained within acceptable limits (below 250Pa).

Another point of view dectates that low discharge mass flow rate combined with low or no discharge pressure simulates the case where the storage cylinders are being close to drain-out. At these operating conditions, the nozzles are not able to operate satisfactory and develop the high turbulence gas cone needed for successful mixing and distribution. However, when applying low pressure (0.1bar, see Figure 82), the nozzles are able to form the jet cones and still achieve the targets for successful distribution. Such low discharge pressure and velocity is expected in the case where the second storage cylinder is used for the metered discharge process. The above two cases set the bottom limits for the nozzle discharge properties.

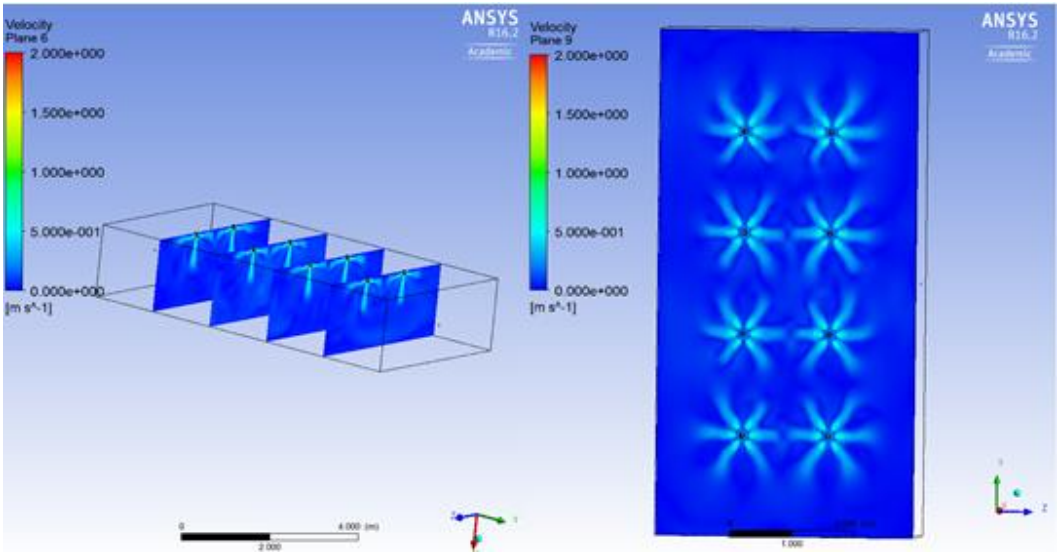

Figure 82 - Full Cargo Nitrogen discharge at 0.1bar

An example case study performed using Halon1301 agent and the nozzle presented in Figure 41, is shown in Figure 83. Halon1301 and HFC-125 vapour properties are inserted as additional species in FLUENT. This case focuses on the metered discharge process designed to prolong the fire protection time. As in the case of Nitrogen with low pressure discharge, Halon1301 agent is distributed uniformly. All nozzles operate as expected, discharging the agent symmetrically and spreading it to the entire control volume. Additionally, the combination of the effects of inlet and outlet ports on the general flow conditions inside the control volume present recirculation enhancement properties.

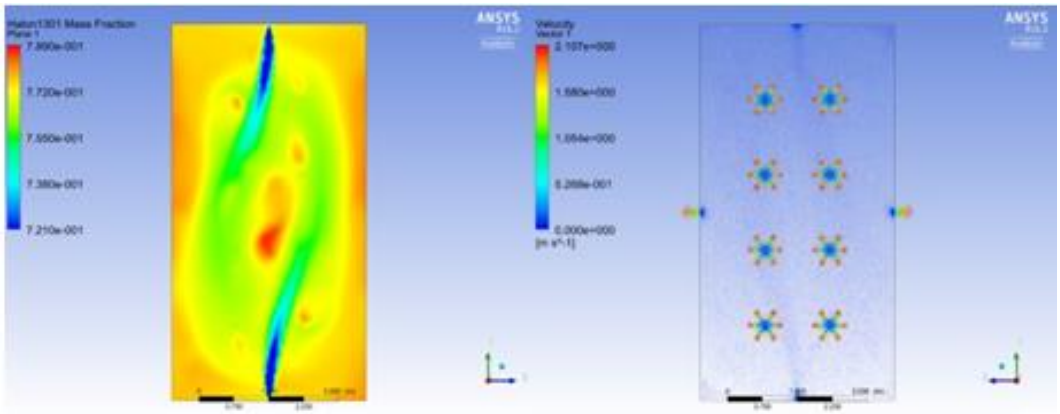

Figure 83 - Full Cargo Halon1301 discharge at pressure 0.1bar

4.2.2.4.3 Full Cargo Transient Simulations

The Full Cargo transient simulations represent the most demanding simulation cases regarding computational cost. The residuals for these cases reached only 10^{-3} (for species and energy 10^{-5} and 10^{-6} respectively) compared to the steady-state which reached 10^{-4}. The time step was selected based on the Partial Cargo models. The Full Cargo transient simulations, except for the increased number of iterations, presented also one order of magnitude larger number of cells which further increased the computational cost. The outcomes summary for the transient cases for 10 seconds duration of Nitrogen discharge is presented in Table 43.

Table 43 - Main CFD outcomes verification for Full Cargo transient simulations

Full Cargo - Transient	Analytical design				CFD predictions				Absolute Delta (%)			
	Nozzles	Door Leaks	Vent Port	Cargo	Nozzles	Door Leaks	Vent Port	Cargo	Nozzles	Door Leaks	Vent Port	Cargo
Total Pressure (bar)	5	NA	NA	<0,015	5	NA	NA	0,00845	0,0000	NA	NA	NA
Static Pressure (bar)	2,36	NA	NA	NA	2,369	NA	NA	NA	0,3814	NA	NA	NA
Total Temperature (K)	253,2	288,2	288,2	288,2	253,5	289,7	289,9	289,8	0,1106	0,5205	0,5795	0,5482
Density (kg/m3)	4,36	1,205	1,205	1,205	4,380	1,212	1,211	1,210	0,4587	0,5809	0,4657	0,4232
Velocity (m/sec)	314,8	NA	NA	NA	316	NA	NA	NA	0,3799	NA	NA	NA
Mach Number	1	NA	NA	NA	0,9921	NA	NA	0,101	0,7900	NA	NA	NA
Inlet Mass Flow (kg/s)	2,63	0	0	NA	2,645	0	0	NA	0,5703	NA	NA	NA
Outlet Mass Flow (kg/s) at t3	NA	1,315	1,315	2,63	NA	1,3251	1,3263	NA	NA	0,7681	0,8593	NA
Agent volumetric fraction at t3	1	NA	NA	<0.86	0,995	NA	NA	0,864	0,5000	NA	NA	NA
											MQF	0,4960

It can be seen that the CFD results present acceptable deviations from the analytical design values and the agent mass-weighted average concentration inside the enclosure reached the desirable value. Additionally, the MQF reached the acceptable value of:

$$MQF_{Full\ Cargo,TR} = 0.496\ \%$$

Figure 84 illustrates the results of Full Cargo Halon1301 agent discharge at 5bar, representative of the current state-of-the-art systems. A modification on the system arrangement was applied by representing the leakages with a single orifice on only one of the sides of the compartment. This was done in an effort to investigate the agent flow path after discharge. The modelling philosophy followed in this case is used to investigate the agent behaviour for loaded cargo compartments. This is due to the fact that current results indicate that as the agent enters the control volume, it is directed towards the leakage orifice. This kind of behaviour can be critical for the system design as in case of loaded cargo, there is high potential for a significant amount of discharged agent to exit the compartment without interacting with the fire. Based on the current set of

assumptions, the results showed that depending on the flow intensity close to the leakage port the agent flow path is affected significantly. However, this phenomenon affects only in the nozzles around the vicinity of the leakage port. Besides that, the results present satisfactory mass-weighted average agent concentration inside the control volume.

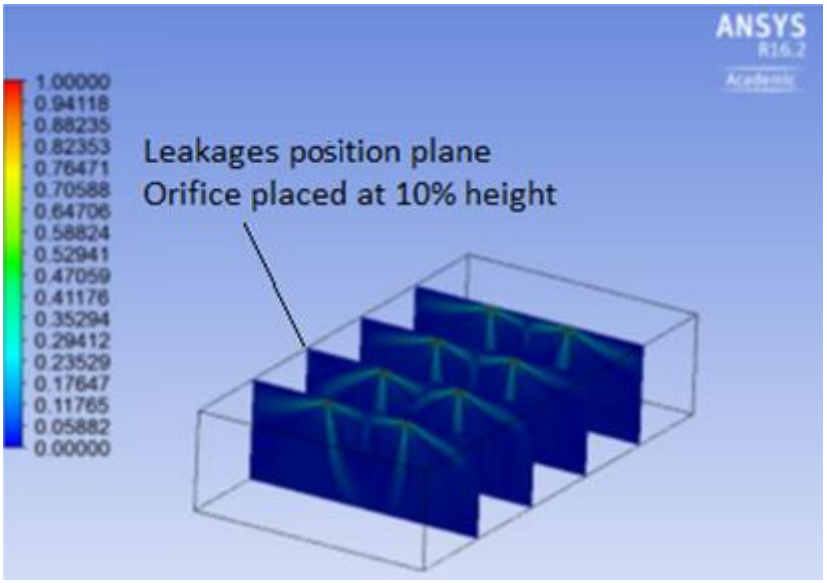

Figure 84 - Full Cargo Halon1301 discharge at the 10sec and 5bar

The outcomes of the CFD cases shown above, drive to the conclusion that the Full Cargo simulations are very demanding with regards to data storage and post-processing. According to these findings, there is a necessity for model scaling in order to examine extended discharge durations and evaluate the fire protection time for at least 30 minutes.

4.2.2.4.4 CFD Models Including Combustion

The simulation of the combustion process inside the cargo is a demanding task. For the consideration of fire inside the enclosure, the model complexity is limited to isolated fires inside the Partial Cargo control volume. This type of information can be useful for the experimental procedure setup.

Figure 85 illustrates the combustion of propane and Jet A fuel inside the control volume. The first picture on the left illustrates the flame of propane gas combustion. The fuel nozzle injects the fuel directly inside the control volume simulating typical open surface fires. The middle and right images illustrate the

combustion of Jet A fuel. In this case, the fuel nozzle injects the fuel inside a small tube, where it mixes with air and ignites. The tube is specifically designed to allow air to enter with an angle, at high velocity and act as turbulence enhancer. These directed flames, which enter the enclosure, attempt to simulate the cases of solid surface fires or aerosol cans explosions.

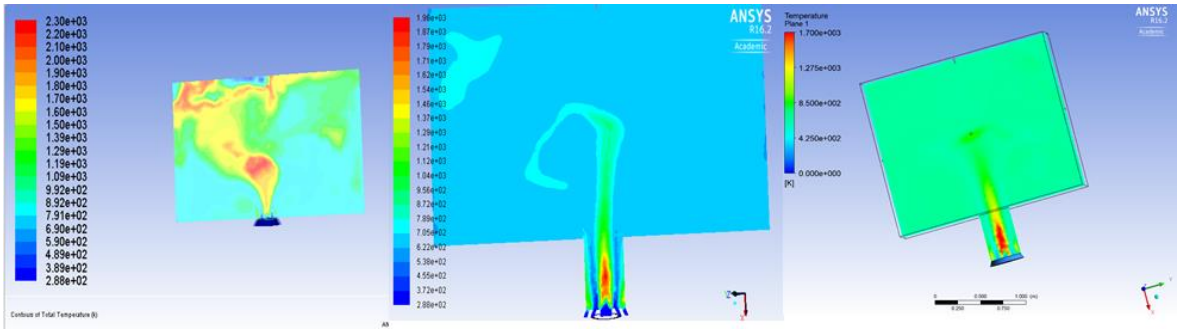

Figure 85 - Models nozzles tested for propane and Jet A fuel

The peak temperatures observed in these simulations presented good agreement with the results from the adiabatic flame temperature calculations (see Table 44). For Jet A fuel, the value was taken from the public domain.

Table 44 - Adiabatic flame temperature calculation for propane and Jet A fuel

Adiabatic flame temperature at 288.15K and 1atm	
Propane	Jet A fuel
1986.85^{o}C	1706.85^{o}C

4.2.2.4.5 Concluding Remarks

Summarising all findings during this phase of the project, the CFD models showed good agreement with the design values for all tested agents (Nitrogen, Halon1301 and HFC-125). Investigations on both Full and Partial Cargo CFD models regarding the appropriate discharge pressure was found appropriate at the higher pressure level of 5bar for all cases.

A general outcome regarding the models quality can be derived by observing the MQF values resulted for each of the CFD simulation cases. It can be seen in Table 45 that all MQFs resulted to be lower than the quality acceptance limit of

0.1%. Nevertheless, it is worth to mention that the Full Cargo models in transient mode resulted to be much more challenging in terms of achieving solution convergence and acceptable accuracy, which in some cases even failed to provide a converged solution. Additionally, the simulation time was significantly larger when using the same CPU and RAM.

Table 45 - MQF Overall summary for the initial CFD models

MQF for each case	
Full Cargo- SS	0,056
Partial Cargo-SS	0,046
Full Cargo- TR	0,496
Partial Cargo-TR	0,279

Additionally, the combustion simulations presented significant challenges both in terms of modelling and calculation time. These facts were discussed both with the *EFFICIENT* project partners as well as with CFD specialists in order to assess the necessity of introducing such complications in the models. Based on the targets of the current research, it is suggested that the work should focus on Scaled models in steady-state mode, simulating the agent discharge only and without the existence of fire. This decision is also supported by the fact that there is already enough information on the public domain regarding the required agent fire extinguishment concentration for each case (cup burner tests) and thus the necessity for experiments is eliminated. However, such information can only be used for verification purposes. For the final models validation and calibration, experimental tests are required.

Furthermore, the transient simulations of the Partial Cargo resulted to be acceptable regarding computational time and satisfactory in simulating the agent discharge process and capturing the effects required for the purposes of this project. Thus, they are suggested to be used for the support of the experimental procedure and the test rig design.

For the Full Cargo models, the final simulations will be limited to steady-state mode and only for the representation of the MPS tests (leakages and ventilation). The suggestion in this case is to scale down the entire model dimensions in an

effort to reduce the computational cost. However, even if reduced, the computational cost level still does not allow for parametric or sensitivity studies. Thus, within the complete duration of the project, only a limited number of simulations can be performed.

Finally, regarding the combustion simulations, a CFD model simulating only the cup burner test procedure could potentially provide a better insight on the derivation of the agent fire extinguishment concentration level. However, such models are recommended for future work.

Summarizing all the above, the final CFD models must focus on:

1. Agent concentration, overpressure and leakages respectively to MPS and to the experimental measurements (gas probes)
2. Agent discharge conditions such as temperature, pressure and mass flow.
3. Agent mixing, distribution and mass loss to the environment
4. Simulations running time reduction

4.2.2.5 Design Space Exploration & Final Selection

This section presents the outcome of the design space exploration performed on the system architecture (location and number of nozzles) and operation using CFD. Additionally, it highlights the options selected as most promising in terms of operability and performance and their relationship to the CFD modelling and simulations setup. Finally, it discusses the CFD model alignment with experiments, its flexibility to modifications and the information it provides regarding system installation on-board commercial aircraft cargo.

Figure 86 presents part of the experimental results of MPS tests using Nitrogen (IG-100), performed by AIRBUS [9]. The figure was adapted to include the times t_1 to t_4, respectively to the setup of the fire extinguish strategy and the time phases for the CFD simulations as well as for verification purposes.

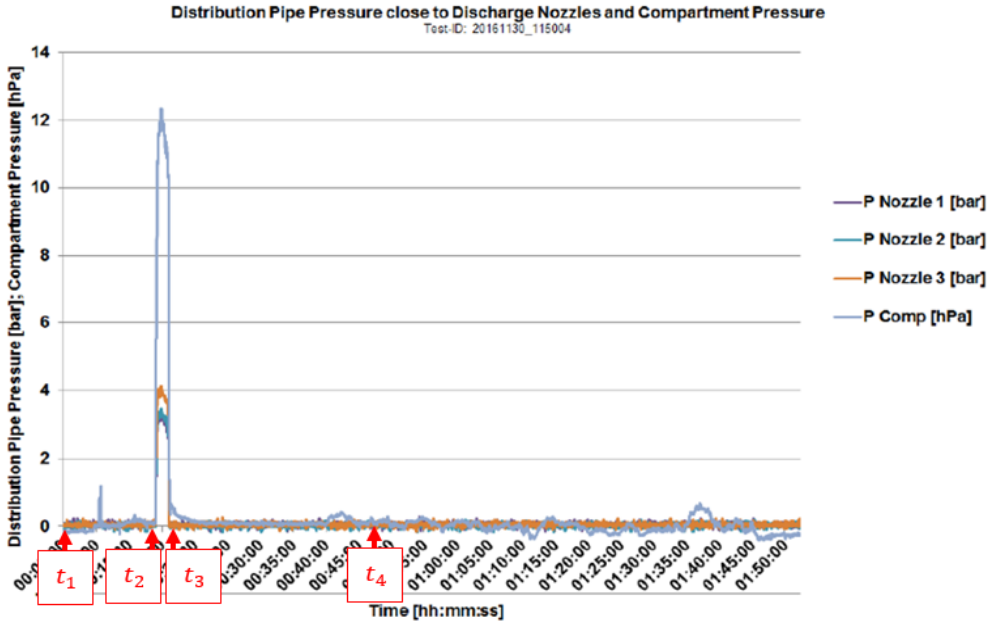

Figure 86 - Experimental measurement of compartment pressure during system operation [9]

The steady-state simulations were set for the instance of full agent discharge described by time t_2. The transient simulations are set for two time periods: a) discharge duration t_2 – t_3 and b) fire protection time t_3 – t_4. The parameters recorded are presented in the list below:

- ✓ Inlet pressure and temperature
- ✓ Inlet Mach number and velocity
- ✓ Inlet density
- ✓ Outlet pressure and temperature or Mass flow
- ✓ Cargo overpressure
- ✓ Cargo N_2 concentration
- ✓ Cargo O_2 concentration

4.2.2.5.1 Final CFD Model Steady-State Simulations

This final part of the system design exploration focused on the selection of the most appropriate number of nozzles for the Full Cargo models. The criteria for this selection have been discussed in Section 3.3.3.1.

The final setup of the Partial Cargo models targeted the assessment of the agent discharge pattern and coverage capability against the number of nozzles, as they

are linearly related to the model dimensions. Based on the outcomes of the current research the most appropriate number of nozzles is 3. This number is also used currently on the actual aircraft cargos and thus minimises the modifications required on the cargo architecture. Although the piping network will need replacement in order to accommodate the new agent, its isometric diagram won't need to change and thus nor any of the other surrounding structures or systems. The selection of the agent discharge conditions was based on the trade-off between the estimated system dimensions, weight and effectiveness, while considering system structural integrity and smooth and safe operability. The top limit for the discharge pressure was based on state-of-the-art land-based Nitrogen systems (≤60bar), including also discharge noise limitations.

The value of 41bar was found to provide the best compromise between the parameters below:

- Forces and velocities of the jets
- Piping network dimensions and weight
- Piping network pressure losses *(Fanno* flow in pipes)
- Nitrogen temperature drop due to throttling (Joule-Thomson effect)
- Margin from maximum acceptable for discharge time variability (60bar)

The discharge time variability is necessary in order to estimate the minimum available discharge time. Additionally, in cases where real fire scenarios present insufficient fire suppression properties for the given time and burning material, an increase of discharge pressure can allow the system to achieve its original goals without any major modifications, besides a small adjustment of the ventilation port size.

The Partial Cargo steady-state simulation for Nitrogen discharge at 41bar is presented in Figure 87. The streamlines illustrate that the targeted distribution and coverage is achieved, confirming again that 3 nozzles are sufficient. It is worth to mention here that a modification on the initial nozzle design resulted out of observing the level of velocities around the nozzle location. In order to minimise the impact of the high velocity regime (≥30m/sec,) on the surroundings, the frontal orifice of the nozzle was removed. The final nozzle design resulted to form jets

with relatively small (~15cm) radius of impact for the high velocity regime (see Figure 87d). Thus, the agent is discharged only through the 6 side orifices forming the targeted flow pattern with the ventilation port and leakages (see Figure 87b, c).

The system design target is not only to achieve sufficient agent spread but also to prolong the agent path before it exits the enclosure and minimise mass leakage to the environment. Minimising agent mass losses directly increases fire protection time and ultimately reduces the final agent quantity or storage weight and size.

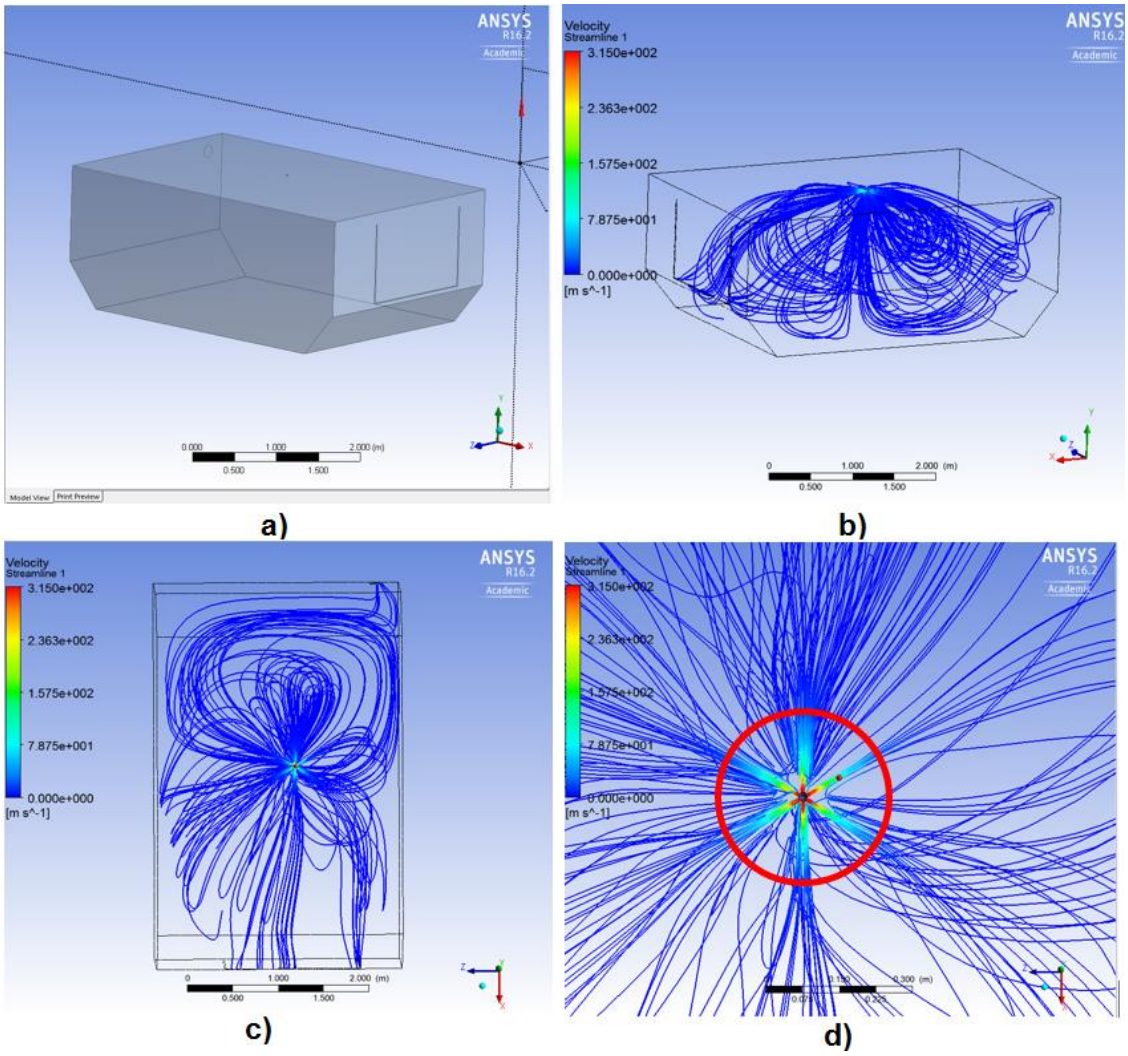

Figure 87 - Partial Cargo Nitrogen discharge at 41bar using 3 nozzles

Similarly to the previous section, the results verification for the above Partial Cargo steady-state simulation is presented in Table 46. The resulted MQF in this case also presented acceptance value.

$$MQF_{Partial\ Cargo,SS} = 0.036\ \%$$

Table 46 - Main CFD outcomes verification for Partial Cargo steady-state simulations

Partial Cargo - Steady-State	Analytical design				CFD predictions				Absolute Delta (%)			
	Nozzles	Door Leaks	Vent Port	Cargo	Nozzles	Door Leaks	Vent Port	Cargo	Nozzles	Door Leaks	Vent Port	Cargo
Total Pressure (bar)	41	NA	NA	<0,015	41,03	NA	NA	0,0143	0,0732	NA	NA	NA
Static Pressure (bar)	21,7	NA	NA	NA	21,706	NA	NA	0,01381	0,0253	NA	NA	NA
Total Temperature (K)	288,1	288,1	288,1	288,1	288,05	288,07	288,05	288,07	0,0174	0,0104	0,0174	0,0104
Density (kg/m3)	29,6	1,205	1,205	1,205	29,59	1,206	1,206	1,206	0,0338	0,0863	0,0846	0,0780
Velocity (m/sec)	314,80	NA	NA	NA	314,69	NA	NA	NA	0,0356	NA	NA	NA
Mach Number	1	NA	NA	NA	0,99981	NA	NA	0,101	0,0190	NA	NA	NA
Inlet Mass Flow (kg/s)	0,1533	0	0	NA	0,15333	NA	NA	NA	0,0000	NA	NA	NA
Outlet Mass Flow (kg/s)	NA	NA	NA	0,1533	NA	NA	NA	0,15346	NA	NA	NA	0,083
Agent volumetric fraction	1	1	1	1	0,9998	0,9998	0,9998	0,9998	0,0200	0,0200	0,0200	0,0200
											MQF	0,036

The Full Cargo steady-state simulation for Nitrogen discharge using 3 nozzles at 41bar is illustrated in Figure 88. This model successfully achieved the targeted agent distribution and coverage as well as the ventilation and leakage rates. In the left picture of this figure, the streamlines illustrate that the agent covers every corner of the control volume. In the right picture, the velocity vectors highlight the low velocity of flow close to the ventilation port and door leakage. It is important to note here that the ‘red’ colour in the picture represents only the velocity at the inlet orifices and not to the surrounding region as it appears. This was due to the fact that in order to capture the low velocity vectors, the selected relative size for display was increased significantly. The general output of this simulation confirms that the specific design presents all the targeted performance features and thus selected as the final model for all Full Cargo simulations.

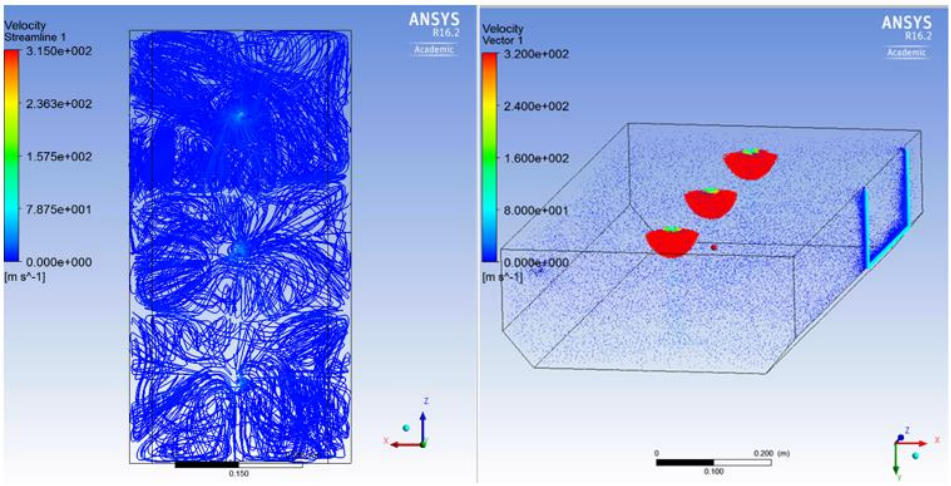

Figure 88 – Full Cargo Nitrogen discharge at 41bar using 3 nozzles

Regarding the agent jets interactions, the results showed that the relative position of the orifices affects the agent distribution pattern (see Figure 89 top). In this case, the nozzles were placed symmetrically with two of their orifices perfectly aligned with the compartment centreline. This design setting leads to the collision of the jets coming from neighbouring nozzles, which reduces their velocity while increases the velocities of the remaining nozzle orifices. In order to improve the agent distribution pattern, the orifices are positioned at a 15° angle from the compartment centreline (see Figure 90). Finally, the high velocity regime resulted to be limited within a radius of ~15cm around the nozzles and at a height of ~5cm (see Figure 91).

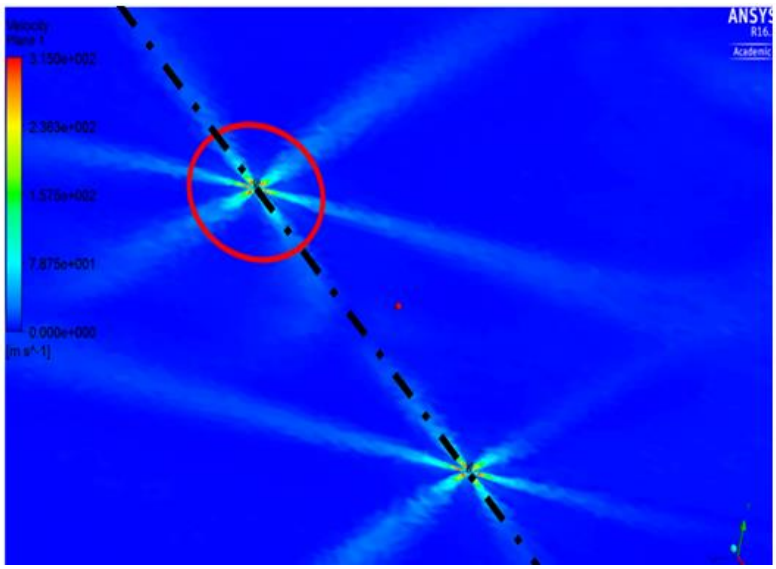

Figure 89 - Nitrogen jets interaction for Full Cargo discharge at 41bar

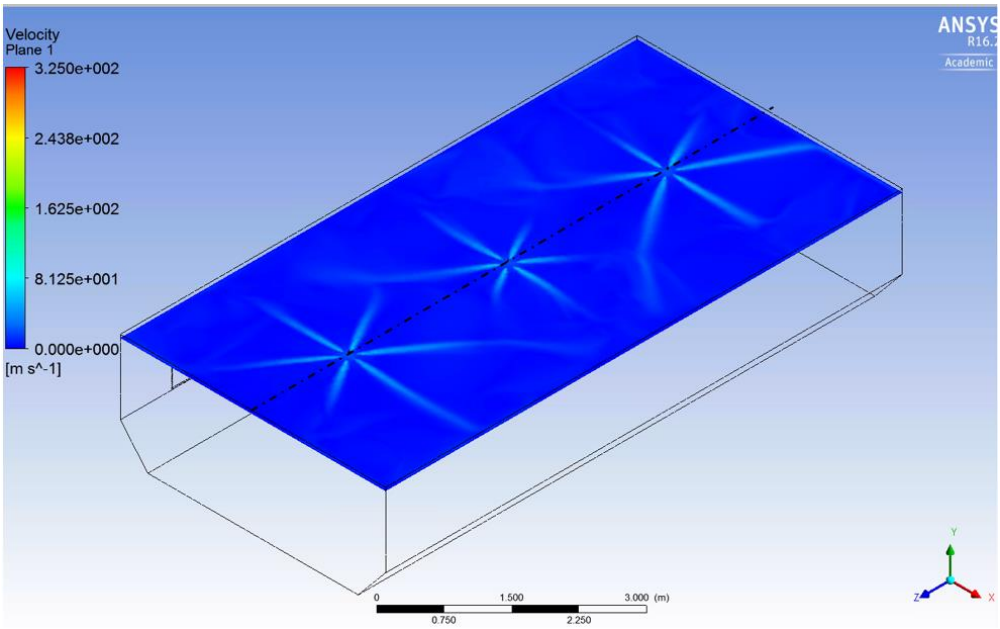

Figure 90 - Nitrogen jets interaction for Full Cargo with nozzles repositioned at 15° angle from the centreline

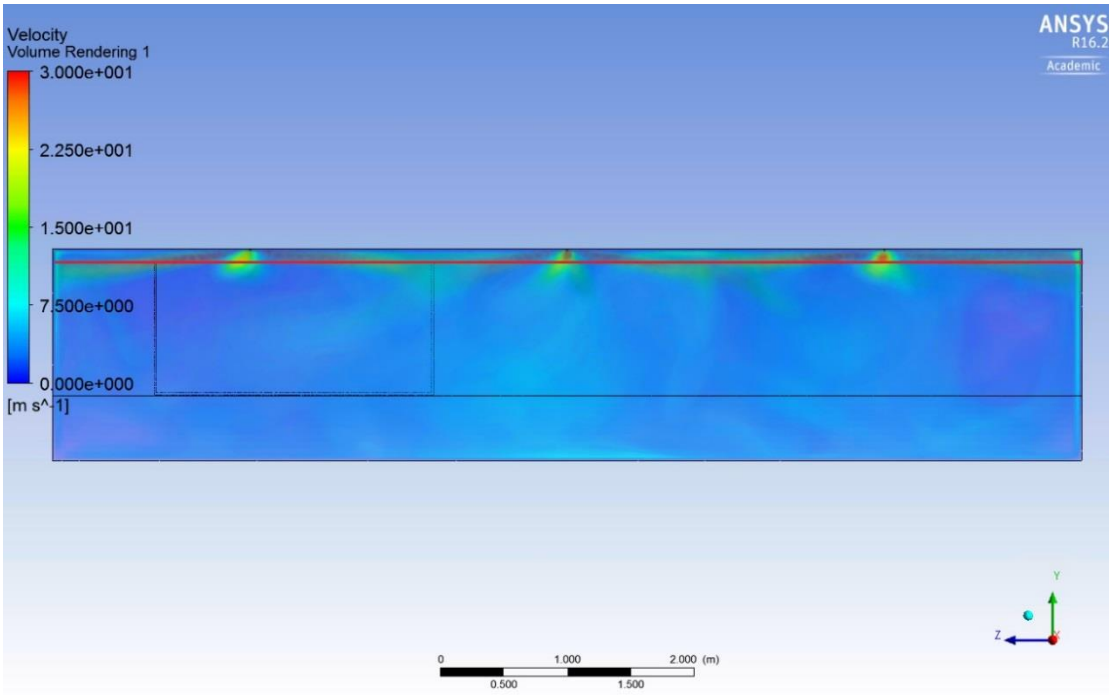

Figure 91 - Nitrogen jets velocity regime of >30m/s limited to 5cm from ceiling on empty cargo

Besides the 30m/s characteristic limit for high velocity, plotting the output in this velocity range allows a closer observation of the agent discharge process.

Observing Figure 92 it can be noted that there is a relatively symmetric agent flow pattern, despite the door leakages and ventilation port, with the central jets intersecting each other allowing improved agent mixing and distribution.

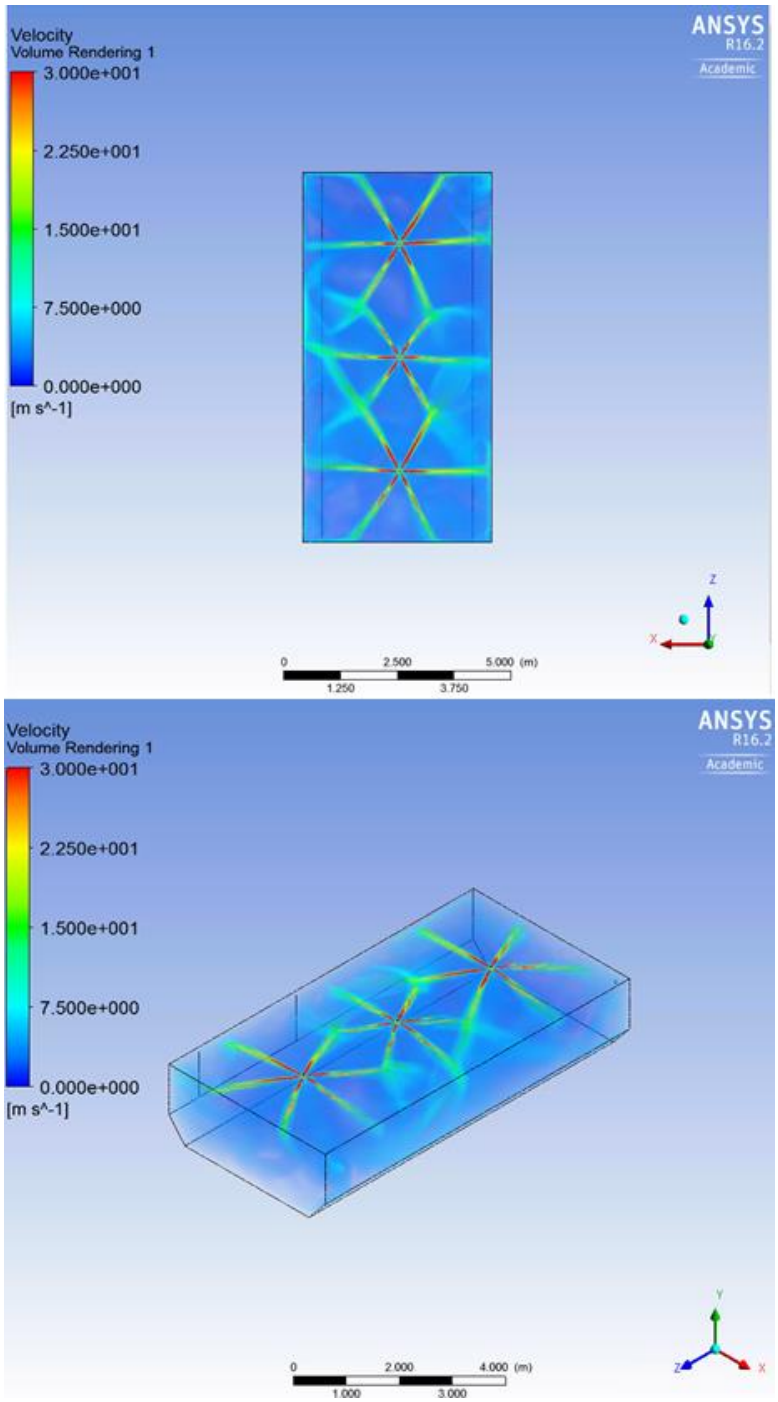

Figure 92 - Nitrogen flow pattern for Full Cargo discharge at 41bar for 3 nozzles

The Full Cargo steady-state simulations supported also the ventilation system arrangement and sizing. Designing the system for a specific level of overpressure

during discharge allows a direct trade-off between the agent discharge pressure and the ventilation ports dimensions. In order to design a system which allows for a range of agent discharge pressures, the compartment ventilation ports must be able to adjust simultaneously. For the CFD models, the design overpressure limit/target was set to be ≤ 1500Pa. The results presented in Figure 93 represent the ventilation port sized at 0.084m in diameter for the 41bar discharge pressure, including the given door leakages. Regarding the location of the ventilation port, it has been decided that it should be placed on the worst possible position in order to maximise its negative impact on the agent distribution patterns. This way, the design assures that even in that case, the agent concentration reaches the design values and the fire won't be able to be sustained. Of course, the final design for the aircraft must consider all the above and select the location away from the ceiling and away from locations of high fire risk. Additionally, it must consider area variability mechanisms or sensitive pressure relief ports to ensure low overpressure levels at any fire scenario.

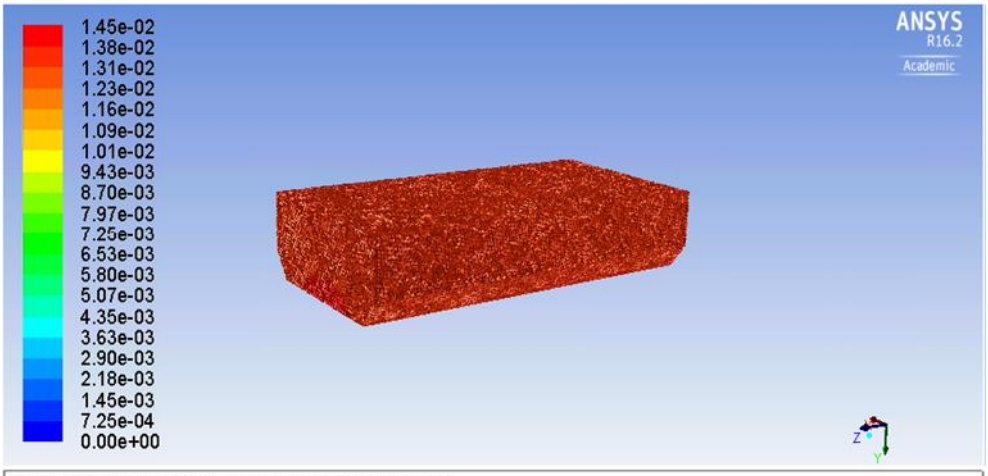


```
Reading "E:\30 month review\Final\filleeee\final.416.dat"...
Parallel variables...
Done.

  iter  continuity  x-velocity  y-velocity  z-velocity      energy           k      epsilon          n2          o2
   120  1.4025e-04  1.5388e-05  1.7490e-05  1.5542e-05  9.9660e-08  2.1263e-04  4.6771e-05  1.5284e-07  1.5388e-05
   121  1.4279e-04  1.5454e-05  1.7536e-05  1.5592e-05  9.8669e-08  2.0824e-04  4.6035e-05  1.5031e-07  1.5592e-05
   122  1.4344e-04  1.5470e-05  1.7546e-05  1.5604e-05  9.8723e-08  2.0724e-04  4.5949e-05  1.3977e-07  1.5470e-05

Interrupting...
   123  1.4410e-04  1.5485e-05  1.7558e-05  1.5616e-05  9.8041e-08  2.0617e-04  4.5953e-05  1.3712e-07  1.5454e-05
Done.

          Area-Weighted Average
                 Total Pressure                (atm)
--------------------------------- ------------------
                interior-solid         0.014482095
```

Figure 93 - Full Cargo average overpressure 1448Pa during Nitrogen discharge at 41bar

Similar, regarding the loaded cargo cases with 30% boxes and for the same discharge pressure of 41bar for 0.7min, the overpressure reached slightly higher but below the limit value of 1500Pa without any adjustment on the ventilation port size. This indicates the level of adjustment required for the ventilation port in order to account for higher load values. Figure below illustrates the Nitrogen jets velocities for the Full Cargo Loaded case.

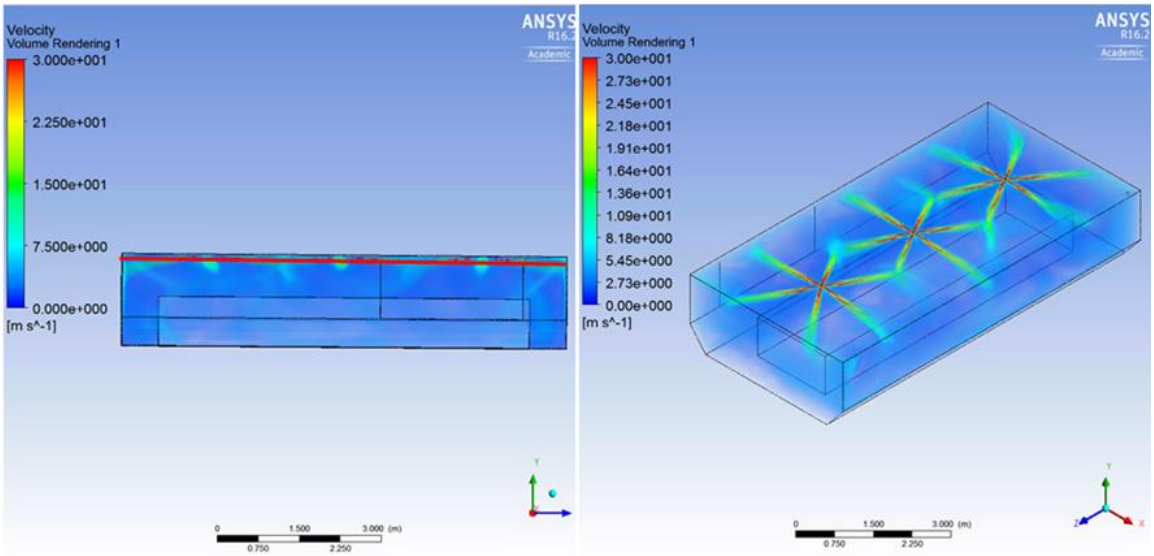

Figure 94 - Nitrogen jets velocity regime of >30m/s limited to 5cm from ceiling on 30% loaded cargo

The resulted MQF in Full Cargo steady-state cases also presented acceptable value.

$$MQF_{Full\ Cargo,SS} = 0.0475\ \%$$

Table 47 - Main CFD outcomes verification for Full Cargo steady-state simulations

Full Cargo - Steady-State	Analytical design				CFD predictions				Absolute Delta (%)			
	Nozzles	Door Leaks	Vent Port	Cargo	Nozzles	Door Leaks	Vent Port	Cargo	Nozzles	Door Leaks	Vent Port	Cargo
Total Pressure (bar)	41	NA	NA	<0,015	41,04	NA	NA	0,0145	0,0976	NA	NA	NA
Static Pressure (bar)	21,7	NA	NA	NA	21,708	NA	NA	0,0138	0,0369	NA	NA	NA
Total Temperature (K)	288,1	288,1	288,1	288,1	288,04	288,02	288,01	288,01	0,0208	0,0278	0,0312	0,0309
Density (kg/m3)	29,6	1,205	1,205	1,205	29,58	1,206	1,206	1,206	0,0845	0,0946	0,0946	0,0830
Velocity (m/sec)	314,80	NA	NA	NA	314,68	NA	NA	NA	0,0379	NA	NA	NA
Mach Number	1	NA	NA	NA	0,99971	NA	NA	0,101	0,0290	NA	NA	NA
Inlet Mass Flow (kg/s)	0,46	0	0	1	0,46	NA	NA	NA	0,0000	NA	NA	NA
Outlet Mass Flow (kg/s)	NA	NA	NA	0,46	NA	NA	NA	0,4604	NA	NA	NA	0,0870
Agent volumetric fraction	1	1	1	1	0,9997	0,9998	0,9998	0,9997	0,0300	0,0200	0,0200	0,0300
											MQF	0,0475

Steady-state simulations following the design strategy discussed above were proved satisfactory because they can deliver converged solutions relatively fast, providing most of the main design data required to manufacture and install such systems. This capability can support future developments on the research topic.

4.2.2.5.2 Final CFD Model Transient Simulations

The transient simulations provided information on the cargo conditions during and after the agent discharge process. The models were set to simulate the time periods $(t_2 \rightarrow t_3)$ and $(t_3 \rightarrow t_4)$. However, these simulations targeted to represent the experimental test cases, in which the agent is discharged at a constant mass flow rate. Thus, the storage cylinders drain-out process is excluded, simplifying the simulations. Based on the system settings, the overpressure inside the empty cargo compartment along with the indicated times are illustrated in Figure 95. The first period represents the continuous discharge of the agent in order to suppress the fire as quickly as possible. The target is to achieve Oxygen concentration 10.4% with overpressure limit/target ≤1500Pa, including considerations about safety factors and fire protection time. This follows the analytical model settings in terms of mass flow and Oxygen concentration. In order to achieve the same level of Oxygen concentration the simulations discharge time was set to 1.74min (at 0.46kg/s constant mass flow), including the agent mass during drain out. After discharge stops, the target was to maintain Oxygen concentration ≤16%, for around 42min, with overpressure limit/target ≤250Pa.

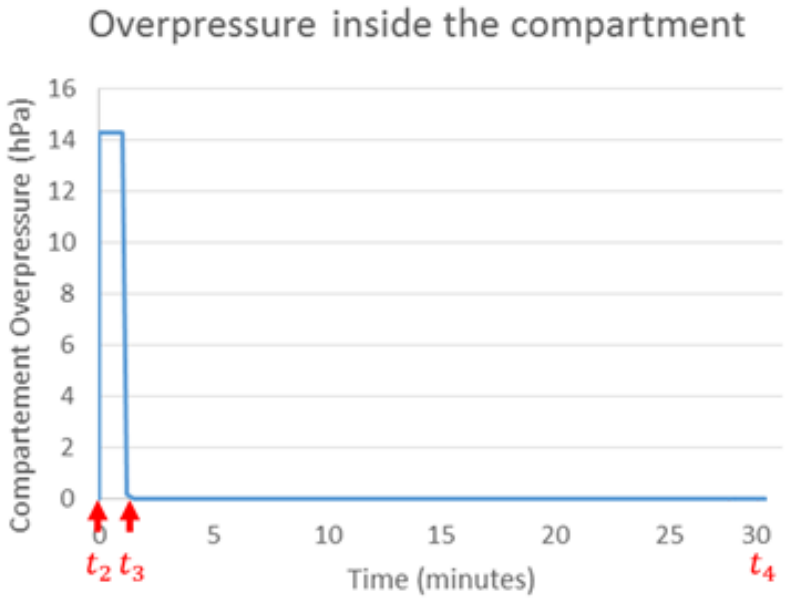

Figure 95 - Full Cargo overpressure for Nitrogen discharge at 41bar - transient simulation setup for two time periods

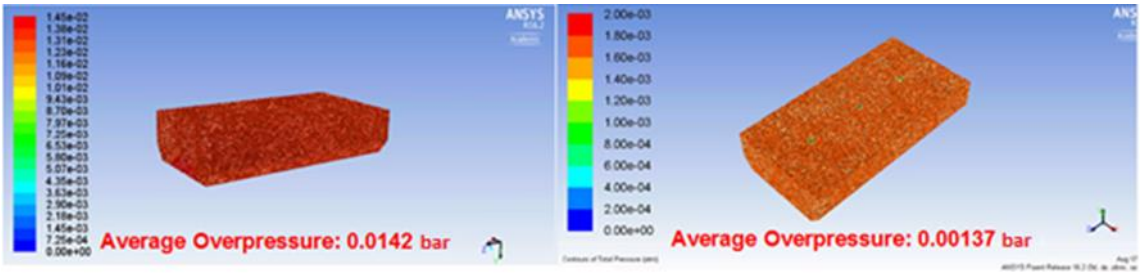

Figure 96 - Full Cargo overpressure (bar) during Nitrogen discharge at 41bar for a) t_3=1.7 min (left) and b) t_4=46.53min (right)

Figure 96 presents the overpressure of the Full Cargo empty case at two time instances: a) at t_3=1.74min and b) t_4=46.53min (≈46min from analytical model). The Nitrogen discharge stopped exactly after t=1.74min, achieving O_2 concentration value of 10.4%. The simulation continued with a 0.023m^3/sec constant door leakage rate until approximately 46min later, where the O_2 concentration reached the value of 15.4% instead of 16%. The difference of 0.6% between the analytical and numerical models shows that the analytical models overestimate the average Oxygen concentration reduction rate compared to the CFD. The assumptions used regarding the homogenous air/agent mixture, the infinitely fast mixing and distribution and the constant inlet and leakage flow rates lead to a relatively faster average Oxygen concentration reduction rate. Thus, based on the CFD results the system can provide even greater fire protection time. Figure 97 illustrates that the Oxygen concentration at the main plane of interest for the two time periods achieved the targets, ensuring adequate fire suppression and fire protection time. Discharging the agent using the same nozzle and pressure, the overpressure level for the 30% loaded cases was found acceptable, with the Oxygen concentration reaching the values of 10.3% at t_2=1.21min and 15.9% at t_2=32.1min (see Figure 98). These values are very close to the predictions of the analytical model, which were 16% at 32.2min.

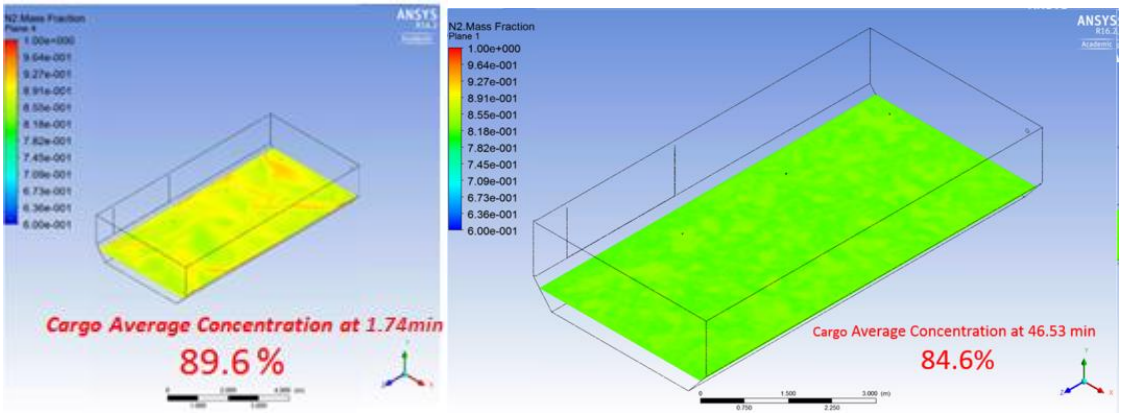

Figure 97 - Full Cargo empty Nitrogen mass fraction at the main plane of interest (height 0.305m) for a) t_3=1.74min (left) and b) t_4=46.53min (right)

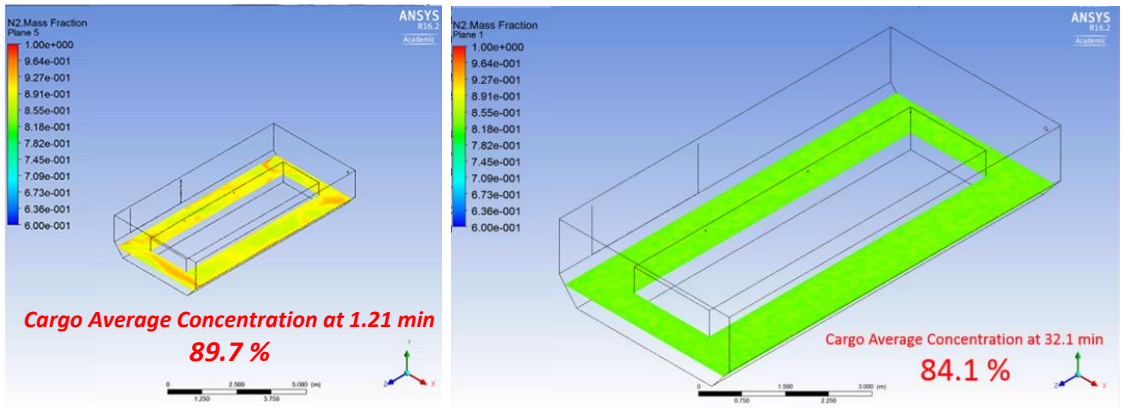

Figure 98 - Full Cargo loaded 30% with boxes, Nitrogen mass fraction at the main plane of interest (height 0.30m) for a) t_3=1.21min (left) and b) t_4=32.11min (right)

Following a similar approach to Section 4.2.2.4.1 for the Partial Cargo transient cases, the trend lines of the transient CFD outcomes were plotted in order to assess the overal system perfromance (see Figure 99 and Figure 100). All cases simulating the time Period 3, agent discharge, showed linear trend while those for Period 4 followed logarithic. These outcomes provide an insight on the exchange between discharge time to achieve the design Oxygen concentration and fire protection time achieved. For the loaded case, since the cargo volume is reduced, fixing the discharge mass flow rate resuls in reduced time to achieve the design concentration. However, after discharge stops, the inverse reason leads to reduced fire protection time. Thus, such outcomes can be extended to cover the complete design space, mapping out the exchange rates between the time until the fire is knocked down and the fire protection time.

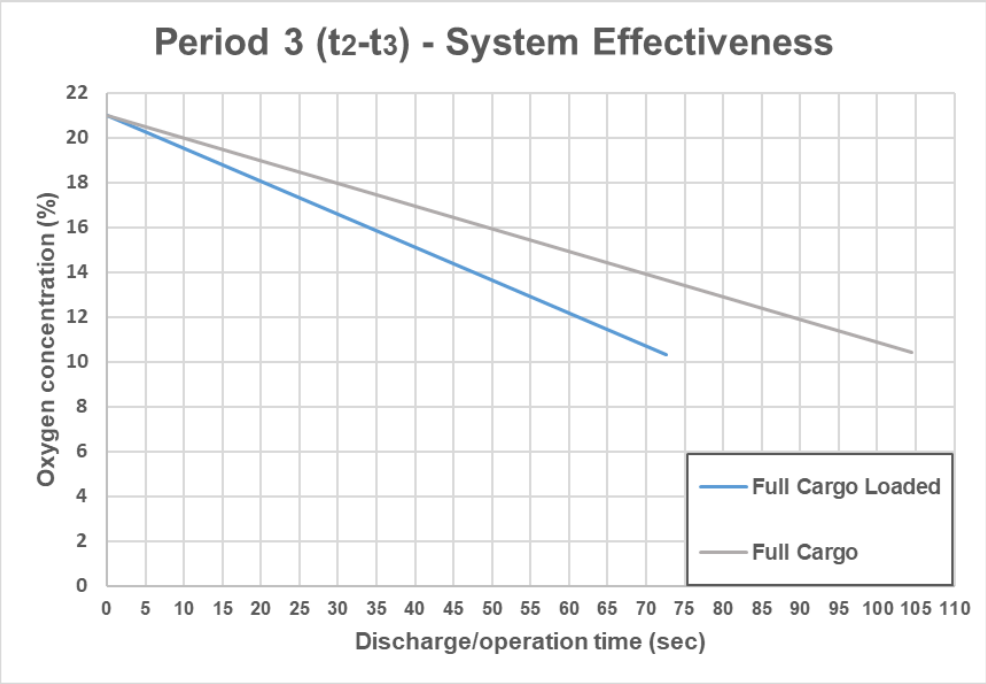

Figure 99 - Transient CFD simulations outcomes for Period 3

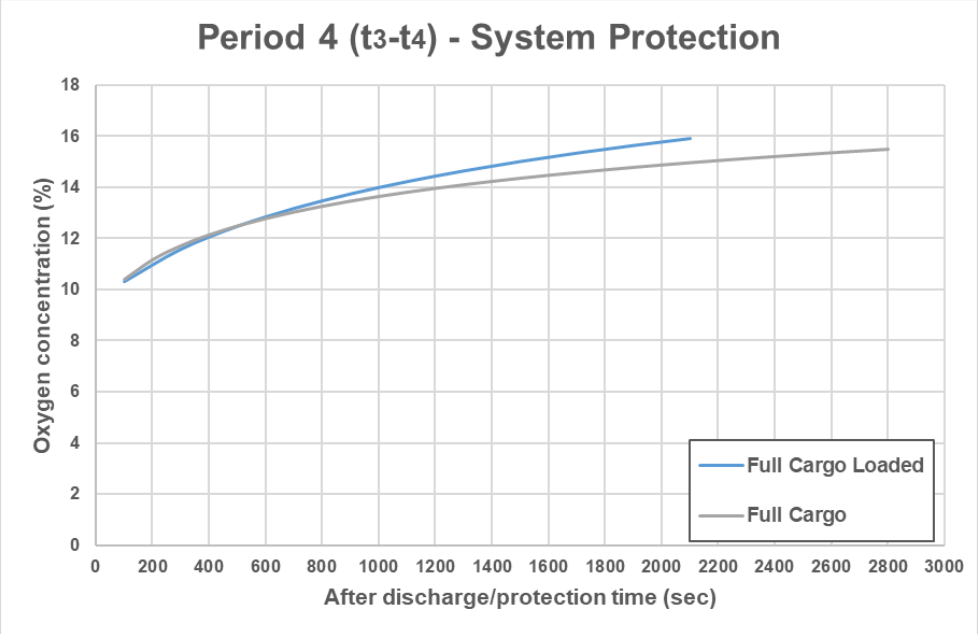

Figure 100 - Transient CFD simulations outcomes for Period 4

Focusing on the transient simulations for the 30% loaded cargo, the results were plotted against the four planes of interest (see Figure 101). Applying the same nozzle geometry and discharge pressure, the required discharge time is reduced respectively to the protected volume decrease. The Oxygen concentration observed in each plane seems to have reached the required level. However,

some unevenness on Oxygen concentration is observed at the critical plane of interest. Generally, close to the short side-walls of the cargo there is an increased level of agent concentration while close to the long side-walls the concentration appears slightly reduced. The most critical region locates near the long side-wall which is opposite to the door leakages. The effect of the ventilation port is negligible at this phase of the system operation.

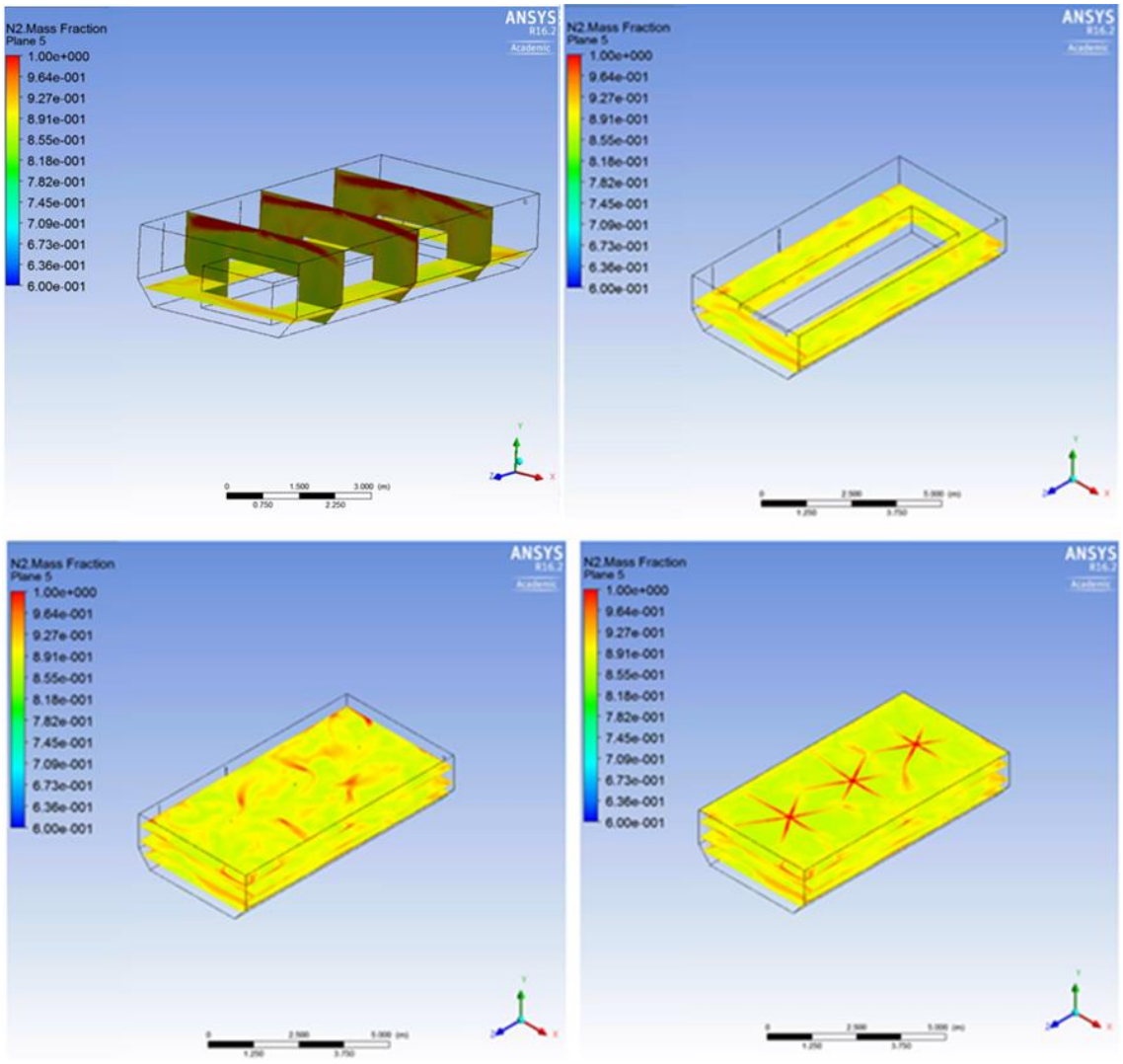

Figure 101 - Full Cargo loaded 30% with boxes Nitrogen mass fraction at four planes and t_3=1.21 min

The recording of overpressure and concentration in these simulations allows the assessment of the ventilation port and leakages areas on the rate of agent mass loss. The presented outcomes resulted out of progressive increase of the

ventilation port area until the overpressure reached acceptable levels during and after discharge. During this process, the resulted fire protection time was reducing, as the ventilation port area was increasing, fact that resulted in a small increase in the agent discharge duration and thus total mass. Nevertheless, the final model met all the design criteria without a significant change in the weight of the agent storage and delivery system.

An important requirement coming from real aircraft operations regards the increase of fire protection time to 3 hours, assuming that the fire event happened at the worst possible time during flight (see Figure 5). Figure 102 shows the simulation for the Full Cargo empty case, after the time of 46.53min where the Oxygen concentration reached 15.4%. At that moment, the setting for the ventilation port mass flow inlet was switched from pure air to hypoxic with 14 % Oxygen concentration. Based on the amount of leakage rate, the flow of the hypoxic air entering the control volume is 0.023m^3/s. These facts lead to the conclusion that with a small addition of Nitrogen (IG-100) mass, the maintenance of Oxygen concentration below the fire re-ignition limit for 3 hours can be achieved.

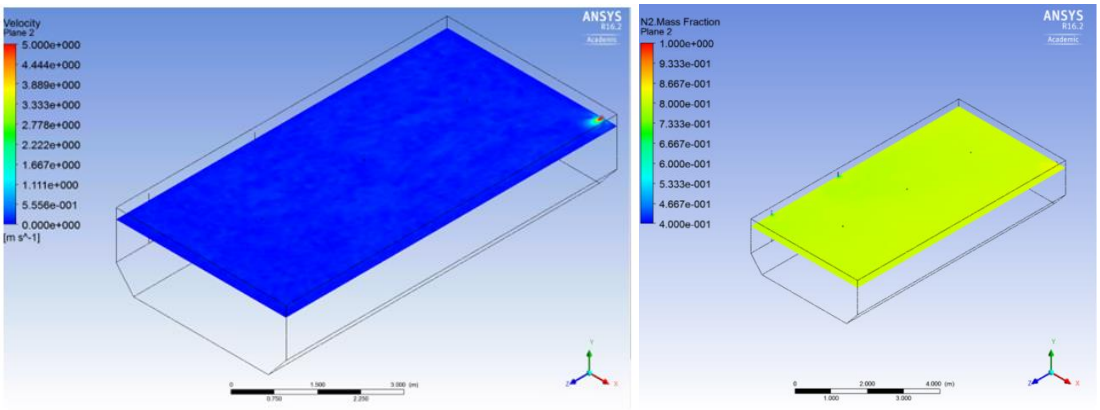

Figure 102 – Velocity and mass fraction contours using hypoxic inlet (14%) Oxygen)

Finally, in the tables bellow, the results verification for empty and 30% loaded Full Cargo transient simulation cases are presented. The outcomes in the transient cases presented relatively lower level of accuracy compared to the steady-state. Nevertheless, the resulted MQFs also presented acceptable values, since the requirements for transient simulations are relaxed compared those of the steady-state.

$$MQF_{Full\ Cargo,Empty,TR} = 0.2619\ \%$$

$$MQF_{Full\ Cargo,30\%load,TR} = 0.2746\ \%$$

Table 48 - Main CFD outcomes verification for empty Full Cargo transient simulations

Full Cargo - Transient	Analytical design				CFD predictions				Absolute Delta (%)			
	Nozzles	Door Leaks	Vent Port	Cargo	Nozzles	Door Leaks	Vent Port	Cargo	Nozzles	Door Leaks	Vent Port	Cargo
Total Pressure (bar)	41	NA	NA	<0,015	41	NA	NA	0,0142	0,0000	NA	NA	NA
Static Pressure (bar)	21,7	NA	NA	NA	21,54	NA	NA	NA	0,7373	NA	NA	NA
Total Temperature (K)	288,1	288,1	288,1	288,1	288,24	288,35	288,41	288,4	0,0486	0,0868	0,1076	0,1145
Density (kg/m3)	29,6	1,205	1,205	1,205	29,840	1,208	1,207	1,207	0,8108	0,2689	0,1920	0,1535
Velocity (m/sec)	314,8	NA	NA	NA	315,81	NA	NA	NA	0,3217	NA	NA	NA
Mach Number	1	NA	NA	NA	0,9991	NA	NA	0,101	0,0900	NA	NA	NA
Inlet Mass Flow (kg/s)	0,46	0	0	NA	0,462	NA	NA	NA	0,3476	NA	NA	NA
Outlet Mass Flow (kg/s-m^3/s) at t3-t4	NA	NA	NA	0,46	0,1914	NA	NA	0,4635	NA	NA	NA	0,7609
Agent volumetric fraction at t3	1	NA	NA	<0.88	0,9985	NA	NA	0,89	0,1500	NA	NA	NA
Agent volumetric fraction at t4	1	NA	NA	<0.84	0,9985	NA	NA	0,846	0,1500	NA	NA	NA
Total Pressure after disharge (atm)	0	NA	NA	<0.0025	0	NA	NA	0,00137	NA	NA	NA	NA
											MQF	0,2619

Table 49 - Main CFD outcomes verification for 30% loaded Full Cargo transient simulations

Full Cargo-Loaded - Transient	Analytical design				CFD predictions				Absolute Delta (%)			
	Nozzles	Door Leaks	Vent Port	Cargo	Nozzles	Door Leaks	Vent Port	Cargo	Nozzles	Door Leaks	Vent Port	Cargo
Total Pressure (bar)	41	NA	NA	<0,015	41	NA	NA	0,01418	0,0000	NA	NA	NA
Static Pressure (bar)	21,7	NA	NA	NA	21,52	NA	NA	NA	0,8295	NA	NA	NA
Total Temperature (K)	288,1	288,1	288,1	288,1	288,28	288,44	288,53	288,5	0,0625	0,1180	0,1493	0,1493
Density (kg/m3)	29,6	1,205	1,205	1,205	29,850	1,209	1,208	1,207	0,8429	0,3436	0,2606	0,1660
Velocity (m/sec)	314,8	NA	NA	NA	315,81	316,18	315,85	NA	0,3194	NA	NA	NA
Mach Number	1	NA	NA	NA	0,999	NA	NA	0,101	0,1000	NA	NA	NA
Inlet Mass Flow (kg/s)	0,46	0	0	NA	0,463	NA	NA	NA	0,6522	NA	NA	NA
Outlet Mass Flow (kg/s) at t3	NA	NA	NA	0,46	NA	NA	NA	0,464	NA	NA	NA	0,8696
Agent volumetric fraction at t3	1	NA	NA	<0.88	0,998	NA	NA	0,896	0,2000	NA	NA	NA
Agent volumetric fraction at t4	1	NA	NA	<0.84	0,998	NA	NA	0,848	0,2000	NA	NA	NA
Total Pressure after disharge (atm)	0	NA	NA	<0.0025	0	NA	NA	0,00135	NA	NA	NA	NA
											MQF	0,2746

Summarizing, the final CFD models were proved sufficient to support and assess the overall system design and performance, providing improved solution accuracy compared to the initial models (compare Table 50 and Table 45). These outcomes provided confidence on the final system design and its targets.

Table 50 - MQF Overall summary for the final CFD models

MQF Final models	
Full Cargo- SS	0,048
Partial Cargo-SS	0,036
Full Cargo Loaded- TR	0,275
Full Cargo-TR	0,262

4.3 Nitrogen System Experimental Testing & Alignment with Analytical/Numerical Models

This section presents the proposed test rig final setup and operation. It includes key measurements of the performance assessment of the system in terms of satisfying the MPS requirements. Additionally, it includes suggestions on CFD model adaptations and calibrations using the available experimental data. Finally, it describes the design iteration needed to be performed between the analytical/numerical and experimental test rig setup in order for the proposed system to reach a higher TRL for aircraft cargo applications.

The MPS based experimental fire tests were primarily built to assess the proposed replacement fire suppression system. Nevertheless, the test rig design was developed in parallel to the development of the numerical 3D-CFD models, using the outputs of the analytical study. However, the test rig assembly was completed at the last phase of the present research, allowing limited time for testing and no time for iterations between the tests and the analytical/numerical models. The test rig operation so far produced two complete sets of measurements: a) No-Fire Tests and b) Open Surface Liquid Fire Tests using Jet-A fuel. Both refer to the Full Cargo Empty cargo compartment cases. These are the experimental measurements that are analysed within the present research. The rest of the required MPS fire tests are going to be completed after the end of the present research and thus are considered as future work.

The MPS based cargo container installed is presented in the figure below. The dimensions match the proposed design while it assures adequate air sealing. Additionally, the pressure and temperature sensors as well as the controls follow the description in Section 3.3.2.

Figure 103 - Test rig cargo compartment structure

The door leakages were represented with the components illustrated in Figure 104. At the centre of this U structure there is a 0.084m in diameter outlet port connected to a pipe, which in turn is connected to a variable speed fan (see Figure 105).

Figure 104 - Cargo door leakage representation on test rig

Figure 105 - Variable speed fan connected for cargo door leakages

The agent storage cylinders as well as part of the piping network can be seen in Figure 106. The cylinders size was based on the agent quantity resulted out of the analytical and numerical calculations while the piping network followed the isometric diagram presented in Figure 64. Figure 107 shows the piping line on the top of the container and the sensors installed for pressure and temperature recording.

Figure 106 - Nitrogen storage cylinders and distribution network

Figure 107 - Nitrogen distribution network

The complete structure of the test rig matches the geometry of the 3D-CFD models as well as the dimensions, conditions and properties of the analytical models. Nevertheless, due to market availability and other similar reasons, some small differences were observed on the installed piping network and discharge nozzles. The effect of such differences on the overall system operation is discussed later in this section.

4.3.1 Experimental Tests without Fire

As mentioned in previous chapters, the main experimental test needed for the validation of both analytical and CFD models, regards the full Nitrogen discharge in the empty compartment without the existence of fire.

The first test rig operation was set to assure that all components are operating as expected. This process included a number of system activations without the existence of fire, while performing a full measurement recording. Such measurements are then used for model validation purposes.

The main measurements for all experimental tests were taken at the time instances t_3 and t_4, as described in Section 3.3.2. Each test was repeated 5 times and the final output for each parameter measured was the resulted average. These main measurements are namely:

- Nitrogen discharge conditions (pressure, temperature and mass flow)
- Cargo conditions (overpressure and leakage flow)
- Agent concentration inside the compartment (v/v %)
- Discharge and protection times (sec or min)

The recording of the discharge pressure against time during the Full Cargo - Empty - No Fire tests is presented in Figure 108. In this case, the system is designed to discharge initially constant mass flow for around 60sec and then continue the discharge allowing the system to expand naturally until the storage cylinders drain out. The recording continues for another two minutes after the cylinders drain out. The average discharge pressure measured for all 3 nozzles presents a trend that closely matches the theoretically expected. The discharge pressure slightly reduces moving from the first to the last nozzle. A close

observation on the data shows that the discharge pressure difference between the first and second nozzles is greater than that of between the second and third at the initial phase of discharge. This doesn't follow exactly the outputs (see Figure 65) of the analytical models due to the fact that the piping network installed on the test rig presented some small differences on the dimensions of the pipes and the discharge nozzles. Nevertheless, the differences are small and they do not affect the primary analysis targets for the system assessment. This is visible when the outputs of the analytical model get superimposed on the experimental outputs. The 41bar constant discharge pressure assumed for 60sec in the analytical model captures the average of the discharge pressures measured for the approximately 55sec main discharge achieved by the actual system. The reason behind the reduced duration of the main discharge phase on this test regard the setting of the first main pressure reducer of the piping network. In the experiment, the pressure reduction after the storage cylinders was more than 120bar, which was used in the analytical model. This fact dictates that during discharge, the cylinder loses mass and thus, its pressure drop. When the pressure inside the cylinder becomes equal to the first pressure reducer setting, the cylinder starts to expand directly into the rest of the piping network. This transition point can be observed on all 3 nozzles discharge pressure curves at the time between 50-60sec, where the curves present a wave-type shape before they start the steep drain out reduction rate. This is due to the pressure reduction valve elastic element which regulates the level of required pressure. Additionally, the linear reduction assumed after 60sec in the analytical model seems to predict relatively accurately the cylinder drain out time.

It has to be noted here that is has been measured that the piping network filling up process requires around 7 kg of agent, which remains unused and locked inside the network.

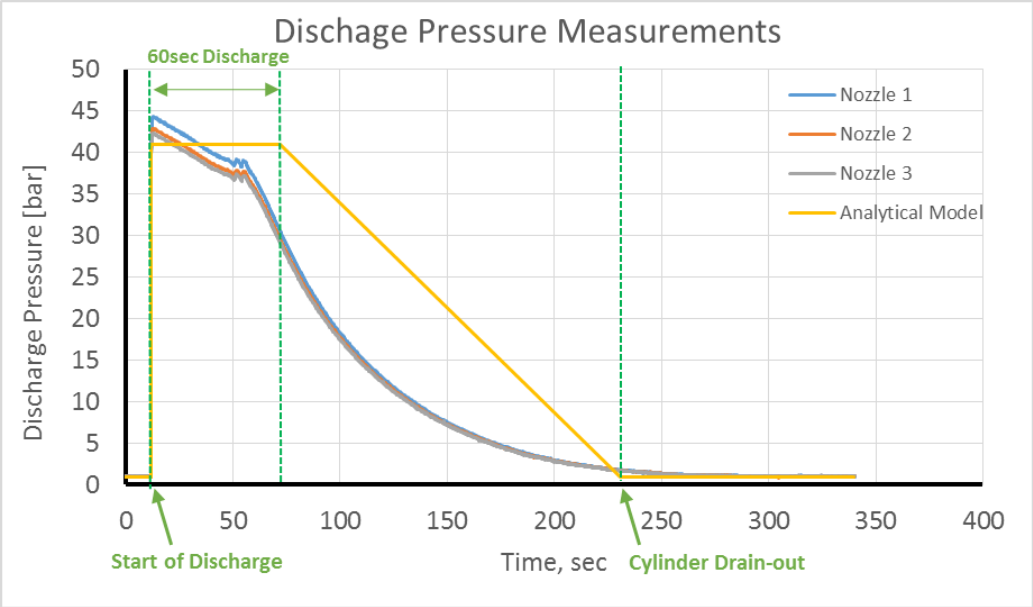

Figure 108– No Fire Experimental Data: Discharge Pressure Measurements vs Time

Figure 109 illustrates the respective results for the discharge temperature against time. The experimental results present several differences to analytical model. This is expected as the set of assumptions applied on the analytical approach targeted the simplification of the problem, to a level appropriate for the purposes of the present research. Thus, in the analytical model the initial discharge temperature is the minimum expected from the Nitrogen expansion process. This is the main agent discharge temperature for 60sec and then due to the cylinders drain out process, the temperature was assumed to reduce linearly to reach the enclosure volume weighted average temperature, which was -1°C. The experimental results present a different trend which is mainly due to the heat transfer effects occurring within the piping network as well as the compartment. It appears that the measured initial discharge temperature resulted to be around 0°C. However, as time progresses the piping network heat transfer affects the surrounding environment and reduces its heat absorption rate. This reduction causes the discharge temperature to reduce for almost 50sec after the main 60 seconds discharge. It is apparent that the minimum level of discharge temperature recorded is around -30°C, which is 10 degrees lower than the analytical prediction. This phenomenon can be explained by assuming higher initial storage pressure or existence of additional substances such as Oxygen, inert gases and humidity. Nevertheless, no evidence were presented so far that

can provide an insight on which of these factors drives this behaviour and to what level. This falls out of the scope of the present research and can be examined in future studies. Finally, observing the temperature evolution, after it reaches a minimum, it start rising again following a fairly linear trend towards the enclosure temperature, which resulted to be very close to the analytically predicted value of -1°C. Of course, these temperature sensors locate on the pipe just before each nozzle and thus they do not represent the enclosure temperature. Only after a significant amount of time their values will become equal. Nonetheless, the experiment showed that the proposed Nitrogen system provides an additional firefighting mechanism by removing heat from the environment, making it more resilient to fire re-ignition.

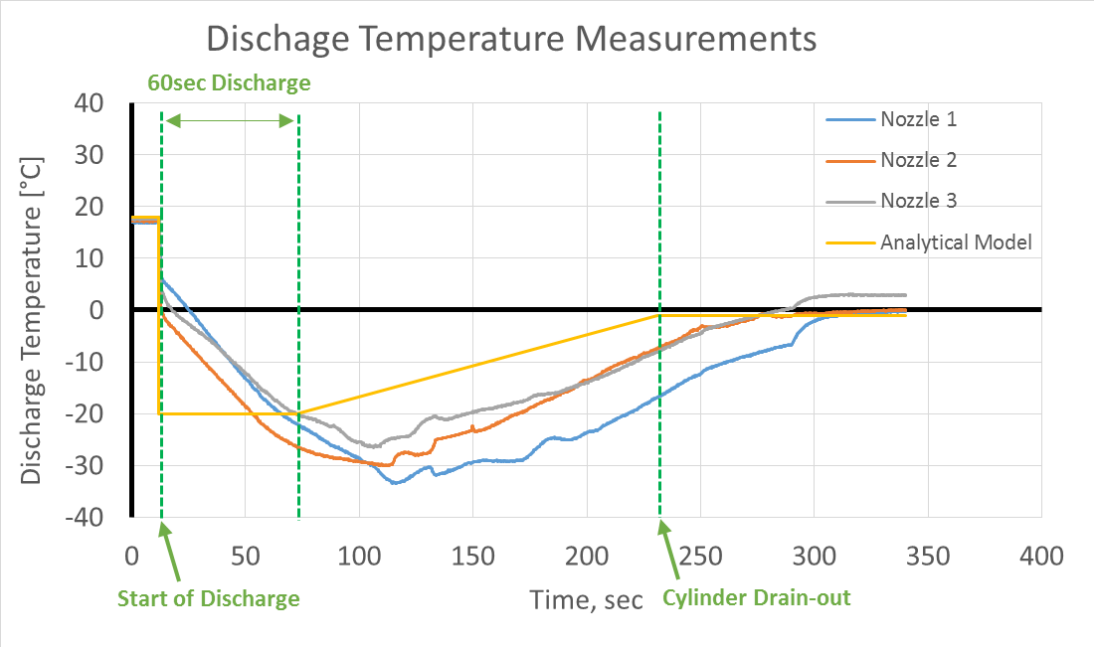

Figure 109 – No Fire Experimental Data: Discharge Temperature Measurements vs Time

The final measurement of interest regarding the Nitrogen discharge conditions is the discharge mass flow rate. The recording of this parameter was made indirectly by measuring the storage system weight reduction with time (see Figure 110). The measurements showed that the total amount of agent discharges was 48kg, matching the value used in the analytical model and verifying the cylinders supplier's claim. Observing the weight reduction rate after the start of discharge,

it is apparent that it follows a linear trend up until 60sec and then a parabolic trend until drain out. This dictates that the mass flow rate is actually fairly constant during the first 60sec of discharge. Thus, the reduction in discharge pressure with time is counter-balanced by the temperature reduction in terms of their effect on the final discharge mass flow. This verifies the assumption of constant mass flow for 60sec used on the models, both analytical and numerical.

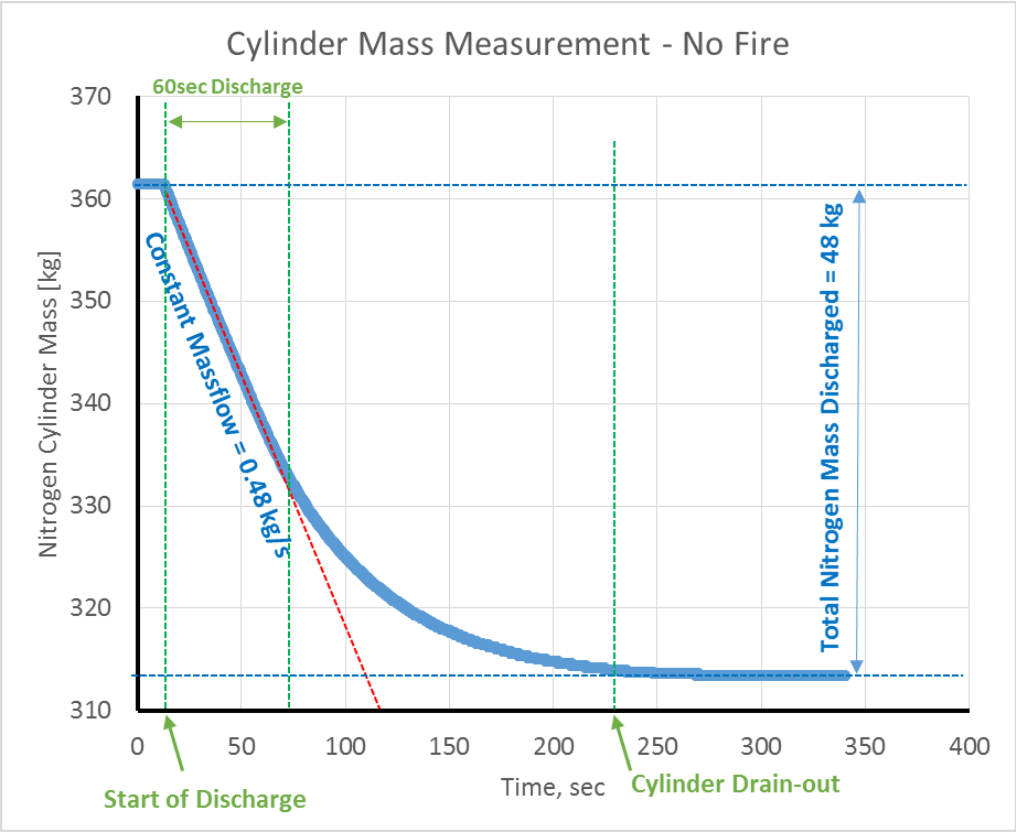

Figure 110 – No Fire Experimental Data: Nitrogen Cylinders Mass Measurements vs Time

Since the installed piping network and nozzles dimensions presented some small differences, the recorded mass flow rate was found slightly larger compared to the analytical calculations. Based on the linear slope, the constant mass flow rate measured was 0.48kg/s while the calculations showed 0.46kg/s. However, it was previously observed on the discharge pressures plot that the actual duration of the discharge with constant mass flow rate was around 55sec. Thus the final agent mass discharged resulted to be very close to the analytically calculated value. Finally, it can be seen that the cylinder drain out time, resulted out of the

cylinder weight recording, was also successfully predicted by the analytical model.

The Nitrogen discharge conditions derived by the analytical model were used as boundary conditions for the numerical simulations, with the assumption that the Nitrogen discharge happens with constant mass flow, pressure and temperature. The numerical CFD models were set to discharge a constant flow of Nitrogen, at 41bar and -20°C for 60sec and then stop the discharge. Such cases resemble only the experimental tests including fire, which were set to discharge exactly 60sec and then stop.

The cargo conditions measured for the Full Cargo Empty No Fire are the compartment overpressure and leakage flow rates. Figure 111 presents the measurements for the compartment overpressure against time. This plot includes the raw data recording along with the “noise” in order to provide an element of the measurement accuracy. Based on the plot, the discharge process increases the overpressure inside the compartment immediately. The level of overpressure measured during discharge satisfies the safety requirements and closely matches the design target of 1500Pa. Additionally, this output matches also the numerical CFD models prediction shown in Figure 93.

The cargo leakage flow rate was set to resemble the actual aircraft cargo leakages as well as the MPS requirements. The variable speed fan was set for a constant flow of 0.023m^3/s. Based on the outcomes for the compartment internal pressure level and the ambient conditions, the leakage flow rate was calculated and the results are shown in Figure 112. Since the ambient conditions were fairly constant during the experiment, the leakage flow rate resulted to be directly related to the overpressure level inside the compartment. Nevertheless, it shows that the system returns to the original leakage flow rate approximately 12sec after the start of discharge and remains fixed thereafter.

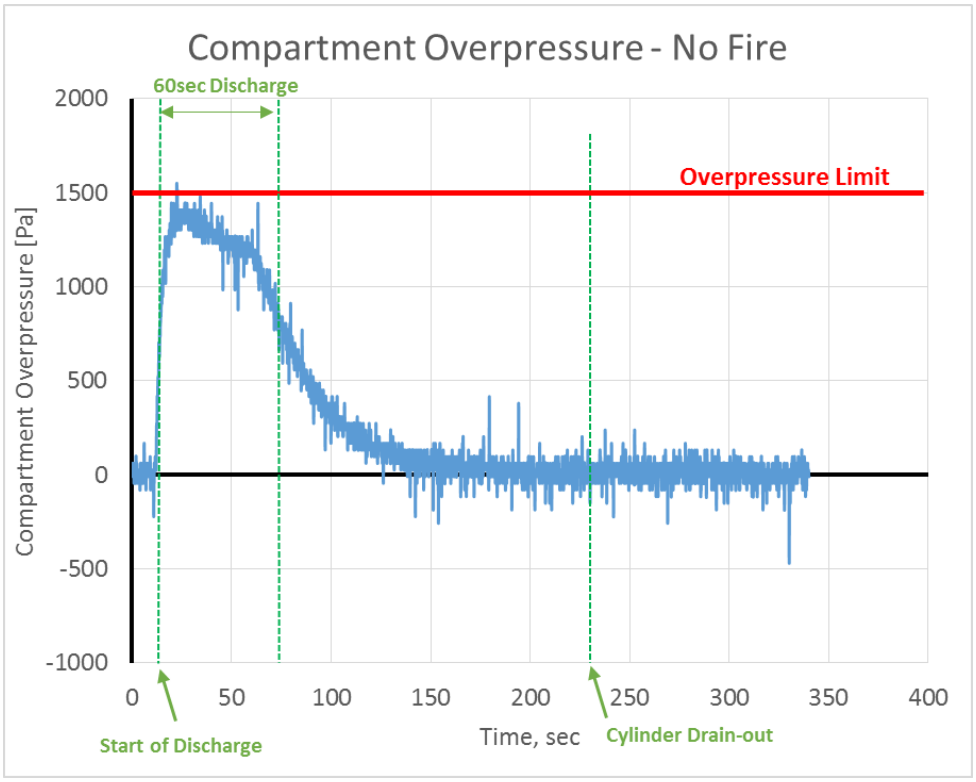

Figure 111 – No Fire Experimental Data: Compartment Overpressure Measurements vs Time

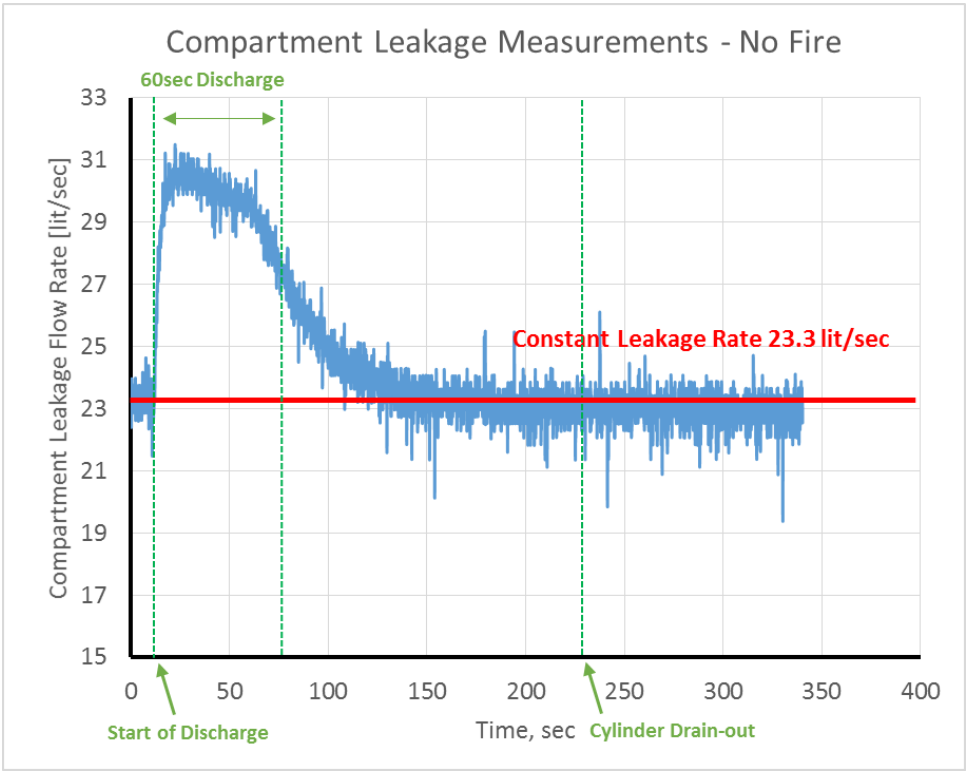

Figure 112 – No Fire Calculated Data: Compartment Leakage Flow Rate vs Time

The main parameter regarding the system fire extinguishing capability is the Oxygen volumetric concentration inside the compartment. The measurements taken from the 3 sensors (ceiling, mid, floor) showed very small differences indicating concentration uniformity within the enclosure. The average value between them is presented in Figure 113.

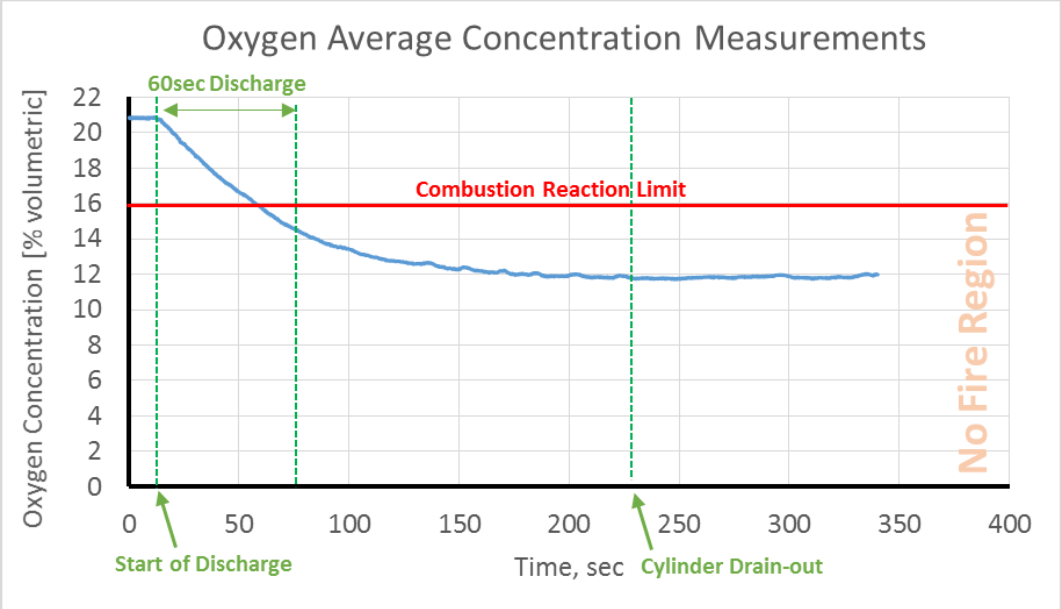

Figure 113 – No Fire Experimental Data: Oxygen Average Concentration Measurements vs Time

Observing the evolution of the Oxygen average concentration evolution with time, it can be seen that it drops as soon as the system begins the Nitrogen discharge. The final level of concentration reached mainly depends on the total amount of agent discharged in the compartment. The rate of its reduction might also present a minor effect on the minimum level reached, however it is considered negligible. Nevertheless, the rate of reduction of Oxygen concentration highly depends on the discharge pressure and temperature. The system was designed to discharge Nitrogen with 41bar initial pressure and achieve 14.2% volumetric Oxygen concentration at 60sec and 10.4% after drain out (see Table 37). The recorded average Oxygen concentration reaches a value of 14.8% at 60sec while the minimum level of reached after drain out was 11.9%. After that time, the Oxygen concentration started to increase at a very slow rate. These outcomes agree with the analytical model due to the reasons below:

- The discharge mass flow measured is slightly larger (0.48kg/s over 0.46 kg/s), however, the duration of constant discharge is smaller (55sec over 60sec) resulting in slightly smaller overall mass discharged at 60sec and thus 14.8% over 14.2% Oxygen concentration. Additionally, although the recorded cylinder weight reduction verifies the mass discharged, the actual mass is reduced to the amount of Nitrogen remained locked in the piping network as mentioned earlier. Thus, the actual mass flow rate is even closer to the analytically predicted value.
- The rate of reduction of Oxygen concentration follows a similar trend on both experimental and analytical results, while the minimum level of concentration reached during the experiment was 11.9%. This was mainly due to the fact that the actual amount of agent discharged was less than design value of 48kg. Nevertheless, the analytical model shows agreement because a reduction on the agent final mass by 7 kg would produce a minimum Oxygen concentration of 11.7%, which is much closer to the measurements, especially those at the top of the container.

4.3.2 MPS Experimental Tests

This section focuses on the fire tests performed based on the MPS requirements for aircraft cargo. The MPS tests are set to assess the system effectiveness for any type of cargo fires (solid, liquid, aerosol can and large container case). At this point of the research, the only set of experiments that has been successfully completed regards the Open Surface Liquid fire tests. Nevertheless, such tests represent the most demanding case of MPS tests on fire suppression. This is due to the fact that the aerosol can explosion tests, which were found the most challenging in previous studies, target to prevent the explosion from happening. However, the conditions that would trigger the aerosol can explosion mainly depend on the cargo temperature levels near the vicinity of the aerosol can. Such scenarios assume an already existing fire inside the compartment, the worst case of which is the Open Surface fire of a liquid fuel. Thus, the Open Surface Liquid fire tests are able to provide a first estimate on the temperature levels inside the

cargo in relation to the aerosol can explosion requirements. Finally, such measurements can be used for CFD model calibration purposes against the MPS fire test scenarios.

Five successful experiments have been performed testing the Nitrogen fire suppression system against the Open Surface Liquid fires using Jet-A fuel. In each case, the system controls were set to perform the same procedure as that for the No-Fire tests, with the exception that the Nitrogen discharge was set to stop after 1 minute. At that instance, the main feeding line valve closes and the agent flow stops. This modification happened in order to control the flow of agent inside the cargo as well as level of Oxygen concentration reached. Based on the findings of the No-Fire tests, during the 1 minute discharge, the agent maintains a relatively constant mass flow rate of 0.48kg/s and reaches 14.2% Oxygen concentration. However, for the Open Surface Liquid fire cases, although the Nitrogen discharge parameters can remain the same, the resulted final Oxygen concentration is expected to be significantly lower due to the existence of the combustion products.

The estimation of the agent discharge mass flow for the Open Surface Jet-A Liquid fire tests is presented in Figure 114. The measurements show that the cylinder mass reduction actually follows a linear trend during discharge, achieving and maintaining the targeted 0.48kg/s. This resulted in 29kg of agent being introduced inside the enclosure in 1 minute, verifying the system expected performance.

The Nitrogen discharge conditions resulted to be similar to those of the No-Fire tests. However, due to sensor sensitivity and protection reasons, for the Open Surface Liquid fire tests a complete recording against time was not performed. Nevertheless, the system resulted to perform very similarly, verifying that the discharge conditions settings were achieved.

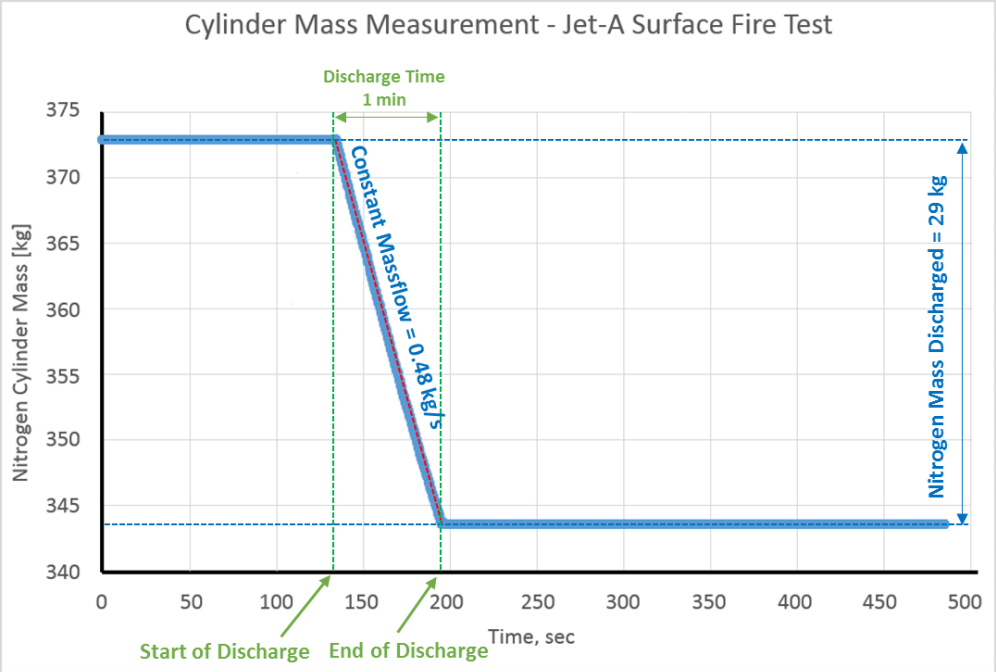

Figure 114 – Liquid Jet-A Open Surface Fire Experimental Data: Cylinder Weight Measurements vs Time

Regarding the cargo compartment internal conditions, there is a strict MPS requirement on the level of overpressure reached during and especially after discharge. This recording was performed by the main pressure transducer (PT_{CON}) placed at the centre of the cargo left side-wall, as shown in Figure 36. The measurements cargo average overpressure against time, are shown in Figure 115. During all tests, the immediate observation was that at the instance of the start of discharge, the signal from the pressure transducer presented a sudden increase in overpressure which reached around 8000Pa. This sudden increase presents the characteristics of a pressure shock that the transducer experiences right at the instance of first discharge, as it disappears immediately after. The appearance of a small duration of time in the plot (around 10sec) only describes the relationship between the speed of the phenomenon and the response of the transducer. The reasons behind this behaviour seem to locate around the fact that the final location (relatively close to the ceiling) and protection housing geometry of the pressure transducer, interacted with the path of one of the discharge jets. Nevertheless, the technical team of the test rig still investigates different methods to avoid this phenomenon in future tests.

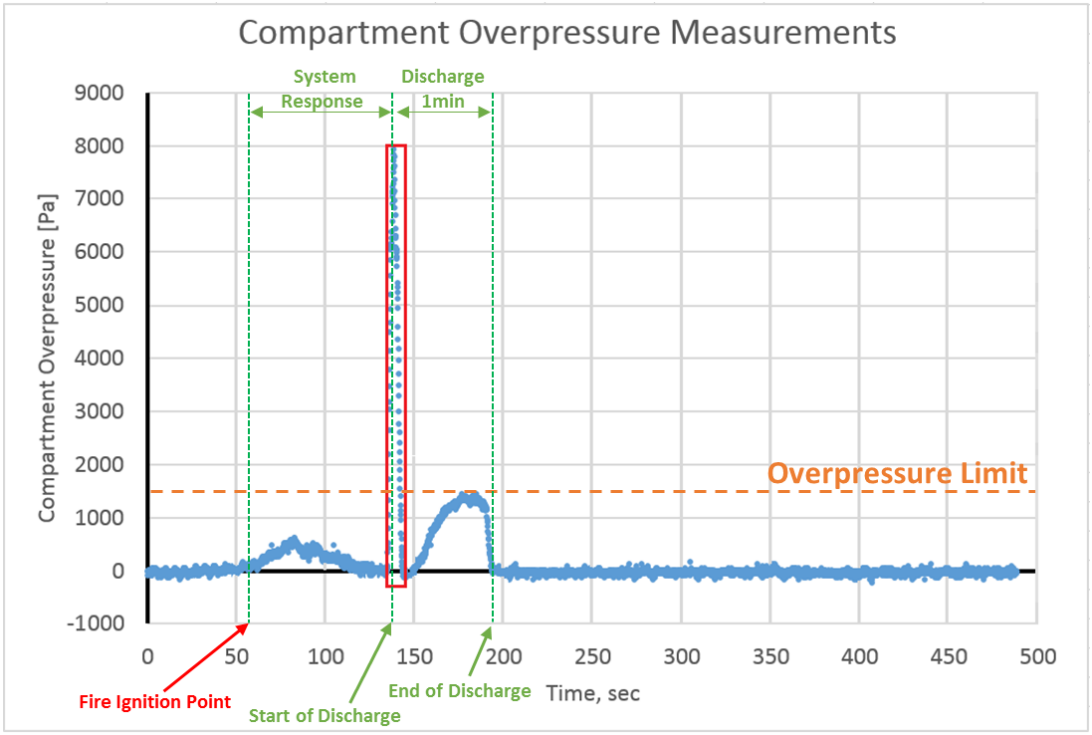

Figure 115 – Liquid Jet-A Open Surface Fire Experimental Data: Cargo Overpressure Measurements vs Time

Based on the nature of the above mentioned phenomenon, it cannot be considered within the MPS assessment of the system in terms of average cargo overpressure levels. However, neglecting that instance of time, the rest of the measurements showed that the system can successfully pass the MPS requirements achieving a maximum level of overpressure of around 1450Pa during discharge, while immediately reducing it to ambient after discharge. Additionally, an interesting observation regards the effect of liquid fires inside the compartment. It can be seen that during the system response time, between the fire ignition point and the start of discharge, the overpressure level increases, reaches a local maximum and then it decreases again. The balance between three parameters dictates this behaviour. The three parameters are: a) combustion heat release rate, b) combustion “hot” pressure losses and c) combustion products generation rate. Based on the measurements, it can be seen that as time passes, the overpressure level increases, increasing the leakage rates of the compartment, up until the point where the balance tilts

towards reaching equilibrium between the combustion generated effects and the compartment leakages.

The temperature levels inside the compartment during the Open Surface Liquid Jet-A fire tests were measured based on the temperature sensors shown in Figure 36. In order to present the recordings from all those sensors in an organised manner, it was assumed that the cargo front door opening represents the front view. Thus, the wall opposing to the door is considered as the rear wall of the compartment, while right and left the respective right and left side-walls. Having established the main four directions relative to the cargo compartment, the measurements of the temperature sensors can be presented in relation to their location. Figure 116 presents the measurements for both ceiling and side-wall sensors, organised into groups of 6 and illustrating the temperature distribution from the rear to the front of the compartment (from curve 1 towards curve 6). For clarity, it is reminded here that the liquid fuel pool and thus the fire locate close to the rear right side of the compartment.

As mentioned in Section 3.3.2, the sensors TC1 on the ceiling, TS19 on the right side-wall and TS25 on the right side of the rear wall are located around the fire region. Thus, they show the highest levels of temperature inside the compartment, with the highest indication coming from TC1 and exceeding 500°C. Observing the temperature evolution and its distribution inside the cargo compartment, a number of important conclusions can be derived regarding the existence of open surface fire and its interaction with the discharged agent. These are:

1. There are 3 distinct periods of temperature evolution observed during the tests: a) from the moment of fire ignition until just before discharge, b) from the start of discharge until the end of discharge and c) from the end of discharge until the MPS required protection time.
2. During the first period, the temperature increases approximately linearly with time, since the hot combustion products are mixed with the surrounding air. This behaviour is best observed using the indication of the TC1 sensor on the cargo ceiling right side. This is the closest to the fire sensor and thus, captures

more accurately the phenomenon. The temperature rises almost to its peak during this period and at this location, while none of the rest of the indications present similar trend. All other sensors presented their peaks later on within the second period, depending on how far they were located from the fire.

3. The differences between the sensors provide an image of the cargo interior gases mixing and distribution rates. For example, focusing on the slopes of the linear temperature evolution of all sensors during the first period, it can be seen that they increase moving towards the cargo compartment rear and right side areas and decrease moving towards the front and left. The rates of increase/decrease of the slopes show the “natural” mixing and distribution of the combustion gases within the enclosure.
4. During the agent discharge period, an enhancement on the mixing and distribution of the cargo interior gases is observed. This is evident in the sudden increase of the slopes of the temperature curves exactly when the agent discharge begins. It is apparent that the temperature starts to increase much more rapidly at all points of the compartment, before it starts to drop at the same rapid rate, until the discharge stops. Thus, the difference between the first and second period temperature increase rates illustrates the extent to which the fire suppression system enhances the mixing and distribution compared to the “natural” process.
5. Regarding the fire extinguishment capabilities of the system, it can be observed that the temperature increase in the compartment stops after 8-10 sec of agent discharge. This is evident in the TC1 measurement for the cargo ceiling right side (red dashed line). Thus, although there might still exist a small flame for a couple of seconds more, it is evident that the fire was successfully supressed within a very satisfactory time. Additionally, the temperature decreases rapidly after its peak, showing enhanced agent mixing and distribution properties and thus enclosure cooling. This is also due to the Nitrogen discharge temperature, which was shown in the previous section to be around -25°C.
6. Regarding the prevention of fire re-ignition and generally the system fire protection capabilities, the experimental recording continued after the agent

discharge for another 5 minutes (MPS requirement). During the third period of the tests, the cargo temperature keeps reducing, however at a much lower rate. This new slope of the temperature curves shows the “natural” evolution, which depends only on the cargo dimensions and leakage rates. Comparing the slops between the first and third periods, it can be stated that the existence of fire at the first period affects significantly the enclosure gases mixing and distribution rate. The combustion introduces a heat source and converts the liquid fuel and surrounding air into combustion products. The heat source rises the temperature and thus the kinetic state of the gases while the combustion reaction introduces products with significantly higher specific heat capacity. This combination leads to a gradual transition from pure air getting heated up relatively quickly, to a mixture of gases cooled down at a much lower rate.

7. Regarding the cargo interior fire safety, it can be noted that the system properties were found satisfactory form the MPS and the respective authorities point of view. Nevertheless, the temperature levels at the rear right corner of the cargo in the event of a liquid fuel open surface fire test remain at around 100°C even 5 minutes after discharge. Based on the temperature evolution trends shown for the third period, it can be assumed that the temperature will drop below 50°C within the next 5 minutes. Accumulating these durations it can be concluded that for approximately 10 minutes after fire ignition, the enclosure average temperature level is higher than typical life supporting conditions. Thus, it is obvious that if any typical living creature (humans, animals, plants, etc.) gets exposed in such conditions inside the compartment has reduced chances of survival.

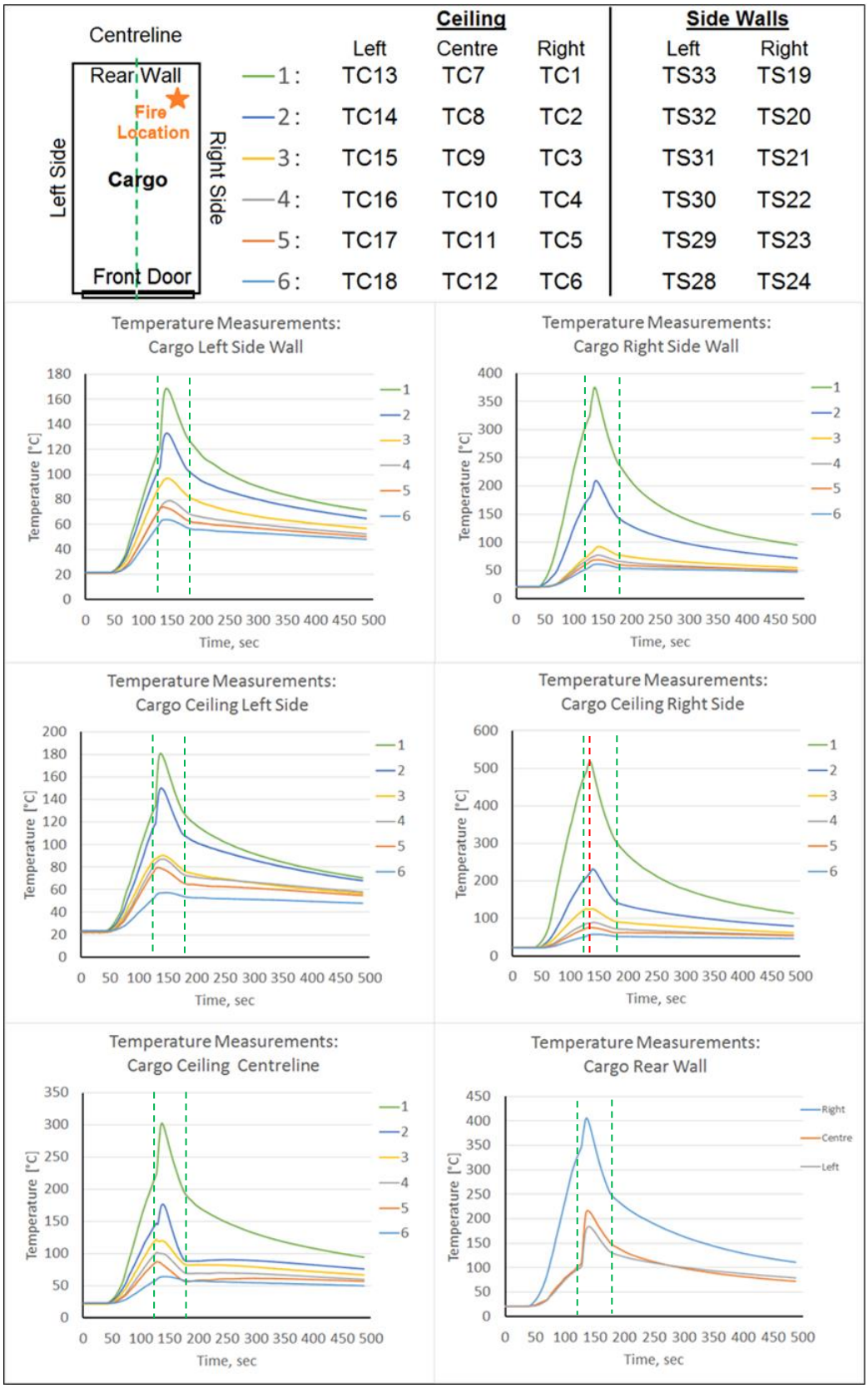

Figure 116 – Liquid Jet-A Open Surface Fire Experimental Data: Compartment Temperature Measurements vs Time

The final metric of interest in terms of MPS requirements is the cargo average Oxygen concertation against time. The recorded measurements as well as their average are illustrated in Figure 117. Three sensors were placed near the vicinity of the fire pool, one near the floor, one on the right side-wall at mid-height and one right on top of the fire pool on the ceiling. Based on the measurements, immediately after the fire ignition point the two top sensors showed a decrease in Oxygen concentration. During the system response time and just before discharge, the Oxygen concentration reached levels around 18% in average and below 16% close to the ceiling. The floor region seems to be unaffected by the presence of fire in terms of Oxygen concentration. This verifies the fact that the Oxygen rich pure air presents higher specific weight compared to the hot combustion gases and the Oxygen depleted air. This outcome shows that the actual Oxygen concentration level before discharge was approximately 3% lower compared to the No-Fire test cases. This 3% reduction illustrates the effects of the Jet-A liquid fuel combustion products, which act similarly to inert gases.

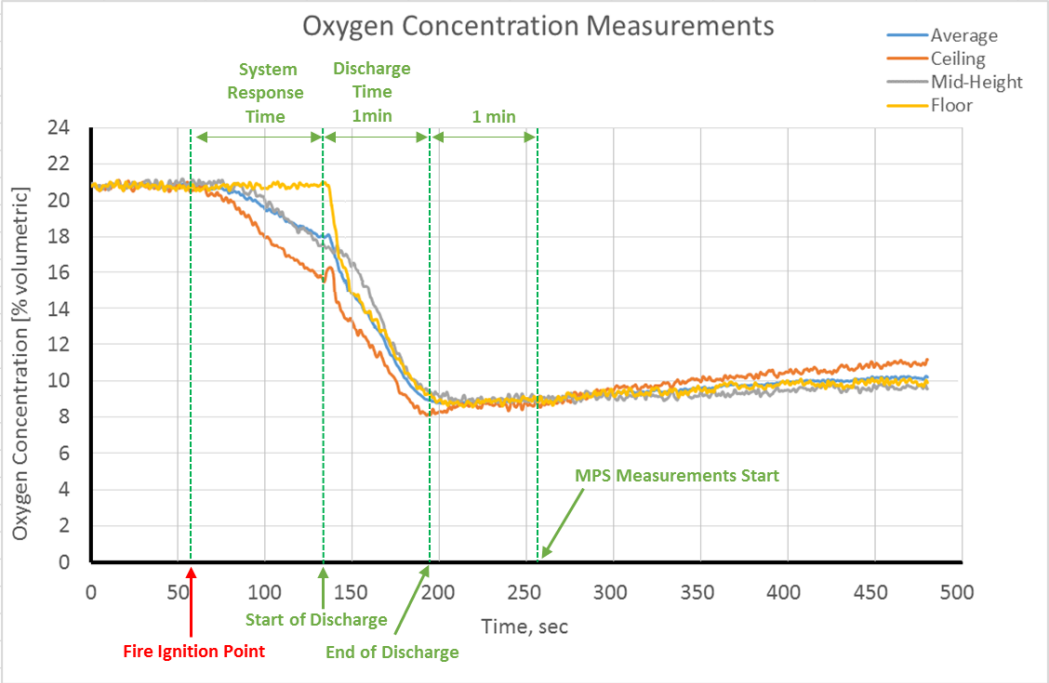

Figure 117 – Liquid Jet-A Open Surface Fire Experimental Data: Cylinder Weight Measurements vs Time

The start of discharge becomes visible on all sensor measurements. The floor sensor presents a very clear change in the Oxygen concentration from the

ambient 20.9% level to approximately 8.4%. At first, the agent discharge enhances the mixing and uniformity level of the compartment interior gases. Thus, the floor sensor quickly drops to average Oxygen concentration levels, after which it continues to drop at a lower reduction rate until discharge stops. Similarly, the other two sensors showed that after discharge started, the Oxygen concertation reduction rate accelerated to the same level with the floor sensor. These facts can be used as evidence for the Nitrogen system mixing and distribution capabilities.

The average Oxygen concentration measurements showed that the system operation against Open Surface Liquid fire tests reduced the level from approximately 18% to 8.4%. This minimum value approaches the limit of 8%, below which the hypoxic air environment becomes toxic. Nevertheless, after suggestions by AIRBUS and in agreement with other authorities, 8.4% was considered as the design value for Open Surface Liquid fire tests, as it includes factors of safety and prolonged fire re-ignition prevention time.

Finally, based on the MPS requirements, the Oxygen concentration levels that occur 2 minutes after the agent discharge stopped are used for the overall system assessment. The average Oxygen concentration was found to be below 9% at 2min after the agent discharge stopped and reached the level of 10.4% at 3min after that, when the test concluded and the recording stopped. These outcomes agree with the MPS requirements and thus the proposed Nitrogen system successfully passed the Open Surface Liquid fire tests.

For the period after the agent discharge stopped, the average Oxygen concentration curve starts to rise again. However, the experimental data present a logarithmic trend (see Figure 118), showing that although the average Oxygen concentration rises with an average rate of 0.006% per second until the end of the experiment, it would take approximately 151.8min to reach the limit of 16% (estimated based on the given logarithmic trend). This is an outcome based on the combination of the dimensions of the leakage ports, the setting of the variable speed fan and the minimum level of average Oxygen concentration reached. This trend shows a satisfactory agreement with the numerical 3D-CFD outputs shown

in Section 4.2.2.5.2. Figure 96 and Figure 97 show the cargo average overpressure and Nitrogen mass fraction respectively. They refer to the time instances just before the agent discharge stops and at 46.53min, which was the time until the average Oxygen concentration reaches 15.4% at the location of the plane of interest. Thus, after discharge stopped, the average Oxygen concentration increased from 10.4% to 15.4% in 46.53min. Using the logarithmic trend shown below, modified in order to start from the value of 10.4% (y'=y+2), the estimated time until the concentration reaches 15.4% results to be 42.1min, which is satisfactory enough for the purposes of the present research.

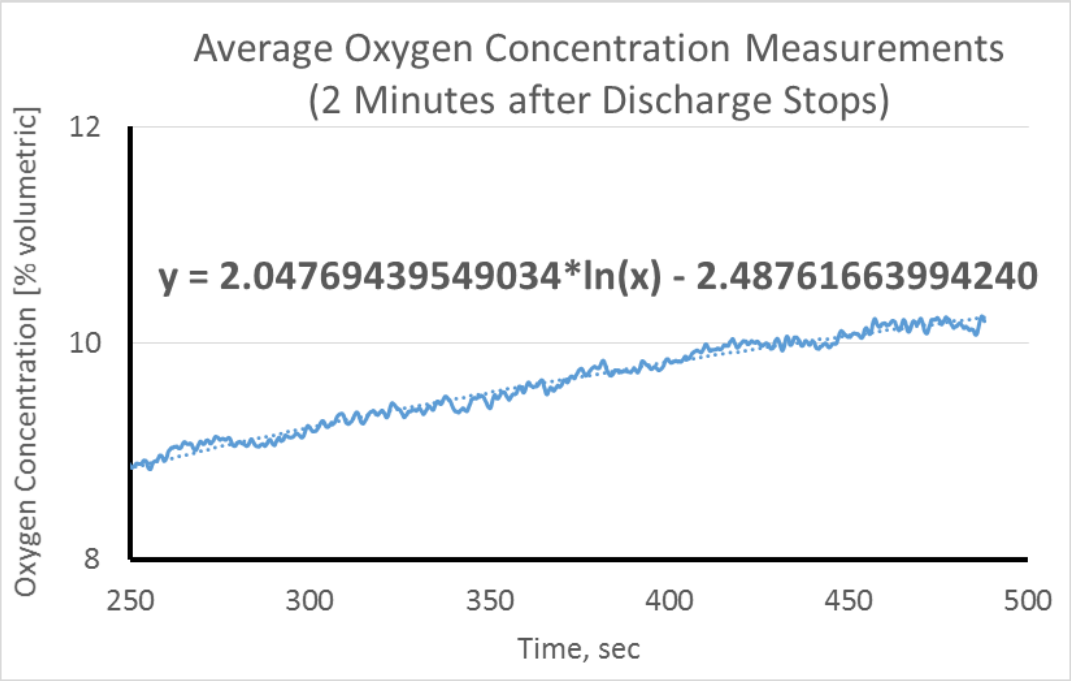

Figure 118 – Liquid Jet-A Open Surface Fire Experimental Data: Average Oxygen Concentration Recovery Trend

4.3.3 Numerical 3D-CFD Models Adaptation & Calibration with MPS Fire Tests

The experimental data received and analysed in the previous section, provide a further insight on the proposed system operation and performance as well as a baseline for comparison with numerical 3D-CFD simulations. Such information can be used for 3D-CFD model adaptation to the details of the finally installed experimental setup. The geometry adaptation of the numerical 3D-CFD models is suggested, since the final dimensions of some components within the test rig resulted to present small differences. Additionally, the boundary conditions and duration for the agent discharge will need to be adapted to the installed bottles, piping network residual agent mass, the actual discharge temperature and the enclosure volume (cargo load adaptation).

The adapted 3D-CFD models are expected to resemble accurately the No-Fire experimental data. Nevertheless, for the MPS fire cases, depending on the type of fire scenario, model calibration is required in order to achieve a satisfactory level of simulation accuracy. This is mainly due to the fact that each type of fire presents unique characteristics in terms of combustion heat releasing rate, enclosure Oxygen depletion rate and temperature distribution. Thus, based on a given system setup, the system response time, the peak temperature and the temperature distribution inside the enclosure are different.

In order to calibrate the 3D-CFD models against the Open Surface Liquid Jet-A fire tests, the data coming from the measurements are used in order to define the parameters that need calibration and derive the required calibration factors. The parameters suggested to be used for calibration purposes are:

1. Compartment initial average Oxygen concentration
2. Nitrogen discharge duration

There are two ways with which the initial average Oxygen concentration of 20.9% can be reduced. The first is to consider the environment filled with hypoxic air of the required average Oxygen concentration. The second is to include CO_2 and H_2O species inside the enclosure. In fact, the simulation can initiate with the

ambient standard value of 20.9% and then introduce from additional inlets CO_2 and H_2O flows, depending on the combustion reaction and product generation rates. Finally, the discharge duration will be set based on the final required agent mass, which depends on the initial level of average Oxygen concentration, the total “empty” volume of the enclosure and the targeted minimum average Oxygen concentration of 8.4%. This way, the 3D-CFD models will be able to simulate accurately the Open Surface Liquid Jet-A fire tests for all cargo load variations.

The above mentioned calibration process is suggested for the rest of the MPS fire tests as well. Activation time and mass flow factors could be also used for a quick assessment of a new system installed during system check test to estimate system response to liquid fire.

Finally, it is worth to note that the proposed iteration between CFD simulations and experiments can significantly reduce the overall development time and cost of respective system designs and test rig installations.

5 CONCLUSIONS & FUTURE WORK

The present thesis contains the main outcomes of the research conducted for the replacement of Halon1301-based fire suppression systems for aircraft cargo applications. The research was performed in parallel and providing support to the EU Clean Sky 2 EFFICIENT project. The scope of this research is to support the transition to Halon-free and environmentally friendly fire suppression systems within the timeframe set by the Montreal protocol.

The proposed “green” replacement agent is Nitrogen (IG-100). The system design is aligned to the MPS requirements, including considerations for retrofit onto already existing aircraft cargo.

5.1 Major Outcomes & Contributions

The outcomes of the project are separated into four categories: a) Conceptual design methods and proof of concept, b) Nitrogen (IG-100) system performance assessment using CFD, c) CFD modelling characteristics and challenges, d) System installation on board the aircraft and on test rigs.

5.1.1 Conceptual Design Methods and Proof of Concept

The conceptual design of the system was based on existing aircraft systems and the MPS. Additionally, it was supported with data coming from experimental cup burner tests regarding the required Nitrogen (IG-100) concentration for fire extinguishment.

The proposed methodology for the analytical and numerical modelling of the replacement system proved to be satisfactory for the given problem. The outcomes of the system performance were verified against first principles as well as public domain information. The established testing procedures and firefighting strategy improve the already existing, contributing towards system certification. Finally, the methodology is adequate to support also further development on Inert Gases systems.

5.1.2 Nitrogen System Performance Assessment using 3D-CFD

Compared to the current state-of-the-art, the proposed Nitrogen (IG-100) system capabilities are:

1. Effectiveness: discharge time achieved 104.4sec (NFPA: 60sec<t<120sec)
2. Cargo protection duration: 46.53min below 16 % O_2 concentration (>30min)
3. Cargo minimum O_2 concentration 10.4%
4. Design aligned to existing Halon1301 systems

Although the cargo protection time target was achieved for the MPS tests, current aircraft cargo scenarios dictate a requirement for extended protection time up to 3 hours until landing [4]. Since the protection time is based on the assumption that the ventilation ports are closed and there is only a constant door leakage rate, two solutions are foreseen in order to extend it significantly. The first involves continuation of agent discharge in a metered manner while the second suggests significant reduction of the initially reached Oxygen concentration by discharging an increased agent mass. The first solution introduces complexity to the system. However, it can still be viable for aircraft cargo. The second solution presents the disadvantage of reducing the Oxygen concentration below survival level and thus the risk of leaking hypoxic air into the cabin. Nevertheless, both solutions depend on the design of the ventilation system and the sealing qualities of the compartment.

A very important observation of the CFD simulations regards the cargo ventilation system. The design of the compartment ventilation ports and any other potential openings are critical for a successful operation. The cargo interior overpressure level during Nitrogen (IG-100) discharge highly depends on the flow capacity exiting the enclosure. In order to achieve reduced fire suppression time, increased discharge pressure is required. This increases the agent discharge flow capacity, which results in increased outlet flow capacity in order to control the overpressure level. Thus, the sizing of the ventilation ports is critical for the success of the proposed design. A more complex solution targeting increased capabilities and degrees of freedom regards the application of a variable area port or the addition of a sensitive pressure relief valve.

Furthermore, the location of the ventilation port was found to affect the agent flow pattern inside cargo during discharge and potentially the agent mass loss. The full scale 3D-CFD simulations confirmed that the Nitrogen system fills the compartment from top to bottom and thus the worst location for the ventilation port in terms of agent mass loss is close to the ceiling and in line with one of the discharge jets. However, placing the port close to the floor presents high risk of feeding a potential fire with Oxygen. Thus, the most favourable location for the ventilation port is around the mid-height of the compartment.

5.1.3 Nitrogen System Performance Assessment using Experiments

The MPS based experimental fire tests for aircraft cargo that take place at Cranfield University focus on the assessment of the proposed replacement fire suppression systems. However, the test rig development and assembly procedures were finalised very close to the end of the present PhD research project. This allowed very limited time for testing and analysis as well as no time for iterations between the tests and the analytical/numerical models. The test rig operation produced two complete sets of measurements during this time: a) No-Fire Tests and b) Open Surface Liquid Fire Tests using Jet-A fuel. Both refer to the Full Cargo Empty cargo compartment cases.

Compared to the current state-of-the-art, operating the proposed Nitrogen (IG-100) system against Open Surface Liquid Fire tests presents improvements on:

1. Effectiveness: discharge time achieved 60sec (NFPA: 60sec<t<120sec)
2. Cargo protection duration: 151.8min below 16% O_2 concentration
3. Cargo minimum O_2 concentration 8.4%
4. Design aligned to existing FAA MPS certification tests requirements

The outcomes of the experimental tests were found satisfactory for the purposes of the present PhD research. The No-Fire tests verified the Nitrogen system design methodology with the measurements showing good agreement to the predictions of the analytical and numerical models. This illustrates the fact that with the given problem definition, relatively simple analytical and numerical predictions can resemble accurately the Nitrogen discharge process inside cargo compartments.

The Open Surface Liquid Fire tests showed that the proposed Nitrogen system succeeded on achieving the MPS requirements regarding the minimum level of average Oxygen concentration, the maximum level of overpressure and the fire protection time after discharge stops. The system managed to extinguish the liquid Jet-A fuel fire within 10sec while both average overpressure and Oxygen concentration resulted within acceptable limits for structural safety and toxicity. Another important observation regards the proposed system response time. Based on the experimental data, the system response time one of the factors that present significant impact on the maximum temperature level reached inside the compartment. Since the Jet-A fuel pool has specific dimensions and quantity of fuel, the combustion based heat release warms the air while consuming the Oxygen. Thus, shorter system response time would result in significantly lower values for both peak and average temperatures inside the compartment. This outcome brings the attention to the system automations, instrumentation and controls, suggesting that significant effort is needed on updating the technology of the system components and achieve rapid system response. Finally, the proposed system operation presents the benefits of allowing the adjustment of the amount of agent discharged based on the amount of luggage existing inside the cargo.

5.1.4 Numerical 3D-CFD Modelling and Adaptation/Calibration against Experiments

The CFD modelling process resulted in valuable information regarding the simulation of Nitrogen discharge inside the aircraft cargo. The Partial Cargo models (1/3 of the Full Cargo) provided the capability to quickly assess the discharge conditions and support the development of the Full Cargo models. The CFD models selected as most appropriate for the specific application are the Full Cargo full scale for steady-state simulations and the Full Cargo scaled at 1/8 for transient. Assessing the final CFD models, the main characteristics and challenges are summarised in the list below:

1. The Full Cargo models are significantly more demanding in terms of computational cost compared to the Partial Cargo. Additionally, they require

significantly more time to setup and verify. Nevertheless, they are deemed necessary for the complete representation of the phenomena. A complete simulation of full scale steady-state is achieved approximately after 200 iterations and the running duration was around 2 hours.

2. The transient simulations of such large control volumes showed high storage memory demands for a single high performance desktop PC, which sometimes resulted in model loading issues. The extended time requirement of the problem was the main reason behind the increased computational cost. A complete simulation for transient cases were achieved during and after discharge at approximately 100 and 50 iterations per time step, respectively. The time step selected for the agent discharge simulation was $1.2*10^{-4}$sec and for the scaled simulation was $1.1*10^{-5}$sec, while for after discharge $2.5*10^{-4}$sec. In order to improve the simulation running time, considerations for time step increment were taken into account.

3. The maximum cell size that was found to be more suitable for the accurate representation the flow phenomena and the mapping of the parameters of interest was 0.012m. This was due to the fact that larger cells present deficiencies in representing a desirable flow mapping resolution.
4. Introducing combustion modelling significantly increases the model complexity and the computational demand. Based on the scope and the timeframe of the present research project, such simulations were deemed unnecessary. Nevertheless, based on the preliminary assessment performed, suggestions for future work are presented in a later section.
5. The nature of all potential replacement agents as well as Halon compounds was found to present minor differences in terms of modelling. The CFD models were found to be adequate for simulating a number of different agents by applying only some minor modifications.
6. The numerical 3D-CFD models were found to provide outputs that agree at a satisfactory level with both the analytical and the experimental data. Nevertheless, model adaptations and calibrations have been suggested in

order to achieve an improved representation of the real tests and provide the capability to simulate fire cases without including combustion.

7. The model calibration against the MPS fire tests can be based on the adjustment of two factors: a) agent required quantity and thus discharge time and b) initial level of Oxygen concentration inside the compartment depending on the type of fire.

5.1.5 System Installation On-Board the Aircraft and on Test Rigs

The proposed system design, weight estimations along with their controls and automations support the development a low cost and complexity test rig as well as a retrofit system for aircraft cargo.

The developed system currently utilises in total 4 Nitrogen (IG-100) storage cylinders, 2 of which are for back-up. Although using Nitrogen instead of Halon increases the required agent mass significantly, an appropriate system design can assure similarity on weight distribution on the aircraft compared to the already existing systems. The isometric diagram of the piping network and thus all piping paths will remain unchanged. Additionally, the system components required for control and operation as largely the same with the only differences appearing at the Nitrogen storage system. The system activation is achieved through a pneumatic system with valves, similarly to the current state-of-the-art.

One of the main differences found during the assessment of the Nitrogen (IG-100) system was the fact that it presented severe temperature drop during isenthalpic expansion in the pressure reducing devices. Nitrogen throttling reduces the temperature depending on the desired pressure drop. Designing for 300bar storage and 41bar discharge pressures, the theoretical temperature drop after the pressure reducer and thus in the piping network was found to be approximately -20°C. However, the experimental results showed that the minimum discharge temperature reached was approximately -30°C. This mainly shows that the storage cylinder initial pressure level and the composition of the gas inside, affect significantly the minimum discharge temperature reached. Setting this case as reference, the average total temperature inside the compartment was designed close to 0°C after the Nitrogen discharge stops

(water freezing point). This fact presents good potential on enhancing the fire extinguishment capability of the system by removing much more of the heat.

In order to account for increased requirements for fire protection time after discharge, the proposed design suggests future improvements as well as potential integration with SPGGs (Solid Propellant Gas Generator) or OBIGGs (On-Board Inert Gas Generator). A parallel connection with SPGG or OBIGGs, can potentially improve overall system weight while providing the capability of maintaining agent inert concentration inside the compartment for longer periods of time. This is due to the fact that if capable, the primary system will stop earlier while the secondary system will maintain the agent concentration as long as required. A similar effect is expected combining the main system with Solid gas or liquid phase secondary system. However, as mentioned previously, this introduces complexity to the system.

Another approach to extending the fire protection time is to extend the agent discharge duration and thus quantity in order to reduce the Oxygen concentration to a lower level. Depending on the amount of cargo leakages suffered and the protection time requirements, the Oxygen concentration can potentially be reduced to levels below 6%, which are very dangerous for human health. Thus, this approach was abandoned.

High quality cargo sealing is desirable from a fire protection perspective. This capability combined with well-designed variable area ventilation ports can improve the fire protection time. Furthermore, the area variability will allow for cargo overpressure control, which in turn can be used as handle for selecting the agent discharge time and thus the fire suppression time.

The results of the current project also indicate further improvements on the MPS tests setup and procedures for future experiments. The test rig design proposed presents improved ventilation system properties, ensuring optimum test conditions and improving the experiments accuracy. This provides the capability of matching adequately the conditions during a fire suppression system operation on-board the actual aircraft cargo.

5.2 Recommendations for Future Work

Based on the outcomes of the present research project, the recommendations for future work are separated in three categories:

1. Execute the rest of the MPS fire tests on the newly developed test rig

Operate the test rig and run the rest of the MPS fire tests required. The complete set of MPS experiments and the post-processing of the outcomes can provide the complete view form the FAA MPS stand point, regarding the proposed system fire suppression capabilities and the ability to achieve the certification requirements.

2. Nitrogen System Design Optimisation Software Development

The complete system design analytical method has been set in a complete sequence of calculations which could be transferred into a computer program. This tool will allow much larger parametric studies and design space explorations for the determination of the relationship between the operating conditions against cargo load and system weight, while respecting safety and fire extinguishment criteria. Finally, it can be linked with an optimiser in order to deliver designs optimised for weight or any other objective.

The future studies suggested should focus on the exchange rates between operating pressure, target discharge time and enclosure volume in order to identify the changes required for the loaded cargo scenarios. Additionally, they should include studies using different inert gases on a given system design and assessing their behaviour in terms of operating pressure, discharge time and desirable agent concentration against the agent specific weight.

3. Small Scale Combustion Simulations and Experiments

The progress of the research on the performance of Nitrogen fire suppression systems will enrich the database regarding the agent concentration required to achieve fire suppression for different fire scenarios. Additionally, it will provide adequate information for the continuation of the investigation of the fire suppression mechanism through small scale experimental or numerical CFD

models. Simulations and cup burner experimental tests should be aligned to the newly found operating conditions and burning material properties. Such cup burner tests can provide further details on the investigation of the fire suppression performance of the system. Additionally, there are experimental data available for temperature inside the compartment and close to the walls. This allows the CFD models to include heat sources to represent fire and enhance the prediction on the fire suppression assessing closely re-ignition possibilities. Finally, such data could support the development of the cargo liner materials and sealing methods.

4. Future System Improvements

Finalising this thesis, a proposition is made for future work on the topic regarding the future fire suppression systems characteristics. Three additional considerations are proposed to be included:

i. System response time enhancement (automations, instrumentation and controls update)
ii. Nozzle arrangement redesign and automation for controlled localized discharge
iii. Integration with OBIGGs and SGPGs
iv. Investigation of inert gases mixtures

In the course of the present research it was found that a potential system response time can offer significant benefits in terms of reducing the impact of fire in the enclosure (reduce maximum temperature levels). An effective and successful fire suppression system should include the capability of rapid response.

In case future new aircraft can afford a fire suppression system redesign, it is proposed that the nozzles should be placed in key areas covering specific locations inside the compartment. Assuming an automatic control mechanism, after fire detection, only the nozzles around the affected area will be activated in an effort to maintain the desired fire suppression conditions only at a part of the enclosure and not to the whole. An even more exotic and complex suggestion would be for the nozzles to be movable or capable to redirect their jet trajectory

by rotation. Although the risk assessment and failure modes would still demand a full cargo coverage, it is interesting to see if in case of low impact fire events the process can be controlled and the agent mass loss minimized.

The reasoning behind the integration with OBIGGs or SGPGs systems has been discussed in previous sections. It has become apparent that this is the next step of development and thus integrated system design as well as CFD simulations should be performed including such systems and targeting extended fire protection time after discharge.

Finally, an investigation on inert gases mixtures for fire suppression enhancement and minimization of agent mass requirement is suggested. Such mixtures should target improved agent behavior in terms of throttling based temperature drop, storage and delivery system sizing and agent required mass to achieve the fire extinguishment concentration.

6 REFERENCES

1 “Montreal Protocol on Substances that Deplete the Ozone Layer”, Final Act, Montreal, Canada, United Nations Environmental Program (UNEP), September 1987

2 R. Beuermann, “Environmentally friendly fire suppression”, A. Operations and E. Consortium presentation, February 2016

3 D.P Bein, “A review of the history of fire suppression on US DOD aircraft”, Naval Air Systems Command (NAVAIR), System Safety, Code 4.1.6.1, Highway 547, B562-2, Lakehurst, 2006

4 D. Lewinski, “Halon Replacement for Airplane Cargo Compartments What it Takes”, Fourth Triennial International Fire and Cabin Safety Research Conference, Lisbon, Portugal, Boieng Company, November 2004.

5 William J. Hughes, “Options to the use of halons for aircraft fire suppression systems”, FAA Report (Updated), Technical Center, Aviation Research Division, Atlantic City International Airport, New Jersey 2012.

6 P. O. Name, “Environmentally friendly fire suppression for cargo using innovative green technology (EFFICIENT),” 2015

7 J. W. R. June, “Minimum performance standard for aircraft cargo compartment halon replacement fire suppression systems ”, N. Technical and I. Service, June 2012.

8 “LSBU report”, EFFICIENT project, Cranfield, 2018

9 Rainer Beuermann, “Preliminary valuation of nitrogen and oxygen depleted Air as Halon 1301 Replacement for Cargo Hold Fire Suppression”, Tech. Notes, Airbus, 2016

10 "Guidance notes on fire fight-systems" , ABS, Updated 2015, May 2005

11 http://www.firesafetyinfo.co.uk/fire-triangle/

12 “Fire Protection: Systems”, FAA, AC 25.869-1A, October 2007

13 T. Flynn, “Service Engineering”, Boeing Comercial Airplanes Croup

14 Boeing official page, “www.boeing.com”

15 “Built-in Fire Extinguishing/Suppression Systems in Class C and Class F Cargo”, FAA, Advisory Circular, AC 25.851-1, May 2016

16 R. Beuerman, “Systems Description Document-Cargo Hold", Airbus, 2016
17 G. N. On, “Fire-Fighting system”, Upadated, 2015
18 J. P Emond, F. Miercier, M. C Nunes, “In-Flight Temperature Conditions in the Holds of an Widebody aircraft”, Air Cargo Transportation Research group, Laval University, Canada, 1999
19 MJ*. Behbahani-Pour and G. Radice, “Cargo Compartment Fire Extinguishing System”, Division of Aerospace Sciences, School of Engineering, University of Glasgow, Glasgow G12 8QQ, UK, 2016
20 I. Douglas, William J. Hughes, “Halon History”, FAA, Fire Safety Section, AAR-422
21 D. Sheinson, R.S., Penner-Hahn, J.E., and Indritz, “The physical and chemical action of fire suppressants”, Fire Safety Journal, vol. Vol. 15, pp. 437–450, 1989
22 “Specifications for halon 1211 and Halon1301”, Fire protection-Fire extinguishing media-Halogenated hydrocarbons, October 1990
23 “Standard on Halon 1301 Fire Extinguishing Systems”, NFPA 12A, 2004
24 H.W. Carhart, J.T Leonard, “Tests of Halon 1301 Test Gas Simulants”, Navy Technology Centre for Safety and Survivability Branch Chemistry Division, Washgton, February 1989
25 J. Jones, C. P. Sarkos, “Design Calculations for a Halon 1301 Distribution Tube for an Aircraft Cabin Fire Extinguishing System”, Report FAA-RD-73-32, April 1973
26 R. N. Coward, J. A. Hillaert, Dennis M. McCrory, “Analytical Methods for Modelling Characteristics of halon 1301 Fire Protection System”, Publication, Washington DC
27 P. J. F. W Dinenno, “Clean agent total flooding fire extinghuishing systems,” Soc. fire Prot. Eng. Handb. fire Prot. Eng., 5th ed, 2016.
28 “Cargo compartment fire protection in large commercial transport aircraf,” N. Technical and I. Service, July 1998.
29 C Grant, “Society of fire protection engineering: Handbook of fire protection engineering,” Halon Des. Calc., 5th ed, 2016.

30 D. Ingerson, "Status of research & testing to replace Halon extinghuish agents in civil aviation”

31 “Class B and F Cargo Compartments”, AC 25.857-1, February 2016

32 https://www.fire.tc.faa.go

33 Y. and B. D. B. Jian C, “Thermodynamics properties of alternatives”, Publication, February 1990

34 R. G. Gann, “FY2004 Annual report next generation fire suppression technology program (NGP)”, 2004.

35 “Review of the Transition Away From Halons in”, U. S. C. A. Applications, September, 2004.

36 “High Pressure CO_2”, Fire Extinguishing System, Janus fire systems, 2016

37 S. Lal, “Denvelopment of water mist nozzles and fire suppression by total flooding” , Publication

38 T. R. Marker, J. W. Reinhardt, "Water Spray as a Fire Suppression Agent for Aircraft Cargo Compartment Fires,” FAA, June 2001

39 J. W. Reinhardt, "The Evaluation of Water Mist With and Without Nitrogen as an Aircraft Cargo," FAA, February 2002

40 D. Blake, "Cargo Compartment Fire Protection in Large commercial Transport Aircraft,” FAA, July 1998

41 T. L. Reynolds, D. B. Bailey, D. F. Lewinski, and C. M. Roseburg, "Onboard Inert Gas Generation System/ Onboard Oxygen Gas Generation System (OBIGGS/OBOGS) Study,” NASA, May 2001

42 M. Burns, W. M. Cavage, R. Hill, R. Morrison, “Flight-Testing of the FAA Onboard Inert Gas Generation System on an Airbus A320”, Final report, FAA, June 2004

43 M. J. Behbahani, G. Radice, “Nitrogen fire extinguishing system in airplanes cargo compartments”, Int J Swarm Intel Evol Comput/6:1, Aerospace Engineering Department, Glasgow University, UK, 2017

44 “Fire suppression system presentation”, FedEx s, June 2017

45 L. Robin and W. Lafayette, “Halon alternatives: Recent technical progress”, Great Lakes Chemical Corporation, Fluorine Chemicals Department, West Lafayette, 1991

46 T.A Penteado, “Analysis of the Concentration of Fire Extinguishing Agent in Baggage Compartments”, Technological Institute of Aeronautics, São José dos Campos, São Paulo, 2004

47 F. Y. Kurokawa, “Numerical simulation of the concentration of fire extinguishing in aircraft cargo compartment”, Proceedings of the 10th Brazilian Congress of Thermal Sciences and Engineering, December 2004

48 D. E. Goldberg and P. E. Rivers, “Computational analysis of aircraft cargo compartment pressurization and extinguishing agent hold time”, 3M Company, SUPDET, July 2008

49 P. J. DiNenno E. K. Budnick,"Halon1301 Discharge testing: A technical Analysis”, National fire protection research foundation, October 1988

50 P. J. Dinenno, E. W. Forsseli, M. J. Ferreira, C. P. Hanauska, B. A. Johnson, and H. Associates, “Modelling of the flow properties and discharge of halon replacement agents”, pp. 117–130, 1984

51 R. Papa, M. Pustelnik and L. C. C. Santos, “A CFD Model for Cargo Compartment Smoke Detection”, Proceedings of IMECE ASME International Mechanical Engineering Congress & Exposition, November 2005

52 I. Batista and N. Júnior, “Numerical simulation of an aircraft cargo”, 19th International Congress of Mechanical Engineering, November 2007

53 Muzzy, G. Wainer, E. Innoceti, “Comparing Simulation Methods for Fire Spreading Across A Fuel Bed”, Online publication

54 J. Lee, “Simulation Method for the Fire Suppression Process Insidethe Engine Core and APU Compartments”, The Boeing Company, 2002

55 K. Zhigang Liu, “A review of water mist fire suppression systems-Fundamentals studies”, Journal of Fire Protection Engineering, October 1999

56 B.H. Cong and G.X. Liao, W.K. Chow, “Review of modeling fire suppression by water sprays by computational fluid dynamics”, International Journal on Engineering Performance-Based Fire Codes, 2005

57 J. C. Hewson, S. R. Tieszen, W. D. Sundberg, P. E. Desjardin, “CFD modeling of fire suppression and its role in optimizing suppresant distribution”, Publication, January , 2003

58 R. N. Coward, J. A. Hillaert, “Numerical analysis of flow characteristics of fire extinguishing agents in aircraft fire extinguishing systems”, Journal of Mechanical Science and Technology, July 2009

59 A. Alizadeh Attar, M. Pourmahdian, B. Anvaripour, “Experimental Study and CFD Simulation of Pool Fires”, International Journal of Computer Applications, May 2013

60 K. J. Kaufmann, M. I. Miller, G. Wozniak, M. D. Mitchell, “Results Of Halon1301 and HFC-125 Concentration Tests on a Large Commercial Aircraft Engine Installation”, Online publication, 1995

61 D. Ingerson , “Test Experience in a Civil Transport Aircraft Engine Nacelle using a Solid Aerosol Fire Extinguishant”, Seventh Triennial International Fire & Cabin Safety Research Conference, December 2013

62 “Minimum Performance Standards for Halon1301 Replacement in the Fire Extinguishing Agents/Systems of Civil Aircraft Engine and Auxiliary Power Unit Compartments”, FAA report, MPSHRe rev04, March 2010

63 G. E. Josephine G. Gatsonides, “Fluorinated halon replacement agents in explosion inerting”, 2015

64 V. I. Babushoka, G. T. Linterisa , O. C. Meierb, “Combustion properties of halogenated fire suppressants”, Combustion and Flame, July 2012

65 G. Holmstedt and P. Andersson, “Investigation of scale effects on halon and halon alternatives regarding flame extinguishing, inerting concerntration and thermal decomposition products”, Department of Fire Safety Engineering, Lund University, Sweden

66 N. Saito, Y. Saso, Y. Ogawa, H. Kikui, “Fire Extinguishing Effect of Mixed Agents of Halon1301 and Inert Gases”, Fire Safety Science 4: 853-864, 1994

67 C . Chivas, J. Bertrand, S. Duplantier, L. Audouin, L. Rigollet, “Method to obtain large scale burning rate of liquids with lab scale test”, International Interflam Conference, Septemper 2007

68 “Prevention of a simulated aerosol can explosion with a mixture of Halon1301 and Nitrogen”, FAA report, N. Technical and I. Service, November, 2008

69 G. Linteris, “Understanding on the combustion promotion by halogen suppressants”, International Halon Replacement Working Group meeting presentation, May 2011

70 G. Linteris, G. and Gmurczyk, “Parametric study of hydrogen fluoride formation in suppressed fires”, Proceedings, Halon Options Tech., 1995

71 G. T. Linteris, J. L. Palgiaro, “Burning Velocity Measurements and Simulations for Understanding the Performance of Fire suppressants in Aircrafts”, NIST, November 2011

72 "Aerosol can explosion simulator”, FAA report, Presentation, 2005

73 J. Reinhard, “Behavior of bromotrifluoropropene and pentafluoropropene when subbjected to a simulated aerosol can explosion”, FAA report, May 2004

74 S. Ravishankara, A.R., Turnipseed, A.A., Jensen, N.R., Barone, S., Mills, M., Howard, C.J., and Solomon, “Do hydrofluorocarbons destroy stratospheric ozone,” *Science ,* Vol. 263, pp. 71–75, 2000

75 Robert D. Gaudette, “Review of Airbus Water Mist Fire Suppression Project”, Airbus Nero Plan, Life Mist Technologies, Inc

76 C. Goodchild, “Firedass”, Air & Space Europe, Volume 2, Issue 1, Pages 96-100, January–February 2000,

77 R. N. Mawhinney, “The development of a CFD based simulator for water mist fire suppression systems: The development of the fire submode”, J. Applied fire science, 2000

78 Robert L. Darwin, Hughes Associates, Frederick W. Williams, “Overview of the development of water-ist systems for US Navy ships”, Halon options technical working conferene, April 1999

79 T. K. Blanchat, A. L. Brown, V Figueroa, “Benchmark enclosure fire suppression experiments and modelling”, Suppression and Detection Research and Applications – A Technical Working Conference (SUPDET 2008), March 2008

80 M. Nilsson and P.Van Hesss, “Advantages and disadnvantages with using hypoxic air venting as fire protection”, Jyly 2013

81 J. Brooks, “Aircaft cargo fire suppression using low pressure dual fluid water mist and hypoxic air”, NIST SP 984-2,Halon Options Technical Working Conference, 14th. Proceedings, 2004

82 S. S. Yoon, V. Figueroa, A. L.Brown, T. K. Blanchat, “Experiments and modeling of large-scale Benchmark enclosure fire suppression”, Research Article, August 2009

83 T. A. Moore, “Nitrogen gas as a Halon replacement”, Halon Options Technical Working Conference, May 1998

84 R. E. Tapscott and L. C. Speitel, “Halon Replacement Options for Aircraft”, International Aircraft Fire and Cabin Safety Research Conference, Atlantic City, New Jersey USA, November 1998

85 A. Horvat, “Fire Modelling in Computational Fluid Dynamics (CFD)”, Presentation, May 2010

86 “Solution methods for Incompressible Navier-Stokes equations”,slides, ME469B/3/G

87 D, William J. Hughes, “Halon History”, Technical Centre Fire Safety

88 C Soares, A. Teixeira, L. Neves, “Probabilistic modelling of offshore pool fires”, In advance in Safety and Reliability, June 1997

89 P. Sarkos, “Status of halon replacement agent evaluation in commercial aircraft and airport application”, FAA techical center, 1994

90 “Clean agents”, NFPA, 2015

91 Professor Paul J. Gans, “Joule-Thomson Expansion”, Physical Chemistry, V25.0651, September 1992

92 Behbahani-Pour MJ* and Radice G, “Cargo Compartment Fire Extinguishing System”, Division of Aerospace Sciences, School of Engineering, University of Glasgow, Glasgow G12 8QQ, UK, 2016

93 “Instalation Manual for Inert Gas System”, Bettati ANTNCENDIO, Italy 2011

94 “Options for aircraft engine fire protection”, International aircraft system fire protection Group, September 2002

95 “Aircraft Fire Fighting- tactics and Techniques”, slides, International Fire Training Centre

96 A. Bandyopadhyay, A. Majumdar, “Modelling of compressible flow with friction and heat transfer using the generalized fluid system simulation program (GFSSP)”, Thermal fluid analysis workshop, Cleveland, September 2007

97 “Rayleigh Flow-Thermodynamics”, slides AE3450, College of engineering, Georgia Tech, 2001

98 R.Yau, V.Cheng, R. Yin, “Treatment of fire source in CFD Models in performance Base Fire Design”, International Journal on Engineering, Performance-Based Fire Codes, Vol 5, May 2003

99 “Meshing Application Introduction-Chapter 2”, ANSYS 2009

100 G. Puigt and H. Deniau, “CFD e-learning – Mesh and Discretization”, Release 1.1, January 2011

101 “Introductory FLUENT Training-Solver Settings”, ANSYS 2006

102 “Introductory FLUENT Training-Modelling Turbulent Flows”, ANSYS 2006

103 F. J Kelecy, “Coupling Momentum and Continuity Increase CFD Robustness”, Applications Specialist, ANSYS, Inc

104 ANSYS Fluent, “Post processing with FLUENT and CFD-Post process”, April 2009

105 W. L. Oberkampf, T. G. Trucano, “Verification and Validation in Computational fluid dynamics”, Albuquerque, New Mexico, March 2002

106 M. Keating, “Accelerating CFD Solutions”, Principal Engineer, ANSYS

107 “Hazard Classification Guidance”, Hazard Communication, 2016

7 APPENDICES

7.1 Literature Review

A. The figure below [7] illustrates several halon compounds properties that can be used for simulation purposes.

Name	FE-13™ (HFC-23)	FE-25™ (HFC-125)	FM-200™ (HFC-227ea)	FE-36™ (HFC236fa)	ITM	BTM	BCF
Chemical Formula	CF_3H	CF_3CF_2H	CF_3CFHCF_3	$CF_3CH_2CF_3$	CF_3I	CF_3Br	CF_2ClBr
Halon No.	13	25	37	36	(13001)	1301	1211
Refrigerant No.	23	125	227ea	236fa	13I1	13B1	12B1
ODP (CFC11 = 1)	0	0	0	0	0.0001	12-13	5.1
100 Year GWP (CO_2 = 1)	11,700	2,800	2,900	6,300	<1	5,400	
Atmospheric Lifetime (years)	264	32.6	36.5	209	<0.005	65	20
Molecular Weight	70.01	120.02	170.03	152.04	195.91	148.90	165.36
Boiling Point (°C)	-82.0	-48.3	-16.36	-1.4	-22.5	-57.8	-4
Freezing Point (°C)	-155	-103	-131	-103	-78	-168.0	-160.5
Vapor Pressure (bar(a) at 25°C)	45.2	13.1	4.5	2.724	5.4	16.0	2.8
Liquid Density ($g.cm^{-3}$ at 25°C)	0.67	1.190	1.43	1.360	2.096	1.54	1.8
Critical Temperature (°C)	25.9	66.3	101.7	124.9	100	67	153.8
Critical Pressure (bar(a))	48.4	35.9	28.7	32	4.04	39.6	41.0
Critical Density ($g.cm^{-3}$)	0.53	0.571	0.621	0.5553		0.745	0.713
Heat of Vaporization ($J.g^{-1}$ @ Bpt)	240	164.4	132.6	160.0	112.3	121	137
Specific Heat Liquid ($J.g^{-1}.K^{-1}$ @ 25°C)	1.377 @-40°C	1.26	1.102	1.1085		0.883	0.783
Specific Heat Vapor ($J.g^{-1}.K^{-1}$ @ 25°C)	0.888 @-40°C	0.800	0.777	0.8444	0.361	0.473	0.460
Inhalation Toxicity (volume%)	>65	>70	>79	>18.9	27.4	80	13
Lowest Concentration Causing an Adverse Cardiotoxic Effect (LOAEL, volume%)	>50	10.0	10.5	15	0.4	7.5	1.0
Highest Concentration Causing No Adverse Cardiotoxic Effect (NOAEL, volume%)	30	7.5	9.0	10	0.2	5.0	0.5
Safety Ratio (NOAEL/Design Concentration)	2.0	0.69	1.2	1.6	0.06	1.3	0.12
EPA SNAP List Approval	Yes	Yes †	Yes	Yes	Yes †	N/A	N/A
Heptane Cupburner (volume%)	12.4	9.0	6.4	6.3	3.0	3.3	3.6
Methanol Cupburner (volume%)	16.3	12.4	10.0	7.4	3.8	5.9	8.2
Inerting Conc. (volume%) Propane	19.8	15.7	11.5		6.5	7.7	5.9
Mass Equivalence Relative to Halon 1301	1.8	2.2	2.2	1.8	1.2	1.0	1.2
Liquid Volume Equivalence Rel. to 1301	4.1	2.7	2.4	2.0	0.9	1.0	1.0
Company	DuPont	DuPont	Great Lakes	DuPont	AJAY	-	-

B. Operating conditions [3]

Low temperature: survival (non-operating)	-55 °C
Low temperature: short-term operation	-40 °C
Low temperature: continuous operation	-15 °C
High temperature: survival (non-operating)	85 °C
High temperature: continuous operation	70 °C

Normal operation	-2,000 to 10,000 ft
Design limit for functioning properly	25,000 ft continuous, 43,000 ft transient (rapid decompression)

	737-800	747-400	747-400 main deck	757-300	767-300	777-300
Initial discharge system						
Quantity of Halon 1301, lb	33	110	294	33	80	137
Max concentration forward*	15%	6.8%	7% (main deck)	9%	7.4%	7%
Max concentration aft*	12%	6.2%	n/a	8%	7.6%	6.6%
Time to 5% concentration	$^1/_2$ min	2 min	$^2/_3$ min	$^1/_2$ min	1 min	2 min
Time to max concentration	$1^1/_2$ min	3 min	1 min	$1^1/_2$ min	$1^1/_2$ min	3 min
Metered discharge system						
Quantity of Halon 1301, lb	n/a	160	920	55	113	**240**
Sustained concentration forward		3.7%	3.2%	8%	3.2%	5.0%
Sustained concentration aft		3.6%	n/a	6%	3.8%	3.6%
Duration above 3%	>60 min	>195 min	>90 min	>195 min	>195 min	>195 min
Sustained compartment test leakage rate in fire mode	4 ft^3/m forward, 12 ft^3/m aft, (11 ft^3/m forward, 19 ft^3/m aft unpressurized)	82 ft^3/m forward, 84 ft^3/m aft	955 ft^3/m	11 ft^3/m forward, 14 ft^3/m aft	61 ft^3/m forward, 57 ft^3/m aft	78 ft^3/m forward, 99 ft^3/m aft
Cabin altitude in fire mode	8,000 ft	8,500 ft	8,000-8,500 ft	9,500 ft	7,500 ft	8,000 ft
Initial cargo ventilation rate For ventilated compartments	None	Up to 1,800 ft^3/m	Up to 1,800 ft^3/m	Up to 300 ft^3/m	Up to 500 ft^3/m	Up to 1,200 ft^3/m
Cargo fire extinguishing total system gross weight	70 lb	410 lb	1,680 lb	150 lb	310 lb	500 lb

C. INTERNATIONAL AIRCRAFT SYSTEM FIRE PROTECTION WORKING GROUP

Options for aircraft engine fire protection [94]

1. Halon compounds

AGENT	HALON 1301	HFC-125	HFC-227ea	FIC-13I1
Manufacturer	None	DuPont	Great Lakes	AJAY
Chemical Formula	CF_3Br	C_2F_5H	C_3F_7H	CF_3I
Molecular Weight	149	120	170	196
Boiling Point @ 1 Atmosphere (°F)	-72	-55	2.6	-8.5
Density @ 25°C (lb/cu.ft)	96.8	74.2	87.1	131
Vapor pressure @ 7 °F (psia)	214	182	58.8	69.5
Vapor pressure @ -6 °F (psia)	31.9	21.5	2.44	6.64
Fire Extinguishing Design Concentration (volume %)	5	10.5	8	3.6
Fire extinguishing mass performan rati	1.0	2.2	2.3	1.3
Fire extinguishing volum performance ratio	1.0	2.8	2.5	0.9
ODP (rel. CFC-11	12	0	0	0.0001
HGWP (rel. CO_2)	5400	2800	2900	< 1
Atmospheric Lifetime (yrs)	65	33	37	< 0.005
Cardio-sensitization LOAEL (vol.%)	10.0	10.0	10.5	0.4
Cardio-sensitization NOAEL (vol.%)	7.0	7.5	9.0	0.2
EPA SNAP Approved	NO	YES	YES	YES

Property	HFC 125	HFC 227ea	HFC 236fa
Molecular weight	120.02	170.03	152
Boiling point @ 760 mm Hg (°C)	- 48.5	- 16.4	-1.4
Freezing point (°C)	- 102.8	- 131.0	-103
Critical temperature (°C)	66.0	101.7	124.9
Critical pressure (kPa)	3,595	2,912	3,200
Critical volume (cc/mole)	210	274	274
Critical density (kg/m^3)	571	621	555.3
Specific heat, liquid @ 25°C (kJ//kg°C)	1.260	1.184	0.844
Heat of vapor at boiling point @ 25°C (kJ/kg)	164.7	132.6	160.1
Viscosity of liquid @ 25°C (centipoise)	0.145	0.184	0.360
Solubility of water in agent	0.07% by weight @ 25 °C	0.06% by weight @ 21 °C	740 @ 20°C
Vapor pressure @ 25°C (kPa)	1,371	457.7	272.4
Global Warming Potential, GWP	2800	2900	6300
Atmospheric Life, Years	32.6	36.5	209
Cup-burner extinguishing concentration (%) by volume Required agent by weight gr/m^3 at 20^0C	8.7 483	6.5 506	6.3 440

7.1 Carbon dioxide

Formula:	CO_2
Molecular Weight:	44.01
Freezing Point:	-78.5°C
Gas Density (at 0°C):	1.977 kg/m^3
Health Hazard:	9-10 Vol.% cause unconsciousness within 5 minutes
Exposure Limit (TLV-TWA):	5000 ppm

(+) CO_2 is heavier than air
(+) CO_2 is available almost everywhere
(-) extinguishing capability is rather poor (numbers found between 30 and 70 Vol.%)
(-) mass: heavy installation (bottles) required
(-) CO_2 is a global warmer
(-) high rate of accidents due to electrostatic charge (being investigated)
(-) System needs to be designed properly. (is odorless, has leaked into the flight compartment and caused asphyxiation of flight crew).

7.2 Nitrogen

Formula	N_2
Molecular Weight	28
Boiling Point:	-195.8°C
Gas Density (at 20°C):	1.251kg/m^3
Health Hazard:	non-toxic down to for breathing necessary oxygen concentration

(+) N_2 is available almost everywhere
(+) very good toxicity values
(+) can be produced out of the ambient air by membranes
(+) lowers burning temperature
(-) extinguishing capability is rather poor (numbers found between 30 and 80 Vol.%)
(-) mass: heavy installation (bottles) required

N_2 is lighter than air. (Molecular weight 28 vs 29)
N_2 is generated by On Board Inert Gas Generating Systems (OBIGGS) on some military aircraft for the purpose of fuel tank ullage inertin

- Weight and storage equivalence relative to Halon1301 [83]

Agent	Based Upon Typical Design Concentration			Based Upon Heptane Cup-Burner Conc.			Based Upon 120% above Heptane Cup-Burner Conc.		
	Conc., Vol.% [a]	Rel. to Halon 1301	Rel. to Halon 1301	Conc., Vol.%	Rel. to Halon 1301	Rel. to Halon 1301	plus 20%, Vol.%	to Halon 1301	Rel. to Halon 1301
IG-100 (150) [b]	40.3	1.8	11.9	33.6	2.5	16.1	40.3	2.6	16.4
IG-100 (180) [c]	40.3	1.8	9.9	33.6	2.5	13.4	40.3	2.6	13.7
Halon 1301	5.0	1.0	1.0	3.0	1.0	1.0	3.6	1.0	1.0

[a] 12 % above cup-burner heptane fuel ext. conc. for IG-100: 170% for Halon 1301.
[b] Agent cylinder pressurized to 150bar (2205 psi).
[c] Agent cylinder pressurized to 180bar (2646 psi).

FULL-SCALE FIRE SUPPRESSION TESTING

- Test result for polyethylene cable (Class C fire)

Agent	Agent Conc, vol.%	Ext. Time, sec	Reignition	Reburning Time, sec
Nitrogen	39.1	11	yes	3
IG-541	40.2	13	yes	6
FM-200	1.6	6	yes	several sec
HFC-23	15.9	6	yes	several sec

- Typical arrangement for Nitrogen fire suppression system [83]:

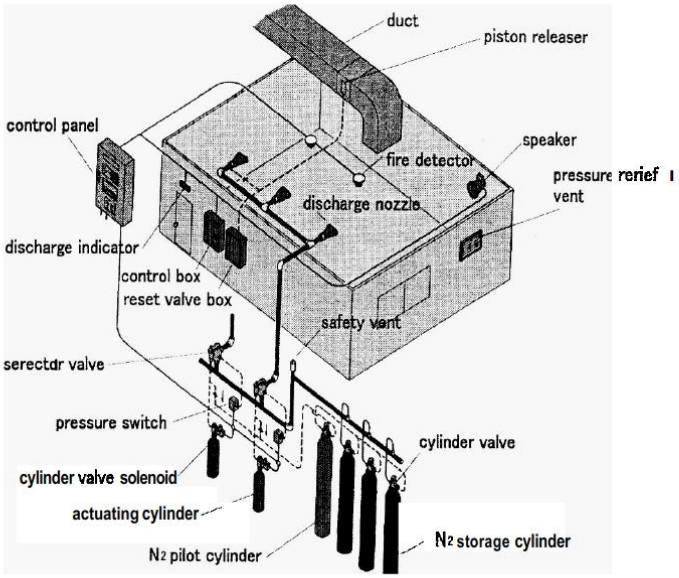

7.2 Safety analysis

This chapter presents the failure modes, the environment and human hazards/risks and the mitigation methods considered during safety analysis:

1. Failure modes

- Ignition wire not sufficient to start the fire.
- Uncontrolled fires/ burn all boxes
- Insufficient distance between the simulator and igniters. High intense explosion (rapid combustion) or no explosion
- Agent contact with reactive material
- Unprotected storage conditions for agent and fuels
- Insufficient ventilation system to clear the enclosure from hazards smokes
- Noise. Discharge of a system can cause noise loud enough to be startling but ordinarily insufficient to cause traumatic injury [90].
- Turbulence. High velocity discharge from nozzles can be sufficient to dislodge substantial objects or injure people directly in the path. System discharge can also cause enough general turbulence in the enclosures to move unsecured paper and light objects [90].
- Decomposition products and exposure time limits for each agent (LSBU) (No personal inside the enclosure during the tests).
- Discharge test failure can be classified as one of the following [90]:
- Primary Failure. The failure of equipment necessary to complete system discharge and achieve initial design concentration (i.e., hydraulic calculations, inoperative containers, control panel malfunction, etc.).
- Secondary Failure. The failure of ancillary equipment that does not inhibit the system from completing discharge and achieving initial design concentration (i.e., dampers, door closures, bells, dry contact relays, etc.).
- Room Integrity Failure. The failure of the room to hold the specified concentration for the specified holding period.

2. Environmental hazards

- Cardboard and paper ashes
- Liquid fuel fire smokes (jet A fuel, propane, ethanol , gasoline)
- Fuel storage

3. Human hazards

- Smoke generation (breathing issues)
- Oxygen Depletion (asphyxiate)
- Fuel leakages, smoke production. Harm in close distance-high temperatures
- The danger in lower agent concentration levels, where some time after extinguishment, a flammable concentration of fuel, air and agent could

possibly be attained through the release or vaporization of additional fuel [90].

- System modifications, refill bottles and fuel transfer during experiments
- Unprotected agent and fuel storage

4. ***Electricity Hazards***

- Low voltage power supply lines
- High voltage transformer and line for ignition spark

5. ***Mitigation***

- Prevent agent exposure for more than 5 minutes for Nitrogen [90].
- Ventilation system operation to clear the air inside enclosure before opening.
- Shut ventilation system to prevent feed oxygen to the fire.
- Ashes will be gathered with the use of specific masks and gloves and placed to designated/protected areas
- Liquid fuel be gathered inside tank with sand from the drain system of the test rig and transfer and disposed in specific allowed designated areas.
- Keep safety distance during the tests and clear the air before opening. Safety distance before ignition.
- Maximum pressure release not sufficient to damage the enclosure.
- Make the ignition smother using gasoline.
- Disconnect/Unplug ignition for test preparation or after test ends.
- Keep away all the equipment regarding fire ignition during test preparation.
- The fumes/smoke will be directed to unoccupied areas as the rest of the tests.
- Inside the enclosure no personal allowed during the tests. The amount of the fuels is not sufficient to damage the enclosure.
- Storage protection (sunlight and harsh conditions), keep safe distance and prevent human exposure.
- System will be tested or shall be appropriate to withstand 10 times higher pressure (or higher than the operating pressure). Air will be pressurized for delivery system leakage and optimum operation checks
- Maintain the cylinder conditions in the desirable flow and discharge conditions. Storage (cylinders) protection with steel fence.
- Pressure equalization valve or door (window) should installed to the test rig.
- Test rig will be capable to open from both sides easily. For the front side two doors opening and one door opening for the back.
- Exposure limits shall be applied depending on the agent (worst case scenario). For example, 5 minutes exposure allowed for 40% design concentration of nitrogen inside the test rig [90]
- Almost all flammable solids begin burning on the surface. In many materials, such as paper and boxes, surface combustion is the only type

that occurs. Although glowing embers can remain at the surface of the fuel following extinguishment of flames, these embers will usually be completely extinguished within 10 or more minutes, provided the agent concentration is maintained around the fuel for this period of time. It is appropriate to consider maintaining the selected agent concentration around the fuel as long as possible.

- Inert gas (nitrogen) system, resulting in low oxygen atmospheres and unnecessary exposure should be avoided. The maximum exposure time in any case shall not exceed 5 minutes for designed concentrations below 43 percent (corresponding to an oxygen concentration of 12 percent, sea level equivalent of oxygen) [90].
- Unprotected personnel shall not enter or get close to the test rig during or after agent discharge.
- Two cameras will be installed, one inside the rig and close to the ignition and one outside the rig focusing on the delivery discharge system and the front doors.
- Sufficient time shall be allowed after every experiment. Temperature and oxygen concentration shall be restored to normal conditions before open the doors of the test rig.
- Special instructions before use of liquid fuels (Jet A fuel, propane, gasoline and ethanol) [90].

Specifically:

1. Do not handle until all safety precautions have been read and understood.
2. Keep away from heat/sparks/open flames/hot surfaces.
3. No smoking.
4. Keep container tightly closed.
5. Ground/bond container and receiving equipment.
6. Use explosion-proof electrical/ ventilating/ lighting/ equipment.
7. Use only non-sparking tools.
8. Take precautionary measures against static discharge.
9. Do not breathe dust/fume/gas/mist/vapour/spray.
10. Wash skin thoroughly after handling.
11. Do not eat, drink or smoke when using these products.
12. Use only outdoors or in a well-ventilated area.
13. Wear protective gloves/ protective clothing/ eye protection/ face protection

Quick response:

1. Immediately call a poison centre/doctor.
2. If on skin (or hair): Take off immediately all contaminated clothing. Rinse skin with water/shower.
3. If inhaled: Remove person to fresh air and keep comfortable for breathing. Call a doctor if you feel unwell.
4. If exposed or concerned: Get medical advice/ attention.

5. Do not induce vomiting.
6. If skin irritation occurs: Get medical advice/attention.
7. Take off contaminated clothing and wash before reuse.
8. In case of fire: Use dry sand, dry chemical or alcohol-resistant foam to extinguish.

Fuels storage:

9. Store in a well-ventilated place. Keep containers tightly closed.
10. Store in a well-ventilated place. Keep cool.
11. Store locked up.

Fuel disposal:

12. Dispose of contents/ containers to an approved waste disposal plant.

7.3 Hazards Classification & Signs

Hazards are classified following the HAZARD COMMUNICATION "Hazard Classifications Guidance" 2016 [107].

The classifications are:

1) Gases under pressure

Decision:

Nitrogen (GI-100) is completely gas at normal conditions (at 15 C or 20 C and 101.3kPa):

i. The gas is contained in a receptacle at pressure at 3000kPa at 15 C
ii. The gas is not dissolved in a liquid phase solvent
iii. The gas is not partially liquid because of it low temperature
iv. The gas is not partially liquid at -50 C it is entirely gas
v. Substance when packed under pressure is entirely gas

Therefore, (Nitrogen) gas is classified as gas under pressure, and categorized as compressed gas:

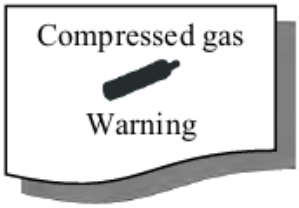

Physical state at 15 C	Gas
Colour	Colourless
Odor	Odorless
Flammability	Non flammable

Critical temperature	-146.96 °C
Vapour density at 15 C	1.1848 kg/m3
State at -50 C	Gas

2) <u>Flammable solid</u>

Cardboard boxes and papers

Decision: depending on burning rate and propagation of the flame (screening test required)

From literature survey,

i. the burning rate is ≥ 2.2 mm/s or burning time ≤ 45 s and
ii. the wetted zone did not stop the propagation of the flame at least in 4min

Therefore, the organic solids are classified as flammable solids Category 2.

3) <u>Flammable liquids</u>

Decision:

i. Kerosene has flash point 38 °C and initial boiling point 149 °C

Therefore, the chemical fulfils the requirements of flammable liquid and is Category 3.

Physical state at 15 °C	Liquid (Kerosene C9-C16)
Colour	Clear light yellow
Flash point (closed cup)	38 °C
Initial boiling point	149 C (at normal pressure)
Flammability/Hazards	Flammable liquid, Carcinogen, Mild skin irritant, Aspiration

ii. Gasoline has flash point -43 °C and initial boiling point 32 °C

Therefore, the chemical fufils the requirements of flammable liquids and is Category 1.

Physical state at 15 °C	Liquid (Gasoline)
Colour	Colourless
Flash point (closed cup)	-43 °C
Initial boiling point	32 C (at normal pressure)
Flammability/Hazards	Flammable liquid, Carcinogen, Mild skin irritant, Aspiration

iii. Propane has flash point -156 °C and initial boiling point 6.6 °C

Therefore, the chemical fulfils the requirements of flammable liquid and is Category 3.

Physical state at 15 °C	Liquid (Propane)
Colour	Colourless
Flash point (closed cup)	-156 °C
Initial boiling point	6.6 °C (at normal pressure)
Flammability/Hazards	Flammable liquid, Carcinogen, Mild skin irritant, Aspiration

iv. Ethanol has flash point 13 °C and initial boiling point 78 °C

Therefore, the chemical fulfils the requirements of flammable liquids and is Category 2.

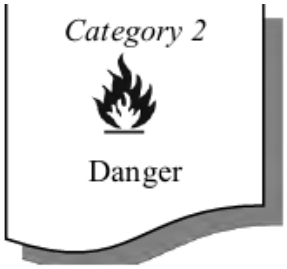

Physical state at 15 C	Liquid (Ethanol)

Colour	Colourless
Flash point (closed cup)	13 °C
Initial boiling point	78 C (at normal pressure)
Flammability/Hazards	Flammable liquid, Carcinogen, Mild skin irritant, Aspiration

4) <u>Flammable spray aerosol</u>

<u>Surface burning fire scenario mixture:</u>

i. The flammable is an aerosol product
ii. Flammable components:
    a) Jet A = 16.5 % (by mass)
    b) Gasoline = 3.5 %
    c) Water =80%
iii. Non-flammable: 80%
iv. The chemical heats of combustion (ΔHc) for gases in the mixture:
    ΔHc (Jet A)= 43 kJ/g
    ΔHc (Gasoline)=46,5 kJ/g
    ΔHc (water)= 0 kJ/g

The chemical heat of combustion (ΔHc) calculated:

(0.165x43)+(0.035X46.5)=8.722 kJ/g

Decision:
The chemical contains 20% flammable components and has heat of combustion of 8.7225 kJ/g and the ignition occurs below 75 cm.

Therefore, the chemical is classified as flammable spray aerosol of Category 2.

<u>Aerosols can explosion test mixture:</u>

i. The flammable is an aerosol product
ii. Flammable components:
    a) Ethanol = 60 % (by mass)
    b) Propane= 20%

c) Water=20%

iii. Non-flammable: 20%

iv. The chemical heats of combustion (ΔHc) for gases in the mixture:
ΔHc (ethanol) = 29,7 kJ/g
ΔHc (propane) =50.4 kJ/g
ΔHc (water) = 0 kJ/g

The chemical heat of combustion (ΔHc) calculated:

(0.6x29.7)+(0.2X50.4)=27.9 kJ/g

Decision:

The chemical contains 80% flammable components and has heat of combustion of 27.9 kJ/g. The ignition of the test should be placed 36 inches (91.4 cm) from the point of discharge.

Therefore, the chemical is classified as flammable spray aerosol in Category 1.

7.4 MPS Fire Scenarios (tests) & Criteria

The figures below illustrate the four fire scenarios (experimental tests) will be performed and the acceptance criteria for each:

Figure 119 - MPS fire test scenarios for aircraft cargo [3]

The main metrics of interest for MPS are: a) the experimental time/duration, b) flame/fire temperature limits and c) pressure allowance inside the test rig. Table 51 and Figure 120 present these limits and the recording data required for analysis.

Table 51 - Flame temperature and pressure limits/criteria for each fire test [3]

Fire Scenario	Maximum Temp. °F (°C)	Maximum Pressure psi (kPa)	Maximum Temp-Time Area °F-min. (°C-min.)	Comments
Bulk Load	720 (382)	Not Applicable	9940 (5504)	Use the data that is between 2 and 28 minutes after suppression system activation. See figure 11.
Containerized Load	650 (343)	Not Applicable	14,040 (7,782)	Use the data that is between 2 and 28 minutes after suppression system activation. See figure 11.
Surface Fire	570 (299)	Not Applicable	1230 (665)	Use the data that is between 2 and 5 minutes after suppression system activation.
Aerosol Can Explosion Simulation	Not Applicable	0.0	Not Applicable	There shall be no evidence of an explosion. No enhancement of explosion at below inert concentrations.

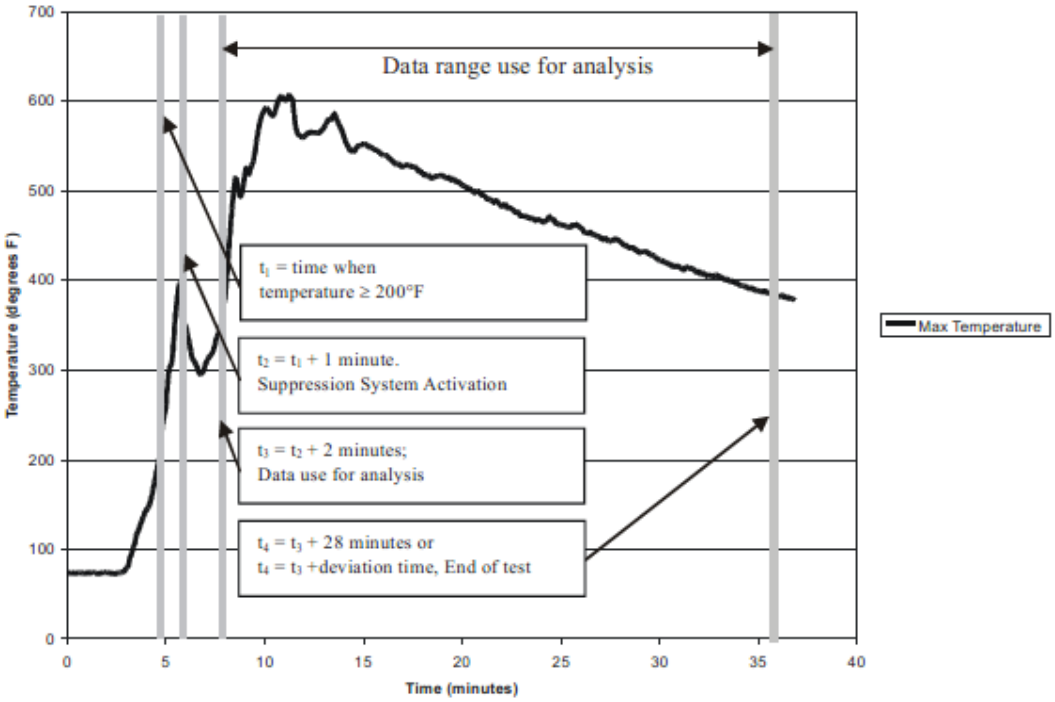

Figure 120 - MPS temperature limits versus time of the experiment [3]

Additionally, Figure 121 describes briefly the experimental procedure, regarding the data for analysis required for each fire scenario.

- *For the bulk-load fire scenario, the average of the five test peak temperatures shall not exceed 720°F (382°C), starting 2 minutes after the suppression system is initially activated until the end of the test. In addition, the average of the five test peak areas under the time-temperature curve shall not exceed 9940°F-min (5504°C-min). The area should be computed from 2 minutes (t_3) after the time of initial suppression system activation (t_2) to 28 minutes after t_3.*
- *For the containerized-load fire scenario, the average of the five test peak temperatures shall not exceed 650°F (343°C), starting 2 minutes after the suppression system is initially activated until the end of the test. The average of the five test peak areas under the time-temperature curve shall not exceed 14,040°F-min (7,782°C-min). The area should be computed from 2 minutes (t_3) after the time of initial suppression system activation (t_2) to 28 minutes after t_3.*
- *For the surface-burning fire scenario, the average of the five test peak temperatures shall not exceed 570°F (299°C), starting 2 minutes (t_3) after the suppression system is initially activated until the end of the test, 3 minutes after t_3. In addition, the average of the five tests peak areas under the time-temperature curve shall not exceed 1230°F-min (665°C-min) for the same period mentioned in the previous sentence.*
- *For the aerosol can explosion simulation scenario, no evidence of an explosion shall be present in the compartment at the time the simulator is activated, such as no overpressure (0.0 psig) or deflagrations. In addition, when the agent concentration is below its inert concentration, the explosion intensity and peak pressures shall not be greater than the values exhibited during an explosive event when no suppression agent is present in the compartment.*

Figure 121 - MPS brief description [3]

Activation and measurement time for each fire test [3]

- ✓ The duration of the bulk- and containerized-load fire scenario tests is 30 minutes after the activation of the suppression system.
- ✓ The fifth test of the bulk and containerized-load fire scenarios must be conducted for at least 180 minutes and must ensure that the temperatures at the end of the test are stable or decreasing. If the system tested is a hybrid system (dual agent), the bulk- and containerized-load fire scenarios must be run for a minimum of 180 minutes.
- ✓ The surface-burning fire test is conducted for 5 minutes from the time the suppression system is activated.
- ✓ The aerosol can explosion simulation fire test shall be conducted for at least 180 minutes or until the aerosol can simulator device is activated, whichever is shorter.

For all fire tests the agent will be discharged until the bottles brain-out (EFKS).

7.5 MPS Fire Scenarios (tests) Setup Description

This chapter describes the set up procedure for the four fire scenarios/tests. These details were taken from MPS 2012 update [3] as it's the main requirement of the project.

For the bulk-load fire scenario [3]

The fire load for this scenario consists of:

- ✓ A single-wall corrugated cardboard boxes, with nominal dimensions of 18 by 18 by 18 inches (45.7 by 45.7 by 45.7 cm) (Figure 122). The weight per unit area of the cardboard is 0.11 lbs/ft^2 (0.5417 kg/m^2).
- ✓ The boxes are filled with 2.5 pounds (1.1 kg) of loosely packed standard weight office paper shredded into strips (not confetti) weighing 4.5 ±0.4 pounds (2.0 ±0.2 kg).
- ✓ The boxes are conditioned to room standard conditions.
- ✓ The flaps of the boxes are tucked under each other without using staples or tape.

- ✓ The boxes are stacked in two layers in the cargo compartment in a quantity representing 30% of the cargo compartment empty volume. For a 2000-cubic-foot (56.6-m^3) compartment, this requires 178 boxes (Figure 122). The boxes touch each other to prevent any significant air gaps between boxes.
- ✓ The fire inside the ignition box (Figure 123) is started by applying 115 Vac to a 7-foot (2.1-m) length of nichrome wire.
- ✓ The wire is wrapped around four folded (in half) paper towels. The resistance of the nichrome igniter coil is approximately 7 ohms. The igniter is placed into the centre of a box on the bottom outside row of the stacked boxes.
- ✓ Finally, several ventilation holes are placed in the side of the box to ensure that the fire does not self-extinguish. Ten 10-inch (2.5-cm) -diameter holes have been shown to be effective

Burning fuel for bulk-load fire

- ✓ cardboard boxes/papers

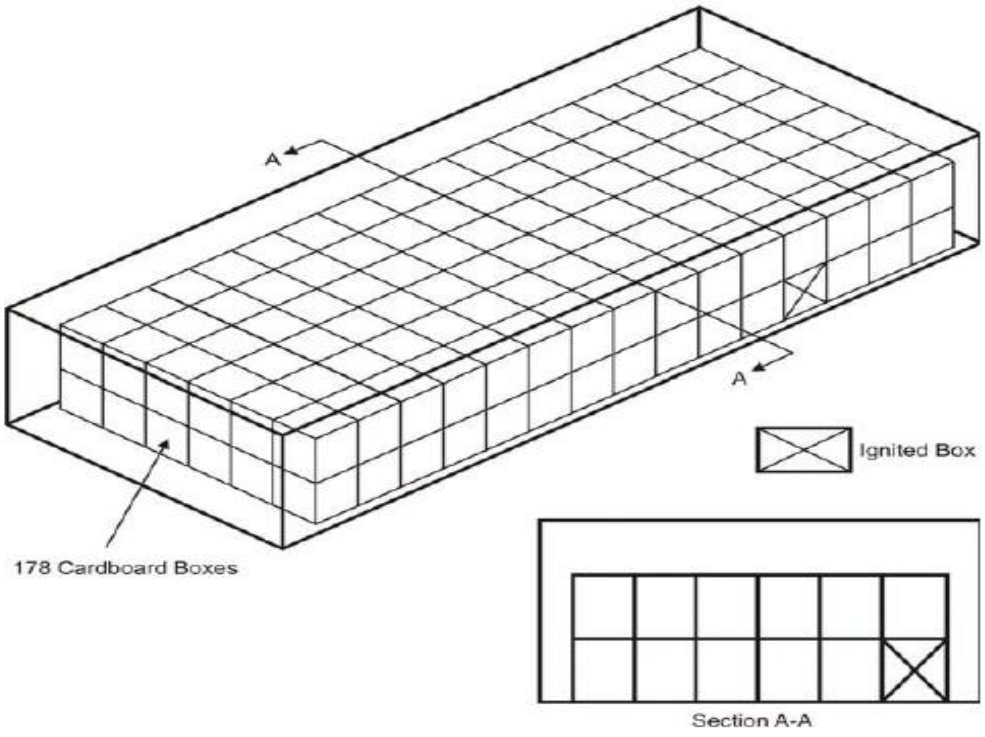

Figure 122 - Bulk-load fire test set up [3]

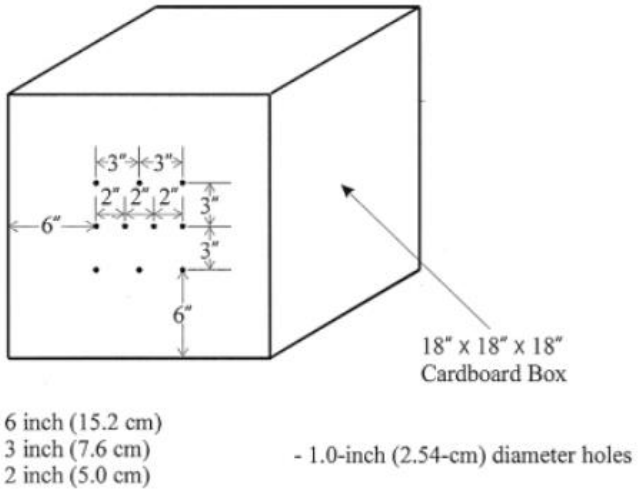

Figure 123 - Igniter box [3]

For the containerized-load fire scenario [3]

- ✓ The same type of paper-filled cardboard boxes and the same type of igniter used in the bulk-load fire scenario is used in this scenario.
- ✓ The boxes are stacked inside an LD-3 container as shown in Figure 124. The boxes touch each other to prevent any significant air gaps between them.
- ✓ The container is constructed of an aluminium top and inboard side, a Lexan (polycarbonate) front, and the remainder of steel (Figure 125). Two rectangular slots for ventilation are cut into the container in the centre of the Lexan front and in the centre of the sloping sidewall. The slots are 12 by 3±1/4 inches (30.5 by 7.6 ±0.6 cm).
- ✓ The igniter is placed in a box on the bottom row (Figure 19), in the centre column next to the sloping side of the container.
- ✓ Ventilation holes are placed on the front face of the box facing the ventilation hole. Ten 1.0-inch (2.5-cm) diameter holes have been shown to be effective.
- ✓ Finally, two additional empty LD-3 containers are placed adjacent to the first container (Figure 126).

Burning fuel for containerized-load fire

- ✓ cardboard boxes/papers

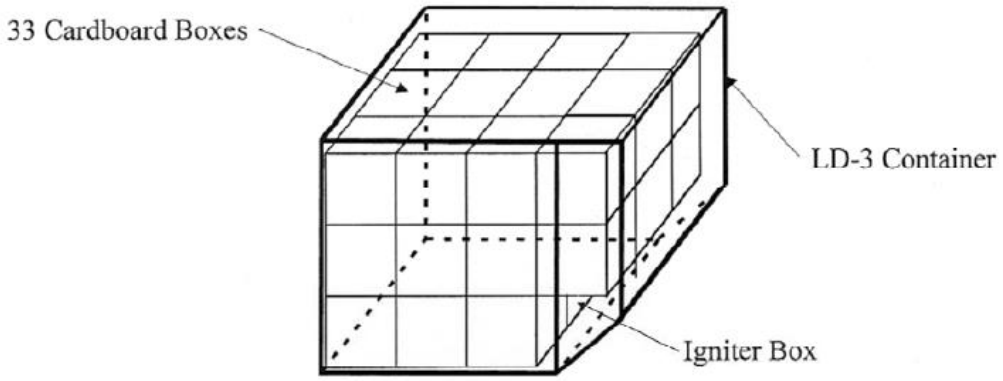

Figure 124 - Containerized-Load fire test set up [3]

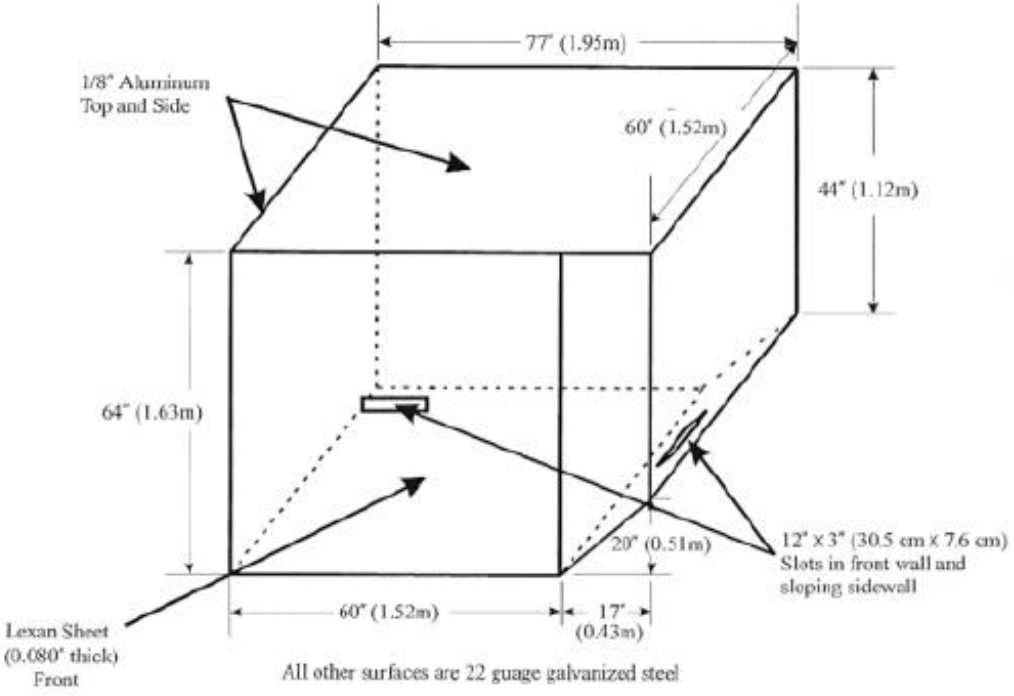

Figure 125 - LD-3 Container [3]

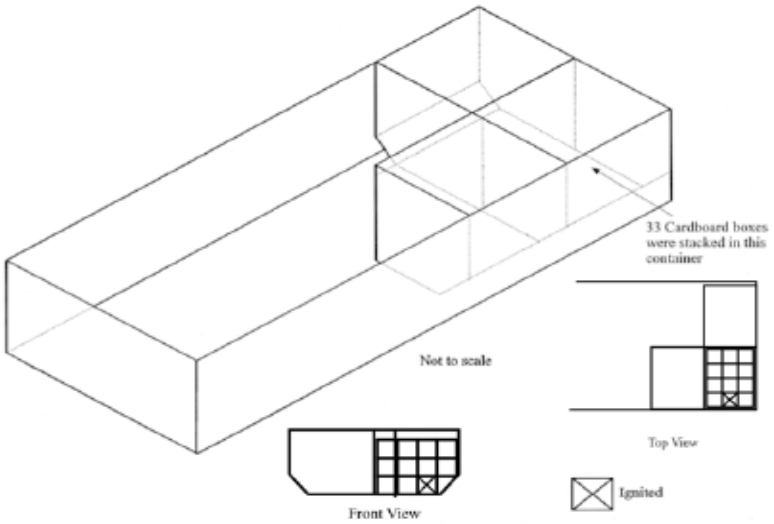

Figure 126 - LD-3 Container arrangement [3]

<u>For the surface burning fire scenario [3]</u>

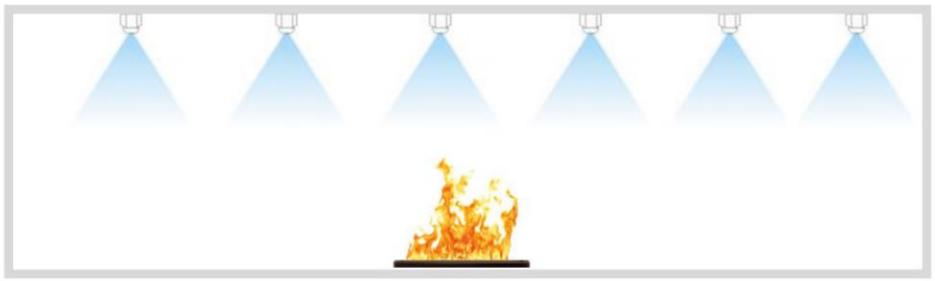

Figure 127 - Surface burning fire scenario arrangement

One-half U.S. gallon (1.9 liters) of Jet A fuel in a square pan is used for this scenario. The pan (Figure 21) is constructed of 1/8-inch (0.3-cm) steel and measures 2 feet by 2 feet by 4 inches high (60.9 by 60.9 by 10.2 cm). Approximately 13 fluid ounces (385 ml.) of gasoline should be added to the pan to make ignition easier. Two and one-half gallons (9.5 liters) of water placed in the pan has been found to be useful in keeping the pan cool and minimize warping. This quantity of fuel and pan size is sufficient to burn vigorously for approximately 4 minutes if not suppressed.

The pan should be positioned in the cargo compartment:

- ✓ At the most difficult location for the particular suppression system being tested.

- ✓ The pan is located 12 inches below the cargo compartment ceiling if the suppression system uses a gaseous agent with a density greater than air at standard pressure and temperature (14.7 psia (101.3 kPa), 59.0°F (15°C)).
- ✓ The pan is 12 inches (30.5 cm) above the floor of the compartment if the suppression system uses a gaseous agent with a density less than air at standard pressure and temperature.
- ✓ The pan is placed in the compartment at mid height when the suppression agent has a density equal to that of air.
- ✓ The pan is located at the horizontal distance from any discharge nozzles for all tests, regardless of the suppression agent used.

Burning fuel for surface burning fire

- ✓ 1.9 L Jet A fuel
- ✓ 385 ml gasoline (smooth and fast ignition)
- ✓ 9.5 L water for coolant

Table 52 - Jet A properties [6]

Property	Jet-A
Heating value (MJ/kg)	43
Flash point (°C) (T at which vapor makes flammable mixture in air)	38
Vapor pressure (at 100°F) (psi)	0.03
Freezing point (°C)	−40
Autoignition temperature (°C) (T at which fuel-air mixture will ignite spontaneously without spark or flame)	210
Density (at 15°C) (kg/m^3)	810

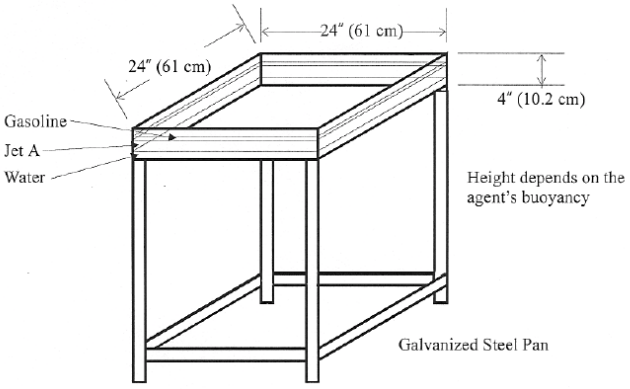

Figure 128 - Surface burning fire pan [3]

<u>For the aerosol can explosion fire scenario [3]</u>

Figure 129 - Aerosol can explosion test

The aerosol can explosion simulator is placed near the centreline of the cargo compartment (as long as there is no agent impingement on the simulator or electrodes), at least 5 feet (1.52 m) forward from the boxes, aft of the boxes containing the igniter and pipes (Figure 130).

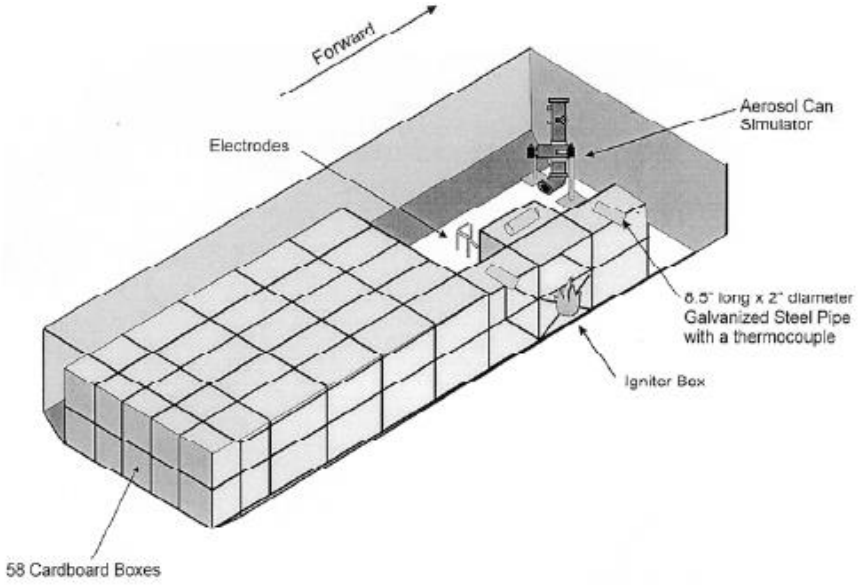

Figure 130 - Aerosol can explosion simulation set up [3]

The simulator's sparking electrodes are located 3 feet in front of the simulator discharge port and 2 feet above the floor. The simulator has a cylindrical pressure vessel for storing the base product hydrocarbon propellant (Figure 23). The pressure vessel is capable of withstanding a minimum pressure of 300 psi (2068.5 kPa). The pressure vessel has a ball valve to rapidly discharge the propellant, capable of withstanding a minimum pressure of 300 psi (2068.5 kPa). The port diameter of the ball must be 1.5 inches (3.8 cm) (note: a ball valve is typically classified according to the diameter of the pipe that it connects to, but this is not necessarily the size of the ball port). The ball valve is capable of rotating from the fully closed position to the fully open position in less than 0.1 second in order to form a vapour cloud. Longer opening durations will significantly affect the size of the vapour cloud formed and, hence, the explosive force. The ball valve can be activated by any suitable means, including pneumatic or hydraulic actuators or manually via the appropriate linkage [3]. The pressure vessel is mounted vertically above the ball valve to allow for complete expulsion of the liquid contents. A discharge elbow located vertically under the ball valve directs the contents horizontally.

The following list describes the major components of the aerosol can simulator (see Figure 131) [3].

- ✓ Pressure Vessel. A steel 2-inch (5.1-cm) -diameter, 11-inch (27.9-cm) -long schedule 80 pipe welded or capped at one end.
- ✓ Ball Valve. The 2-inch (5.1-cm) valve is constructed of a material capable of withstanding interaction with ethanol and propane. A DynaQuip stainless steel valve has been found suitable for this application.
- ✓ Ball-Valve Actuator. A pneumatic rotary actuator is suitable for quickly and reliably rotating the ball valve from closed to fully open. A Speedaire 90-degree actuator with a 2-inch (5.1-cm) bore performs well.
- ✓ Propellant Heater. A system for heating the pressurized propellant mix after transfer to the pressure vessel is provided. This could include a hot-air gun directed toward the pressure vessel, a hot-wire wrap, or other suitable means.

- ✓ Pressure Gauge. A suitable device for measuring the pressure of the contents is installed on the simulator pressure vessel, capable of measuring the pressure to within ±5 psi (34.5 kPa).
- ✓ Propellant Mix.
    i. The base product/propellant mix is 20% liquid propane (3.2 ounces [0.09 kg]),
    ii. 60% ethanol (denatured alcohol, 9.6 ounces [0.27 kg]),
    iii. 20% water (3.2 ounces [0.09 kg]).
- ✓ The total weight of the base product/propellant mix is 16 ounces.

Spark Igniters. A set of direct current (DC) spark igniters is used to ignite the propellant/base product mix discharged from the pressure vessel. An ignition transformer capable of providing a 10,000-volt output has been found to be suitable for powering the igniters, which should be placed 36 inches (91.4 cm) from the point of discharge. The spark igniter gap is set at 0.25 inch (0.64 cm). The igniter should be protected from the rapidly discharged simulator contents by shielding it. A bent piece of sheet metal, like a ramp, provides adequate protection.

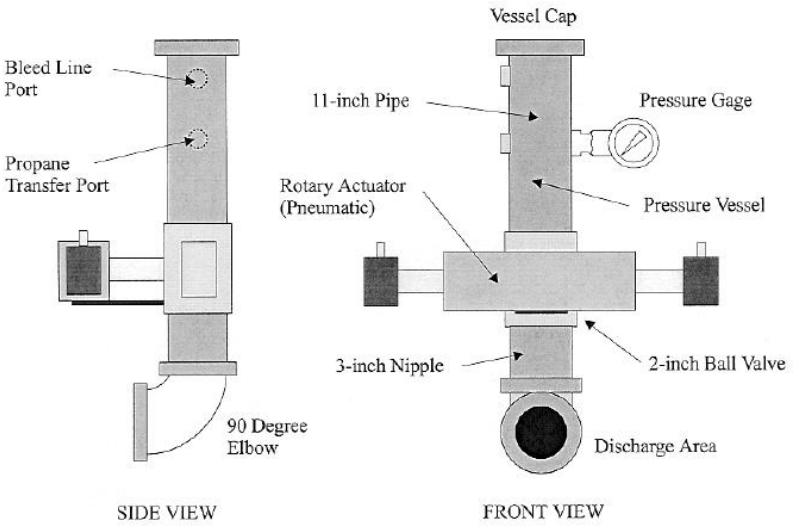

Figure 131 - Schematic of aerosol can explosion simulator [3]

The procedure for setting up the aerosol can explosion simulator is as follows:

- ✓ Weigh the empty aerosol can explosion simulator device on a suitable scale and zero the scale.

- ✓ Place 9.6 ounces (0.27 kg) of ethanol (denatured alcohol) and 3.2 ounces (0.09 kg) of water into the pressure vessel. Transfer 3.2 ounces (0.09 kg) of liquid propane into the pressure vessel.
- ✓ Remove all transfer lines and check final mass.
- ✓ Mount the simulator device in the forward compartment bulkhead in a manner that directs the discharge across the spark igniters.
- ✓ The simulator device discharge port and the spark igniter are 2 feet (60.9 cm) above the compartment floor, and the spark igniter is 3 feet away from the discharge port.
- ✓ The simulator device discharge port is located on the centreline of the aircraft, 5 feet forward of the first rows of cardboard boxes spanning the width of the compartment.
- ✓ Finally, heat the pressure vessel to raise the pressure of the contents to 240 ±5 psi (1655 ±34.4 kPa).

Aerosol can explosion (SHORT VERSION)

Shorter version of the aerosol can explosion simulation test protocol may be used for gaseous agents. Therefore, this version will be executed during EFFICIENT project fire tests. In the short version, the aerosol can explosion simulator device is placed inside the empty standard compartment (see Figure 132). The simulator device is prepared as specified previously at the long version. This test starts when the fire suppression agent is discharged.

- ✓ The simulator device is activated at least 2 minutes after agent discharge.
- ✓ The activation time is dictated by the measured volumetric concentration, within ±0.1% of the minimum protection concentration.
- ✓ The minimum concentration is measured 2 feet (60.9 cm) above the floor, near the sparking electrodes.
- ✓ The agent concentration must be measured during the test, and calculation of agent concentration based on the leakage rate is not permitted.
- ✓ The gas-sampling probe is 36 inches (91.4 cm) from the exit of the simulator device and 18 inches (45.7 cm) to the side of the spark igniters (starboard or portside).

- ✓ The applicant must demonstrate that the system is capable of providing sufficient agent, at least to maintain the minimum inert concentration.
- ✓ The exploding aerosol can test scenario shall be conducted for at least 180 minutes or until the simulator device is activated, whichever is shorter.

Burning fuel: Mixture inside pressure vessel

- ✓ *3.2 ounces (0.09 kg) of liquid propane*
- ✓ *9.6 ounces (0.27kg) of ethanol*
- ✓ *3.2 ounces (0.09kg) water*
- ✓ *Vessel pressure 240 ±5 psi (1655 ±34.4 kPa) (using heat source)*

Table 53 - Fuels properties

Specific Energy, Energy Density & CO2				
Fuel	Specific Energy kj/g	Density KWH/gal	Chemical Formula	lbs CO2/gal
Propane	50.4	26.8	C3H8	13
Ethanol	29.7	24.7	C2H5OH	13
Gasoline	46.5	36.6	C7H16	20

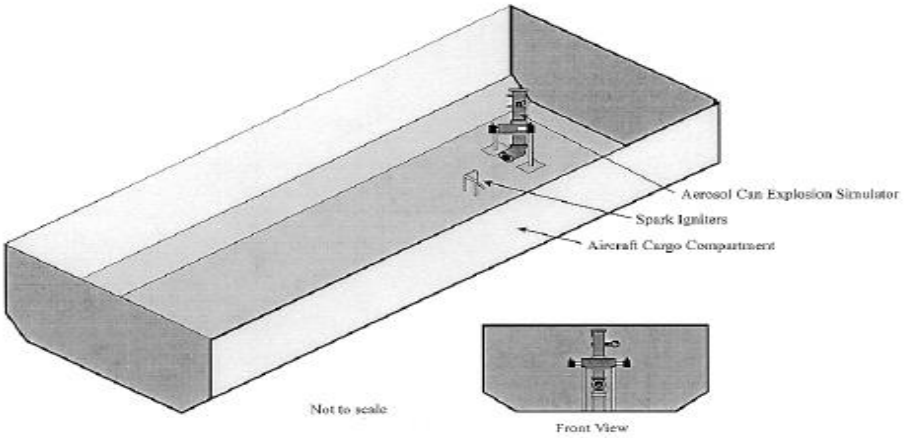

Figure 132 - Aerosol can explosion simulation test set up (short version) [3]

7.6 MPS Fire scenarios (tests) Equipment for Measurements

Figure bellow illustrate the general arrangement and instrumentation of cargo (test rig) suggested in MPS.

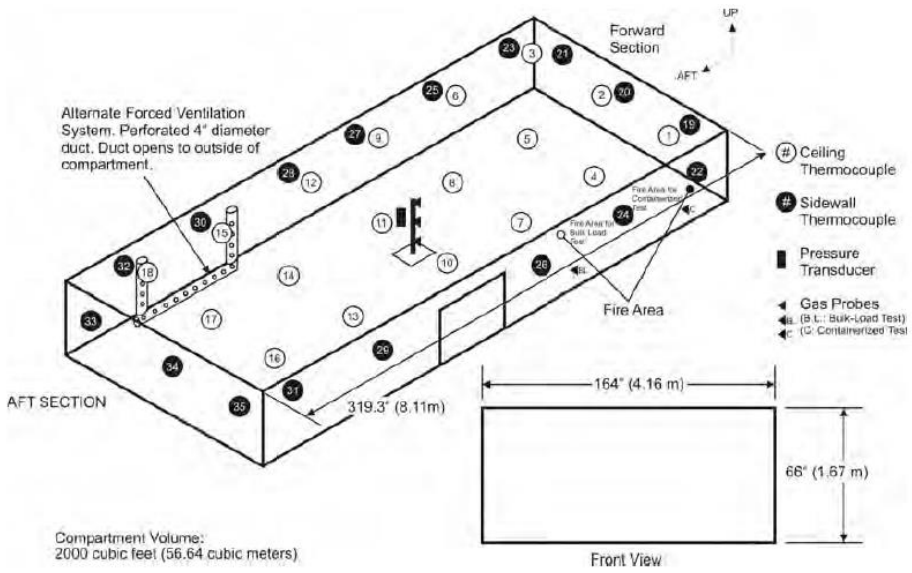

Figure 133 - General arrangement and instrumentation

Hardware, software, controls systems and electrical connections

Temperature measurements are taken throughout the cargo compartment. Type K chromel/alumel 22-gauge thermocouples (1300 C) have been found to be effective at measuring temperatures in the range these fire scenarios produce [3]. The positions and number of the thermocouples goes as follow:

- ✓ Ceiling thermocouples are evenly spaced along the compartment ceiling at 5-foot intervals
- ✓ One ceiling thermocouple is installed directly above the initial ignition location for all fire scenarios.
- ✓ The beads of the ceiling thermocouples are 1 inch (2.5 cm) below the compartment ceiling.
- ✓ At least one thermocouple is placed on the compartment sidewall 1 foot below ceiling level and centred on the fire ignition location. The sidewall

thermocouple is installed on the compartment wall nearest the ignition location.

- ✓ At least two additional thermocouples are placed in and above the box containing the igniter for the bulk- and containerized-load fire scenarios. The purpose of these two thermocouples is to monitor and verify the ignition of the boxes. The readings are not part of the acceptance criteria.
- ✓ Care should be taken to prevent these thermocouples from contacting the energized coil of the nickel-chrome wire.
- ✓ The total number of thermocouples are 37 (18 ceiling,15 sidewall, 2 for ignition verification and 2 for other points of interest or backup)
- ✓ Three thermocouples were selected for measuring the temperature close to the nozzles. Type K chrome/alumel differential thermocouples with temperature range -100 to 50 C.

For the rest of the equipment:

- ✓ A continuous gas analyser with a real-time display of the gas (extinguishing agent) volumetric concentration is required for the aerosol can explosion simulation fire scenario, when the suppression system is a gaseous total flood system (short-test version).
- ✓ A continuous gas analyser may also be required, depending on the suppression system design, for the bulk- and containerized-load fire scenarios. The accuracy of the analyser shall be ±5% of the reading. The gas analyser is used to measure the concentration of oxygen and agent. The data sampling rate for all the temperature measurements and the gas concentrations should be at least one data point every 5 seconds.
- ✓ A pressure transducer is also required for the aerosol can explosion simulation fire scenario. The maximum transducer pressure range is 0-50 psig. The minimum frequency response of the transducer is 3000 Hz. The transducer is mounted on the ceiling in the geometric centre of the compartment. The data sampling rate for the pressure transducer is at least 3000 data points per second.

- ✓ Two more pressure transducers were selected for measuring the pressure inside the container/test rig and inlet of the fan. The range is 0-1 psig (0-0,07bar)
- ✓ Three pressure transducers were selected for measuring the pressure close to the nozzles (range is 0- 50bar).
- ✓ A barometric high pressure transducer was selected for measuring the ambient temperature.
- ✓ Two cameras, one for inside the test rig/container close to the fire ignition (high temperature resistance camera (night/dark vision or heat camera)) and one outside focusing to the storage delivery system and front doors of the test rig.
- ✓ Equipment for measuring and transferring liquid fuels
- ✓ Two personal computers (LAB view software) will be used for recording the measurements for temperature, pressure, agent concentration (mass flow rate if applicable) inside the enclosure and other points of interest such as nozzles etc.
- ✓ Hardware housing close to the test rig. Use of smaller room (house)
- ✓ Hardware board/box and electrical box
- ✓ Control panel, switches, buttons, indicators lamps etc.
- ✓ Electrical wiring, protection tubes and automation equipment.
- ✓ Test rig/container cover protection when not in use